THE ROLE OF MAP KINASE PHOSPHATASE 2 (MKP-2) IN EXPERIMENTAL AUTOIMMUNE ENCEPHALOMYELITIS, AN ANIMAL MODEL OF MULTIPLE SCLEROSIS

A thesis presented by

Mark J. Barbour BSc Hons, MRes

A thesis submitted in the fulfilment of the requirements for the degree of Doctor of Philosophy

September 2015

Strathclyde Institute of Pharmacy and Biomedical Sciences (SIPBS)

University of Strathclyde

Glasgow, UK

This thesis is the result of the author's original research. It has been composed by the author and has not been previously submitted for examination which has led to the award of a degree.

Signed:

Date:

Abstract

Experimental Autoimmune Encephalomyelitis (EAE) is an animal model of multiple sclerosis (MS), causing a demyelinating central nervous system (CNS) inflammation which resembles the main pathological features of MS. Mitogen-activated protein kinases (MAPKs), which are key components in the molecular response leading to MS/EAE pathogenesis, are regulated by MAPK phosphatases (MKPs), enzymes which dephosphorylate phosphotyrosine and phosphothreonine residues. It has previously been shown that MKP-2 modulates the inflammatory response during both acute lung injury and sepsis. Therefore in the present study we investigated the role of MKP-2 in the development of the neurological autoimmune disease, MS, using a murine EAE model.

We first observed significantly increased expression of MKP-2 mRNA in the spinal cord of EAE mice compared with PBS controls. Subsequently, to understand the function of MKP-2 *in vivo*, we utilised MKP-2 deficient mice, inducing EAE in MKP-2 KO and WT littermates. Our data show that MKP-2 KO mice displayed significantly reduced EAE susceptibility, associated with diminished CNS inflammation and cellular infiltration, decreased expression of key cytokines and chemokines (IL-17, IFNγ, IL-6, IL-2 and CCL2), reduced frequency of $CD4^+$ T cells, $CD8^+$ T cells and B cells in spleen and dLN tissue as well as downregulated nitric oxide (NO) production in MKP-2 KO EAE mice. We further analysed the role of MKP-2 in two key immune cells involved in EAE pathogenesis. Upon LPS stimulation, MKP-2 deficient bone marrow-derived dendritic cells expressed less MHC-II while producing more IL-6, TNF-α and IL-10, whereas MKP-2 KO bone marrow-derived macrophages displayed a unique M1 and M2 mixed phenotype, with reduced NO production (M1) and increased CD206 expression (M2) but increased IL-6 and TNF-α, which are more associated with M1 responses.

Therefore this report suggests that MKP-2 is essential to the pathogenic response of EAE, and that inhibition of MKP-2 expression or function may be a viable strategy in the treatment of autoimmune inflammatory diseases such as MS.

Publications

Papers

Pei C, **Barbour M**, Fairlie-Clarke KJ, Allan D, Mu R, Jiang HR. Emerging role of interleukin-33 in autoimmune diseases. *Immunology*. 2014;141:9–17

Barbour M, Allan D, Xu H, Pei C, Chen M, Niedbala W, Fukada SY, Besnard AG, Alves-Filho JC, Tong X, Forrester JV, Liew FY, Jiang HR. IL-33 attenuates the development of experimental autoimmune uveitis. *Eur J Immunol*. 2014;44(11):3320-9

Tong X, Jiang HR, **Barbour M**, Hou K, Gao C, Cao S, Zheng J, Zhao Y, Mu R, Zhang J. Interleukin-33 predicts poor prognosis and promotes ovarian cancer cell growth and metastasis through regulating MAPK/ERK and MAPK/JNK signalling pathways (In preparation)

Conference Posters

Barbour M, Jiang HR, Plevin R. The Role of the Dual Specificity Phosphatase DUSP4 (MKP-2) in Experimental Autoimmune Encephalomyelitis. British Society for Immunology Congress 2013. Liverpool, UK

Acknowledgements

I would like to thank Dr Hui-Rong Jiang for her continued support, encouragement and guidance throughout the course of this project. Her door was always open when I needed help or advice. I would also like to thank my second supervisor, Prof Robin Plevin, for his help during my studies, providing new ideas or a different view which I had perhaps not considered, and also for providing the MKP-2 KO mice which I used in this study. In addition I would like to thank Roy and Robin for genotyping these mice.

In addition, Dr Karen Fairlie-Clarke sacrificed countless hours helping me in the lab, giving me good advice and generally making work a bit more fun, for which I'm extremely grateful. I also wish to thank two other previous lab colleagues for their help, Debbie Allan and Ava Noofeli, as well as the animal unit staff, particularly Carol Whitehouse, who were always willing and able to provide assistance. As ours was a very small lab group, I also got help from other kind SIPBS people, including Justyna, Lamyaa, Stuart, Gary, Emma, Julianne and Thikryat, all of whom I would like to thank. I would also like to thank Dr John Dempster for his help with statistical analysis.

Also, I want to thank the friends I made here in SIPBS. Studying for a PhD is by no means the hardest job in the world, but it comes with unique experiences and can be a rollercoaster at times, and so having good people around you all going through the same things and supporting each other makes it that bit easier when nothing works! Finally, I would never have made it this far without the unwavering support of my mum, sister, LJ and RW. I know how lucky I am to have a good family and people in my life who care about me. They have all given me the drive to try and be better and to make the most of the opportunities I get, and so I hope by completing this I can make them proud of me.

Abbreviations

ADEM	Acute disseminated encephalomyelitis
ALI	Acute lung injury
AMPA	Alpha-amino-3-hydroxy-5-methylisoxazole-4-propionic acid
APC (conjugate)	Allophycocyanin
APC	Antigen presenting cell
APS	Ammonium persulfate
Arg1	Arginase-1
ASK1	Apoptosis signal-regulating kinase 1
ATF2	Activating transcription factor 2
BAL	Bronchoalveolar lavage
BBB	Blood brain barrier
BCR	B cell receptor
bmDC	Bone-marrow derived dendritic cell
BMM	Bone-marrow derived macrophage
BSA	Bovine serum albumin
CCL	Chemokine (CC) ligand
CCR	Chemokine (CC) receptor
CD	Cluster of differentiation
cdc	Cell division cycle
cDMEM	Complete Dulbeccos Modified Eagle Medium
cDNA	Complementary DNA
CFA	Complete freunds adjuvant
CIA	Collagen-induced arthritis
CIITA	Class II, major histocompatibility complex, transactivator
CNS	Central nervous system
ConA	Concanavalin A

COX-2	Cyclooxygenase 2
CREB	cAMP response element-binding protein
cRPMI	Complete RPMI
CSF	Cerebrospinal fluid
CXCL	Chemokine (CXC) ligand
CXCR	Chemokine (CXC) receptor
DC	Dendritic cell
dH_2O	Distilled water
DLK1	Delta-1 like homolog
dLN	Draining lymph node
DNA	Deoxyribonucleic acid
DPX	Distyrene, plasticizer, xylene
DTT	Dithiothreitol
DUSP	Dual-specificity protein phosphatase
E2F1	E2F transcription factor 1
EAE	Experimental autoimmune encephalomyelitis
EBV	Epstein-Barr virus
ECL	Enhanced chemiluminescence
EDTA	Ethylenediaminetetraacetic acid
ELISA	Enzyme-linked immunosorbent assay
Elk-1	Ets-like transcription factor-1
ERK	Extracellular signal-regulated kinase
ERα	Estrogen receptor alpha
FACS	Fluorescence-activated cell sorting
FAK	Focal adhesion kinase
FasL	Fas ligand
FDA	U.S. Food and Drug Administration
FDCP1	Factor-dependent cell progenitor 1

FITC	Fluorescein isothiocyanate
GAPDH	Glyceraldehyde 3-phosphate dehydrogenase
GMCSF	Granulocyte-macrophage colony-stimulating factor
Grb2	Growth factor receptor-bound protein 2
GTP	Guanosine-5'-triphosphate
H&E	Haematoxylin and eosin
H2AFX	H2A histone family, member X
HEK 293	Human embryonic kidney 293 cells
HHV-6	human herpes virus 6
HLA-DRB1	Major histocompatibility complex, class II, DR beta-1
HRP	Horseradish peroxidase
HSVTK	Herpes simplex virus thymidine kinase
HUVEC	Human Umbilical Vein Endothelial Cells
i.p.	Intraperitoneal
IFN-β	Beta interferon
IFN-β1a	Type 1a beta interferon
IFN-β1b	Type 1b beta interferon
IFNγ	Interferon gamma
Ig	Immunoglobulin
IHC	Immunohistochemistry
IL	Interleukin
iNOS	Inducible nitric oxide synthase
IRF-1	Interferon regulatory factor 1
JIP1	JNK-interacting protein 1
JNK	c-Jun N-terminal kinase
KO	Knockout
Lck	Lymphocyte-specific protein tyrosine kinase
LCMV	Lymphocytic choriomeningitis virus

LN	Lymph node
LPS	Lipopolysaccharide
M1	Classically activated macrophages
M2	Alternatively activated macrophages
MAPK	Mitogen-activated protein kinase
MAPKK	Mitogen-activated protein kinase kinase
MAPKKK	Mitogen-activated protein kinase kinase kinase
MBP	Myelin basic protein
M-CSF	Macrophage colony-stimulating factor
mDC	Myeloid dendritic cell
MHC-I	Major histocompatibility complex class I
MHC-II	Major histocompatibility complex class II
MIP1α	Macrophage inflammatory protein 1 alpha
MKP	Mitogen activated protein kinase phosphatases
MLK3	Mixed lineage protein kinase 3
MOG	Myelin oligodendrocyte glycoprotein
MP1	MEK partner 1
MRI	Magnetic resonance imaging
mRNA	Messenger RNA
MS	Multiple sclerosis
NaCl	Sodium chloride
NES	Nuclear export sequence
NFAT	Nuclear factor of activated T cells
NF-κB	Nuclear factor kappa beta
NK	Natural killer cell
NKT	Natural killer T cell
NLS	Nuclear localisation sequence
NO	Nitric oxide

OPC	Oligodendrocyte precursor cells
OVA	Ovalbumin
Pax5	Paired box 5
PBS	Phosphate buffered saline
PBST	Phosphate buffered saline-Tween 20
PCR	Polymerase chain reaction
pDC	Plasmacytoid dendritic cell
PE	Phycoerythrin
PerCPCy5.5	Peridinin chlorophyll cyanine5.5
p-ERK	Phosphorylated ERK
p-JNK	Phosphorylated JNK
PLE	Plevin MKP-2 mice
PNS	Peripheral nervous system
PPMS	Primary progressive multiple sclerosis
PRMS	Progressive relapsing multiple sclerosis
PTX	Pertussis toxin
qPCR	Quantitative polymerase chain reaction
Raf	Rapidly accelerated fibrosarcoma
RFX5	Regulatory factor X 5
RIPA	Radioimmunoprecipitation assay
RRMS	Relapsing remitting multiple sclerosis
RT	Room temperature
RT-PCR	Reverse transcription polymerase chain reaction
Runx	Runt-related transcription factor
s.c.	Subcutaneous
S1P	Sphingosine-1-phosphate
SDS	Sodium dodecyl sulfate
SDS-PAGE	Sodium dodecyl sulfate polyacrylamide gel electrophoresis

SEM	Standard error of the mean
siRNA	Small interfering ribonucleic acid
SPMS	Secondary progressive multiple sclerosis
STAT	Signal Transducer and Activator of Transcription
STWS	Scotts tap water substitute
TBS	Tris buffered saline
TBST	Tris buffered saline-Tween 20
TCR	T cell receptor
TEMED	Tetramethylethylenediamine
Tfh	T folicular helper cell
Th	T helper cell
TMB	3,3',5,5'-Tetramethylbenzidine
TNFα	Tumour necrosis factor alpha
Treg	Regulatory T cell
TRITC	Tetramethylrhodamine
TYK2	Tyrosine kinase 2
UVB	Ultraviolet B
VCAM-1	Vascular cell adhesion molecule
VH1	Vaccinia virus H1 protein
VLA-4	Very late antigen 4
WT	Wild type
$ZnSO_4$	Zinc sulfate

List of Figures

List of Tables

1 General Introduction

1.1 Multiple Sclerosis

Multiple sclerosis (MS) is an autoimmune, inflammatory disease of the central nervous system (CNS). It was originally described by Jean-Martin Charcot in 1866 when, during autopsy, he observed disseminated plaques in the brain and spinal cord of three patients who had suffered progressive disability which he originally believed was the result of neurosyphilis [1], [2]. By 1868, he and his colleague Edme Vulpain had elucidated important aspects of disease pathology such as myelin loss, axonal damage, and macrophage involvement. In addition, they were also able to identify clinical manifestations of the condition. This included visual problems caused by plaques on the optic nerve, tremors, speech difficulty, cognitive impairment and the fluctuating nature of symptom intensity.

Following on from Charcot, further research has continued over the years to elucidate the pathological and immunological aspects of MS – the disease was officially named as such in 1955 having been primarily known as disseminated sclerosis prior to the publication of Douglas McAlpine's seminal book, Multiple Sclerosis [2].

It is now known that MS is caused by autoreactive immune cells which target myelin and axonal proteins within the CNS. Myelin is a fatty material composed of lipids and proteins that surrounds the axon of each neuron, creating an electrically insulating layer known as the myelin sheath. Myelin is produced by schwann cells in the peripheral nervous system (PNS) and by oligodendrocytes in the CNS. The main function of the myelin sheath is to enable faster propagation of action potentials along axons [3]. In MS demyelination occurs, in which the myelin sheath is damaged by an autoimmune inflammatory response. This results in axonal damage which impairs the conduction of nerve impulses, causing a variety of physical and mental problems.

Approximately 2.5 million people worldwide are thought to suffer from the disorder [4]. In the UK it is estimated that around 125,000 people have MS, with 6,000 newly diagnosed each year [5]. In particular, Scotland has one of the highest incidence rates of MS in the world, with a prevalence of around 190 cases per 100,000 compared to a

UK average of just 164 according to the 2013 Atlas of MS produced by the Multiple Sclerosis International Federation (MSIF). Women are 2-3 times more likely to develop MS than men [4]–[6]. Onset usually occurs in early adulthood, with the majority of individuals diagnosed between the ages of 20-40, although it can affect people of any age. Prevalence is variable, but tends to increase the greater the distance from the equator [7], [8], although there are exceptions to this, with lower prevalence in certain populations such as the Inuit, Norwegian Lapps, and the Maori of New Zealand [9], [10]. Therefore ethnic background is clearly another factor to consider, with MS most common in Caucasians of northern European ancestry [11].

1.1.1 Diagnosis of MS

There is no single test currently available to enable positive diagnosis of MS, making it difficult to diagnose. Instead, a number of criteria to diagnose MS have been established based on patient clinical symptoms and various neurological tests including neuroimaging and cerebrospinal fluid (CSF) analysis. These current criteria for correct diagnosis of MS have been developed from the McDonald criteria originally published in 2001, and subsequently revised in 2005 and again in 2010, as well as by the International Panel on Diagnosis of MS [12]. It must be demonstrated that there is a minimum of two unique T2 lesions in at least two out of four areas of the CNS (perivascular, juxtacortical, infratentorial and spinal cord) as analysed by Magnetic Resonance Imaging (MRI), unless the patient has previously suffered more than one clinical attack, in which case evidence of one lesion would suffice.

In addition the physician must obtain evidence for dissemination of lesions in time, and will therefore perform a follow up MRI, typically at least one month after the baseline test to look for new T2 lesions. Cerebrospinal fluid (CSF) analysis can also aid in MS diagnosis. CSF is obtained by lumbar puncture and examined for the presence of two or more oligoclonal bands, which is seen in at least 80 – 95 % of MS patients [13], [14].

1.1.2 MS Aetiology

The initiating factor(s) of MS remains unknown. However, like many autoimmune disorders, it is likely that both genetic and environmental factors are involved. Several genes have been associated with MS susceptibility in previous studies, which suggests potential genetic predisposition to development of the condition. This includes HLA-DRB1, IL-2Rα, IL-7R and tyrosine kinase 2 (TYK2) [15], [16]. Although these are not specific to MS, with variations in HLA-DRB1 in particular linked to increased risk of developing other autoimmune conditions including rheumatoid arthritis and type 1 diabetes [17], [18]. More recently, genome-wide association studies have identified novel loci with links to disease susceptibility [19], [20], including classes of genes which function as part of the immune system, in particular those associated with T cell activation and proliferation [21]. Nevertheless these risk factors are not sufficient to cause MS on their own; merely convey susceptibility to the disease which can be triggered by an environmental factor or viral infection [22], [23], [24]. However any links between MS and viral or environmental factors remain inconclusive.

Vitamin D deficiency was originally linked to MS in 1974 as an explanation for the geographical distribution of disease, with a general increase in incidence correlating with increased latitude [25]. Therefore it was proposed that the higher prevalence of MS in those individuals further from the equator was due to reduced exposure to UVB radiation, the primary source of vitamin D. Previous studies have shown that people with a high intake or high serum levels of vitamin D are at lower risk of developing MS [26], [27]. Serum samples from MS patients contain lower levels of vitamin D than healthy individuals [28], [29].

Unhealthy lifestyles confer an increased risk of developing chronic diseases. Strong evidence has been obtained from previous studies which have associated cigarette smoking with development of MS [30], [31]. A recent meta-analysis of 14 previous studies that had investigated cigarette smoking as a potential risk factor for MS found that smoking increased MS susceptibility, with a risk ratio of 1.48 [32]. In addition, a large cohort study of 1465 MS patients carried out by researchers at Harvard University observed increased MS severity and disability status in smokers relative to non-smokers [33]. They also found that the rate of disease progression and T2 lesion

volume increased significantly faster compared to non-smokers, suggesting smoking not only increases MS susceptibility but also worsens disease progression if continued.

Of the potential viral infections thought to be risk factors for MS, Epstein-Barr virus (EBV) has been the most extensively studied, however its association with MS development remains inconclusive [22]. In support of EBV as a causative agent for MS, previous reports have observed an increased risk of MS in individuals with a history of glandular fever, an infection caused by EBV, with one meta-analysis of 14 studies concluding a risk factor or 2.3 [34]. High serum EBV-specific antibody titers have also been associated with increased MS susceptibility, and have been shown to precede disease onset by several years [35], [36]. Similarly, the risk of developing MS is reduced in EBV seronegative individuals relative to seropositive [37], [38].

Serum samples from many MS patients also contain increased prevalence and titers of antibodies against human herpes virus 6 (HHV-6) compared to healthy individuals [39], [40] , suggesting that HHV-6 may be implicated in MS aetiology. In addition to a potential role in MS onset, HHV-6 infection might also increase the risk of relapses, with HHV-6 antibody titer positively associated with periods of relapse [41]. However, as with EBV, the link between MS susceptibility and HHV-6 infection remains as yet unconfirmed. This lack of conclusive disease initiating factor makes MS so difficult to prevent.

1.1.3 MS Symptoms

There are a wide variety of symptoms associated with MS. However, as the symptoms are caused by axonal damage resulting in impaired action potentials, the location of the lesions within the CNS determines the nature of the symptoms. Therefore each patient will exhibit a unique repertoire of MS signs/symptoms, making the nature and severity of disease that each individual will suffer extremely unpredictable.

Amongst the most common issues that affect MS patients is fatigue, which is thought to occur in 80 % of cases. Other common symptoms include bladder dysfunction, with increased frequency of urination and incontinence. Numbness/tingling of the face and

body, particularly in the extremities, is often one of the first symptoms of MS. Visual problems can also occur first in many patients. It is caused by inflammation and lesions of the optic nerve which leads to blurred/double vision, nystagmus (involuntary eye movement) and potentially vision loss. Individuals with MS may also suffer speech problems such as slurring of words and a disjointed speech pattern, which can range from mild to severe.

Spasticity, increased muscle stiffness and spasms, occurs in around 60 % of patients with progressive disease, particularly in the legs. It is caused by excessive muscle contraction resulting from the loss of inhibition of motor neurons. Muscles can also become weak as a result of deconditioning and demyelination of nerve fibres. Spasticity and muscle weakness contribute to walking difficulties. Uncontrollable shaking of limbs, known as a tremor, is present in up to 50 % of MS patients. In addition, patients may also struggle with balance and coordination, with dizziness a common issue. Cognitive dysfunction affects approximately 50 % of MS patients, and can include problems with memory, concentration, information processing and reasoning. Patients can also suffer from emotional changes, including depression, stress, anxiety and mood swings. Previous studies have suggested that the incidence of depression is higher in individuals suffering from MS than in the general population [42], [43].

1.1.4 MS Subtypes

MS has been categorised into four different subtypes based on the course of disease progression. The most common is relapsing remitting MS (RRMS) which affects around 80-85 % of all MS patients. This subtype involves periods of relative disease latency which can last months or years interspersed with unpredictable bouts of symptoms which dissipate partially or completely. Relapse severity is variable, ranging from mild to severe, and usually continue for around 4-6 weeks although this is also variable between individuals. It is unclear what causes periods of relapse; however certain factors have been associated such as stress or infection.

Secondary progressive MS (SPMS) describes those patients whose condition deteriorates from RRMS such that there is no longer any periods of disease quiescence. Around 50-60 % of individuals with RRMS go on to develop SPMS after 10-15 years. If a patient never has any periods of disease inactivity following the initial onset of MS but instead suffers a steady decline in cognitive function and increase in symptom severity, they are described as having primary progressive MS (PPMS). In PPMS, patients usually initially present with mild symptoms which gradually worsen over time. It is typically diagnosed in older individuals (age 40-60) and, unlike the other forms of MS, it is equally as common between men and women. The final, and least common, subtype of MS is progressive relapsing (PRMS) in which the patient undergoes a continual decline in neurologic function but also suffers distinct spells of more severe attacks. Around 5 % of patients develop PRMS. Often they are initially diagnosed as having PPMS until they suffer an exacerbatory attack/relapse. The disease continues to gradually worsen between relapses.

1.1.5 MS Treatments and Drugs

At present there is no cure for MS. Current FDA-approved treatments are aimed at managing the condition by relieving symptoms and reducing the frequency/severity of relapses, allowing the patient to continue functioning and improving their quality of life. To date there are four beta-interferon (IFN-β) drugs used in MS. Two are type 1a interferons (IFN-β1a), Avonex and Rebif, and two are type 1b interferons (IFN-β1b), Betaseron and Extavia [44], [45]. The precise mechanism of action of these drugs in MS is not fully understood, but they are thought to work by reducing the inflammatory response and increasing regulatory effects. Known functions of IFN-β include decreasing antigen presentation, inhibiting Th1 cell proliferation and increasing IL-10 production [46]–[48] . These drugs reduce the rate of relapse by approximately one third in patients with RRMS. They also reduce the severity of relapses. Inflammatory lesions have been shown to be reduced by 50-80 % in MS patients treated with beta-interferons [49], [50], with improved quality of life and cognitive function also observed [51], [52].

Glatiramer acetate is a synthetic copolymer polypeptide mix consisting of random sequences of L-glutamic acid, L-lysine, L-alanine and L-tyrosine. It is prescribed as first-line treatment against RRMS in patients intolerable to the beta-interferons [44], reducing the frequency of relapses by between 30 – 75 % in different clinical trials [45], [53], as well as decreasing the onset of disability, progression from RRMS to SPMS, and development of new lesions[53]–[55]. Similar to the beta-interferons, the exact mechanism of action remains unknown. It is believed to compete with myelin basic protein (MBP) by binding MHC-II molecules, reducing the amount of myelin-specific T cells by downregulating autoantigen presentation [56].

Mitoxantrone is a synthetic anthracenedione antineoplastic agent originally used in the treatment of certain types of cancer, but is also used to treat RRMS and SPMS [44]. It is a type II topoisomerase inhibitor, disrupting DNA synthesis and repair [57], [58]. Mitoxantrone suppresses the activity and proliferation of T cells, B cells and macrophages, downregulates IFNγ, TNF-α and IL-2 secretion and induces apoptosis of B cells and monocytes/macrophages [57], [59], therefore substantially decreasing the immune response and thus reducing inflammation, demyelination and axonal damage. Clinical trials have shown that treatment with this drug can decrease the frequency of relapses and slow the onset of disability [60], [61].

Natalizumab, a second line MS treatment, is a recombinant humanized monoclonal antibody recommended for patients with RRMS. It binds the α4-chain of α4β1 integrin, also known as VLA-4, preventing binding of VLA-4 to the cell adhesion molecule VCAM-1 expressed on endothelial cells [62], [63]. Therefore Natalizumab decreases leukocyte transendothelial migration into the CNS. Patients who receive this treatment display reductions in rate of relapse, disability progression and lesion accumulation [64], [65]. However there have been reported cases of patients developing progressive multifocal leukoencephalopathy following treatment with this drug [66], highlighting the need for better, safer therapies to treat MS.

Fingolimod is another second line therapy for the treatment of RRMS. Unlike other MS drugs it is administered orally and functions as a sphingosine-1-phosphate (S1P) receptor modulator [44], [45]. T and B cell migration from lymph nodes and thymus is dependent on the S1P receptor [67]; therefore fingolimod prevents lymphocytes

egress from these tissues, reducing the amount of cells reaching the CNS. It significantly reduces the relapse rate of MS patients [68].

However, as mentioned above, none of the currently available treatments cure MS but are used to try and control the symptoms and episodes of relapse. In addition, many patients do not respond to these therapies and thus there is an essential requirement for further research into MS onset and pathogenesis in order to enable the development of more effective therapeutic strategies and, perhaps, a cure.

1.2 Experimental Autoimmune Encephalomyelitis

Experimental autoimmune encephalomyelitis (EAE) is the most commonly used animal model for studying MS, causing a demyelinating CNS inflammation similar to that seen in MS [69], [70]. This model was first used in 1933 by researchers at the Rockefeller Institute for Medical research - now The Rockefeller University [71]. Rivers *et al* originally sought to investigate a potential link between viral infections such as smallpox and measles, as well as vaccines for diseases like rabies, and subsequent paralysis in some patients. They had observed that the paralysis was caused by acute disseminated encephalomyelitis (ADEM) and perivascular demyelination, and thus EAE was not first established to examine MS, but instead to investigate ADEM.

Since then the model has been developed to include pathological and clinical features of MS including demyelination and axonal damage as well as relapsing and remitting episodes of paralysis, allowing researchers to study specific aspects of MS within individual models [72], [73]. It has also been induced in several different animal species and therefore EAE is considered a collection of animal models rather than simply one model.

1.2.1 Induction of EAE

Autoantigenic peptides derived from myelin, such as MBP or myelin oligodendrocyte glycoprotein (MOG) are commonly used as immunization agents to initiate EAE. Complete freunds adjuvant (CFA) is often included in the immunization to potentiate the immune response and induce a faster onset of disease. CFA is a solution of inactivated and dried *Mycobacterium tuberculosis* emulsified in mineral oil which was developed by Jules Freund. When used together with an initiating antigen only one injection is required to induce disease, compared to the multiple injections required by Rivers group in 1933 (as many as three injections a week per monkey for 7 months).

As well as this, Pertussis toxin (PTX) is often added to enhance EAE development. This toxin is believed to increase blood brain barrier (BBB) permeability, enabling immune cells to reach the CNS more readily [74], [75]. In addition, PTX may upregulate adhesion molecule expression to enhance CNS infiltration [76]. Studies have shown it can also increase expansion of antigen specific $CD4^+$ T cells (Th1 and Th2) via CNS and lymphoid-resident antigen presenting cells (APCs) [77]. EAE can be induced with distinct disease activity, and immunology and pathology characteristics depending on the antigen and animal being used. As mentioned above, EAE can be induced in a number of species including mice, rats, guinea pigs, rabbits and primates when immunised with different myelin proteins or peptides of these proteins.

The most commonly used animal species for EAE models is the mouse, with the first induction of EAE in mice reported in 1949 via immunization with brain homogenates emulsified in CFA [78]. This report also observed the differences in EAE susceptibility between different strains of mice, an important finding which would influence the subsequent development of different EAE models in different mouse strains with different initiating agents. For example, active EAE induction in SJL mice by immunization with myelin proteins or protein peptides (e.g. MBP or MOG) emulsified in CFA is characterized by a relapsing-remitting disease course, enabling the study of these stages of relapse which are indicative of RRMS, the most common form of the human disease. Researchers continue to develop unique variations of

mouse strain and immunizing agent combinations to elicit particular responses which represent different aspects of MS presentation and pathogenesis.

EAE can also be induced via adoptive transfer of autoreactive $CD4^+$ T cells as well as $CD8^+$ T cells specific to myelin protein [79], [80]. These cells are isolated from EAE mice immunized with myelin protein or peptide, stimulated *in vitro* with an encephalitogenic peptide and injected into naïve recipient mice. Adoptive transfer experiments allow for improved analysis of myelin-specific T cell function in EAE. More recently, spontaneous EAE models have been developed in transgenic C57BL/6 mice and SJL/J mice [81], [82]. These mice contain T cells expressing receptors specific for peptides MOG_{35-55} or MOG_{92-106} respectively, and will spontaneously develop EAE with either a chronic progressive (C57BL/6) or relapsing-remitting (SJL/J) disease course without the need for immunization or adoptive transfer which more closely represents MS onset.

This project will use C57BL/6 mice and transgenic MKP-2 KO mice which, upon induction of EAE with subcutaneous injection of MOG_{35-55} peptide emulsified in CFA together with intraperitoneal injection of PTX, typically suffer a monophasic disease course [83].

1.2.2 EAE as an Appropriate Model of MS

In the mouse model of EAE, there is a general progression of weakness and paralysis starting from the tail and working its way up to the hind-limbs, spine and fore-limbs. In terms of pathology, there are several aspects within EAE that make it a viable model of MS. This includes destruction of the myelin sheath; numerous disseminated CNS lesions, particularly in the brain stem and spinal cord; and the presence of immunoglobulin in the CNS and cerebrospinal fluid.

However EAE is not a perfect representation of MS. Firstly, the majority of EAE models are not spontaneous diseases; instead they require induction by myelin antigens or transfer of autoreactive T cells, whereas no definitive initiating autoantigen has been identified in MS. Furthermore, as mentioned earlier, immunisations often include

reagents to further enhance immune responses such as CFA, containing mycobacterium tuberculosis which initiates immune responses via several classes of pattern recognition receptors (PRRs) including Toll-like receptors (TLRs) 2, 4 and 9. Therefore immunisation with CFA, as well as PTX, may give a false or over-exaggerated example of the immune situation in MS. In spite of this, EAE provides a valuable research tool in CNS autoimmune diseases including MS. It has contributed to our knowledge and understanding of MS pathogenesis and has also led to the development of some of the clinically approved therapies mentioned earlier, such as Glatiramer and mitoxantrone [69].

1.2.3 MS and EAE Pathophysiology

The main pathophysiological aspects of MS are increased BBB permeability, the development of inflammatory and demyelinating lesions in the brain and spinal cord and oligodendrocyte loss (Fig 1.1). Many MS lesions are found in white matter close to ventricles of the cerebellum, brain stem, spinal cord and optic nerve [84]–[86]. However they can also develop in other areas of white matter as well as grey matter but to a lesser extent [86], [87]. At the early stages of disease a process known as remyelination can occur in which oligodendrocytes generate new myelin sheaths on demyelinated axons, allowing the axon to continue functioning. However as disease pathogenesis progresses, remyelination begins to fail as the extent of myelin damage becomes too severe, and oligodendrocyte numbers dwindle as a result of immune-mediated apoptosis.

The mechanisms which lead to increased BBB permeability are still not fully understood but this process is known to be a crucial step in disease development as it allows autoreactive myelin-specific T cells to enter the CNS via upregulation of adhesion molecules on the BBB vasculature and the relevant ligands (e.g. α4-integrin) on the cell surface. EAE pathophysiology is similar to that of MS, save for the initiating antigen. Myelin-specific T cells are primed in spleen and lymph nodes (the afferent compartment) by professional APCs which present antigen loaded onto an MHC molecule. These are recognized by T cell receptors (TCRs) on the surface of

the lymphocyte, along with costimulatory signals (CD80 and CD86 on APCs; CD28 on T cells). T cells then proliferate and differentiate into myelin antigen-specific $CD4^+$ and $CD8^+$ T cells.

These cells migrate from the afferent compartments and across the tight endothelial junctions of the BBB to the CNS. Here they are reactivated by local and infiltrating antigen presenting cells (APCs) presenting myelin fragments loaded onto MHC molecules. Activated autoreactive $CD4^+$ T cells release proinflammatory and cytotoxic mediators (e.g. IFNγ, TNF-α). This can induce further CNS infiltration by other immune cells and/or initiate inflammatory responses in both CNS resident cells and infiltrating phagocytes.

Inflammation leads to lesion development. These lesions contain activated $CD4^+$ and $CD8^+$ T cells, B cells, microglia/macrophages, dendritic cells (DCs) and astrocytes, which all contribute to demyelination and oligodendrocyte destruction, either via direct damage or production of inflammatory and cytotoxic mediators (e.g., IFNγ, TNF-α, and nitric oxide). However the exact role each cell plays in disease pathogenesis varies, with particular cell types capable of contrasting functions.

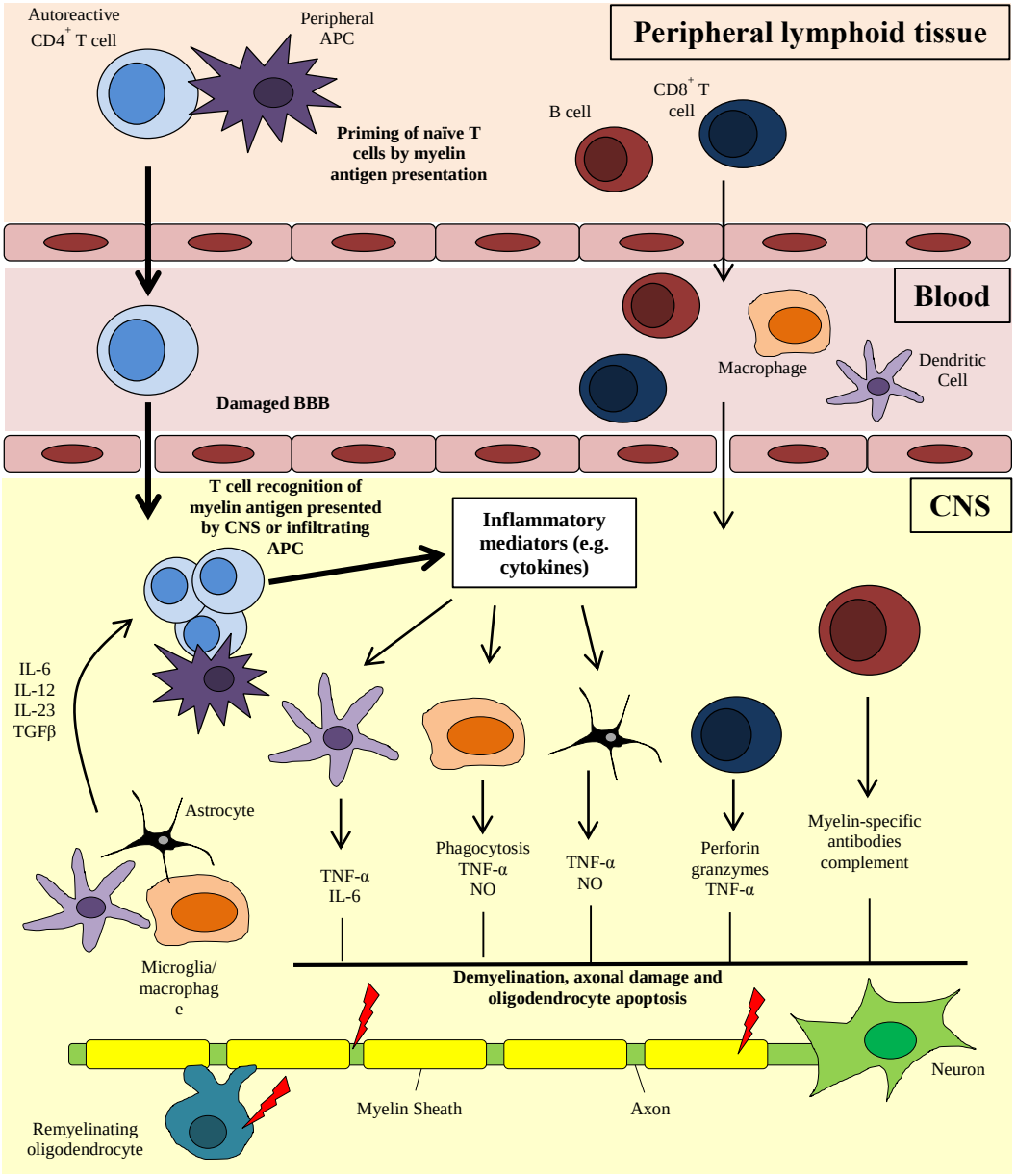

Figure 1.1: Schematic diagram displaying the key pathological features of MS/EAE pathogenesis. Autoreactive $CD4^+$ T helper cells are activated in peripheral lymphoid organs by APCs following immunisation with myelin proteins (EAE) or by a currently unknown mechanism such as a viral or bacterial trigger (MS). Activated $CD4^+$ T cells adhere to and then cross the damaged BBB endothelium via adhesion molecules. Following entry into the CNS, $CD4^+$ T cells are reactivated by local or infiltrating APC. Following reactivation, $CD4^+$ T cells release proinflammatory mediators which amplify local inflammation by activating resident microglia and astrocytes as well as other immune cells such as B cells, DCs, and macrophages. These cells produce cytokines which upregulate T cell differentiation. Demyelination, axonal damage and oligodendrocyte loss occur due to direct damage or production of inflammatory and cytotoxic mediators by activated immune cells. Red bolts indicate primary targets of immune damage.

1.2.3.1 $CD4^+$ T cells

MS/EAE is a complex autoimmune condition characterised by a multitude of effector functions exerted by numerous different cell types, however $CD4^+$ T cells are the key immune cells involved in disease initiation and progression. T cells are lymphocytes which are an essential part of the adaptive immune response. Lymphoid progenitor cells arise in the bone marrow and migrate to the thymus. The earliest thymocytes do not express CD4 or CD8 and are therefore classed as double-negative ($CD4^-CD8^-$) cells. As cells progress through their development, they become double-positive thymocytes ($CD4^+CD8^+$) before undergoing positive and negative selection and finally mature to single-positive ($CD4^+CD8^-$ or $CD4^-CD8^+$) thymocytes.

Thymocytes that interact with MHC molecules on cortical epithelial cells receive a survival signal. Those expressing TCRs specific for MHC-class-I differentiate into $CD8^+$ T cells, whereas those expressing TCRs specific for MHC-class-II ligands mature into $CD4^+$ T cells. Thymocytes that bind too strongly to self antigen presented on MHC complexes of medullary thymic epithelial cells are removed via apoptosis to prevent them exiting the thymus and entering general circulation. Remaining cells are then released from the thymus to peripheral tissues. Several different subsets exist based on their molecular phenotype and effector function.

$CD4^+$ T helper cells (Th cells) are activated following presentation of peptide antigen loaded onto MHC-II molecules on the surface of APCs, along with costimulatory signals via CD28-CD80/CD86 interactions. The primary function of these cells is in regulation of the immune system via their effects on other immune cells, including assisting in B cell maturation and activation of $CD8^+$ cytotoxic T cells and macrophages. $CD4^+$ T cells can differentiate into one of several subtypes, including Th1 cells, Th2 cells, Th9 cells, Th17 cells, Th22 cells or Tfh cells, which all have unique differentiation profiles, phenotypes and effector functions (Fig 1.2).

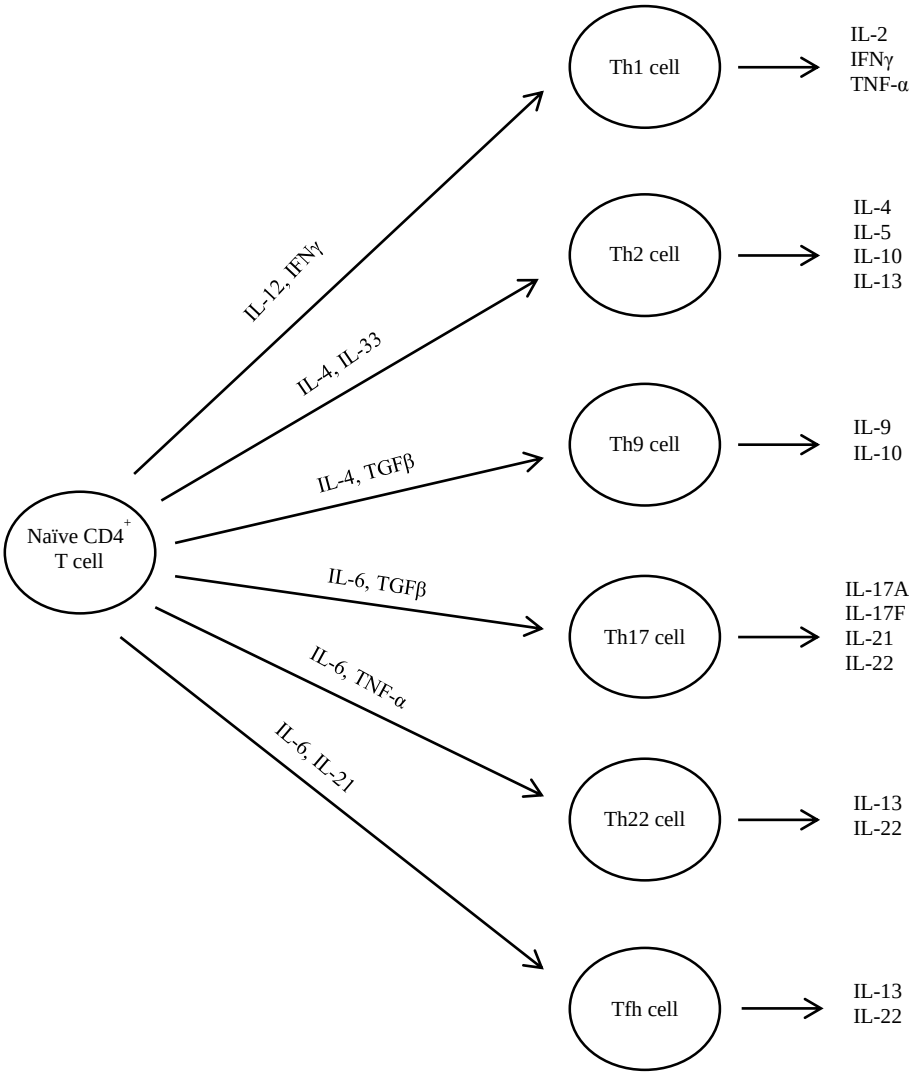

Figure 1.2: CD4$^+$ helper T cell subsets. Naïve CD4$^+$ T cells can differentiate into different T helper cell subsets depending on the cytokines present within the local environment. The specific stimulatory conditions influence transcription factor expression, which determines the differentiation program that the T cell will follow and thus the cytokines that it will subsequently produce.

Prior to the definitive identification of Th17 cells as a unique $CD4^+$ T cell subset, MS/EAE was considered a Th1-cell mediated disease. This was confirmed by adoptive transfer of myelin-specific $CD4^+$ Th1 cells into naïve mice which were sufficient to induce EAE whereas Th2 cells were not [88]. IFNγ is considered the archetypal Th1 cytokine and is produced in vast quantities by these cells. As IFNγ was detected in MS/EAE lesions [89], and treatment of MS patients with IFNγ enhanced disease severity [90], Th1 cells and IFNγ were considered to be the primary mediators of pathogenesis. However IFNγ and IFNγ receptor deficient mice were found to develop more severe EAE [91], [92]. Therefore it became apparent that although Th1 cells were essential in EAE, and IFNγ contributed to disease pathogenesis, this cytokine was not itself essential and thus other Th1 related cytokines were investigated.

As IL-12 is required for the differentiation of Th1 cells, EAE was induced in p35 and p40 deficient mice, the two protein subunits that compose IL-12. While IL-12p40 deficient mice were resistant to EAE, IL-12p35-deficient mice remained susceptible [93], [94]. The IL-12p40 chain is also a component of IL-23 along with the IL-23p19 subunit. IL-12p19 deletion conferred resistance to EAE [95], confirming the importance of IL-23 in EAE development.

IL-23 was subsequently shown to be essential for the development and expansion of a novel IL-17-producing $CD4^+$ T cell subset, Th17 cells [96], [97]. Adoptive transfer of Th17 cells into naïve mice could induce EAE [97], [98], thus establishing Th17 cells as mediators of EAE pathogenesis along with Th1 cells. The primary pathogenic function of $CD4^+$ T cells in MS/EAE is the production of cytokines (Fig 1.1) which can activate infiltrating peripheral immune cells as well as CNS resident cells involved in disease pathogenesis.

1.2.3.2 Regulatory T cells

In addition to Th cells, a specialized subset of $CD4^+$ T cells exist which function to maintain self-tolerance and immune homeostasis, known as regulatory T cells (Tregs). Natural Tregs (nTreg) develop within the thymus and are important in maintaining

immune homeostasis. In addition, inducible Tregs (iTreg) are differentiated from naïve conventional T cells (Tconv) in the periphery under certain conditions and play key roles in tolerance. Tregs suppress the effector functions of myelin-specific $CD4^+$ and $CD8^+$ T cells and thus are protective in MS/EAE. This has been confirmed by adoptive transfer of either purified Tregs, or Tregs isolated from EAE mice, which can reduce EAE severity in recipient animals associated with IL-10 production decreased CNS infiltration [99], [100]. A greater number of Tregs isolated from the peripheral tissue (spleen, lymph nodes) of EAE mice are required to decrease the severity and incidence of EAE compared to those collected from CNS tissue [100], suggesting these CNS-infiltrating Tregs have a stronger inhibitory effect.

Treg cell accumulation and frequency in the CNS positively correlates with EAE recovery, constituting as much as one third of the CNS $CD4^+$ T cell population during the recovery stage [100]. In addition, depletion of Treg cells using an anti-CD25 monoclonal antibody results in increased susceptibility to EAE [101], confirming the essential role these cells play in ameliorating disease severity and contributing to recovery.

1.2.3.3 $CD8^+$ T cells

The main function of $CD8^+$ cytotoxic T cells is direct killing of infected or cancerous cells mediated by secretion of perforin and granzymes which induce apoptosis of target cells. $CD8^+$ T cells are activated following recognition of peptide antigen loaded onto MHC-I molecules, which are present on the surface of all nucleated cells, along with costimulatory signals via CD28-CD80/CD86 interactions. $CD4^+$ T cells were initially thought to be almost entirely responsible for the pathogenesis of MS and EAE. However this disease paradigm was re-assessed following continued recognition of the presence of $CD8^+$ T cells within MS/EAE lesions and inflammatory infiltrates, particularly in close proximity to demyelinated axons [102], [103]. In fact, $CD8^+$ T cells predominate in MS lesions, with as many as 10-fold more $CD8^+$ compared to $CD4^+$ T cells [104], [105]. Furthermore, there is an increased frequency of clonally

expanded $CD8^+$ T cells in MS CSF samples [106], [107]. Axonal damage is positively correlated with the number of $CD8^+$ T cells [108], [109].

Depletion of $CD4^+$ T cells using a monoclonal anti-CD4 antibody in an MS clinical trial failed to reduce MS activity, with no changes in relapse rate or lesion development as assessed by monthly MRI [102]. In contrast, using anti-CD52 monoclonal antibody to deplete both $CD4^+$ and $CD8^+$ T cells reduced relapses and new lesion development [110], thus confirming the importance of $CD8^+$ T cells in MS/EAE pathogenesis. CNS resident cells, including astrocytes and microglia can express MHC-I molecules, particularly under inflammatory conditions, including within MS lesions [111] and thus can provide the means for $CD8^+$ T cell expansion and activation, along with peripheral APCs which have migrated into the CNS. The exact pathogenic mechanisms of $CD8^+$ T cells in MS/EAE have not yet been fully confirmed. Once activated, $CD8^+$ T cells can produce inflammatory mediators such as IFNγ, IL-17 and TNF-α which would contribute to the inflammatory response. Several studies have also highlighted the potential for $CD8^+$ T cells to further contribute to tissue damage by directly targeting oligodendrocytes, astrocytes and axons/neurons [112]–[114].

1.2.3.4 NK/NKT cells

Protective roles have been attributed to both Natural Killer (NK) cells and Natural Killer T (NKT) cells in EAE. NK cells are innate lymphoid cells essential in the innate immune response. Their main functions include perforin and granzyme-mediated apoptosis of infected cells and cytokine production (e.g. IFNγ, IL-17, and TNF-α). NKT cells are a small subset of T cells that, unlike conventional T cells, recognize antigen presented via CD1d on the surface of APCs. Once activated, these cells can produce cytokines (e.g. IFNγ, IL-2, IL-4 and IL-17) and directly kill infected cells. The addition of anti-NK cell antibodies worsens disease severity [115] while enhancing NK cell activity using the drug Linomide restricts EAE development [116], both of which strongly suggest NK cells are involved in disease suppression. The addition of spleen-derived NKT cells to C57BL/6 TCR knockout mice by adoptive

transfer can induce recovery from passive EAE [117] thus NKT cells may also be protective.

1.2.3.5 B cells

B cells are key lymphocytes involved in the humoral immune aspect of the adaptive immune system. B-cell development occurs within the bone marrow and peripheral lymphoid tissues (e.g. spleen). In the bone marrow, development progresses through the pro-B-cell, pre-B-cell and immature-B-cell stages. Each stage represents rearrangements at the immunoglobulin locus resulting in the generation and surface expression of the pre-B-cell receptor (pre-BCR) and finally a mature BCR which is capable of binding antigen. At this stage of development, B cells undergo positive and negative selection to prevent the development of self-reactive cells which are removed by clonal deletion. Surviving cells leave the bone marrow as immature B cells, eventually maturing into mature naive B cells. Following an immune response and subsequent B cell activation, antigen-specific B cells differentiate into either plasma B cells, which secrete large amounts of antibody, or memory B cells which are essential in developing a more rapid immune response upon re-infection.

Contrasting roles have been reported for B cells in EAE/MS pathogenesis. The presence of oligoclonal bands of Immunoglobulin (Ig) in CSF and the deposition of Ig and complement activation products in MS lesions clearly indicate the involvement of B cells in MS pathology [118]–[121]. In a phase II clinical trial, treating RRMS patients with rituximab, a monoclonal antibody which depletes B cells by specifically targeting CD20, resulted in reduced lesion development and reduced the rate of relapse by 50 % [122]. This suggests B cells are involved in the pathogenic response of MS. In EAE studies, B cells are shown to produce antigen-specific autoantibodies which contribute to inflammation and demyelination, enhancing the severity of EAE pathogenesis [123]. Although some studies have shown that B cells promote the induction of EAE via facilitating antigen presentation to myelin-specific T cells [124], similar EAE onset and clinical sign development in B cell deficient mice when

compared with WT counterparts suggest that B cells are not required for the initial activation of autoreactive T cells [125].

In contrast, B cells can also be beneficial in EAE recovery as other studies have shown that in the absence of B cells, EAE mice do not begin to recover, instead continuing to display high clinical severity [126]. This is due to a lack of IL-10 producing B cells which are required for EAE remission. B cell-derived IL-10 contributes to the amelioration of EAE pathogenesis by downregulating Th1 responses [127]. Therefore current research evidence suggests that B cells are capable of contrasting functions in EAE which may be due to the presence of unique B cell subsets or the stage of disease pathogenesis.

1.2.3.6 Dendritic Cells

DCs are innate immune cells derived from hematopoietic bone marrow progenitor cells and act as professional APCs. Their main function is to process antigenic material, and present it on the cell surface to T cells. Therefore they are considered to be an essential link between the innate and adaptive immune responses. Immature DCs express a large repertoire of phagocytic receptors with high endocytic activity and low T-cell activation potential. Upon phagocytosis of a foreign pathogen they become activated into mature DCs. The antigen is transported to lysosomes where it is degraded into peptide epitopes. The fragments are then loaded onto MHC molecules before translocation to the plasma membrane to be displayed on the cell surface which allows presentation to, and activation of, T cells. Mature DCs also upregulate expression of the co-receptors CD80, CD86 and CD40 required for T cell activation. DCs are divided into two main groups. Firstly, the conventional myeloid-derived DCs (mDCs) which can be further subdivided into mDC-1 and the extremely rare m-DC2. The second group comprises the lymphoid-derived plasmacytoid DCs (pDCs). This report will focus on mDCs unless otherwise stated.

Adoptive transfer of DCs pulsed with MOG_{35-55} peptide, with or without accompanying PTX and CFA injections, into naïve C57BL/6 mice can induce EAE [128], confirming DCs as key antigen presenting cells involved in the initiation of EAE

via activation of myelin-specific T cells. Once the autoreactive T cells have migrated into the CNS during EAE/MS, they require reactivation to exert effector functions which induce disease pathogenesis. DCs have been shown to be present in increased numbers within regions of CNS inflammation during EAE development, particularly in the meninges and perivascular infiltrate, appearing just before disease onset [129]. Therefore in addition to resident APCs which can present endogenous myelin peptides to T cells, DCs are also involved in this [130]. Another important facet of DC functioning that contributes to EAE pathogenesis is the production and release of inflammatory mediators such as TNF-α, IL-6 and IL-1β which can contribute to inflammation and axonal damage, as well as IL-12 and IL-23 which promote Th1 and Th17 differentiation respectively [130].

In contrast, another subtype of DCs distinct from myeloid DCs, plasmacytoid dendritic cells (pDCs), can contribute to resolution of EAE. Within the CNS these cells are inefficient in antigen presentation to T cells [130], yet constitute over 5 % of the total mononuclear cell population in EAE and make up over one third of all CNS infiltrating DCs [130], [131], suggesting the potential for an important function. Specific pDC depletion at the onset of EAE, as well as during the relapse phase, significantly enhances clinical severity [131]. This was associated with enhanced $CD4^+$ T cell activation and IL-17 and IFNγ production in the CNS. In addition, CNS myeloid DC production of IL-17, IFNγ and IL-10 is suppressed by CNS pDCs in cocultures with CNS-isolated $CD4^+$ T cells [131].

1.2.3.7 Macrophages/microglia

Macrophages are key cells involved in the early immune response as well as initiating adaptive immune responses. Most tissues within the body contain tissue-resident macrophages which are derived from yolk sac erythro-myeloid progenitors in the embryo [132]. Circulating macrophages are derived from bone marrow myeloid progenitor cells. Upon tissue damage or infection, monocytes are rapidly recruited from the circulation to the tissue, where they differentiate into macrophages. The main

function of macrophages is phagocytosis of apoptotic cells and pathogens and presentation of antigen to T cells via MHC molecules.

Macrophages are involved in the development of MS and EAE, although both detrimental and protective effects have been reported. Depletion of macrophages by injection of dichloromethylene diphosphonate liposomes just prior to onset of clinical signs of disease decreases the severity of EAE, confirming a pathogenic role of macrophages in EAE [133]. This effect is seen when using liposomes which can cross the BBB due to the addition of mannose in the lipid layers but not when liposomes cannot enter the CNS, confirming the main pathogenic responses of macrophages are exerted within the CNS. CNI-1493 (now known as semapimod) is an inhibitor of inflammatory responses in macrophages, suppressing production of inflammatory cytokines (TNF-α, IL-6, IL-1β) and NO. Administration of this compound significantly reduces EAE severity [134], providing further confirmation that macrophages contribute to the pathogenic response of EAE.

Microglia are a type of glial cell, and the resident macrophages of the CNS. They are the primary immune cell of the CNS and, as with macrophages, their main function is phagocytosis of cellular debris and pathogenic material and antigen presentation via MHC molecules. Selective paralysis of microglial cells using CD11b-herpes simplex virus thymidine kinase (HSVTK) transgenic mice and systemic Ganciclovir treatment prevents activation of these cells, resulting in the inability of microglia to produce inflammatory mediators include cytokines, chemokines and NO [135]. EAE clinical severity and CNS inflammation are substantially reduced in these mice, confirming the importance of CNS-resident microglial cells in the pathogenesis of EAE. Macrophages and microglia are also important in re-activation of autoreactive T cells within the CNS during EAE via antigen presentation, with upregulated MHC-II expression observed in EAE [136].

Similar to B cells, the dual roles of macrophage and microglia cells in MS and EAE development may be due to the presence of unique phenotypes. Classically activated macrophages (M1) produce nitric oxide (NO) and inflammatory cytokines such as TNF-α, IL-6, IL-1β which can contribute to inflammation and axonal damage. Whereas alternatively activated macrophages (M2) produce arginase and IL-10 while

downregulating production of NO and M1 macrophages and thus can aid in recovery. Therefore it is hypothesised that M1 macrophages are responsible for the deleterious functions in MS/EAE while M2 macrophages convey protection.

In support of this hypothesis, using a rat model of relapsing EAE it has been shown that M2 macrophage frequency decreases during relapse whereas the percentage of M1 macrophages remains unchanged, suggesting an inhibition of M2 macrophages promotes relapse [137]. Administration of M2-polarized macrophages into EAE mice after the onset of clinical disease significantly ameliorated disease severity, with reduced macrophage/microglia activation within the CNS [137]. In addition, treating mice with M2 macrophages before MOG immunization decreases EAE severity and increases IL-10 production while treatment with M1 macrophages does not alter EAE development [138].

Microglia/macrophages can also aid in recovery by removing tissue debris via phagocytosis of degraded myelin products within active inflammatory lesions [139]. This is an essential step in EAE recovery as myelin debris can inhibit axonal regeneration and oligodendrocyte precursor cell differentiation, preventing remyelination [140].

1.2.3.8 Astrocytes

As well as microglia, other CNS-resident glial cells are also involved in MS/EAE pathogenesis, including astrocytes. These are the most abundant cells within the human brain and perform a variety of functions including the uptake and release of neural transmitters, maintenance of the BBB, and nutrient support for neurons as well as immune effector functions. Activated astrocytes are detected in both MS and EAE lesions [141], [142] and in EAE have been associated with axonal damage before T cell infiltration [143]. In response to CNS injury/disease, astrocytes undergo reactive astrogliosis, characterized by a variety of functional, molecular, biochemical and morphological changes. The transcription factor NF-κB regulates many of these processes that occur in activated astrocytes. In a transgenic model in which NF-κB is inactivated specifically in astrocytes, EAE severity is markedly reduced with

decreased pro-inflammatory gene expression within the CNS and decreased adhesion molecule expression [144]. There is also an improvement in clinical recovery when astrocyte function is suppressed, associated with reduced immune cell infiltration at the later stages of EAE (not associated with increased BBB permeability) as well as higher myelin compaction (better quality of myelin) and increased remyelination [145]. Furthermore, astrocytes can secrete cytokines such as IL-12 and IL-23 which promotes differentiation of Th1 and Th17 cells respectively [146]. In addition, astrocytes produce inflammatory mediators such as NO and TNF-α, contributing to increased inflammation, demyelination and oligodendrocyte apoptosis [147]. They can also function as APCs to reactivate T cells [146].

Astrocytes also have the potential to contribute to EAE protection and recovery. Astrocytic perivascular endfeet are associated with the basal lamina of blood vessels, forming part of the BBB and providing a cellular link to neurons. Damage to these perivascular astrocytes, which has been observed in MS/EAE [141], can contribute to the increase in BBB permeability and thus increased immune cell infiltration. They produce chemoattractants which induce migration of oligodendrocyte precursor cells (OPCs) from the brain parenchyma towards the site of inflammation/demyelination, enhancing remyelination [144]. In cocultures with microglia, upon stimulation with LPS and/or IFNγ they inhibit the production of IL-12 by microglia which would reduce Th1 responses [148]. Astrocytes can also secrete IL-27 [149], an IL-12 family cytokine that suppresses Th17 cell development and IL-6-mediated T cell proliferation [150], [151]. IL-27 receptor-deficient mice are more susceptible to EAE as a result of these functions being inhibited [152].

1.2.3.9 Oligodendrocytes

Oligodendrocytes are glial cells which produce the myelin that surrounds and insulates axons of the CNS. The differentiation of oligodendrocyte progenitor cells (OPCs) within the CNS gives rise to oligodendrocytes. The myelin sheath increases conduction velocity of axonal action potentials [3]. In MS and EAE lesions, oligodendrocyte apoptosis is a key aspect of disease pathogenesis [153]. It is caused

by immune and CNS-resident cells, including lymphocytes and microglia, producing mediators such as TNF-α, IFNγ, perforin, granzymes and reactive oxygen species which can induce apoptosis and necrosis of oligodendrocytes [154]–[156]. In addition, direct cell contact via the death receptor Fas can induce oligodendrocyte death following stimulation with FasL [154].

Oligodendrocytes can aid in EAE/MS recovery by providing a new, but thinner, myelin sheath to axons which have undergone demyelination, leading to functional recovery by allowing the restoration of action potentials. Therefore oligodendrocyte death prevents efficient remyelination of exposed axons during recovery from a relapse attack.

1.3 MAP Kinase signalling

Mitogen-activated protein kinases (MAPKs) are enzymes that have a critical role in signal transduction pathways involved in cellular responses initiated by extracellular stimuli (such as growth factors or chemical and physical stress). Therefore MAPKs can regulate functions such as cell survival, proliferation, differentiation and gene transcription [157], [158]. There are three main groups of MAPKs: the extracellular signal-regulated kinases (ERK-1/ERK-2), the c-Jun N-terminal kinases (JNK-1/2/3) and the p38 MAPK proteins (p38-α/β/γ/δ). There are also other, less well-defined MAPK pathways such as ERK5 and ERK7/8, however these remain poorly characterised.

MAPK activity is regulated through a signalling cascade (Fig 1.3). This cascade is initiated by small GTP-binding proteins or by adaptor proteins that transmit an activatory signal to MAPK kinase kinases (MAPKKK; also known as MEKKs). These subsequently activate the MAPK kinases (MAPKK/MEKs) by phosphorylation which in turn phosphorylate, and thus activate, MAPKs. MAPK phosphorylation is achieved through dual phosphorylation of threonine and tyrosine residues. Once activated, MAPKs phosphorylate their respective targets, including transcription factors and

effector kinases (e.g. p53, c-myc, NFAT) which result in altered gene expression and cell physiology.

The MAPK pathway is a very intricate signalling cascade, with various stimuli and receptors initiating the events which lead to kinase activation. In addition, some MAPKKs which activate the MAPKs are not specific to one substrate: MEK1 and MEK2 activate ERK1/2, MKK3 and MKK6 activate p38 and MKK7 specifically activates JNK however MKK4 is associated with JNK-1/2/3 as well as p38. Activation of the MAPKKs by MAPKKKs can also initiate different cascades (e.g. ASK1). Therefore, due to the severe complexity of signalling in this pathway, several mechanisms exist that regulate specificity in MAPK activation. Scaffold proteins interact with MAPKKs and their relevant MAPKs, organising them into a specific signalling module. JNK-interacting protein 1 (JIP1) brings together MKK7 and JNK1/2 as well as the MAPKKK, MLK1 [159]. Another scaffold protein, MEK partner 1 (MP1), is involved in ERK1 activation through interactions with MEK1 and ERK1 [160].

An additional mechanism to regulate activity of the MAPKs is in the ability of MAPKs to indirectly create both positive and negative feedback loops to control signalling. This is achieved by regulating the expression of agonists and antagonists of receptors mediating the relevant MAPK signalling pathway.

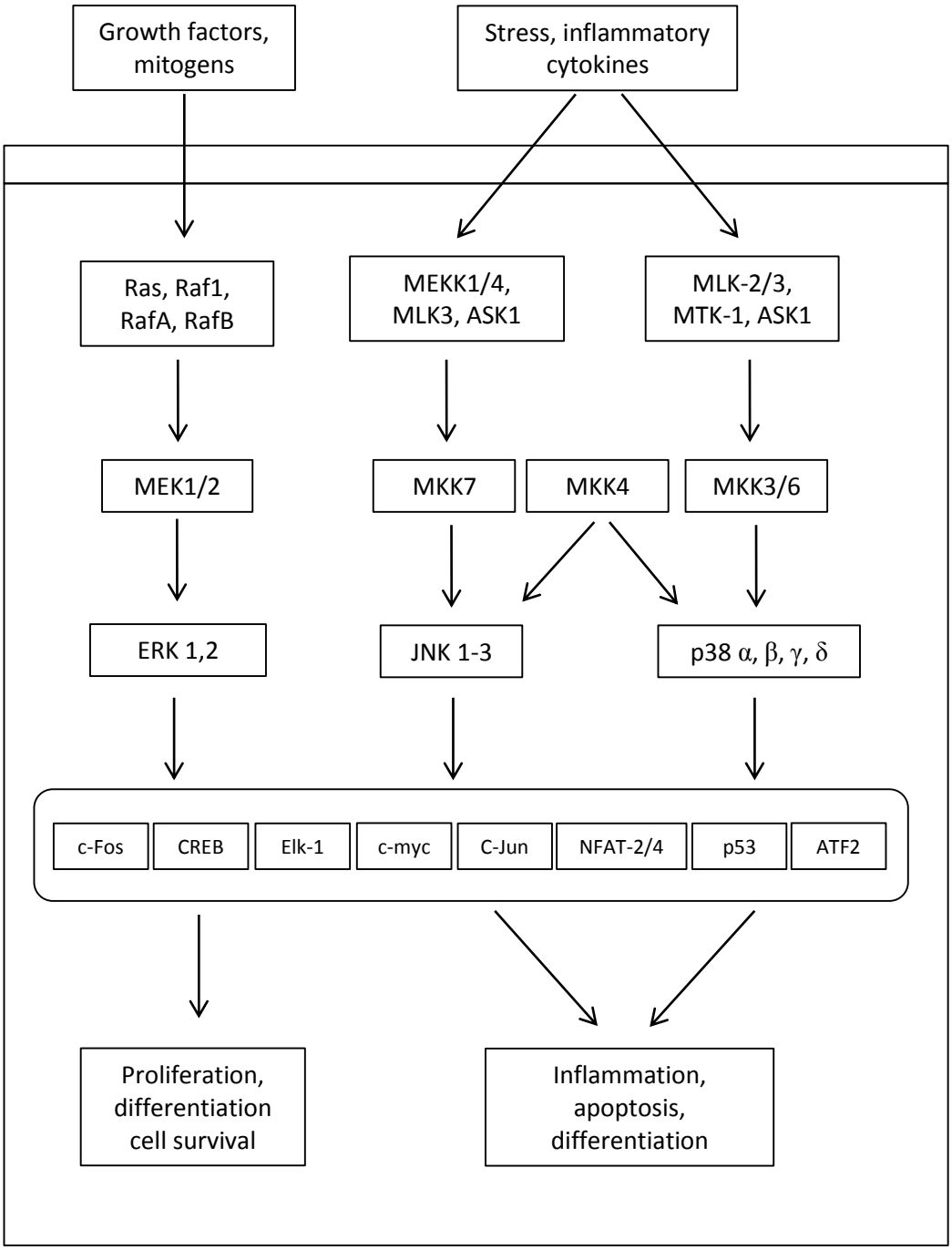

Figure 1.3: Simplified schematic diagram of the ERK, JNK and p38 MAPK signalling pathways. The MAPKs are activated by dual phosphorylation of the threonine and tyrosine residues within a conserved 'TXY' motif following a three-tiered kinase cascade consisting of a MAPK kinase kinase (e.g. Raf, MEKK1, ASK1), MAPK kinase (e.g. MEK1, MKK3-7) and then the MAPKs (ERK, JNK, p38). Once activated, MAPKs can phosphorylate their transcription factor and effector kinase targets (e.g. Elk1, c-Jun, p53) to induce a variety of cellular responses such as cytokine production, apoptosis, proliferation and differentiation.

1.3.1 Extracellular Signal-Regulated Kinases (ERK)

The ERK family were the first MAPKs to be discovered [161] and are the best characterized to date. Several isoforms exist [162], however the majority of research has focused on ERK1 and ERK2. Signalling is initiated predominantly by growth factors binding cell-surface tyrosine kinase receptors or cytokines/chemokines binding G-coupled receptors resulting in activation of the GTPase Ras, via the Grb2/Sos complex [158]. Ras, which has three isoforms (H-Ras, N-Ras and K-Ras), specifically phosphorylates and activates Raf which itself has three unique isoforms (Raf-A, Raf-B and Raf-C). Raf is a MAPKKK which subsequently phosphorylates its MAPKK target, either MEK1 or MEK2 [157], [158]. ERK1/ERK2 can then be activated by dual phosphorylation of threonine and tyrosine residues within a threonine-glutamic acid-tyrosine motif [163]. Once phosphorylated, ERK1/ERK2 can activate several downstream targets including transcription factors and protein kinases. This gives ERK the ability to modulate the transcription of genes involved in cellular proliferation [164] as well as cell survival by preventing apoptosis [165], [166].

1.3.2 c-Jun N-terminal Kinases (JNK)

This particular MAPK signalling cascade is part of the stress-activated MAPKs, as the primary initiating factor that stimulates JNK signalling is chemical or mechanical stress. There are three JNK isoforms (JNK1, JNK2 and JNK3) [167], [168] which can be further subdivided into 10 different splice variants (four JNK1, four JNK2 and two JNK3 variants) [169]. JNK1 and JNK2 are expressed in all cell types and tissue whereas JNK3 expression is limited primarily to the brain [169]. As stated above, JNK signalling is activated in response to stress stimuli, including inflammatory cytokines and ultraviolet radiation. This leads to activation of JNK-associated MAPKKKs (e.g. MEKK1, MEKK4 and ASK1) which phosphorylate and activate MKK4 / MKK7 [170], [171]. The now activated MAPKKs are able to phosphorylate JNK1 / JNK2 by dual phosphorylation of threonine and tyrosine residues within a threonine-proline-tyrosine motif found in kinase domain VIII [172]. Active JNKs have a number of downstream substrates which can be specific to different cell types

or the stimulus involved. These include constituents of activator protein 1 (AP-1), Elk1, c-myc and Histone H2AX. Previous studies have shown that JNK can be both pro- and anti-apoptotic [173], [174] as well as being involved in cell migration [175], differentiation [176], [177] and inflammatory gene production [178], [179].

1.3.3 p38 MAPK proteins

Like JNK, the p38 signalling cascade is activated by various stress stimuli and growth factors, thus p38 is also known as a stress-activated MAPK. Four isoforms exist (p38-α, β, γ and δ) [180]–[182] which are expressed in different regions of the body and at different levels depending on the cell type and stimuli involved [183]. Initiation of the p38 signalling module by the relevant stimuli activates MAPKKKs involved in this pathway (e.g. MLK3, DLK1 and ASK1) which phosphorylate the p38-specific MAPKKs MKK3 and MKK6 [184], as well as MKK4 which can interact with both JNK and p38 [185], [186]. These MAPKKs can then activate p38 by dual phosphorylation of threonine and tyrosine residues within the activation loop sequence threonine-glycine-tyrosine [183]. Active p38 MAPK can increase mRNA stability [187], induce chemotaxis [188], [189] and, like JNK, regulates cell differentiation [190], [191] and inflammatory gene production [192], [193] via downstream targets such as p53 and ATF2.

1.4 MAPK Phosphatase Overview

Mitogen activated protein kinase phosphatases (MKPs) are a subgroup of the larger family of dual-specificity protein phosphatases (DUSPs). Their function is to regulate MAPK signalling by dephosphorylation. MKP's remove phosphate groups from phosphotyrosine and phosphothreonine residues within the T-X-Y activation site of MAPKs, thereby deactivating them [194]. All MKPs share a common structure, with a C-terminal catalytic domain and an N-terminal domain which is important in MAPK substrate recognition and binding as it contains clusters of positively-charged amino–acid residues [195], [196]. Also, all MKPs comprise two cdc25 homology domains

(CH2A and CH2B) within the N-terminus [194] while the catalytic domain (PTP domain) can be found on the C-terminus.

There are 10 active MKP enzymes and one inactive protein (MK-STYX) which lacks the active site cysteine, instead containing a naturally occurring glycine residue [197]. The 10 active MKP's can be further subcategorized into three groups according to their subcellular location, substrate specificity, gene structure and sequence homology [198]. Group one comprises MKP-1/DUSP1, PAC-1/DUSP2, MKP-2/DUSP4 and DUSP5/hVH3 which are all inducible and found within the nucleus. The second group is made up of MKP-3/DUSP6, MKP-4/DUSP9 and MKP-X/DUSP7 which are constitutively expressed in the cytoplasm because they contain nuclear export sequences (NES). This group is ERK-specific. The final group of MKPs (MKP-5/DUSP10, MKP-7/DUSP16 and hVH5/DUSP8) are categorised based on their selective targeting of the stress-activated MAPK, JNK and p38, and can be expressed in both the nucleus and cytoplasm.

1.4.1 MKP-1

Mitogen activated protein kinase phosphatase 1 (MKP-1 / DUSP1) was the first of the MKP family to be discovered in 1985 [199]. It was originally identified as an immediate-early gene, induced by serum growth factors, in a BALB/c cDNA library and was termed 3CH134. The corresponding human cDNA was isolated and characterized in 1992 as CL100, a stress-inducible tyrosine phosphatase with sequence similarity to the dual specificity phosphatase of vaccinia virus, VH1 [200].

The name MKP-1 was later proposed for 3CH134/CL100 upon recognition of its dual dephosphorylation activity towards phosphotyrosine and phosphothreonine residues of ERK [201]. It is located within the nucleus [202] and can be induced as an early gene by a variety of stimuli such as growth factors, cytokines, bacterial toxins and physical or chemical stress. MKP-1 is ubiquitously expressed and was originally thought to specifically dephosphorylate ERK [201], [203]. However subsequent reports successfully demonstrated substrate specificity is varied between different cell

types, with dephosphorylation activity towards p38 and/or JNK over ERK observed in cells such as macrophages and mouse embryonic fibroblasts (MEFs) [204], [205].

MKP-1 is important in cell survival as MAPK-mediated apoptosis is decreased in MKP-1 KO MEFs [204]. In human breast cancer cells, MKP-1 mediates reductions in cell proliferation via ERK phosphorylation [206]. MKP-1 has also been shown to be involved in regulating the production of several immune mediators using cell stimulation experiments, with MKP-1 either overexpressed or deleted in macrophages and DCs. From these studies, MKP-1 appears to negatively regulate the production of the inflammatory cytokines TNF-α, IL-6, IL-1β and the anti-inflammatory IL-10 [207]–[209]. In addition, chemokine production is also enhanced in MKP-1 deficient cells, including CCL2-CCL4 and CXCL2 [210]–[212] as well as other inflammatory mediators such as iNOS [213], [214] and COX-2 [215]. Increased immune responses are also seen in MKP-1 deficient mice when LPS is administered systemically [210], [211]. MKP-1 can be detrimental in disease conditions such as *Leishmania major* (*L.major*), with inhibition of MKP-1 resulting in reduced parasite load [216]. Furthermore, MKP-1 is crucial for T cell activation, proliferation and function [217]. As a result of this, MKP-1 deficient mice are less susceptible to EAE and do not mount an effective immune response to influenza viral infection.

1.4.2 MKP-2

Mitogen activated protein kinase phosphatase 2 (MKP-2 / DUSP4) was first characterised in 1995 as an inducible MKP expressed in a wide range of tissues and cells [218]. MKP-2 is synthesized as an immediate early gene in response to many of the same stimuli that activate the MAPKs. It is found exclusively within the nucleus as a result of two nuclear localisation sequences (NLSs), however only one of these NLSs is required for nuclear localisation of MKP-2, therefore if one is damaged it can still be targeted to the nucleus [219]. Mutations in both NLSs do not prevent MKP-2 interacting with and dephosphorylating JNK, suggesting NLS-1 and NLS-2 are not involved in these processes in relation to JNK [219]. However it appears that NLS-1 is required for MKP-2 interactions with the other MAPKs as it is contained within a

sequence at the N-terminus of the enzyme, which is responsible for its interactions with ERK and p38 [220].

An alternative splice variant of MKP-2 (known as MKP-2-S) has recently been identified with several differences in function, cellular location and substrate specificity relative to the previously known form (MKP-2-L). This variant form arises from alternative initiating codons on exons 1 and 3 [221]. It still contains the phosphatase catalytic domain but lacks the MAPK binding site. MKP-2 is ubiquitously expressed, and originally displayed dephosphorylation specificity towards JNK and ERK *in vitro*, but was also found to bind p38 without dephosphorylating this MAPK [220]. However several functional studies have confirmed that, *in vivo*, substrate specificity varies, with MKP-2 able to regulate ERK, JNK and p38 depending on the cell type.

MKP-2 reduces stress-induced cellular apoptosis in HEK 293 cells by dephosphorylating JNK, but not ERK or p38 [222] In addition, MKP-2 protects against apoptosis in human endothelial cells as a result of specific regulation of JNK, again with no effect on ERK or p38 activity [223]. Conversely, MKP-2 is a mediator of cell death in the E2F-1 pathway via selective regulation of ERK activity [224]. These results suggest that MKP-2 is involved in cellular apoptosis by means of MAPK dephosphorylation; however its exact role appears to be dependent on the cell type involved. This is further confirmed when analysing the role of MKP-2 in the regulation of cellular proliferation. MKP-2 deficient mouse fibroblasts and macrophages show a significant reduction in proliferation relative to WT counterparts due to a greater amount of cells accumulating in the G2/M phase [225]. This was attributed to an increase in cyclin B1 expression and cdc2 phosphorylation. In contrast to this, a previous study which used MKP-2 knockdown mouse tumour cells demonstrated that the arrest of cells in G2/M phase was mediated by an abrogation in cyclin B1 expression and cdc2 kinase activity [226]. MKP-2 has previously been linked to colorectal cancer, in which MKP-2 may potentially function as a tumour suppressor. MKP-2 expression is negatively correlated with T classification (the size of the primary tumour), lymphatic and vascular invasion, increasing stages of cancer (I-IV) and liver and lung metastases [227].

Further studies utilising KO mice have demonstrated that MKP-2 has the ability to modulate immune responses in a variety of conditions. MKP-2 deficient mice display a greater susceptibility to *Leishmania Mexicana* (*L.mexicana*) infection with increased lesion size and parasite burden [228]. This is due to significantly upregulated Th2 responses in MKP-2 deficient mice when the parasite is injected into the rump, including increased antigen specific serum IgG1 levels and splenocyte IL-4 and IL-13 production, without affecting Th1 responses. In contrast, when *L.mexicana* is administered into the footpad, the increased severity is the result of significantly downregulated Th1 responses (specific IgG2a and IFNγ production) with no alteration in Th2 responses. This is in part due to the differences in immune control of *L.mexicana* infection at different injection sites. In the footpad, the non-healing response to *L.mexicana* is primarily associated with deficient IFNγ production, whereas in the rump the response is Th2 dependent [229].

Furthermore, MKP-2 deficient mice are more susceptible to *Toxoplasma gondii* (*T.gondii*) infection, with increased mortality rates and parasite burden [230]. However, unlike with *L.mexicana* infection, T cell responses were unchanged in the absence of MKP-2. Instead, following *T.gondii* infection, MKP-2 deficient mice have reduced NO levels but increased splenic arginase-1 expression. MKP-2 KO macrophages are also more susceptible to *L.major* infection [231]; however the course of infection in the mice is not altered by MKP-2 deletion, with comparable lesion sizes and parasite burdens between WT and KO.

Cornell et al have further shown, using KO models, that MKP-2 regulates the inflammatory response in acute lung injury (ALI) [232] and sepsis [233]. In a model of ALI, MKP-2 deficient mice develop an attenuated early inflammatory response, with reduced production of inflammatory mediators in BAL fluid (TNFα, MIP-1α) and decreased lung neutrophil infiltration. MKP-2 deficient mice also mount a decreased inflammatory response to endotoxin challenge as a model of sepsis, with decreased serum TNF-α, IL-6 and IL-1β and display improved survival rates.

1.4.3 MKP-3

Mitogen activated protein kinase phosphatase 3 (MKP-3 / DUSP6) is constitutively expressed within the cytoplasm and preferentially targets ERK [234]. It is highly expressed in various tissues, with highest levels in heart, brain, spleen, liver and kidney. MKP-3 has mostly been studied in the context of cancer and whether it could have a protective role. It has been shown to be inactivated in various types of cancers. A recent study demonstrated that MKP-3 can regulate ERK in adenocarcinoma progression via negative feedback, and thus may be able to suppress tumour development [235]. In addition, MKP-3 has similar anti-tumour effects in non-small-cell lung cancers, again by negative regulation of ERK [236]. MKP-3 is also involved in regulating cell proliferation via its control of ERK activity as shown in corneal epithelial cells [237] and epididymal cells [238]. In an immune context, MKP-3 can protect against *L.major* infection [216]. The addition of a lentiviral vector that overexpresses MKP-3 to *L.major* infected mice increases parasite clearance and reduces parasite load. MKP-3 is a negative regulator of platelet-derived growth factor-induced chemotaxis in the fibroblast cell line NIH3T3 [239].

By blocking MKP-3 expression in oligodendrocytes, alpha-amino-3-hydroxy-5-methylisoxazole-4-propionic acid (AMPA) receptor-induced cell death is significantly reduced [240]. This suggests MKP-3 may be involved in oligodendrocyte death via regulation of ERK activity, and could therefore play a role in MS / EAE pathogenesis by reducing the amount of oligodendrocytes available for remyelination. MKP-3 is also important in regulating ERK and p38 activity in spinal cord microglia and neurons, aiding in the resolution of mechanical allodynia following mouse paw incision which was used as an animal model for the persistent postoperative pain experienced by many patients after surgery [241].

1.4.4 MKP-5

Mitogen Activated Protein Kinase Phosphatase 5 (MKP-5 / DUSP10) is widely expressed throughout the body, particularly in the heart, liver, kidney and skeletal muscle and can be found in both the nucleus and cytoplasm of the cell [242]. It is

induced by various stress stimuli and preferentially targets p38 and JNK, but not ERK [242]. Mice deficient in this phosphatase have an increased $CD4^+$ and $CD8^+$ T cell response and cytokine production (TNF-α, IFNγ) following secondary lymphocytic choriomeningitis virus infection (LCMV) [243]. MKP-5 deficient mice also mount an increased inflammatory response against LPS-induced vascular injury involving enhanced TNF-α and IL-6 production in addition to increased neutrophil infiltration and superoxide production [244].

Furthermore, MKP-5 may play a role in regulating the immune response to malaria, with the severity of *Plasmodium yoelii* infection (a mouse model of malaria) reduced in MKP-5 KO mice, associated with decreased parasite burdens, increased survival rates and upregulated IFNγ [245]. In addition, MKP-5 overexpression decreases p38-mediated production of the inflammatory mediators (IL-6, IL-8 and COX-2) in prostatic epithelial cells following TNF-α and IL-1β stimulation [246]. These reports clearly demonstrate that MKP-5 is involved in the regulation of immune responses. MKP-5 has previously been studied in the context of an EAE model, with MKP-5 deficient mice less susceptible to disease due to decreased $CD4^+$ T cell responses [243].

1.4.5 MKP-7

Mitogen Activated Protein Kinase Phosphatase 7 (MKP-7 / DUSP16) is found exclusively in the cytoplasm and is highly expressed in mouse brain and kidney [247]. MKP-7 preferentially dephosphorylates JNK and p38 [247]. In T cells, MKP-7 is involved in regulating the balance between Th1 and Th2 responses [248], [249], as well as $CD8^+$ T cell proliferation and effector functions such as cytokine production (IL-2, IL-4, IL-5, IL-13 and IFNγ) by regulating JNK activity [249]. LPS-stimulated MKP-7 deficient macrophages produce significantly less IL-12, IL23 and TNF-α, with reduced myeloid cell differentiation also observed in the absence of MKP-7, suggesting a role in cytokine production and differentiation of myeloid cells [250].

Previous research has highlighted other potential functions for MKP-7, including regulation of adhesion molecule expression [251]. siRNA knockdown of MKP-7 in

HUVECs decreases expression of VCAM-1 by downregulation of the transcription factor IRF-1 via increased JNK activity in the absence of MKP-7. Endothelial cell migration induced by the proangiogenic chemokine CXCL12 (stromal cell-derived factor-1-α) is, in-part, regulated by MKP-7 and its effect on JNK3 activity [252].

1.4.6 MKP-x

Mitogen Activated Protein Kinase Phosphatase x (MKP-x / DUSP22) is an atypical DUSP which is expressed in various tissues, with highest expression in the brain, heart, liver and kidney [253]. Atypical DUSPs share a degree of similarity with MKPs; however they do not contain a common regulatory site, the cdc25 homology domain [254], [255]. Different reports have suggested DUSP22 can dephosphorylate JNK and p38 [253], [255], but can also target non-MAPK substrates. These include STAT3; with DUSP22 overexpression in HEK293T cells reducing IL-6 mediated phosphorylation and activation of STAT3 [256]. This was further confirmed with siRNA transfection of HeLa cells to knockdown DUSP22 expression, resulting in upregulated STAT3 activity. Another report found that overexpression of DUSP22 decreases β-estradiol-induced phosphorylation of estrogen receptor-α (ERα), while knockdown of DUSP22 by siRNA increases ERα-mediated transcriptional activation in breast cancer cells [257] suggesting another potential target for regulation by DUSP22. Focal adhesion kinase (FAK) has also been identified as a novel target for DUSP2 as overexpression downregulates FAK phosphorylation and decreases cell motility in H1299 cells (human non-small cell lung carcinoma cell line) [258]. Furthermore, DUSP22 knockdown enhances FAK phosphorylation and cell migration. TCR signalling and T cell activation is enhanced in DUSP22 deficient mice, with increased proliferation, activation and IFNγ and IL-2 production [259].

DUSP22 deficient mice also develop more severe EAE [259]. These effects were attributed to a reduction in dephosphorylation of Lck, allowing continued activation of this tyrosine kinase which is integral to TCR signalling. Therefore DUSP22 functions to dephosphorylate Lck, decreasing TCR signalling and T cell responses. This would make DUSP22 a potentially important regulator of MS/EAE pathogenesis

by reducing autoreactive T cell effector function. In addition to these functions, DUSP22 can also selectively activate JNK [253].

1.4.7 DUSP5

Similarly to MKP-1 and MKP-2, dual-specificity phosphatase 5 (DUSP5) is an inducible MKP localised within the nucleus and is expressed in a variety of tissues, particularly in the brain and pancreas. However, unlike MKP-1 and MKP-2, DUSP5 selectively dephosphorylates ERK1 and ERK2, with no activity towards JNK or p38 [260]. DUSP5 overexpression decreases T cell development in the thymus, reducing the number of $CD4^+$ and $CD8^+$ single positive cells by blocking progression at the double positive stage [261]. IL-2-mediated T cell proliferation and gene induction was also decreased in transgenic DUSP5 mice, suggesting an important role for DUSP5 in normal thymocyte development and T cell-mediated immune responses. DUSP5 overexpression attenuates the incidence and severity of collagen-induced arthritis (CIA), suggesting a protective role in rheumatoid arthritis [262]. This was associated with reduced Th17 cell frequency, reduced inflammatory cytokine production (IL-6, TNFα and IL-1β) and reduced antigen-specific antibody levels while regulatory T cell frequency was increased.

DUSP5 is also involved in regulation of cell survival and permeability [263]. HUVECs were transfected with siRNA oligonucleotides to knockdown DUSP5 expression, resulting in increased baseline and serum-induced cytotoxicity and caspase 3/7 activity while also preventing the attenuation of vascular permeability by angiopoietin-1. Overexpression of DUSP5 upregulates proliferation of FDCP1 progenitor cells induced by M-CSF and also alters the pattern of differentiation of the multipotent hematopoietic cell line, EGER-Fms, with reduced macrophage but increased granulocyte differentiation, suggesting a role for DUSP5 in myeloid cell lineage commitment [264]. DUSP5 has also been implicated in cardiovascular diseases, with roles in cardiac hypertrophy [265] and myogenic responses in rat cerebral arteries [266], [267].

1.5 How might MKPs be involved in MS

As MAPKs are involved in control of cellular proliferation and survival, these enzymes need to be tightly regulated to help maintain cell function and tissue homeostasis within the human body. In autoimmune conditions such as MS, where cells of the immune system are activated and damage self-tissue, this is even more important. MKPs can downregulate MAPK signalling by dephosphorylating, and thus deactivating, MAPKs. Therefore in a biological context such as a patient suffering from MS, regulating the expression of transcription factors, proliferation of immune cells and production of cytokines could play a vital role in determining the severity of disease. Also, as MS has been associated with predominantly Th1 and Th17 responses and MAPKs have been shown to play an important role in the activation and polarization of T cell subsets and macrophages, regulation of MAPK activity by MKPs could be important in disease pathophysiology. However, one important consideration is that MKPs have pleiotropic functions in different cell types, thus their potential role in disease conditions could be very complicated depending on which cells are involved and the stage of disease.

Three previous studies have been carried out to understand the roles of MKPs in MS development utilising MKP deficient mice in EAE, with disease severity ameliorated in the absence of MKP-1/DUPS1 and MKP-5/DUSP10 whereas MKP-x/DUSP22 deficient mice are more susceptible to EAE. These reports clearly demonstrate the integral role MKPs play in conditions such as MS, however they also suggest that different MKPs have the potential to be either deleterious or protective in EAE/MS and thus must be analysed individually to fully understand the MKP network in MS.

1.6 Research aims

This thesis aimed to understand the function of MKP-2 during the development of EAE, an animal model of MS, in order to determine whether this may provide a novel therapeutic target in the treatment of neurological inflammatory disorders.

Recently MKPs, which negatively regulate MAPK activity, have emerged as critical players in immune responses and thus are now known to be important in immune mediated diseases. While MKP-1 and MKP5 deficient mice were shown to develop less severe EAE with decreased immune cell activation, MKP-2 deficient mice developed an attenuated inflammatory response in animal models of ALI and sepsis. I therefore hypothesise that MKP-2 deficient mice will develop less severe EAE due to diminished inflammatory responses in the absence of MKP-2

The primary aims of this report are as follows:

- Establish a working model of EAE and characterise the immunological changes associated with disease onset and progression.
- Analyse the expression and activation of the main MAPKs, ERK, JNK and p38, in EAE tissue as well as the expression of selected MKPs within CNS and lymphoid tissue of EAE mice.
- Investigate the potential role of MKP-2 in the pathogenesis of EAE using MKP-2 deficient mice.
- Determine which aspects of the immune response and MAPK signalling are regulated by MKP-2 during EAE development, progression and recovery.
- Determine the role of MKP-2 in regulating the phenotype and function of two key cells involved in EAE pathogenesis, DCs and macrophages.

2 Materials and Methods

2.1 Materials

All chemicals and reagents obtained from Sigma-Aldrich or Thermo Fisher Scientific unless otherwise stated.

2.1.1 Phosphate buffered saline (PBS)

1 L of 20 x PBS: 160 g Sodium chloride (NaCl), 4 g Potassium chloride, 28.8 g Sodium phosphate dibasic and 4.8 g Potassium phosphate monobasic; pH 7.4 in 1 L dH_2O

For 1 L of 1x PBS (working conc): 50 mL of 20 x PBS in 950 mL dH_2O

2.1.2 Tris buffered saline (TBS)

1 L of 10 x TBS: 24 g Tris base, 88g NaCl; pH 7.5 in 1 L dH_2O

For 1 L of 1x TBS (working conc): 100 mL of 10 x TBS in 900 mL dH_2O

2.1.3 Genotyping lysis buffer

100 mM Tris base, 5 mM Ethylenediaminetetraacetic acid (EDTA), 200 mM NaCl, 0.2 % Sodium dodecyl sulfate (SDS) and 200 µg/ml Proteinase K

2.1.4 Immunohistochemistry (IHC) fixative solution

1 L ice cold solution: 750 mL Acetone and 250 mL Ethanol absolute

2.1.5 IHC blocking buffer

10 mL TBS with 0.1 g Bovine serum albumin (BSA; 1 %), 10 µL Triton X-100 (0.1 %) and 5 µL Tween-20 (0.05 %)

2.1.6 IHC wash buffer (TBST-0.05 %)

1 L of TBS with 0.5 mL of Tween-20 (0.05 %)

2.1.7 Scotts tap water substitute (STWS)

10 g Magnesium sulphate, 0.67 g Sodium bicarbonate in 1 L H_2O

2.1.8 ELISA wash buffer

1 L of PBS with 0.5 mL of Tween-20 (0.05 %)

2.1.9 ELISA blocking buffer

900 mL of PBS with 100 mL Foetal calf serum (FCS; 10 %)

2.1.10 ELISA stop solution

1M Sulphuric acid

2.1.11 FACS Buffer

1 L of PBS with 10 g of BSA (1 %)

2.1.12 Laemmli sample buffer

63mM Tris-HCL, (pH6.8), 2mM Sodium pyrophosphate, 5mM EDTA, 10% (v/v) glycerol, 2% (w/v) SDS, 50mM Dithiothreitol (DTT), 0.007% (w/v) bromophenol blue

2.1.13 Western blot electrophoresis buffer

1 L of dH_2O with 2.7 g Tris base, 12.96 g Glycine and 0.9 g (SDS)

2.1.14 Western blot transfer buffer

800 mL of dH_2O with 2.7 g Tris base, 12.96 g Glycine and 200 mL Methanol

2.1.15 Western blot wash buffer (TBST-0.1 %)

1 L of TBS with 1 mL of Tween-20 (0.1 %)

2.1.16 Western blot blocking buffer

100 mL of TBST-0.1 % with 5 g BSA (5 %)

2.1.17 Western blot antibody diluent

100 mL of TBST-0.1 % with 0.5 g BSA (0.5 %)

2.1.18 Western blot gel buffers

Buffer 1: 90.75 g Tris base 1.5M, 2 g SDS 0.4% w/v; pH 8.8 in 500 mL dH_2O

Buffer 2: 30.25 g Tris base 0.5M, 2 g SDS 0.4% w/v; pH 6.8 in 500 mL dH_2O

2.1.19 Western blot 10 % Resolving gel

For 1 thick (1.5 mm) gel: 3.6 mL dH_2O, 2.25 mL Gel buffer 1, 3 mL Acrylamide (Carl Roth GmbH and Co.), 7.5 µL Tetramethylethylenediamine (TEMED) and 75 µL 10 % Ammonium persulfate (APS; 0.1 g in 1 mL PBS)

2.1.20 Western blot stacking gel

For 1 thick (1.5 mm) gel: 3.65 mL dH_2O, 1.4 mL Gel buffer 2, 0.6 mL Acrylamide, 7.5 µL TEMED and 56.2 µL 10 % APS

2.1.21 Western blot stripping buffer

100 mM β-mercaptoethanol, 2% SDS, 62.5 mM Tris-HCl, pH 6.7

2.1.22 Complete RPMI medium (c-RPMI)

RPMI-1640 (Lonza) supplemented with 10 % heat inactivated FCS (Biosera Gold), 100 mg/mL streptomycin, 100 U / mL penicillin and 2mM L-glutamine

2.1.23 Complete Dulbeccos Modified Eagle Medium (c-DMEM)

DMEM (GIBCO, Life Technologies) supplemented with 10 % heat inactivated FCS (Biosera Gold), 100 mg/mL streptomycin, 100 U / mL penicillin and 2mM L-glutamine

2.2 Methods

2.2.1 Animals

Female MKP-2 -/- mice and MKP-2 +/+ littermate controls on a C57BL/6 background were obtained from Professor Robin Plevin (University of Strathclyde). Knockout (KO) mice were generated as previously described (Al-Mutairi *et al*., 2010). In this thesis 5th, 6th and 7th generation backcross mice were used. These mice, as well as naive C57BL/6 mice used throughout this study, were bred and maintained within the Strathclyde Institute of Pharmacy and Biomedical Science animal unit. Animals were used at 6–8 weeks of age and were age and sex matched within each experiment. All animal experiments adhered to the UK Animals (Scientific Procedures) Act 1986 and were conducted under a Project License to Dr Hui-Rong Jiang (PPL60/4136 ‘‘Pathophysiology of autoimmune diseases’’) granted by the UK Home Office and with local ethical approval.

2.2.2 Genotyping

Genotyping was carried out to confirm MKP-2 gene deficiency. To do this, tail biopsy was performed and 0.5 mL of lysis buffer added to each tail sample in a 1.5 mL microcentrifuge tube. This was incubated overnight at 65 °C on an orbital shaker before centrifugation at 14,000 x *g* for 20 minutes. Supernatant was transferred to a new 1.5 mL microcentrifuge tube and 50 µL sodium acetate (NaAc, pH 5.5; 3M) and 250 µL isopropanol added. Samples were centrifuged at 14,000 x *g* for 5 minutes to pellet DNA. The pellet was then washed in 0.5 mL of ice cold 70 % ethanol. After removing the ethanol, the DNA pellet was allowed to air dry and then resuspended in 50 µL of dH_2O and heated at 65 °C for 30 minutes. Polymerase chain reaction (PCR) was performed using the GoTaq Polymerase kit and nucleotide mix (both Promega). Initial denaturing of the DNA template was performed at 95 °C for 2 minutes. This was followed by 35 cycles of denaturing (95 °C, 30s), annealing (58 °C, 30s) and extension (72 °C, 5 minutes) before a final extension step at 72 °C for 5 minutes.

Samples were cooled to 4 °C and then separated on a 1 % agarose gel by electrophoresis (120V for 45 minutes).

Primers used were as follows (5'-3'): WT forward primer, CCTCAGACT GTCCCAATCAC; WT reverse primer, GACTCTGGATTTGGGGTCC. KO forward primer, TGACTAGGGGAGGAGTAGAAGGTGGC; KO reverse primer, ATAGTGACGCAATGGCATCTCCAGG.

2.2.3 EAE Induction and assessment

Female, 8-week old C57BL/6 mice or MKP-2 KO (-/-) and wild-type littermates (WT; +/+) were immunized subcutaneously on day 0 with 100 µg MOG_{35-55} (ChinaPeptides Co Ltd) emulsified in complete freunds adjuvant (CFA; Sigma) supplemented with 2.75 mg or 3.65 mg Mycobacterium *tuberculosis* (BD Biosciences). Every mouse received 100 µL of this MOG and CFA mixture, 50 µL on each side of the lower back which was shaved and sprayed with 70 % ethanol prior to injection. In addition, each mouse received 100 ng pertussis toxin (PTX; Tocris Bioscience) in 100 µL PBS injected intraperitoneally (i.p.) on day 0 and again on day 2.

Mice were weighed and monitored daily for signs of disease development and given a clinical score based on the following evaluation system : 0 = no clinical sign; 0.5 = partial loss of tail tone; 1.0 = Complete loss of tail tone; 1.5 = Altered gait; 2.0 = Hind limb weakness; 2.5 = Paralysis of one leg; 3.0 = Hind limb paralysis; 3.5 = Hind limb paralysis with significantly reduced mobility; 4.0 = Forelimb involvement; 5.0 = Moribund. To control for subjective bias, mice were scored blind as recommended in the ARRIVE guidelines [268]

2.2.4 Tissue preparation for staining

Naïve or PBS/MOG_{35-55} immunised mice were sacrificed at days 9, 17 or 28 and, following PBS perfusion, intact spinal cords were flushed out with PBS by hydrostatic pressure using a sterile 19G needle and 2.5 mL syringe (both BD Medical). Tissue

was submerged in OCT mounting medium (VWR International) and rapidly frozen on dry ice before being cut into 7 µM thick sections on a Shandon cryotome (Thermo Scientific).

2.2.5 Haematoxylin and Eosin staining

Tissue sections were stained with haematoxylin and eosin (H&E). Briefly, slides were fixed using fixative solution for 10 minutes before staining in Gill 2 haematoxylin (Thermo Scientific) for 6 minutes. Slides were then washed in running water for 5 minutes. This was followed by blueing in STWS for 3 minutes, another 5 minute wash and then counterstaining in eosin Y solution (Thermo Scientific) for 5 minutes. Slides were then washed for a final time until the desired colour intensity of eosin was achieved (by periodically checking slides under microscope) before dehydration through 70 % ethanol (1 dip), 95 % ethanol (1 dip) and 100 % ethanol (5 minutes). Finally, slides were cleared in histoclear II (National Diagnostics) for 5 minutes and mounted with DPX (Fisher Scientific).

2.2.6 Immunohistochemical staining

Sections were stained with different cell-surface marker antibodies as listed in Table 2.1. Firstly, slides were fixed using fixative solution for 10 minutes before blocking non-specific binding sites by incubating with blocking buffer for 1 hour at room temperature (RT). This was then replaced with the relevant primary antibody diluted in IHC blocking buffer and slides incubated overnight at 4 °C. The following day slides were washed (3 x 5 minutes) in IHC wash buffer before adding a biotin-conjugated secondary antibody diluted in blocking buffer for 1 hour at RT. After another wash step, sections were incubated for 30 minutes at RT with streptavidin-HRP (eBioscience) diluted in TBS before one more wash. Tissue was then incubated at RT with ImmPACT AMEC red peroxidase substrate (Vector Laboratories) until optimal colour development achieved before a brief rinse in dH_2O then counterstaining with haematoxylin for 1 minute. Slides were then mounted with hydromount

mounting medium (National diagnostics). Images were obtained using the Nikon Eclipse 50i microscope, the Nikon Digital Sight DS-U3 microscope camera controller and Nikon NIS Elements microscope imaging software.

2.2.7 Immunofluorescent staining

Sections were stained with different cell-surface marker antibodies (Table 2.1). Firstly, slides were fixed using fixative solution for 10 minutes before blocking non-specific binding sites by incubating with blocking buffer for 1 hour at RT. This was then replaced with the relevant primary antibody diluted in blocking buffer and slides incubated overnight at 4 °C. The following day slides were washed (3 x 5 minutes) in wash buffer before adding a biotin-conjugated secondary antibody diluted in blocking buffer for 1 hour at RT. After another wash step, sections were incubated for 1 hour at RT in the dark with fluorochrome-conjugated streptavidin (Vector Laboratories) diluted in TBS before one more wash. Slides were then mounted with Vectashield mounting medium containing DAPI (Vector Labotatories). Images were obtained using the Nikon Eclipse TE2000 inverted microscope and IPLab imaging software.

Table 2.1: List of Immunohistochemical antibodies used

Antibody	**Species**	**Manufacturer**	**Cat No.**
MKP2	Rabbit	Santa Cruz Biotechnology	sc-1200
IL-22	Rat	R&D Systems	MAB582
CD4	Rat	eBioscience	14-0193-85
CD45	Rat	eBioscience	14-0451-85
F480	Rat	eBioscience	14-4801-85
Rabbit IgG	Rabbit	Santa Cruz Biotechnology	sc-2027
Rat IgG	Rat	BD Biosciences	553986
Anti-Rabbit Biotin	Goat	BD Biosciences	550338
Anti-Rat Biotin	Mouse	eBioscience	13-4813-85
Anti-Rabbit AlexaFluor 568	Goat	Life Technologies	A11036
Fluorescin-HRP	N/A	Vector Laboratories	SA-5001

2.2.8 Cell preparations from spleen and inguinal lymph nodes

Mice were sacrificed at various time points and spleen and draining lymph nodes (inguinal) harvested for cell culture. The tissue was placed in complete RPMI medium and disrupted using the back of a syringe to form a cell suspension. This was filtered through nitex nylon mesh (Cadisch precision meshes). Spleen cell pellets were resuspended in lysis buffer (BD Biosciences) for 5 minutes before both spleen and lymph node cells were washed twice with PBS, resuspended in RPMI, counted and resuspended to an appropriate concentration for use.

2.2.9 CNS cell isolation

Mice were sacrificed at different time points and brain and spinal cord tissues harvested and placed in c-RPMI medium. Brain and spinal cords were pooled together for each individual mouse to ensure an adequate number of CNS cells were obtained for FACS analysis. The CNS tissue was cut into smaller pieces in a petri dish using a scalpel blade and further homogenised by passing it through a 21G needle to form a cell suspension. This was filtered through a mesh cell strainer (BD Falcon) into a 50 mL centrifuge tube and washed in c-RPMI (1600 rpm for 10 minutes). Supernatant was removed and the pellet resuspended in 2 mL of c-RPMI containing collagenase D (1mg/mL; Roche) and DNase (1mg/mL; Roche) and incubated at 37 °C and 5% CO_2 for 30 minutes. After the incubation, 8 mL of c-RPMI was added to each sample and the cells were passed through a cell strainer into a fresh 50 mL tube before another wash step as above. Supernatant was then removed and the pellet resuspended in 5 mL of 30 % percoll (Fluka)/70 % c-RPMI. This suspension was carefully overlaid on 70 % percoll/30 % PBS in a 15 mL centrifuge tube and centrifuged at 2000xg for 20 minutes. Cells were carefully removed at the interphase between the layers, washed with c-RPMI and cells counted.

2.2.10 Generation of Bone Marrow Derived Macrophages

Macrophage growth medium was composed of c-DMEM supplemented with 30 % L-cell (L929 cell culture derived). Bone marrow-derived macrophages (BMDMs) were generated from the culture of bone marrow from 7-8 week old C57Bl/6 mice. Both tibia and femurs were collected from mice and the epiphyses removed. Bone marrow was subsequently flushed out with c-DMEM using a 25 gauge needle and disaggregated to form a single cell suspension. This was pelleted (1400 rpm for 5 minutes) and resuspended in growth medium, with 15 mL added to a sterilin petri dish (Fisher Themro Scientific) and cultured at 37 °C with 5 % CO_2. Fresh growth medium was added on day 2 of the culture. On day 5 all medium was removed and replaced with 20 ml of fresh growth medium. The BMDMs were harvested on day 7. Medium was removed and discarded, and 5 ml cold PBS added to each dish and incubated at 37 °C for 2-3 minutes to remove cells from the bottom of the petri dishes. Cells in the PBS were then collected in a 50 mL centrifuge tube. The petri dishes were washed 2 more times with cold PBS to ensure all the cells were collected. Cells were counted using a haemocytometer and resuspended to an appropriate concentration for use.

2.2.11 Generation of Bone Marrow Derived Dendritic Cells

Dendritic cell growth medium was composed of c-RPMI supplemented with 10 % GMCSF-containing supernatant (X-63 cell culture derived). Bone marrow-derived dendritic cells (BMDCs) were generated from the culture of bone marrow from 7-8 week old C57Bl/6 mice. As described in section 2.2.10, a single bone marrow cell suspension was obtained from mouse tibia and femurs. The cells were then cultured in sterilin petri dishes (10 mL / dish) and cultured at 37 °C with 5 % CO_2. Fresh growth medium was added on day 3 of culture. On day 5 all medium was removed and replaced with 20 mL of fresh growth medium. The BMDCs were harvested on day 7. In brief, the culture medium was removed and collected, and then 10 mL cold HBSS (GIBCO, Life Technologies) was added to each dish and incubated at RT for 5 minutes. Adherent cells were gently detached from the bottom of the dishes using a cell scraper. Both adherent cells as well as unattached cells within the culture

supernatant were collected and counted using a haemocytometer. Cells were then resuspended to an appropriate concentration for further experiments.

2.2.12 Spleen and inguinal lymph node stimulation

Spleen and lymph node cells were cultured in 24-well tissue culture plates at $4x10^6$ cells/well for spleen and $1\text{-}2x10^6$ cells/well for lymph node. Cells were stimulated for 72 hours with media alone, media and 40 µg/ml $MOG_{35–55}$ or media and 40 µg/ml conA (Sigma-Aldrich).

2.2.13 Enzyme-linked immunosorbant assay (ELISA)

ELISA was utilised to examine soluble cytokine levels in the samples using ready-set-go kits (eBioscience) or antibody pairs with recombinant cytokine as the standard (eBioscience). Briefly, high binding 96-well ELISA plates (Greiner Bio-One) were coated with capture antibody (using concentrations stated on the certificate of analysis; Table 2.2) diluted in coating buffer provided within the ready-set-go kits and incubated overnight at 4 °C. The following day, plates were washed 5 times with ELISA wash buffer. Plates were then incubated with ELISA blocking buffer for 1 hour at RT. Plates were washed again before adding recombinant standards and samples and incubating for 2 hours at RT. Wells were aspirated and washed, and then detection antibody added for 1 hour at RT followed by another wash step. Avidin-HRP (eBioscience) was subsequently added and plates incubated for 30 minutes at RT. Following a final wash step, TMB substrate solution (BD Bioscience) was added to each well until a definitive blue colour had developed at which point stop solution was added and the plate read at 450 nm.

Table 2.2: List of ELISA antibodies used

Antibody	**Manufacturer**	**Cat No.**
IL-2 capture	eBioscience	14-7022-68
IL-2 detection	eBioscience	33-7021-68
IL-2 recombinant	eBioscience	39-8021-60
IL-6 capture	eBioscience	14-7061
IL-6 detection	eBioscience	13-7062
IL-6 recombinant	eBioscience	14-8061
IL-10 capture	eBioscience	14-7101
IL-10 detection	eBioscience	13-7102
IL-10 recombinant	eBioscience	14-8101
IL-17 capture	eBioscience	14-7175
IL-17 detection	eBioscience	13-7177
IL-17 recombinant	eBioscience	14-8171
IL-22 capture	eBioscience	14-7221-68
IL-22 detection	eBioscience	13-7222-68
IL-22 recombinant	eBioscience	39-7222-60
CCL2 capture	eBioscience	14-7391-68
CCL2 detection	eBioscience	33-7096-68
CCL2 recombinant	eBioscience	88-7391-60
IFN-γ capture	eBioscience	14-7313-68B
IFN-γ detection	eBioscience	13-7312-68C
IFN-γ recombinant	eBioscience	39-8311-60
TNF-α capture	eBioscience	14-7325
TNF-α detection	eBioscience	13-7326
TNF- α recombinant	eBioscience	14-8321

2.2.14 Fluorescence-activated cell sorting (FACS)

Cells from tissues or culture were first counted, and then 0.5 x 10^6 cells added to each FACS tube, to which 1 mL FACS buffer was added. The cells were pelleted at 1400 rpm for 5 minutes and supernatant removed. To block non-specific Fc receptors, cells were resuspended in α-mouse CD16/CD32 Fc block (eBioscience) at 4 °C for 10 minutes. Following this, the appropriate antibodies which were diluted in 100 µL FACS buffer (Table 2.3) were added to each tube, mixed well, and incubated for 30 minutes at 4 °C in the dark. 2 mL of FACS buffer was added and cells pelleted again as previously. This was repeated one more time before cells were resuspended in 0.5 mL FACS buffer and analysed using a BD FACSCanto system and BD FACSDiva software (both BD Biosciences).

For staining of intracellular antigens, the Fixation and Permeabilization Solution Kit with BD GolgiStop (BD Biosciences) was used per manufacturers' instructions. Briefly, following cell surface antigen staining, cells were washed twice in staining buffer before resuspension in fixation/permeabilization solution for 20 minutes at 4 °C. Cells were washed two times with BD Perm/Wash buffer to maintain cell permeabilization and then incubated with the appropriate antibodies for 30 minutes at 4°C in the dark. Following two more wash steps in BD perm/wash solution, cells were resuspended in staining buffer and analysed as above.

Table 2.3: List of Flow cytometry antibodies used

Antibody	Conjugate	Manufacturer	Cat No.
CD3	PE	BD Biosciences	553063
CD4	FITC PerCPCy5.5	eBioscience eBioscience	53-0041-82 45-0042-82
CD8	PE PerCPCy5.5	BD Pharmingen eBioscience	553033 45-0081-82
CD11b	PE	eBioscience	12-0112-82
CD11c	PE	eBioscience	12-0114-82
CD19	APC	eBioscience	17-0193-80
CD25	FITC	eBioscience	53-0251-82
CD40	FITC	eBioscience	53-0251-82
CD206	FITC	BioLegend	123005
MHC-II	APC	eBioscience	17-5321-82
Foxp3	APC	eBioscience	17-5773-82
F4/80	APC	eBioscience	17-4801-82

2.2.15 RNA Extraction and Reverse Transcription PCR

Mice were sacrificed at various time points and spinal cord and brain tissue collected and placed in RNAlater (Life Technologies). RNA isolation was performed using TRIzol reagent (Life Technologies). In brief, tissue samples were homogenized in TRIzol (approx. 1 mL TRIzol per 50 mg tissue) using a power homogenizer and incubated for 5 minutes at RT. Chloroform was added (0.2 mL per 1 mL of TRIzol) and mixed vigorously. Samples were incubated for 2 minutes at RT and then centrifuged at 12,000 x *g* for 15 minutes at 4°C to achieve phase separation. The top aqueous layer (which contains the RNA) was transferred to a new tube (if subsequent protein extraction was performed, the interphase and organic phenol-chloroform phase

were retained and stored at 4°C until required). To the RNA-containing aqueous layer, 100 % isopropanol was added (0.5 ml per 1 ml TRIzol) and then incubated at RT for 10 minutes before being centrifuged at 12,000 x *g* for 10 minutes at 4 °C. The supernatant was removed and the RNA pellet washed in 70 % ethanol (1 ml per 1 ml TRIzol). This was centrifuged at 7,500 x *g* for 5 minutes at 4 °C. Ethanol was discarded and the pellet vacuum dried before resuspension in 50 µl RNase-free water and incubation in a heat block at 60 °C for 10-15 minutes. Total RNA was quantified using the NanoDrop 2000c spectrophotometer (Thermo Scientific).

2 µg total RNA was reverse transcribed using the High Capacity cDNA Reverse Transcription Kit (Life Technologies). The 2X RT master mix was prepared using the components and specifications provided in the manufacturers' protocol (Table 2.4) and 10 µl added to each tube.

Table 2.4: High capacity cDNA Reverse Transcription kit 2X RT master mix

Component	**Volume (µl) per reaction**
10X RT Buffer	2.0
10X RT Random Primers	2.0
25X dNTP Mix (100 mM)	0.8
Multiscribe Reverse Transcriptase	1.0
Nuclease Free H_20	4.2
Total per Reaction	**10**

To this, 10 µl of sample (composed of 2 µg RNA and RNase-free water) was added. Reverse transcription was performed in the Veriti 96-well Thermal Cycler (Applied Biosystems) using the following conditions: 25 °C for 10 minutes, 37 °C for 120 minutes and 85 °C for 5 minutes.

2.2.16 Quantitative PCR

The cDNA obtained from reverse transcription was analysed for expression of various mRNA transcripts (primer details are listed in Table 2.5). Quantitative PCR was carried out using 2x Fast SYBR Green master mix (Life Technologies) as the detection agent. This master mix contained SYBR Green I Dye, AmpliTaq Fast DNA Polymerase, Uracil-DNA Glycosylase (UDG), ROX dye Passive Reference, dNTPs and optimized buffer components. Each 20 µL reaction was prepared in MicroAmp Fast Optical 96-Well reaction plates (Applied Biosystems) with 10 µL of Fast SYBR Green master mix, 1 µL of each primer (to give a final primer concentration of 500 nM) and 2 µL of cDNA (20 ng cDNA per reaction). RNase-free water was added to complete the 20 µL final reaction volume. Plates were sealed with an optical adhesive cover (Applied Biosystems) and briefly centrifuged to spin down the entire reaction volume and remove air bubbles. The PCR reaction was performed in the Applied Biosystems StepOnePlus real-time PCR system. Melt-curve analysis was carried out each time to ensure specificity of the reaction. The full reaction conditions were as follows: 95 °C for 20 seconds, followed by 40 cycles of 95 °C for 3 seconds and 60 °C for 30 seconds, and a standard melt curve stage of 95 °C for 15 seconds, 60 °C for 1 minute and 95 °C for 15 seconds. Primers were obtained from Sigma-Aldrich and designed used Primer3 software.

Table 2.5: List of qPCR primers used

Molecule	Forward Primer (5' – 3')	Reverse Primer (5' – 3')
β-actin	GTGGGCCGCTCTAGGCACCAA	CTCTTTGATGTCACGCACGATTTC
TATA-binding protein	CTCAGTTACAGGTGGCAGCA	ACCAACAATCACCAACAGCA
Tubulin beta 5	AGGTGGTAGTGCCTGGAATG	AGGGACATACTTGCCACCTG
MKP-1 / DUSP-1	GACAAAACAGGGCAGAAGAG	CCACCGACCTACACAAAAAT
MKP-2 / DUSP-4	TGCCAGAGAAGACTTGGTTT	TCCTCTTTCCTTTCCCTCTC
MKP-3 / DUSP-6	GAATAATCCGGCGAGAAACA	AATGAAGGTGCCCAGTTTTG
DUSP5	GAGTGCGTCTGAGATTCTGTCCAG	AAGTCCAAGGTCACCGAGGAAC
MKP-5 / DUSP-10	ACAGCACCCCATGGTAGAAG	AGGCCTTGGGTACAACTGTG
MKP-7 / DUSP16	GCACACCACCATTACATCATCG	AACAGTCTGAAGAGAGAGAGGC
MKP-x / DUSP-22	CCCCTTGCTTCTTGACTCTG	AAAGCAGGAAAACTGGCTCA

2.2.17 Protein Isolation

Protein was isolated either from the organic phenol-chloroform phase produced during TRIzol RNA extraction or directly from tissue/cells using RIPA Buffer (Thermo Scientific). For the Trizol method; 100 % ethanol (0.4 ml per 1 ml of TRIzol) was added to the organic phase, mixed, and incubated at RT for 2-3 minutes. Samples were then centrifuged at 2000 x *g* for 5 minutes at 4 °C to pellet the DNA. The phenol-ethanol supernatant (containing protein) was removed and transferred to a new tube. Isopropanol (1.5 ml per 1 ml of TRIzol) was added to the supernatant, mixed, and

incubated for 10 minutes at RT. Following this, samples were centrifuged at 12,000 x *g* for 10 minutes at 4 °C to pellet the protein. The protein pellet was washed 3 times with 0.3 M guanidine hydrochloride in 95 % ethanol (by incubating in this solution for 20 minutes at RT followed by centrifugation at 7500 x *g* for 5 minutes). After washing, 2 ml of 100 % ethanol was added to the pellet, incubated at RT for 20 minutes and centrifuged at 7500 x *g* for 5 minutes at 4 °C. The ethanol was then removed and the pellet allowed to air dry before being resuspended in 200 µl RIPA Buffer and stored at -20 °C.

For protein extraction directly from tissue (spinal cord and brain), RIPA buffer was used. Tissue was harvested, placed in a 1.5 ml microcentrifuge tube and snap frozen on dry ice. The frozen spinal cord or brain was defrosted, placed in a 6-well tissue culture plate and disrupted using the back of a syringe through a nitex mesh to form a cell suspension. This was centrifuged at 400 x *g* for 5 minutes at 4 °C to pellet the cells. Supernatant was removed and the cell pellet washed twice in cold PBS. Following the last wash, PBS was removed and the pellet resuspended in 50 µl of complete RIPA buffer containing a Halt Protease & Phosphatase Inhibitor Cocktail (Thermo Scientific). Samples were incubated on ice for 30 minutes and then centrifuged at full speed for 15 minutes at 4 °C. The supernatant containing protein was transferred to a new 1.5 ml microcentrifuge tube and stored at -20 °C

Protein concentration within each sample was determined using the Quick Start Bradford 1x Dye Reagent (BIO RAD). BSA was used as the relative protein standard. The absorbance of all standards and unknown samples were measured using a spectrophotometer at 595 nm. From this, a BSA standard curve could be generated to calculate the protein concentration within the unknown samples.

2.2.18 Western Blotting

2.2.18.1 Sample preparation

Once protein concentration was determined by Bradford assay, 30 µg from each tissue or cell sample was transferred to a 1.5 mL microcentifuge tube and 4x Laemmli's

sample buffer added. Samples were boiled at for 5 minutes to denature proteins and then stored at -20 °C until required for use.

2.2.18.2 SDS-Polyacrylamide Gel Electrophoresis (SDS-PAGE)

Resolving gels were prepared as described in 2.1.19 and the mixture added between two glass plates assembled vertically in a frame according to the manufacturer's instructions (Bio-Rad) and topped with 300 µl of 0.1% (w/v) SDS to level the surface. The SDS was removed after gel polymerisation and a stacking gel (2.1.20) was added directly on top of the resolving gel with a Teflon comb immediately inserted into the mixture between the glass plates. After stacking gel polymerisation the comb was removed and the glass plates containing the gels were assembled in a Bio-Rad Mini-PROTEAN II^{TM} electrophoresis tank, with reservoirs filled with electrophoresis buffer. Gels were run at 120V for 1 hour 30 minutes using the Bio-Rad PowerPac basic power supply.

2.2.18.3 Electrophoretic Transfer of Proteins to Nitrocellulose Membrane

Proteins separated by SDS-PAGE were transferred to nitrocellulose membrane by electrophoretic blotting. Briefly, the gel was pressed firmly against a nitrocellulose sheet and assembled in a transfer cassette sandwiched between two Whatman 3MM paper and two sponge pads. The cassette was immersed in transfer buffer in a BIO-Rad Mini Trans-Blot ^{TM} tank and the tank was cooled by inclusion of an ice reservoir. A constant current of 300mA was applied for 105 minutes.

2.2.18.4 Immunological Detection of Protein

Following transfer of the proteins to the nitrocellulose membrane, the membrane was removed and any remaining protein blocked by incubation in 15 mL western blot blocking buffer for 2 hours with gentle agitation on a platform shaker. The blocking buffer was removed and membranes incubated overnight with HRP-conjugated primary antibodies (Table 2.6) diluted in western blot antibody diluent. On the

following day membranes were washed with western blot washing buffer three times for 5 minutes each wash. Immunoreactive protein bands were detected by incubation with enhanced chemiluminescence (ECL) (reagents from Amersham International Plc) for 3 minutes. The membranes were blotted on a paper towel, mounted onto an exposure cassette and covered with cling film. The membranes were then exposed to Kodak X-OMAT LS film for the appropriate time under dark room conditions and developed by KODAK M35-M X-OMAT processor.

2.2.18.5 Reprobing of Nitrocellulose Membrane

The used nitrocellulose membranes were stored at 4^{o}C in a sealed container containing TBST-0.1% until reprobing was desired. Antibodies were then stripped from the nitrocellulose membrane by incubating for 1 hour in 15 mL of stripping buffer at 60^{o}C on a shaker (Stuart Science Equipment). After the incubation period the stripping buffer was discarded and membranes were rinsed in western blot wash buffer four times for 15 minutes to remove residual stripping buffer. Finally, immunological detection of protein was carried out as described in section 2.2.18.4 however the blocking step was not required after stripping.

2.2.18.6 Scanning Densitometry

X-ray films were scanned on an Epson perfection 1640SU scanner using Adobe photoshop 5.0.2 software. The captured images were then normalised to a control and quantified using Scion Image (Scion Corp., Maryland, USA).

Table 2.6: List of western blot antibodies used

Antibody	Species	Manufacturer	Code
pERK	Mouse	Santa Cruz Biotechnology	SC-7383
Total ERK	Rabbit	Santa Cruz Biotechnology	SC-94
pJNK	Rabbit	Cell Signalling	9251S
Total JNK	Rabbit	Santa Cruz Biotechnology	SC-571
GAPDH	Rabbit	Cell Signalling	2118S
anti-mouse IgG	Donkey	Jackson ImmunoResearch Laboratories	715-005-150
anti-rabbit IgG	Goat	Jackson ImmunoResearch Laboratories	111-005-144

2.2.18 Serum nitric oxide assay

Serum nitric oxide levels were determined by measuring one of its stable oxidation products, nitrite (NO_2-) by Griess assay. Following euthanasia on day 28 post EAE induction, the thoracic cavity was opened and a small incision made in the right ventricle to allow collection of whole blood in a sterile 1 ml syringe. Samples were centrifuged at 13,000 rpm for 15 minutes at 4 °C and serum retained and stored at -20 °C. Griess microplate assays were performed using the Griess reagent kit for nitrite determination (G-7921, Molecular Probes; Invitrogen) per manufacturers' guidelines. For this, protein was removed by adding 15 mg/ml zinc sulfate ($ZnSO_4$) to 100 µl serum samples, and centrifuged at 13,000 rpm for 10 minutes. 75 µl of supernatant was added to each well of a 96 well plate, together with 10 µl Griess reagent and 65 µl deionized water, and incubated for 30 minutes at RT. Absorbance was measured at 548 nm in a spectrophotometric microplate reader. Nitrite concentrations were determined using a standard curve of known nitrite concentrations between 1-100 µM.

2.2.19 Statistics

All data are shown as mean ± SEM. The distribution of each data set was determined using the normality test tool on minitab. Normally distributed data was analysed by two-tailed, unpaired student's t test and data not normally distributed was analysed by Mann-Whitney U test on minitab. Statistical analysis of EAE clinical score data was performed using 2-way ANOVA with repeated measures and bonferroni post hoc tests on OriginPro. A *P* value of less than 0.05 was considered significant.

3 Analysing the expression of MAPKs and MKPs in EAE, an animal model of MS

3.1 Introduction

EAE is the most widely used animal model in the study of MS, causing a demyelinating CNS inflammation which resembles the key pathological features of MS [69], [70]. This response is driven by myelin-specific T cells which migrate across the BBB to the CNS. Here they become re-activated via presentation of antigen and inflammatory mediators, predominantly cytokines, which induce further CNS infiltration of circulating mononuclear phagocytes to the CNS which themselves become activated along with resident phagocytic cells (e.g. microglia and astrocytes). Subsequent inflammation, demyelination, axonal loss and oligodendrocyte apoptosis occur due to the damaging effects of activated phagocytic cells as well as the inflammatory and cytotoxic mediators produced by activated T cells and B cells.

MAPKs are protein kinases that have a critical role in signal transduction pathways involved in cellular responses initiated by extracellular stimuli such as growth factors, chemical and physical stress or inflammatory cytokines. Once activated, MAPKs can regulate several key cellular functions including cell proliferation and differentiation, apoptosis and inflammatory gene activation, among others. In particular, MAPKs have been shown to be important in T cell and B cell proliferation, differentiation and function, as well as in cytokine production within DCs and macrophages; all key mediators of EAE pathogenesis. [269]–[272] Therefore it is likely that the MAPK pathway is a key component in the molecular response leading to EAE pathogenesis. Several studies utilising MAPK KO mice further support this hypothesis [273]–[275].

As discussed in Chapter 1, the MAPK signalling cascade is a very complex pathway due to the various stimuli, receptors and protein kinases involved. In addition, the

outcome of MAPK phosphorylation is determined by the duration and extent of activation, therefore various mechanisms have developed to regulate MAPK activity. One of the most prominent examples of this is the MKPs, enzymes which dephosphorylate phosphotyrosine and phosphothreonine residues, thus deactivating MAPKs [276], [277].

Therefore, the aims of this chapter were firstly to establish a working model of EAE, and then characterise the immunological changes associated with disease onset and progression. Following this, expression and activation of the main MAPKs, ERK, JNK and p38, in EAE tissue was assessed. Finally, the expression of selected MKPs within CNS and lymphoid tissue of EAE mice was investigated to determine whether there is an association between MKP expression levels and EAE severity, with emphasis on one particular MKP of interest, MKP-2.

3.2 Results

3.2.1 EAE induction and monitoring of disease progression

EAE was induced in 8 week old female C57BL/6 mice following immunization with myelin oligodendrocyte glycoprotein peptide fragment 35 - 55 (MOG_{35-55}). MOG is a protein found exclusively within the CNS and is expressed on the surface of oligodendrocytes and on the myelin sheath that surrounds axons. MOG_{35-55} was emulsified in CFA and injected subcutaneously in the lower back on day 0. In addition, mice received PTX i.p. on day 0 and day 2 (Fig 3.1 A).

Two control groups were included, a naïve group which did not receive any immunisations and a PBS group which received PBS in place of MOG_{35-55}. This group was included to investigate any non MOG-specific response caused by the CFA supplemented with M. *tuberculosis* and PTX. Mice were randomly allocated to each group per recommendations set out in the ARRIVE guidelines [268]

Mice were subsequently monitored daily for clinical signs of disease, and assigned a score between 0 and 5 based on a standard EAE scoring system (Fig 3.1 B).

(A)

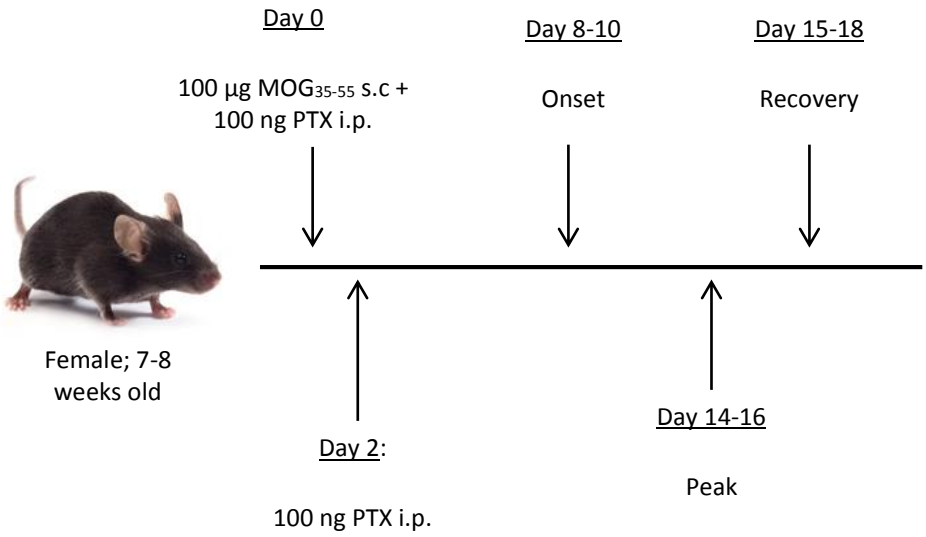

(B)

Score	Sign
0	No clinical signs of disease
0.5	Partial loss of tail tone
1.0	Complete loss of tail tone
1.5	Altered gait
2.0	Hind limb weakness
2.5	Paralysis of one hind limb
3.0	Complete hind limb paralysis
3.5	Hind limb paralysis and significantly reduced mobility
4.0	Bilateral paralysis
5.0	Moribund

Figure 3.1: EAE induction and clinical scoring. (A) Schematic diagram showing the method of EAE induction and time course of disease development. (B) Standard clinical scoring system used to evaluate disease severity.

As shown in Fig 3.2 A, naïve and PBS mice did not develop any clinical signs of disease, and therefore all mice within these groups maintained a clinical score of 0 over the full period of the experiment. Mice immunized with MOG_{35-55} developed a monophasic disease course, which is typical with the use of this particular initiating agent in C57BL/6 mice. EAE onset occurred around day 8 – 9. By day 10, 50 % of MOG mice were displaying clinical signs of EAE (Fig 3.2 B). Disease incidence reached a peak of 90 % by day 14 (Fig. 3.2 B). Most mice reached their maximum level of EAE severity between day 16 and 18, with the greatest average clinical score observed at day 16 (score = 2.25). From day 19 onwards mice began to gradually recover, with a steady decrease in clinical score. However full recovery was never achieved within the 28-day time course, mice still displayed an average clinical score of 1.4.

As well as checking for clinical signs of disease, we also monitored the weight of each animal throughout. Mice were weighed on day 0 and then daily from day 6 onwards and the relative percentage weight change calculated. Naïve and PBS mice, which did not develop EAE, steadily gained weight over the 4-week time course (Fig. 3.2 C). In contrast, the weight of MOG peptide-immunised mice fluctuated with the changes in disease severity. Weight began to decrease at disease onset around day 9-10. Mice were at their lightest at days 14-17 just as they were reaching maximum disease severity (between days 16-18). After this, mice steadily began to regain weight again as they recovered.

(A)

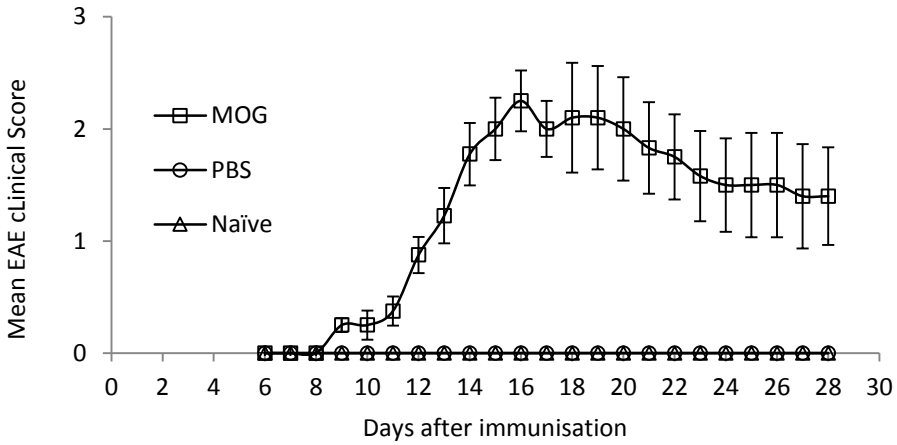

(B)

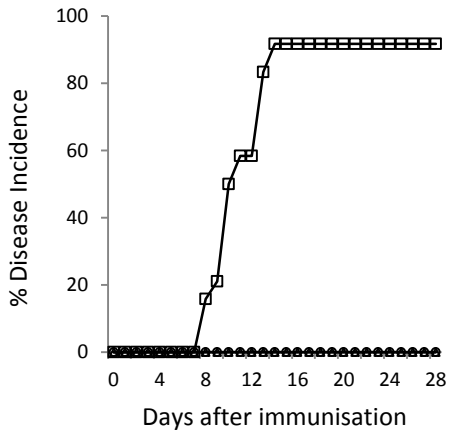

(C)

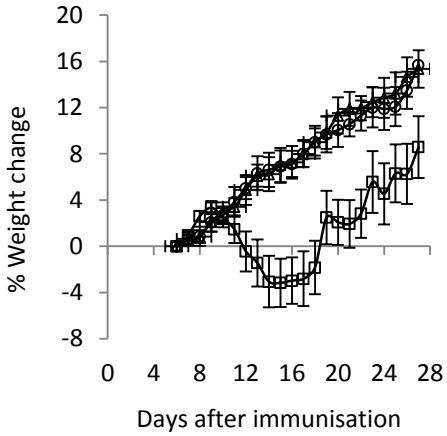

Figure 3.2: EAE clinical evaluation. C57BL/6 mice (Female, 8 weeks) were injected subcutaneously with 100 µg MOG_{35-55} or PBS in CFA supplemented with 2.75 mg/ml *M.tuberculosis* on day 0 as well as 100 ng of Pertussis toxin i.p. on day 0 and day 2. Results represent (A) mean clinical score ± SEM as assessed using the scoring system described in figure 3.1, (B) percentage disease incidence and (C) percentage weight change of all animals in each group. These graphs show representative data from one of three individual experiments. Naïve, n =3; PBS, n = 15; MOG, n= 20.

3.2.2 Histological analysis of CNS tissue

Histological examination was employed to allow us to investigate the extent of inflammation in mouse spinal cords at various stages of disease progression. Tissue was removed, flash frozen and cut into 7 micron sections. Haematoxylin and eosin (H & E) staining was then performed. The data show that there were no obvious signs of inflammation in PBS spinal cords at any time point (Fig 3.3 B). All PBS tissue analysed mirrored that of naïve counterparts (Fig 3.3 A).

In EAE mice there was increased cellular infiltration around the peak of disease, day 17 (Fig 3.3 C) compared to naïve and PBS tissue. Infiltration was predominantly focused within the white matter region of the spinal cord. In contrast, no obvious signs of inflammation or leukocyte infiltration were observed in day 9 or day 28 MOG peptide-immunised mice tissues.

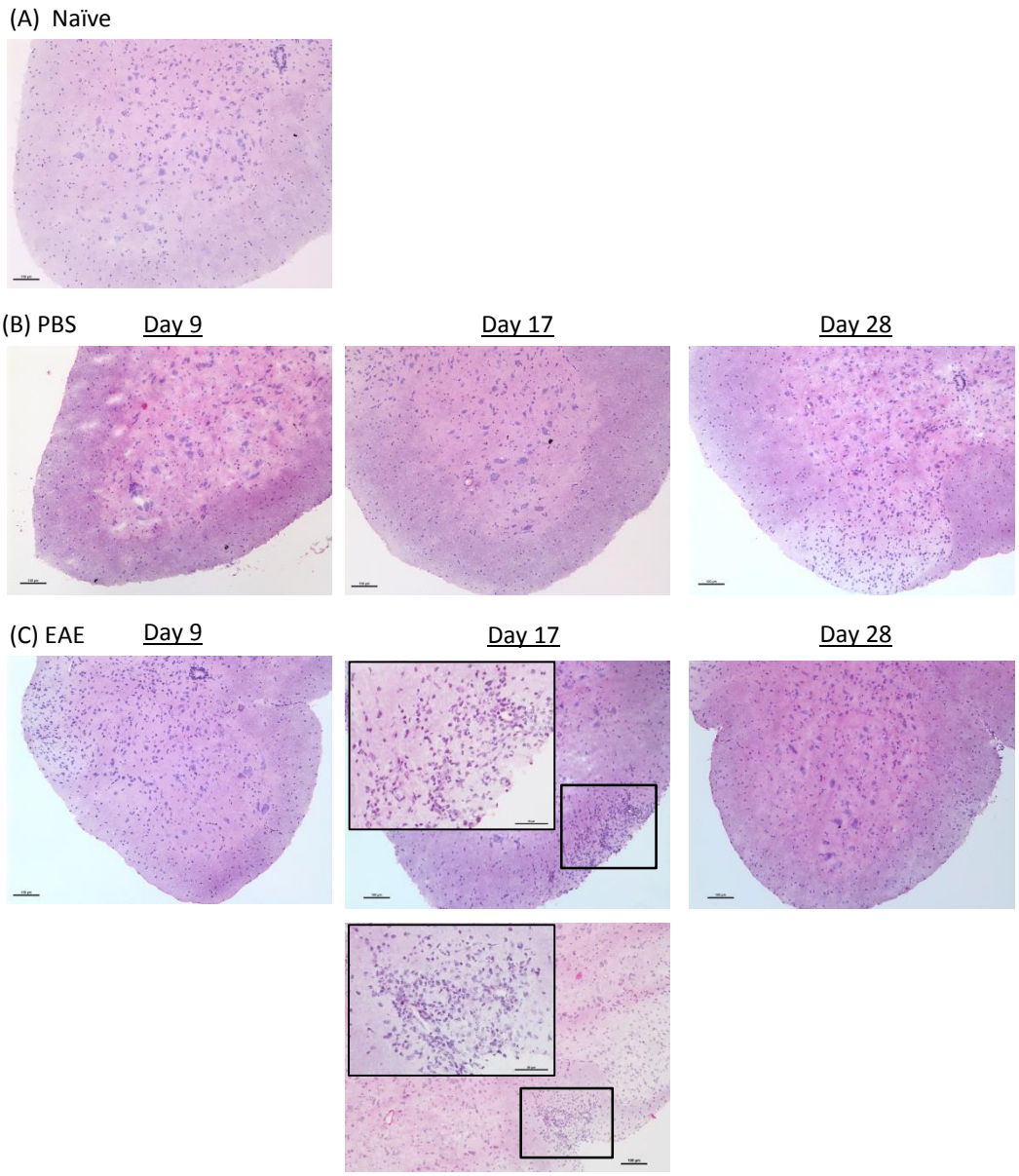

Figure 3.3: Immunopathology of Naïve, PBS and MOG_{35-55}-immunised mouse spinal cords. Spinal cords were removed from naïve mice or at EAE Day 9, 17 or 28 from MOG_{35-55} and PBS-immunised mice and flash-frozen in OCT. Seven micron sections were cut and stained with H & E. (A) Naïve tissue. Mice received (B) PBS in CFA or (C) 100 µg MOG_{35-55} in CFA. Primary images 100X magnification, scale bars = 100µm; EAE day 17 secondary images 400X magnification, scale bars = 50µm Images are representative of total mice in each group from one of three individual experiments. Naïve, n = 3; EAE and PBS, n = 6 each time point per experiment.

3.2.3 Increased MOG-specific cytokine production in EAE spleen cells

To examine the immunological phenotype and changes in cytokine profile over the course of EAE, we analysed cytokine production from splenocytes obtained from EAE mice or PBS control mice. Spleens were harvested at 9, 17 and 28 days post-immunisation and pooled within each group and analysed in triplicate. Day 9 (MOG n = 6; PBS n = 6); Day 17 (MOG n=7; PBS n=6); Day 28 (MOG n=7; PBS n=5). Thus differences represent technical replicates rather than biological replicates.

Single spleen cell suspensions were prepared and cultured with media alone or media supplemented with MOG_{35-55} peptide for 72 hours and the supernatant assayed by ELISA for expression of cytokines known to be essential in EAE pathogenesis. Cells were also stimulated with conA as a positive control to ensure cells were functional and cytokine production could be determined (data not shown).

No cytokine production was detected by spleen cells from PBS immunised mice cultured with media or MOG_{35-55} at any time point (Fig 3.4). EAE day 9 spleen cells cultured in media alone produced 1033±143 pg/ml IFNγ (mean±SEM). Upon antigen challenge this increased significantly, to 2058±37 pg/ml. As with day 9, by day 17 only EAE cultures contained detectable levels of IFNγ. When cultured with media alone, these cells produced 452±157 pg/ml. However, in response to MOG_{35-55}, IFNγ production increased to 2506±125 pg/ml. Antigen specific IFNγ production was reduced in day 28 EAE spleen cells (1548±37 pg/ml) compared to day 9 and day 17. No cytokine was detected in day 28 EAE spleen cell media cultures.

No detectable levels of IL-17 or IL-6 were observed in media-only cultures from all groups at each time point. Naïve and PBS mice spleen cells did not produce any detectable levels of IL-17 or IL-6 following *in vitro* culture with the antigen. Cells from EAE mice produced high levels of IL-17 at day 9 (1100±159 pg/ml), which had increased further by day 17 to 1267±19 pg/ml. IL-17 production then decreased in day 28 MOG_{35-55} cultured EAE cells. Interestingly, antigen specific IL-6 production was at its highest at day 9 (937±20 pg/ml) before decreasing by day 17 and day 28.

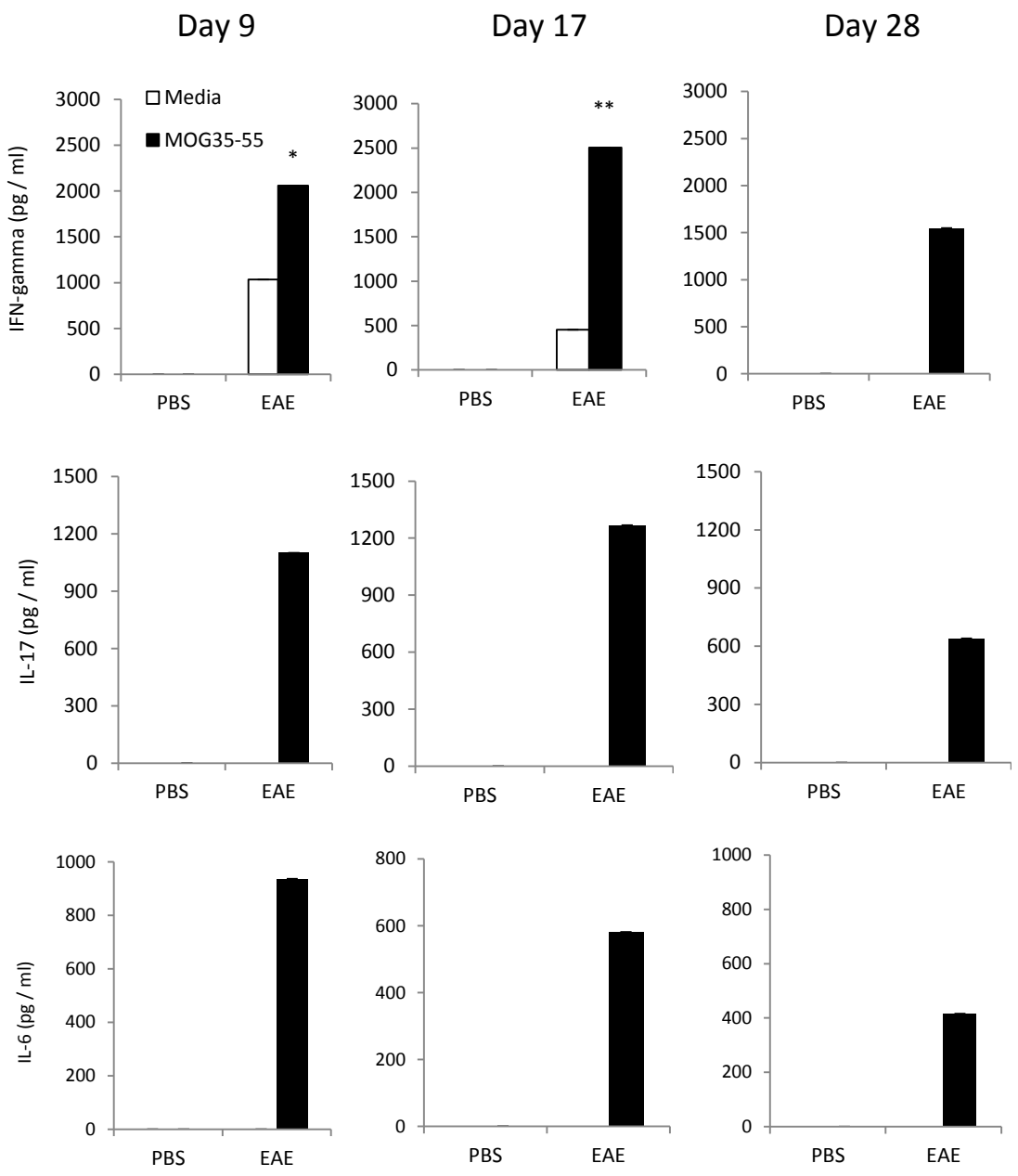

Figure 3.4: Cytokine production by spleen cells of PBS or MOG_{35-55} immunised mice. Spleens were harvested at Day 9, 17 and 28 after immunisation from PBS and EAE mice. Single cell suspensions were prepared and incubated ($4x10^6$ cells / well) in a 24-well tissue culture plate for 72 hours (37°C and 5% CO_2) in presence of complete RPMI alone or RPMI supplemented with 40 µg/ml MOG_{35-55}. Supernatants were collected and cytokine expression analysed by ELISA. Values represent mean ± SEM. Graphs show representative data from one experiment. Samples were pooled and analysed in triplicate. Day 9 (MOG n = 6; PBS n = 6); Day 17 (MOG n=7; PBS n=6); Day18 – 28 (MOG n=7; PBS n=5). *P<0.05; **P<0.01 compared to unstimulated EAE cells, two-tailed unpaired student's t test.

3.2.4 MAPK mRNA expression in EAE Lymphoid and CNS tissue

As mentioned previously (Section 3.1), EAE is initiated by autoreactive T cells primed and activated by APCs. The MAPK signalling pathway controls several important functions within these cells, including proliferation, differentiation and inflammatory gene activation, and thus it is an integral part of disease pathogenesis. Therefore, to establish what changes occur in MAPK expression at various stages of EAE development, we analysed the relative mRNA levels of total ERK, JNK and p38 within the spleen, draining lymph nodes (inguinal lymph nodes; dLNs) and CNS using quantitative PCR (qPCR).

3.2.4.1 Spleen and dLNs

Spleen and dLNs were collected from naïve and EAE day 21 mice. RNA was isolated using TRIzol and reverse transcribed to cDNA to allow analysis of mRNA expression by qPCR using the 2-ΔΔCT method, with values in EAE samples expressed as relative to naïve. This date (EAE day 21) was chosen as clinical severity is still high, and it allowed maximal use of various tissues and biological samples by other members of the lab group, thus adhering to 'the 3Rs' of animal testing (replace, reduce and refine).

An insufficient number of naïve samples prevented statistical analysis of these results (n=2), however our data suggest that the mRNA levels of total ERK2 and JNK1 may be increased in day 21 EAE spleens relative to naïve expression with mRNA on average 7.4-fold and 6.6-fold greater respectively than untreated mice (Fig 3.5 A), as well as ERK2 expression in EAE dLNs (2.3-fold relative to naïve; Figure 3.5 B). All other MAPKs analysed appear to remain unchanged in EAE samples but statistical analysis is required to confirm this.

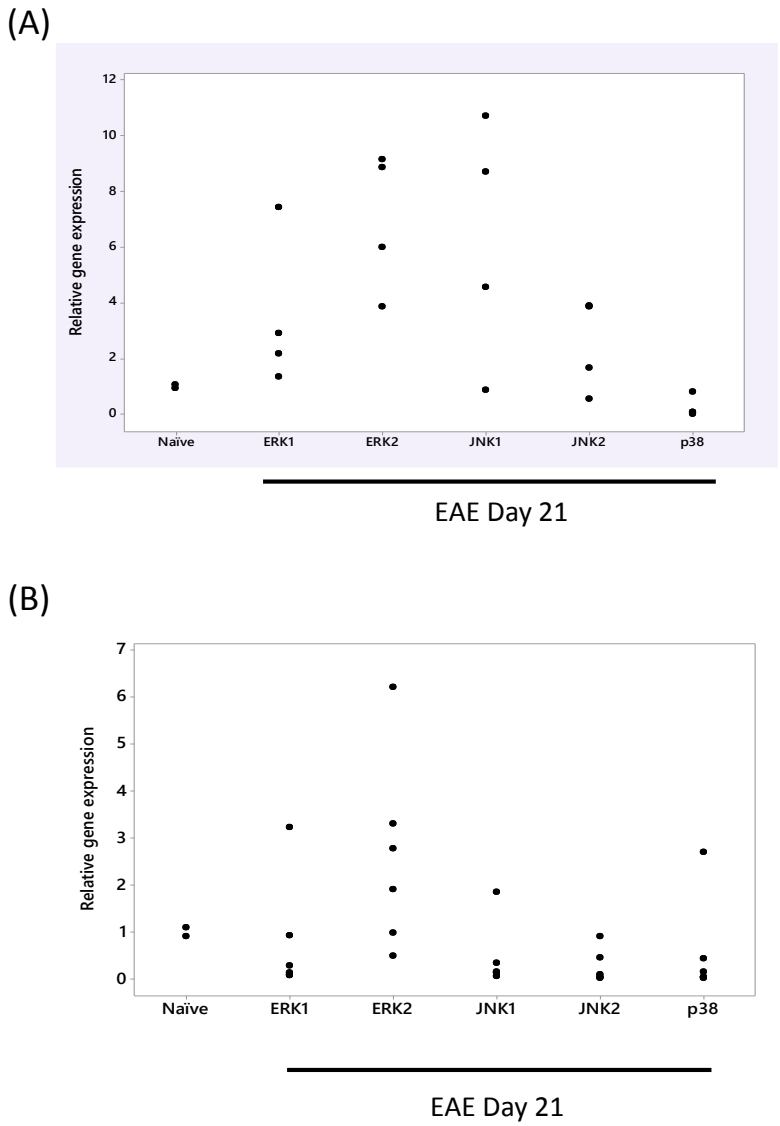

Figure 3.5: Relative MAPK mRNA expression in naïve and EAE day 21 spleen and dLN tissue. (A) Spleen and (B) dLNs were harvested from naïve and day 21 EAE mice. RNA was isolated and reverse transcribed to allow analysis of cDNA by quantitative PCR. The housekeeping gene TATA-binding protein was analysed simultaneously to allow normalisation of target gene expression. Results show changes in ERK1, ERK2, JNK1, JNK2 and p38 mRNA expression in MOG tissue relative to naïve mice tissues using the 2-ΔΔCT method. Naïve n = 2; EAE spleen n=4, EAE LN n=6.

3.2.4.2 Spinal cord

Spinal cord tissue was collected from PBS-control and EAE day 9, 17 and 28 mice. RNA was isolated using TRIzol and reverse transcribed to cDNA to allow analysis of mRNA expression by qPCR using the 2-ΔΔCT method, with values in EAE samples expressed as relative to naïve.

Upon disease onset at day 9, expression of all isoforms tested - ERK1, ERK2, JNK1, JNK2 and p38 - within MOG-immunised spinal cord tissue remained unchanged relative to PBS control mice (Fig 3.6 A). By day 17, the peak of EAE severity, expression of all MAPKs again remained unchanged in EAE mice compared to PBS (Fig 3.6 B). In contrast, JNK1 mRNA levels were significantly increased in EAE day 28 samples relative to PBS (2.9-fold; Fig 3.6 C).

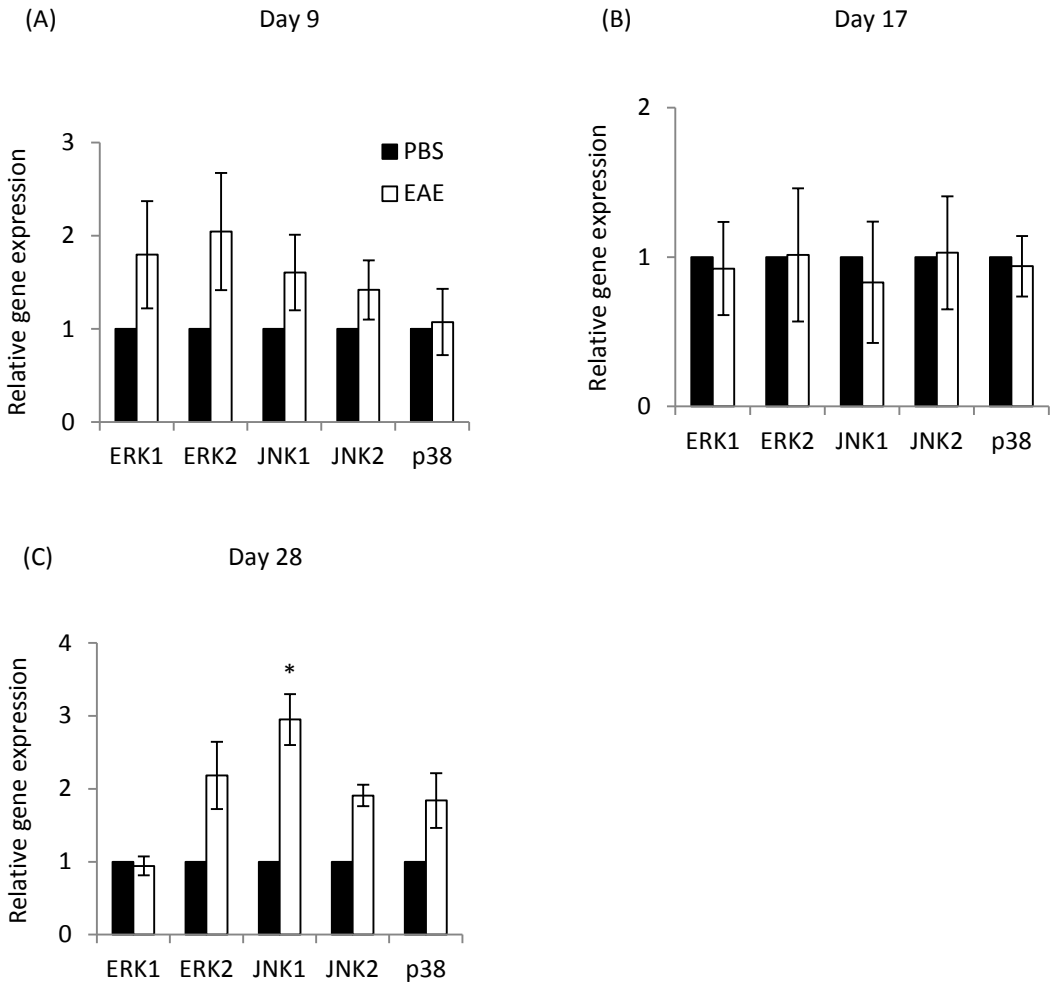

Figure 3.6: Relative MAPK mRNA expression in PBS and EAE spinal cords. Spinal cords were harvested at (A) day 9, (B) day 17 and (C) day 28 from mice immunized with either PBS or MOG. As described in the methods section, RNA was isolated and reverse transcribed to allow analysis of cDNA by quantitative PCR. The housekeeping gene tubulin beta 5 was analysed simultaneously to allow normalisation of target gene expression. Results show changes in ERK1, ERK2, JNK1, JNK2 and p38 mRNA expression EAE tissue relative to PBS using the 2-ΔΔCT method. Values represent mean ± SEM from 2 individual experiments. PBS n = 6; EAE n = 10 each time point. *P<0.05 compared to PBS, Mann-Whitney U test.

3.2.5 p-ERK and p-JNK expression in EAE CNS tissue

MAPK phosphorylation is a key component involved in regulation of inflammatory responses within T cells, B cells, dendritic cells and macrophages among others. The MAPKs are also known to be involved in the immune response of MS/EAE. Therefore ERK and JNK phosphorylation in EAE brain and spinal cord tissues was investigated by western blot. Membranes were probed for phospho-ERK/JNK, then stripped and re-probed for respective total kinase levels and GAPDH.

For densitometry analysis, GAPDH levels were used as a loading control. Total kinase expression was then used to ensure changes in phosphorylated levels were not simply due to the varying levels of ERK or JNK. Finally, phospho-ERK / JNK values in PBS and EAE mice were expressed as relative to naïve samples.

3.2.5.1 ERK

Firstly, p-ERK1 and p-ERK2 expression in naïve, PBS and EAE spinal cord tissue was examined (Fig 3.7 A-C; Fig 3.8 A-C). However analysis of more tissues is required to permit statistical analysis in order to confirm our results.

No changes in ERK1 or ERK2 phosphorylation were observed in day 9 or day 17 EAE samples relative to expression within naïve and PBS control samples (Fig 3.7 D).

By day 28 there remained no difference in p-ERK1 or p-ERK2 expression between naïve, PBS and EAE spinal cords, (Fig 3.8 D).

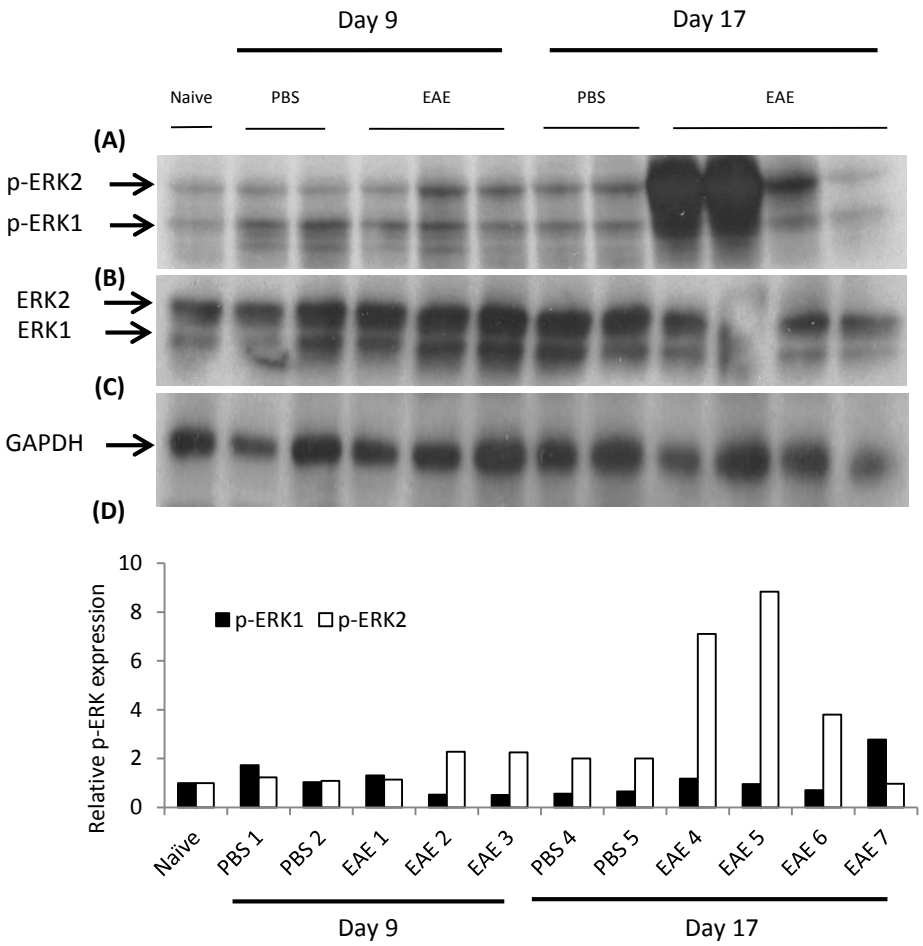

Figure 3.7: p-ERK expression in spinal cord tissue of naïve, PBS or EAE mice at day 9 and day 17. Spinal cords were harvested from naïve, PBS and MOG_{35-55} immunised mice at day 9 or 17 and whole protein lysate prepared using RIPA buffer. (A) p-ERK expression was analysed by western blotting. Membranes were stripped and re-probed for (B) total ERK and (C) GAPDH. (D) Densitometry was utilised to determine changes in p-ERK1 and p-ERK2 expression relative to naïve, with GAPDH used as a loading control and total ERK used as a control for variances in overall ERK levels between samples. Data shown is from one experiment.

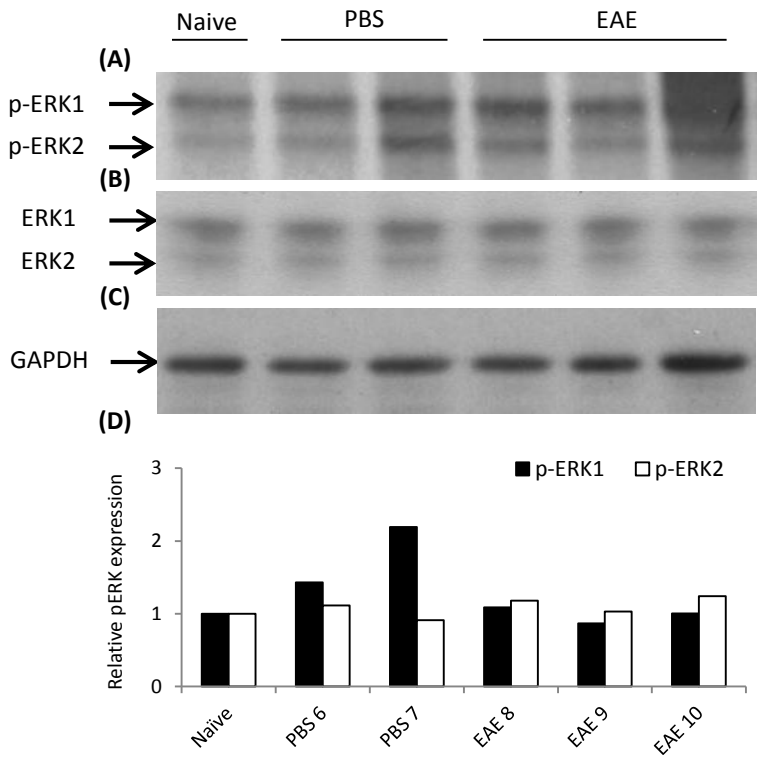

Figure 3.8: p-ERK expression in spinal cord tissue from naïve, PBS and EAE mice at day 28. Spinal cords were harvested from naïve, PBS and MOG_{35-55} immunised mice at 28 and whole protein lysate prepared using RIPA buffer. (A) p-ERK expression was analysed by western blotting. Membranes were stripped and re-probed for (B) total ERK and (C) GAPDH. (D) Densitometry was utilised to determine changes in p-ERK1 and p-ERK2 expression relative to naïve, with GAPDH used as a loading control and total ERK used as a control for variances in overall ERK levels between samples. Data shown is from one experiment.

We next analysed ERK phosphorylation in corresponding brain samples from day 9, day 17 (Fig 3.9 A-C) and day 28 (Fig 3.10 A-C) EAE-induced mice. Our data show no change in p-ERK1 expression in day 9, day 17 (Fig 3.9 D) or day 28 (Fig 3.10 D) EAE mice relative to naïve and PBS counterparts.

Levels of p-ERK2 were significantly increased in EAE day 9 brain tissues compared to PBS controls (Fig 3.9 D), while a similar trend was also observed at day 17 (Fig 3.9 D) and day 28 (Fig 3.10 D) however increased sample numbers would be required to confirm this via statistical analysis and thus increased phosphorylation at these later stages of EAE has to be confirmed.

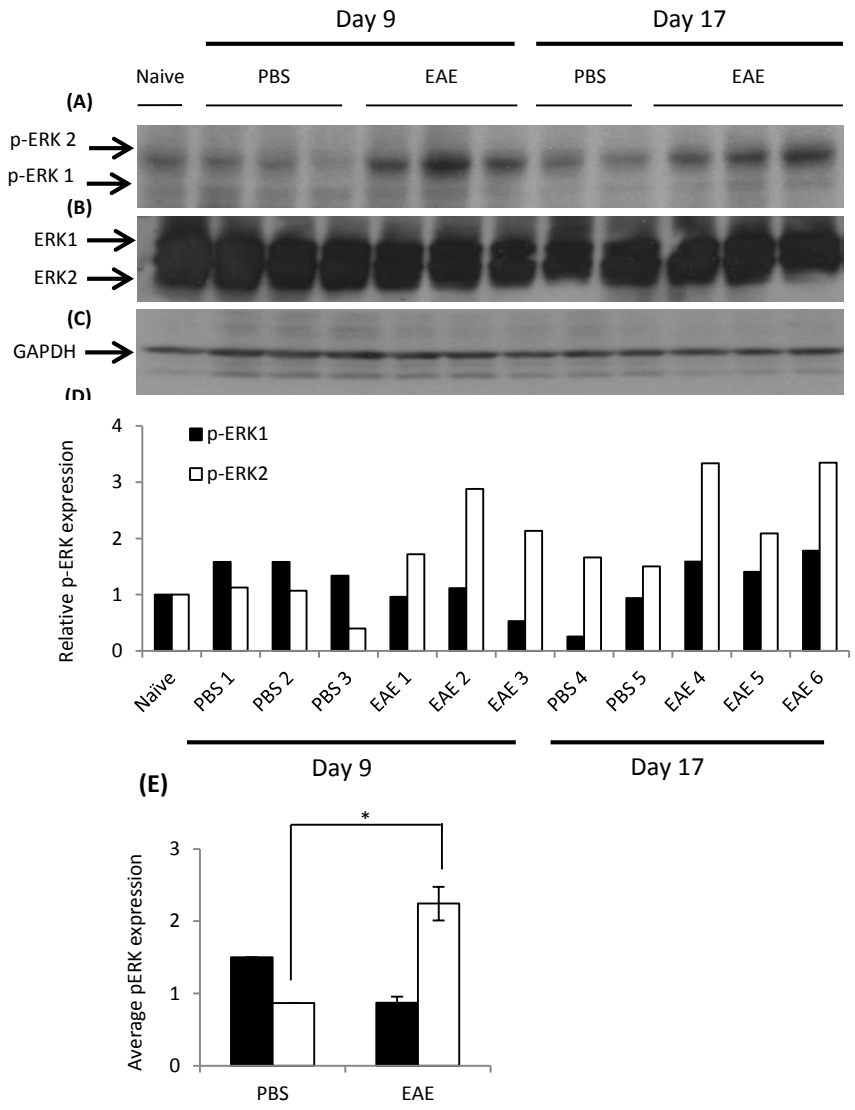

Figure 3.9: p-ERK expression in brain tissue of naïve, PBS or EAE mice at day 9 and day 17. Brains were harvested from naïve, PBS and MOG_{35-55} immunised mice at day 9 or 17 and whole protein lysate prepared using RIPA buffer. (A) p-ERK expression was analysed by western blotting. Membranes were stripped and re-probed for (B) total ERK and (C) GAPDH. (D) Densitometry was utilised to determine changes in p-ERK1 and p-ERK2 expression relative to naïve, with GAPDH used as a loading control and total ERK used as a control for variances in overall ERK levels between samples. (E) Graph represents average change in expression ± SEM in PBS and EAE groups at day 9. Data shown is from one experiment. *P<0.05 EAE p-ERK2 compared to PBS, two-tailed unpaired student's t test.

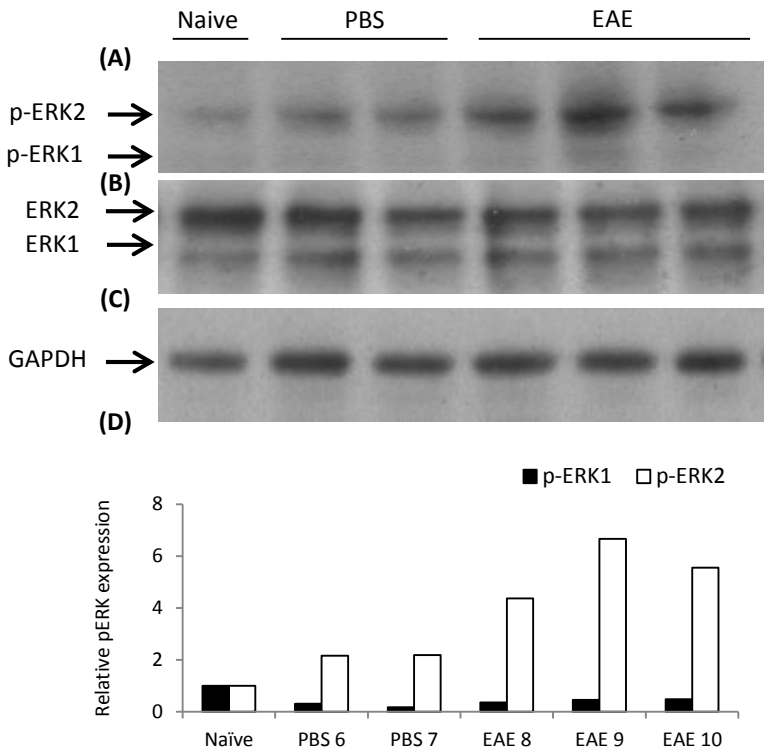

Figure 3.10: p-ERK expression in brain tissue of naïve, PBS and EAE mice at day 28. Brains were harvested from naïve, PBS and MOG_{35-55} immunised mice at 28 and whole protein lysate prepared using RIPA buffer. (A) p-ERK expression was analysed by western blotting. Membranes were stripped and re-probed for (B) total ERK and (C) GAPDH. (D) Densitometry was utilised to determine changes in p-ERK1 and p-ERK2 expression relative to naïve, with GAPDH used as a loading control and total ERK used as a control for variances in overall ERK levels between samples. Data shown is from one experiment.

3.2.5.2 JNK

Following this, we subsequently analysed phosphorylation levels of the two primary JNK isoforms, JNK1 and JNK2 (Fig 3.11; Fig 3.12). Our data suggest a possible, but inconclusive, increase in expression of p-JNK1 at day 9 EAE onset and day 17 EAE peak relative to naïve and PBS controls (Fig 3.11 D).

We observed no difference in p-JNK2 expression between naïve, PBS and EAE samples at day 9 or day 17 (Fig 3.11 D). Both JNK1 and JNK2 phosphorylation were unchanged in EAE day 28 spinal cords compared to naïve and PBS counterparts (Fig 3.12 D). However analysis of more tissues is required to allow statistical analysis to confirm this, and therefore these observations remain as yet inconclusive.

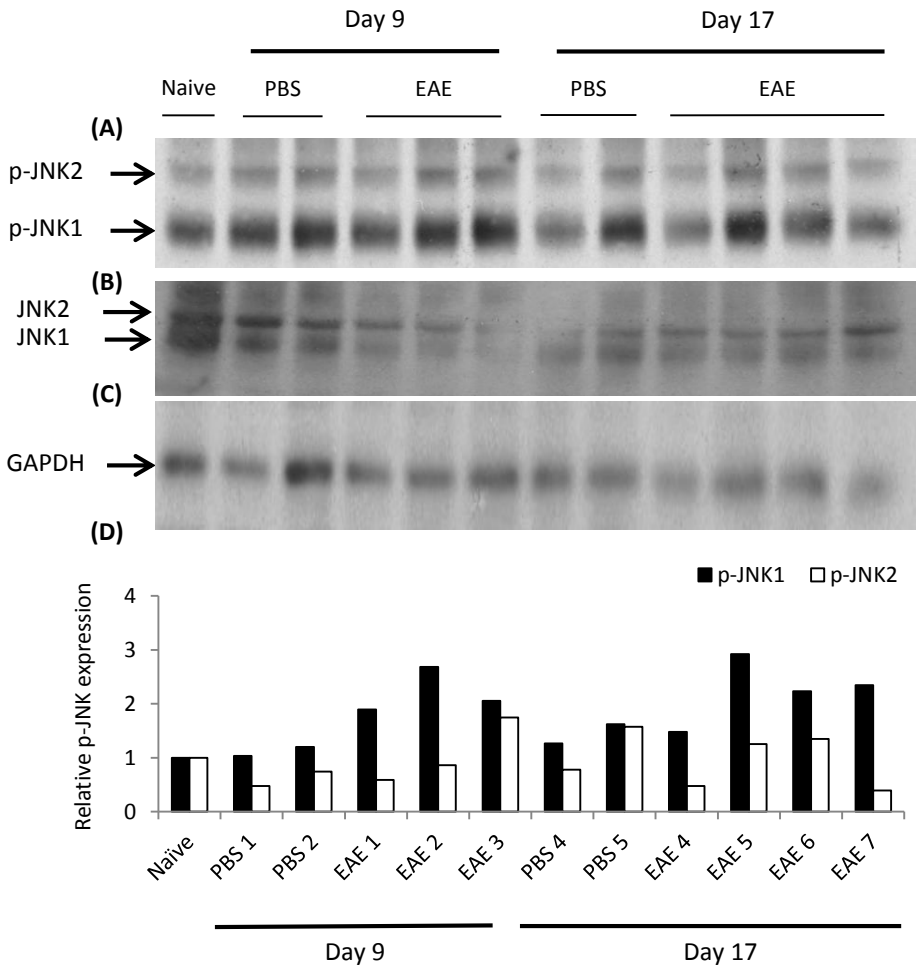

Figure 3.11: p-JNK expression in spinal cord tissue of naïve, PBS and EAE mice at day 9 and day 17. Spinal cords were harvested from naïve, PBS and MOG_{35-55} immunised mice at day 9 or 17 and whole protein lysate prepared using RIPA buffer. (A) p-JNK expression was analysed by western blotting. Membranes were stripped and re-probed for (B) total JNK and (C) GAPDH. (D) Densitometry was utilised to determine changes in p-JNK1 and p-JNK2 expression relative to naïve, with GAPDH used as a loading control and total JNK used as a control for variances in overall JNK levels between samples. Data shown is from one experiment.

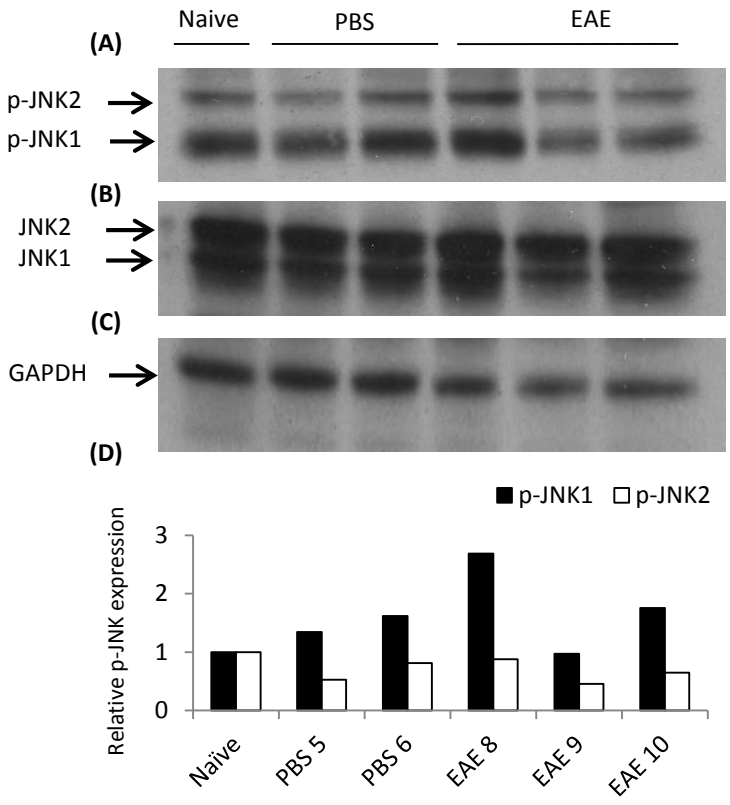

Figure 3.12: p-JNK expression in spinal cord tissue of naïve, PBS and EAE mice at day 28. Spinal cords were harvested from naïve, PBS and MOG_{35-55} immunised mice at 28 and whole protein lysate prepared using RIPA buffer. (A) p-JNK expression was analysed by western blotting. Membranes were stripped and re-probed for (B) total JNK and (C) GAPDH. (D) Densitometry was utilised to determine changes in p-JNK1 and p-JNK2 expression relative to naïve, with GAPDH used as a loading control and total JNK used as a control for variances in overall JNK levels between samples. Data shown is from one experiment.

In EAE brain tissue (Fig 3.13 A-C; Fig 3.14 A-C), the levels of p-JNK1 and p-JNK2 remained consistent between naïve, PBS and EAE samples at each time point analysed, day 9 (Fig 3.13 D), day 17 (Fig 3.13 D) and day 28 (Fig 3.14 D), thus suggesting no change in the level of JNK phosphorylation in brain tissue of EAE mice.

However analysis of more tissues is required to allow statistical analysis to confirm this between naïve and EAE samples, and between PBS and EAE samples at day 17 and day 28. There was no statistical difference between PBS and EAE samples at day 9.

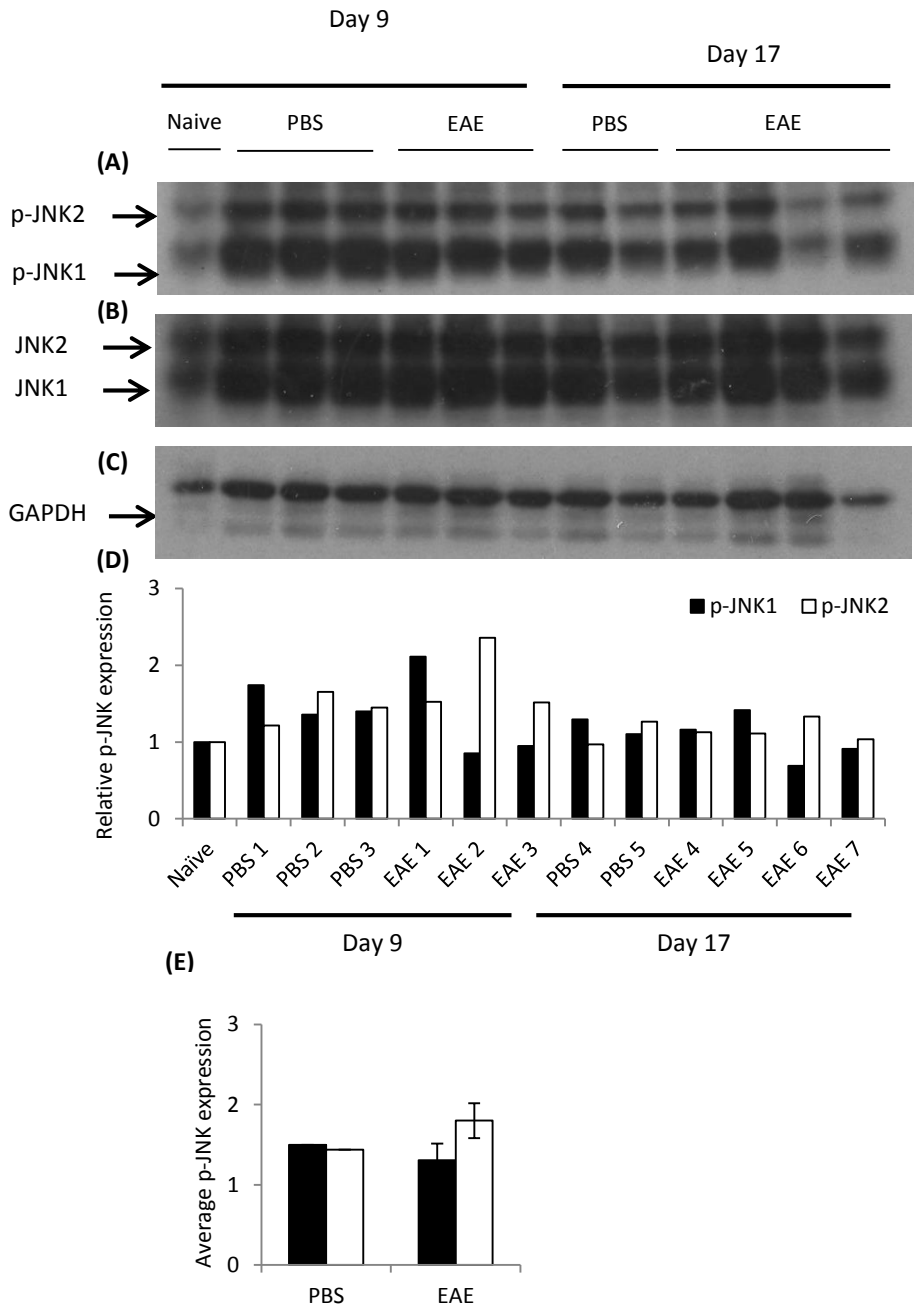

Figure 3.13: p-JNK expression in brain tissue of naïve, PBS and EAE mice at day 9 and day 17. Brains were harvested from naïve, PBS and MOG_{35-55} immunised mice at day 9 or 17 and whole protein lysate prepared using RIPA buffer. (A) p-JNK expression was analysed by western blotting. Membranes were stripped and re-probed for (B) total JNK and (C) GAPDH. (D) Densitometry was utilised to determine changes in p-JNK1 and p-JNK2 expression relative to naïve, with GAPDH used as a loading control and total JNK used as a control for variances in overall JNK levels between samples. (E) Graph represents average change in expression ± SEM in PBS and EAE groups at day 9. Data shown is from one experiment. Not statistically significant, two-tailed unpaired student's t test.

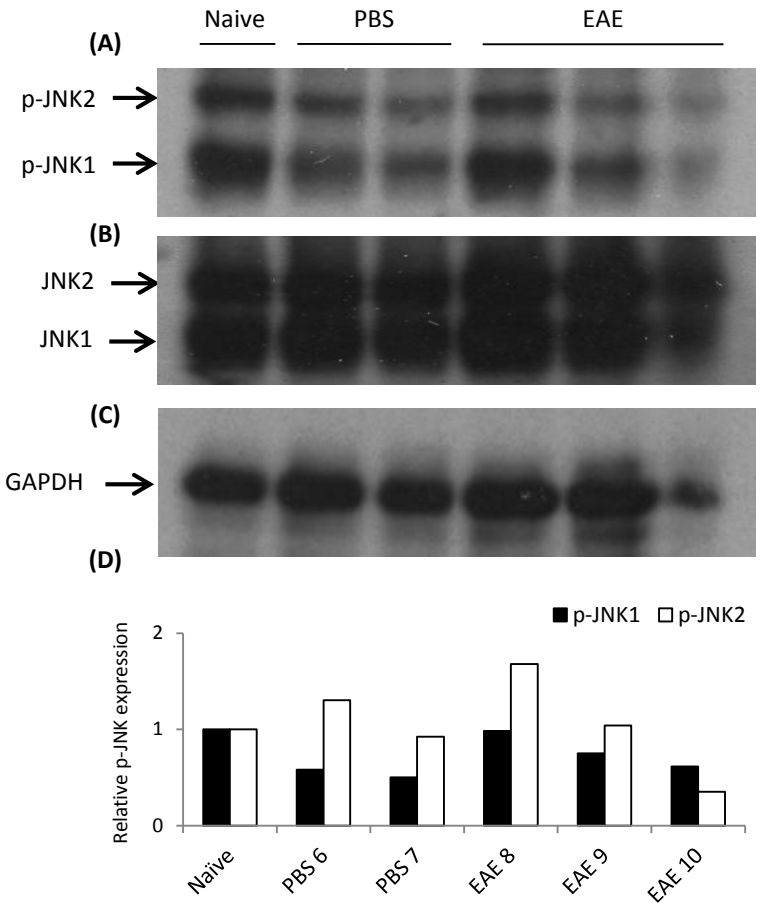

Figure 3.14: p-JNK expression in brain tissue naïve, PBS and EAE mice at day 28. Brains were harvested from naïve, PBS and MOG_{35-55} immunised mice at 28 and whole protein lysate prepared using RIPA buffer. (A) p-JNK expression was analysed by western blotting. Membranes were stripped and re-probed for (B) total JNK and (C) GAPDH. (D) Densitometry was utilised to determine changes in p-JNK1 and p-JNK2 expression relative to naïve, with GAPDH used as a loading control and total JNK used as a control for variances in overall JNK levels between samples. Data shown is from one experiment.

3.2.6 Analysing MKP-2 expression in EAE CNS tissue by immunohistochemistry

Regulation of MAPK activity is an integral part of the signalling pathway in the initiation and development of immune responses. One mechanism for this is MAPK dephosphorylation by MKPs. Previous reports have shown a role for MKP-1 in various conditions, including EAE. However, less is known about the role of the closely related MKP-2, which has a similar expression profile and functional repertoire. To understand the function of MKP-2 in the development of EAE, we first examined its expression in the CNS tissues.

Firstly, we investigated whether MKP-2 is expressed by CNS tissues and if EAE induction affected expression levels of MKP-2 in CNS tissue using immunohistochemical staining. Naïve and MOG immunised spinal cord and brain tissues were stained with two different anti-MKP-2 antibodies (details listed in Chapter 2, Table 2.1) using both biotin-conjugated and fluorescent-conjugated secondary antibodies (Fig 3.15 A, D). Several controls were also used, including isotypes and various negative controls (Fig 3.15 B, C, E, F). However successful specific staining was never confirmed as identical results were observed between MKP-2 WT and KO tissue stained with anti-MKP-2 as well as tissues stained with isotype antibodies. Therefore the staining obtained was deemed to be non-specific.

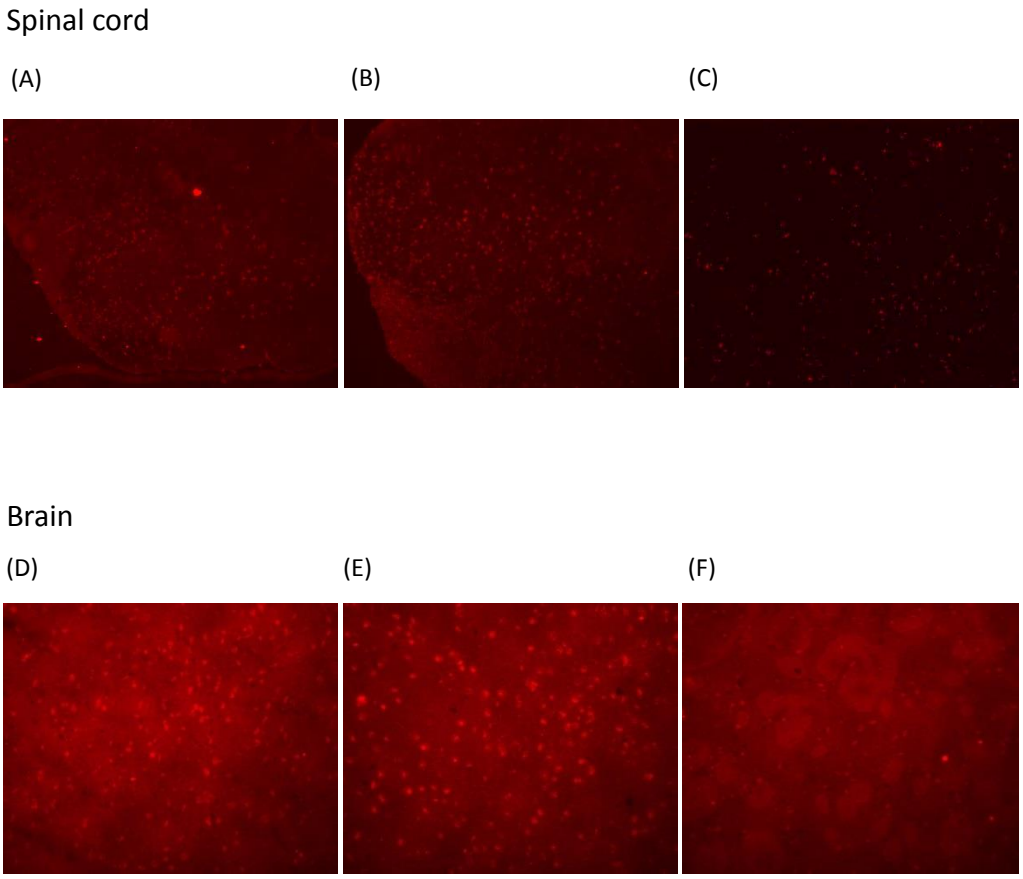

Figure 3.15: Immunohistochemical staining of MKP-2 CNS tissue. Brain and spinal cords were harvested from naïve C57BL/6, MKP-2 +/+ or MKP-2 -/- mice and flash frozen in OCT mounting compound. Tissue was cut into 7 micron sections and immunofluorescent staining performed. Naïve spinal cord stained with (A) rabbit anti-MKP-2 or (B) rabbit IgG isotype control. (C) MKP-2 -/- spinal cord stained with rabbit anti-MKP-2. Naïve brain sections stained with (D) rabbit anti-MKP-2 or (E) rabbit IgG isotype control. (F) MKP-2 -/- brain stained with rabbit anti-MKP-2. Secondary antibody was an Alexa Fluor 568 labelled goat anti-rabbit.

To ensure the experimental technique was okay, sections were also stained with anti-IL-22 and anti-IL-33, two antibodies known to work from previous experiments within our lab. We observed positive, specific staining for both of these controls (data not shown).

Following that we used embryonic fibroblast cell cultures, which are known to highly express MKP-2, as a final positive control. However no expression could be detected (Fig 3.16 A, B). From this, it was concluded that the functional problem was with the MKP-2 antibodies, which seemed unable to be utilised for IHC techniques. Therefore detection of MKP-2 expression had to be achieved using an alternative method.

(A) (B)

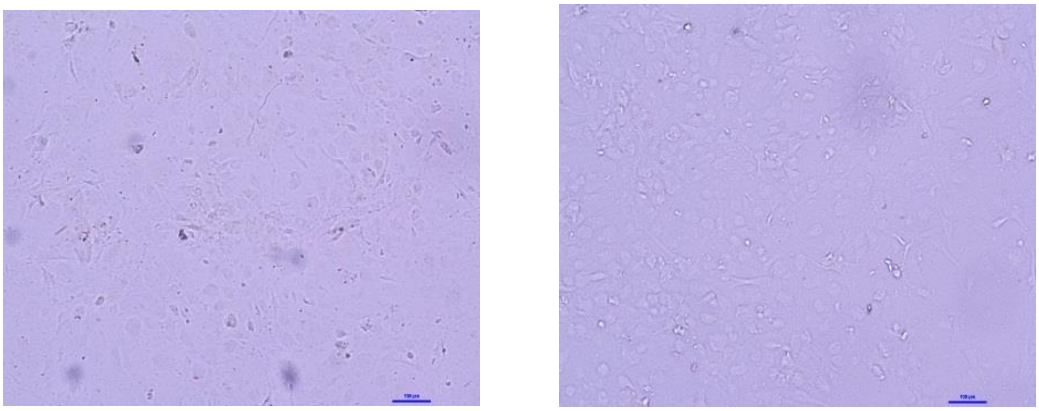

Figure 3.16: MKP-2 staining in mouse embryonic fibroblasts. (A) MKP-2 +/+ and (B) MKP-2 -/- mouse embryonic fibroblasts were cultured in multiwall chamber slides for 24 hours before staining with anti-MKP-2 antibody followed by a biotin-conjugated secondary antibody and Vector DAB substrate.

3.2.7 Effect of EAE on MKP mRNA expression

As immunohistochemical staining of MKP-2 was unsuccessful, we instead focused on analysing the mRNA expression of MKP-2, as well as other selected MKPs, in the CNS by qPCR. Spinal cords from PBS and MOG immunized mice were removed at days 9, 17 and 28. RNA was then extracted, quantified and reverse transcribed to allow analysis of mRNA expression by qPCR. Values in EAE samples are expressed as relative to PBS using the 2-ΔΔCT method.

3.2.7.1 MKP-2

Firstly, MKP-2 was analysed. On day 9, our data shows that MKP-2 mRNA expression is unchanged in EAE tissue relative to PBS (Fig 3.17). In contrast, by day 17, MKP-2 was significantly upregulated in EAE mice, with mRNA expression 3-fold higher than PBS controls. Equivalent levels of MKP-2 mRNA were observed at day 28 in EAE and PBS spinal cord tissue.

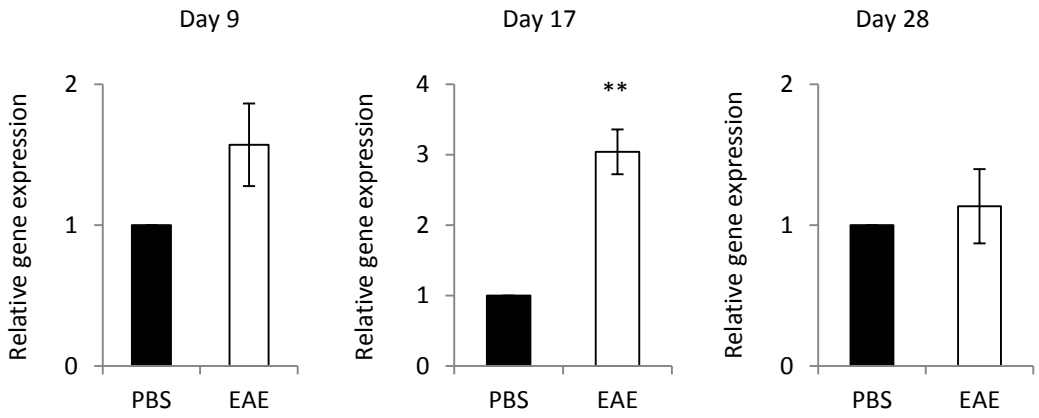

Figure 3.17: Relative MKP-2 mRNA expression in tissues of PBS or EAE mice. Spinal cords were harvested at day 9, 17 and 28 from C57BL/6 mice immunized with either PBS or MOG. RNA was isolated and reverse transcribed to allow analysis of cDNA by quantitative PCR. The housekeeping gene tubulin beta 5 was analysed simultaneously to allow normalisation of MKP-2 expression. Results show mean±SEM changes in MKP-2 mRNA expression in MOG immunised mice tissue relative to PBS using the 2-ΔΔCT method. Data is from two individual experiments. PBS n=6 at day 9 and day 17, n=7 at day 28; MOG n=7 at day 9, n=8 at day 17, n=9 at day 28. **P<0.001 compared to PBS, Mann-Whitney U test.

As well as MKP-2, we also analysed other MKPs/DUSPs. These were chosen based on previous links to EAE or other inflammatory/autoimmune disorders, as well as trying to ensure representation from different MKP sub-groups (Section 1.4).

3.2.7.2 MKP-1

MKP-1 mRNA expression between EAE and PBS control spinal cord tissues was analysed. Our data show that MKP-1 was potentially upregulated in day 9 EAE spinal cord tissue with a general, but not statistically significant, increase of 2.3-fold relative to PBS (Fig 3.18). However no differences in MKP-1 levels were observed at either day 17 or day 28 samples between EAE and mice.

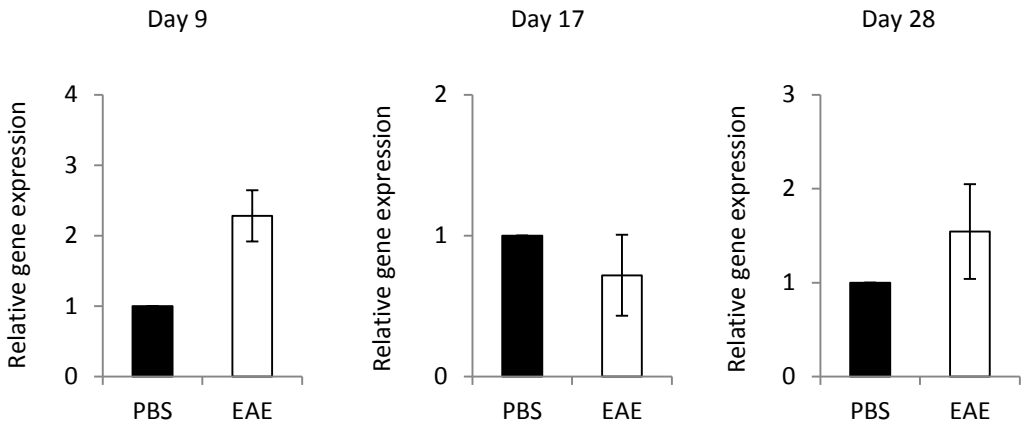

Figure 3.18: Relative MKP-1 mRNA expression in tissues of PBS or EAE mice. Spinal cords were harvested at day 9, 17 and 28 from C57BL/6 mice immunized with either PBS or MOG. RNA was isolated and reverse transcribed to allow analysis of cDNA by quantitative PCR. The housekeeping gene tubulin beta 5 was analysed simultaneously to allow normalisation of MKP-1 expression. Results show mean±SEM changes in MKP-1 mRNA expression in MOG immunised mice tissues relative to PBS using the 2-ΔΔCT method. Data is from two individual experiments. PBS n=7; MOG n=7 at day 9, n=9 at day 17, n=10 at day 28. Not statistically significant, Mann-Whitney U test.

3.2.7.3 DUSP5

DUSP5 is a nuclear MKP known to be involved in regulation of T cell functions and has been previously studied in a CIA model. In our study, DUSP5 mRNA expression in spinal cord tissues was unaltered, with no statistical differences between EAE mice and PBS controls at any time point analysed, day 9, day 17 or day 28 post immunisation (Fig 3.19).

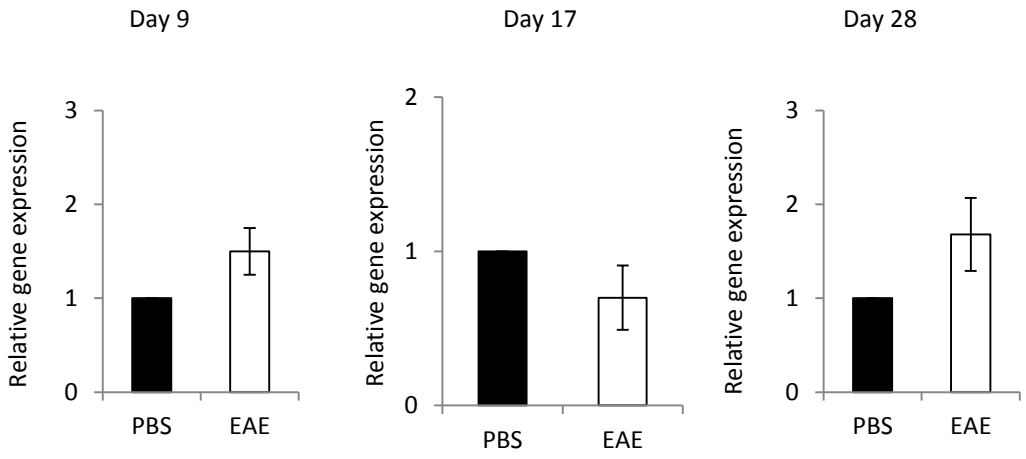

Figure 3.19: Relative DUSP5 mRNA expression in tissues of PBS or EAE mice. Spinal cords were harvested at day 9, 17 and 28 from C57BL/6 mice immunized with either PBS or MOG. RNA was isolated and reverse transcribed to allow analysis of cDNA by quantitative PCR. The housekeeping gene tubulin beta 5 was analysed simultaneously to allow normalisation of DUSP5 expression. Results show mean±SEM changes in DUSP5 mRNA expression in MOG immunised mice tissue relative to PBS using the 2-ΔΔCT method. Data is from two individual experiments. PBS n=6 at day 9, n=7 at day 17 and day 28; MOG n=8 at day 9, n=9 at day 17 and day 28. Not statistically significant, Mann-Whitney U test.

3.2.7.4 MKP-7

MKP-7 is expressed in both the nucleus and the cytoplasm. Like DUSP5, it is involved in regulation of various T cell functions. Our data show that MKP-7 mRNA expression is significantly decreased by 0.33-fold in day 17 EAE spinal cord tissue relative to PBS samples (Fig 3.20). No statistical differences were observed at day 9 or day 28 between EAE samples and PBS controls.

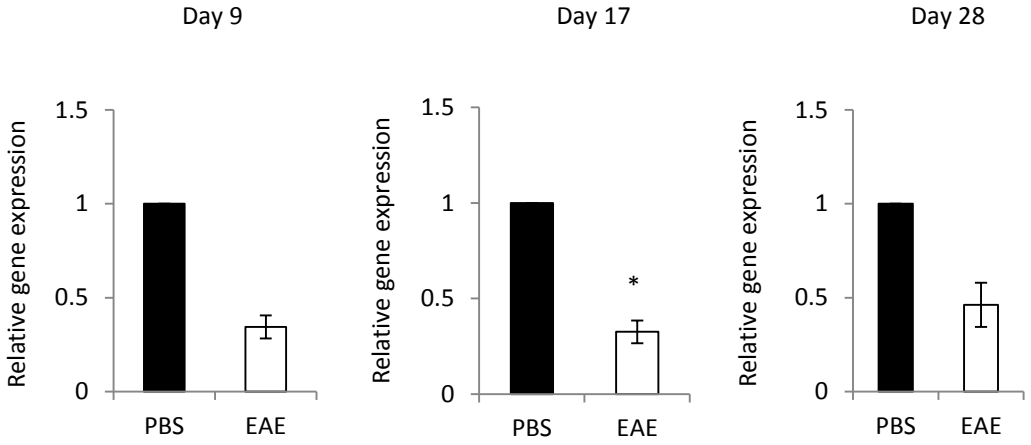

Figure 3.20: Relative MKP-7 mRNA expression in tissues of PBS or EAE mice. Spinal cords were harvested at day 9, 17 and 28 from C57BL/6 mice immunized with either PBS or MOG. RNA was isolated and reverse transcribed to allow analysis of cDNA by quantitative PCR. The housekeeping gene tubulin beta 5 was analysed simultaneously to allow normalisation of MKP-7 expression. Results show mean±SEM changes in MKP-7 mRNA expression in MOG immunised tissues relative to PBS using the 2-ΔΔCT method. Data is from two individual experiments. PBS n=3; MOG n=3 at day 9; n=5 at day 17 and day 28. *P<0.05 compared to PBS, Mann-Whitney U test.

3.2.7.5 MKP-5

MKP-5 also shows both nuclear and cytosolic localization. Previous research has suggested it is involved in EAE pathogenesis. Here we examined the expression of MKP-5 mRNA in the spinal cord tissues of EAE and PBS control group mice at day 9, day 17 or day 28 after immunisation. Our data show that there was a wide variation in MKP-5 mRNA levels between individual mice in both groups, and that there was no difference in the expression levels between EAE and PBS controls at any time point (Fig 3.21).

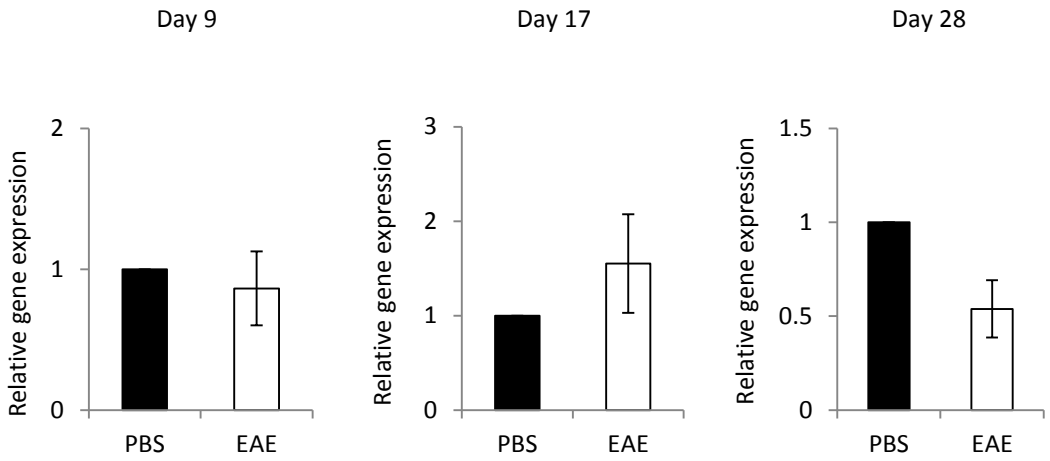

Figure 3.21: Relative MKP-5 mRNA expression in tissues of PBS or EAE mice. Spinal cords were harvested at day 9, 17 and 28 from C57BL/6 mice immunized with either PBS or MOG. RNA was isolated and reverse transcribed to allow analysis of cDNA by quantitative PCR. The housekeeping genes tubulin beta 5 was analysed simultaneously to allow normalisation of MKP-5 expression. Results show mean±SEM changes in MKP-5 mRNA expression in MOG immunised mice tissues relative to PBS using the 2-ΔΔCT method. Data is from two individual experiments. PBS n=3; MOG n=6 at day 9 and day 17; n=5 at day 28. Not statistically significant, Mann-Whitney U test.

3.2.7.6 MKP-x

The final MKP investigated, due to previous implications in EAE, was MKP-x. Our data show that the relative expression of MKP-x mRNA in EAE mice spinal cord tissues remained unchanged at day 9, day 17 and day 28 when compared to PBS controls (Fig 3.22).

In summary, this study has determined the mRNA expression levels of various MKPs including MKP-1, MKP-2, MKP-5, MKP-7 and DUSP-5 in the inflammatory spinal cord tissues from EAE mice at disease onset, peak and resolution stages and compared with tissues of PBS immunised mice which had no CNS inflammation. The main changes we observed were significantly increased MKP-2 mRNA expression in the spinal cord of EAE mice compared with controls at the peak of clinical severity, day 17 after immunisation, whereas MKP-7 is decreased at this time. The data may suggest MKP-2 and MKP-7 are involved in the development of CNS inflammation but potentially with different roles

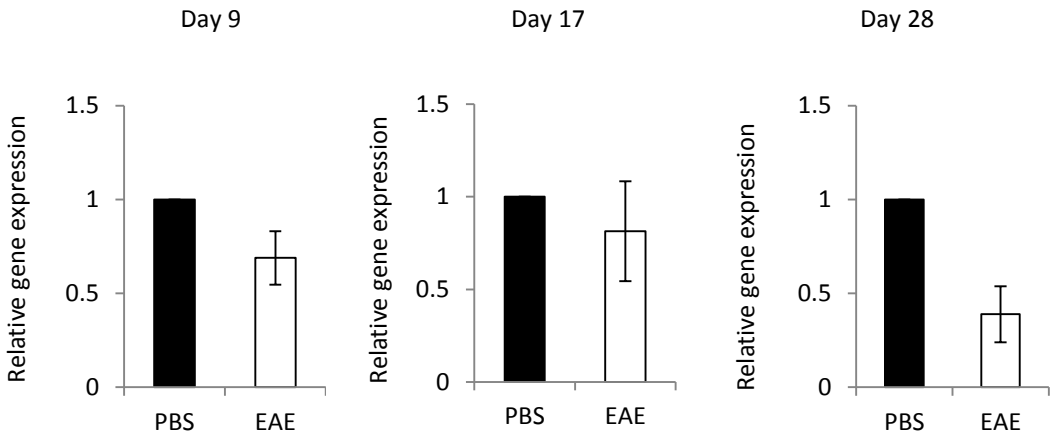

Figure 3.22: Relative MKP-x mRNA expression in tissues of PBS or EAE mice. Spinal cords were harvested at day 9, 17 and 28 from C57BL/6 mice immunized with either PBS or MOG. RNA was isolated and reverse transcribed to allow analysis of cDNA by quantitative PCR. The housekeeping gene tubulin beta 5 was analysed simultaneously to allow normalisation of MKP-x expression. Results show mean±SEM changes in MKP-x mRNA expression in MOG immunised mice tissues relative to PBS using the 2-ΔΔCT method. Data is from two individual experiments. PBS n=3; MOG n=6 at day 9 and day 17; n=5 at day 28. Not statistically significant, Mann-Whitney U test.

3.3 Discussion

In line with previous studies [278], [279], C57BL/6 mice developed an acute, monophasic form of EAE following immunisation with MOG_{35-55}. EAE severity reached a peak at days 16-18, with 90 % of MOG-immunised mice showing clinical signs of disease, confirming the effectiveness of MOG_{35-55} in inducing this animal model. Mice receiving PBS instead of MOG peptide did not develop any clinical signs of EAE, proving that EAE is only induced by specific CNS autoantigens, and not by adjuvants included in the immunisation (e.g. CFA, PTX) which only serve to enhance the immune response. To further discount for the role of these 'immunological boosts,' and to confirm the cytokine profile involved in EAE, spleens from naïve, PBS and MOG peptide immunised mice were harvested at different time points (initiation, peak and resolution stages of EAE) and cells re-challenged with MOG_{35-55} ex vivo. Only cells from mice originally immunised with MOG peptide in vivo responded to a second challenge from the antigen, with higher levels of IFNγ, IL-17 and IL-6 compared with naïve or PBS immunised groups, verifying the specificity of the autoimmune response in EAE. Naïve and PBS-immunised mice spleen cell cultures contained no detectable levels of cytokine following MOG stimulation, confirming a lack of autoreactive T cells when mice are only immunised with CFA and PTX without MOG peptide.

Increased IL-6 production by EAE mice spleen cells following MOG stimulation suggests an important role for this cytokine in EAE development. Previous research supports this finding, with increased IL-6 observed in MS serum and CSF samples [280], MS brain samples [281] and EAE animals [282], [283]. The functional role of IL-6 in EAE has also been investigated utilising IL-6 -/- mice. Animals deficient in this cytokine are fully resistant to EAE, associated with reduced proliferation and effector function of autoreactive T cells as well as reduced myelin-specific antibody levels [284]–[286], suggesting IL-6 exacerbates EAE severity. However IL-6 may be more involved in the early inflammatory response. Our data shows reduced expression at later time points, emphasising the shift to an adaptive response driven predominantly by T cells, particularly Th1 and Th17 cells as evidenced by increased IFNγ and IL-17 expression respectively at day 17, correlating with disease peak. These results are in

agreement with several previous studies which have also shown increased IL-17 and IFNγ, predominantly from $CD4^+$ T cells, in EAE mice as well as in MS lesions [89], [287]–[289]. In addition, EAE can be induced by adoptive transfer of myelin-specific Th1 and Th17 cells [88], [98], confirming the essential role of Th1 and Th17 cells and their cytokines in MS/EAE pathogenesis. IL-6 may also be downregulated at later stages of EAE in an attempt to reduce disease pathogenesis as IL-6 is known to be involved in the differentiation of MOG-specific Th17 cells [290].

Upon development of EAE, mice began to lose weight, with peak weight loss coinciding with peak of disease. This is in agreement with previous reports which have monitored the weight of mice following EAE induction [291], [292]. The decreased weight is most likely attributable to side effects of inflammation; but may also be a result of reduced appetite or inability to reach food and water due to paralysis. Mice were monitored daily and provided with wet food when EAE was most severe. Following amelioration of disease, MOG immunised mice began to regain lost weight and grow beyond initial starting weight.

As would be perhaps expected, there were no obvious indications of cellular infiltration or inflammation in spinal cord tissues of naïve or PBS-immunised mice at any time. This reflects the lack of CNS-specific response as no initiating myelin peptide has been given. In those mice that received MOG peptide immunisation, only at day 17 were there substantial signs of an inflammatory response within the CNS, predominantly in the white matter of each spinal cord. The majority of EAE lesions occur in the white matter [84]–[86], which would explain why most cells migrate to these areas. This was not seen at day 9, when the clinical signs of EAE manifest, or at day 28 when most mice have shown signs of recovery. Thus confirming that it takes time for cell infiltration to occur, and that disease pathogenesis is driven by these cells migrating across the disrupted BBB into the CNS, here becoming reactivated to cause axonal damage via myelin destruction.

MAPKs are involved in regulation of innate and adaptive immune responses, including T cell proliferation and differentiation and inflammatory gene activation within several different cell types including T cells, B cells, DCs, macrophages/microglia and astrocytes [178], [193], [269], [293]–[295]. As a result of this, the MAPK pathway is

considered a key component of the molecular response leading to MS and EAE pathogenesis [296]. Our data suggest that ERK2 may be involved in EAE pathogenesis as its relative mRNA expression appeared to be increased in EAE day 21 spleen and dLNs, although these changes could not be analysed for statistically differences due to the low sample n numbers and therefore this would have to be confirmed with further experiments. However we did observe a significant increase in ERK2 phosphorylation in EAE day 9 brain samples compared to PBS controls, suggesting a potential role within the CNS for ERK2 in EAE development. In contrast, total ERK1 mRNA levels were unchanged in spinal cord and spleen tissue, with no increase in p-ERK1 expression. These results would perhaps suggest ERK1 may not be as important in EAE development.

Most work looking at the role of ERK in EAE to date has primarily focused on ERK1, with conflicting results. In one study, increased EAE susceptibility in ERK1 -/- mice was observed; associated with enhanced CNS inflammation as well as increased Th1 cytokine production and MOG-specific antibody titers [297]. This would imply ERK1 is involved in regulating certain aspects of the autoimmune response associated with EAE and may, therefore, contribute to amelioration of disease. However, another group found that deletion of ERK1 had no effect on EAE severity, T cell effector function and CNS infiltration or cytokine production [298], suggesting ERK1 is not essential for EAE development. They also postulated a possible compensatory mechanism of ERK2, but with little evidence to back this up. Finally, Brereton *et al*., utilised an inhibitor of MEK1/2 (kinases which phosphorylate ERK1 and ERK2) to prevent ERK activation, and found EAE severity was significantly reduced along with Th1 and Th17 responses [273]. As both ERK1 and ERK2 activity were blocked in this experiment, it would suggest that both must be simultaneously targeted to successfully ameliorate EAE pathogenesis otherwise one will compensate in the absence of the other. Our data presented here remains inconclusive, but suggests ERK2 may warrant further analysis to determine a possible role in EAE development.

JNK1 may also be involved in EAE progression as a previous study reported decreased EAE severity in JNK1 -/- mice as a result of reduced MOG-specific Th1 responses [274]. In our study, total JNK1 mRNA expression was significantly increased in EAE

day 28 spinal cord tissue relative to PBS controls. In addition, although not statistically significant, our data display a possible increase in JNK1 mRNA in EAE spleen and p-JNK1 levels in EAE day 9 and day 17 spinal cords. However, as with ERK, this needs to be confirmed by repeating experiments to allow statistical analysis. JNK2 only displayed a moderate upregulation in spleen and day 9 spinal cord tissue and showed little change in phosphorylation. These results would suggest JNK2 is not as important in EAE pathogenesis as JNK1, and is in agreement with a previous report which showed that JNK2 deficient mice are fully susceptible to EAE, with no change in T cell proliferation or function and equivalent levels of demyelination and inflammation [299]. Similarly, in the CIA model, JNK1 deletion results in almost complete resistance while JNK2 -/- animals remain highly susceptible [300]. CIA is an animal model of rheumatoid arthritis, another condition associated with chronic inflammation. Taken together, the results of our study and others indicate that JNK1 is likely involved in the pathogenesis of inflammatory disorders while JNK2 appears to be more dispensable.

The final MAPK analysed, p38, does not appear to be involved in the immune response of EAE as mRNA expression remained unchanged in CNS, spleen and dLN tissue. However to confirm the role of p38 signalling in EAE pathogenesis in this study, phosphorylation levels would have to be analysed for a stronger representation of kinase activity. From previous literature, deletion of p38α results in mice being completely resistant to EAE [275]. To determine which cells p38α deficiency was most affecting, they generated mice selectively lacking this gene in T cells, marcophages or DCs. EAE was only ameliorated in p38α KO DC mice, with a lack of p38α signalling in DCs leading to reduced Th17 function. In contrast, mice with p38α deficiency in T cells or macrophages developed EAE equivalent to WT counterparts. This suggests p38 is essential in EAE pathogenesis, and that this is due to its role in DCs and the subsequent effect this has on T cell function. The role of p38 in EAE was further supported by another report which found that the use of a p38 inhibitor renders mice totally resistant to EAE [301]. The p38 MAPK pathway required continuous blocking by daily administration of the inhibitor, suggesting p38 is important in disease development as well as progression of the autoimmune response and that this effect was due, in part, to impaired IL-17 production by $CD4^+$ T cells.

The MAPK pathway is subject to negative regulation by MKPs, which inactivate MAPKs via dephosphorylation. Therefore MKPs can control the level of differentiation, proliferation and inflammatory cytokine production mediated by MAPK signalling. Very few studies to date have looked at MKPs in the context of autoimmune conditions such as MS and EAE; however a potential role for two particular phosphatases, MKP-1 and MKP-5, as well as the atypical DUSP22, in EAE pathogenesis has emerged [217], [243], [259]. In addition, MKP-2 has been linked to other inflammatory conditions including sepsis and acute-lung injury (ALI) [232], [233].

In the present study, a significant increase in MKP-2 mRNA expression was observed in spinal cord tissue at day 17, the peak of EAE severity, relative to PBS controls suggesting MKP-2 is likely to be involved in EAE pathogenesis. MKP-2 expression in EAE mice tissues returned to comparable PBS group levels by day 28. This suggests that MKP-2 possibly plays a role in the CNS-specific response leading to inflammation and axonal damage, before expression of this molecule is reduced to help facilitate recovery.

MKP-1 was the first discovered member of the MKP family [199] and, like MKP-2, is ubiquitously expressed throughout the body [201], with nuclear localisation [202] and varied substrate specificity in different cells [205], [206], [302]. It has previously been demonstrated that MKP-1 deficient mice are less susceptible to EAE development, associated with reduced $CD4^+$ T cell proliferation and CNS infiltration as well as decreased IL-17 and IFNγ production [217]. These data support a role for MKP-1 in EAE pathogenesis. Surprisingly our study did not show any changes in MKP-1 mRNA in spinal cord tissues at the onset, peak and resolution stages of EAE when compared to PBS immunised mice controls. Increased sample numbers in the experiment groups will help to determine whether the mRNA expression levels of MKP-1 are correlated with EAE severity.

We observed no difference in DUSP5 expression within the spinal cord at any time point between EAE and PBS mice, suggesting this gene may not be important in immune response within the CNS. DUSP5 has previously been shown to ameliorate CIA by decreasing the frequency of Th17 cells while increasing Treg cell populations

as well as reducing proinflammatory cytokine production and ERK activation [262]. Therefore DUSP5 may perform a similar protective role in this animal model by regulating the immune response.

Overall expression levels (based on Ct values) were low for MKP-7. This may be due to EAE being a predominantly Th1/Th17-driven disease rather than Th2 cells. Previous research has shown that MKP-7 expression decreases when $CD4^+$ T cells differentiate into Th1 cells but is upregulated in Th2 cells [248]. The upregulation of MKP-7 expression in Th2 was also supported by another study in which transgenic mice expressing a dominant negative form of MKP-7, specifically in T cells, display an enhanced Th1 phenotype, with a corresponding reduction in Th2 cytokine expression [248], [249]. Therefore if MKP-7 is more associated with Th2 responses, and can drive the immune response towards this phenotype; it would explain the decreased expression observed in the day 17 EAE spinal cord tissue.

Levels of MKP-5 and MKP-x mRNA were found to be unchanged in EAE mice relative to PBS controls at any time point, suggesting that neither is likely to be involved in the CNS-specific inflammatory response of EAE. Previous research contradicts this hypothesis. EAE severity, as well as $CD4^+$ T cell proliferation and infiltration into the CNS have been shown to be reduced in MKP-5 deficient mice [243]. This would in fact suggest an important role for MKP-5 in autoimmune pathogenesis via regulation of autoreactive T cell expansion and function. In addition, MKP-x deficient mice are more susceptible to EAE via enhanced T-cell-mediated immune responses [259] which alludes to a potential protective role in EAE.

In summary, EAE induced by immunisation with MOG, in addition to CFA and PTX, is a viable and antigen-specific disease model associated with many of the hallmarks of MS including limb weakness, inflammation and immune cell infiltration in the CNS and upregulation of key cytokines such as IL-17, IFNγ and IL-6. MAPK signalling has previously been linked with EAE. Our study observed potential but as yet inconclusive changes in ERK2 and JNK1 mRNA expression in the lymphoid organs, and ERK and JNK phosphorylation in CNS tissues of EAE mice relative to PBS controls. Our results also indicate that some MKPs, such as MKP-2 and MKP-7, may have roles in the development of EAE, but likely at different disease stages and in

different aspects of the autoimmune inflammatory response during disease development, perhaps in ameliorating disease or exacerbating CNS inflammation. The altered expression of these phosphatases is almost certainly an attempt to control MAPK activation and thus regulate the cellular functions initiated by these signalling cascades.

4 Investigating the role of MKP-2 in EAE development and pathogenesis

4.1 Introduction

It has previously been shown that MKP-2, modulates the inflammatory response during ALI [232]. Proinflammatory cytokine and chemokine production (TNFα, MIP1α), as well as neutrophil infiltration in the lungs, were both reduced in MKP-2 KO mice in response to LPS without impacting on clearance of bacteria. Another inflammatory model in which a potential role for MKP-2 has been investigated is sepsis. MKP-2 deficient mice displayed a significantly reduced mortality rate, associated with decreased serum levels of pro-inflammatory cytokines such as TNFα, IL-1β and IL-6 [233]. IL-10, an anti-inflammatory cytokine, was also reduced. At the MAPK signalling level, phosphorylation of ERK was increased while JNK and p38 phosphorylation decreased in KO bone marrow macrophages compared to WT, leading to decreased TNFα and IL-10 production in these cells.

These data clearly indicate that MKP-2 has an important function in diseases with a prominent inflammatory element. As EAE is an inflammatory disease of the CNS, and MKP-2 mRNA is significantly upregulated within the CNS during the course of this disease model as shown in Chapter 3, we hypothesise that MKP-2 exacerbates EAE development which is associated with changes in the immune response. The primary aim of this chapter therefore was to determine the function and underlying mechanisms of this phosphatase in the development of CNS inflammation using gene deficient mice.

To do this, MKP-2 deficient mice were utilised. Firstly, EAE was induced in MKP-2 KO mice and MKP-2 WT littermates, with EAE clinical score and body weight monitored throughout the course of disease. At selected time points, CNS tissue, lymphoid organs and serum samples were harvested and analysed to determine what changes occur in various aspects of the immune response, as well as the MAPK

signalling pathway, as a result of MKP-2 gene deletion. In addition, any potential compensatory effects exerted by other MKPs were investigated by analysing changes in the expression of selected MKPs in MKP-2 deficient mice during EAE development.

4.2 Results

4.2.1 MKP-2 KO mice

Mice were obtained from Professor Robin Plevin. Briefly, an 9.9 kb SwaI DUSP4/MKP-2 genomic fragment containing exons 2–4 was replaced by a PGK-Neo cassette flanked by LoxP sites (Fig 4.1) [228]. Both arms were introduced into a pBluescript vector in either side of the neomycin cassette. The final vector was transfected into a 129Sv mouse embryonic stem cell. Male chimeras were obtained and crossed with C57BL/6 female to obtain the F1 generation. Heterozygous mice were then backcrossed against C57BL/6 for further generations, with 5^{th}, 6^{th} and 7^{th} generations used during this thesis.

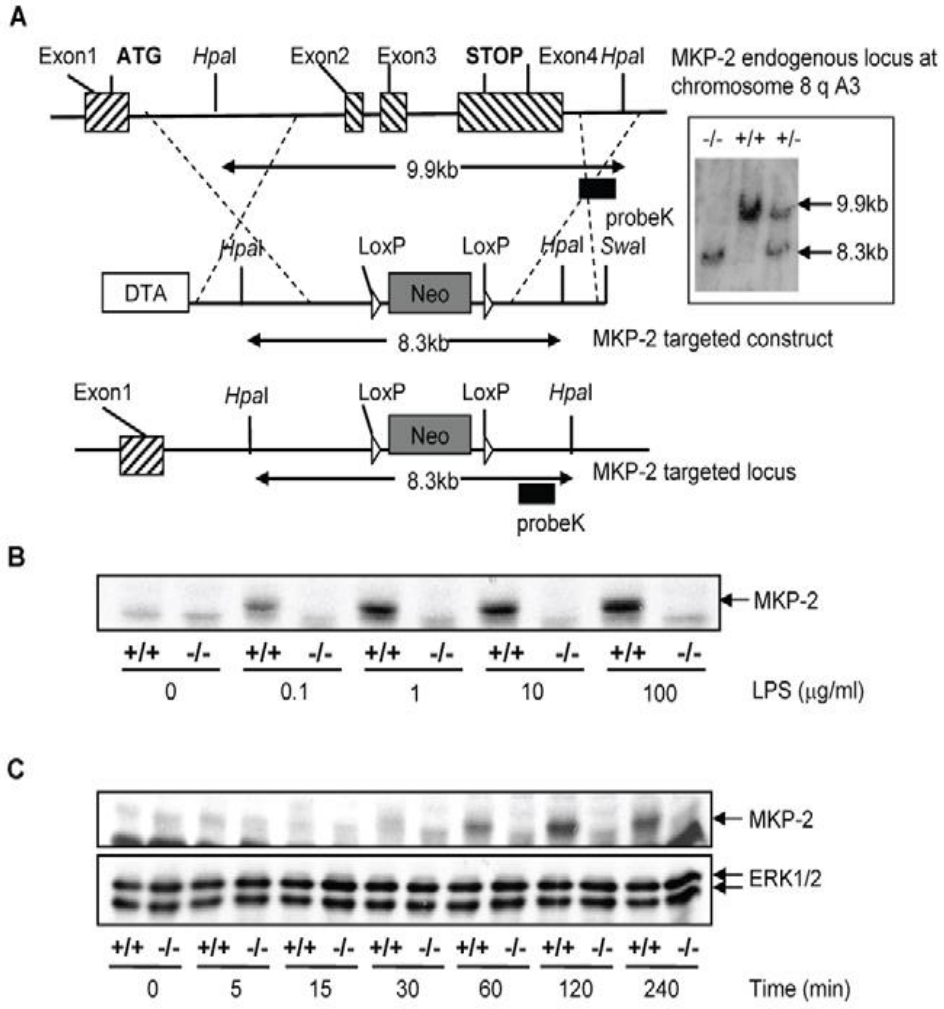

Figure 4.1: Al Mutairi at al., 2010. Generation of mice lacking DUSP4/MKP-2 gene by targeted homologous recombination. (Panel A): Schematic showing the DUSP4/MKP-2 gene locus, the targeted construct and the resulting targeted allele. Recombination events are indicated by dashed lines and show the replacement of an 8.3 kb SwaI DUSP4/MKP-2 genomic fragment containing exons 2–4 by the PGK-Neo cassette. SwaI and HpaI described the restriction sites for the respective enzymes. The pGK-Neo cassette is flanked by LoxP sites. DTA represents the negative selection cassette. (Inset) An example of the 39 southern blot analysis of mouse tail tip genomic DNA following digestion with HpaI using an external Probe K as indicated in panel A. The autoradiography revealed the 9.9 kb (wild type) and 8.3 kb (targeted) fragments representing the two different alleles discriminating wild type, heterozygote or homozygote mutant animals. B & C: Concentration (LPS mg/ml for 60 min) and time dependent (LPS 100 ng/ml) expression of MKP-2 in bone marrow derived macrophages. The blot represents at least 4 individual experiments. doi:10.1371/journal.ppat.1001192.g001

4.2.2 Confirmation of MKP-2 deletion

MKP-2 gene knockout was confirmed by PCR. Tail tips were removed from 6 week old, MKP-2 WT and MKP-2 KO mice and DNA extracted and analysed by PCR. All MKP-2 WT mice analysed contained only the 1.3 kb WT fragment while only the 2.4 kb KO fragment was detected in MKP-2 KO samples (Fig 4.2 A). However the KO primers produced a streaked band in some of the KO samples, perhaps due to issues with sample preparation or primer aliquots. Genotyping was repeated by others on a regular basis to ensure correct characterisation of the mice.

Successful gene deletion was further verified by quantitative PCR (qPCR). RNA was extracted from EAE day 28 spleen cells of MKP-2 KO and WT littermates cultured ex vivo with MOG_{35-55} peptide for 72 hours and MKP-2 mRNA expression by these cells analysed. No expression was detected in MKP-2 KO cells, confirming MKP deletion in these KO mice (Fig 4.2 B). Abundant expression of MKP-2 was observed in WT cells, confirming their MKP-2 WT phenotype, and also serving as a positive control for the primers.

(A)

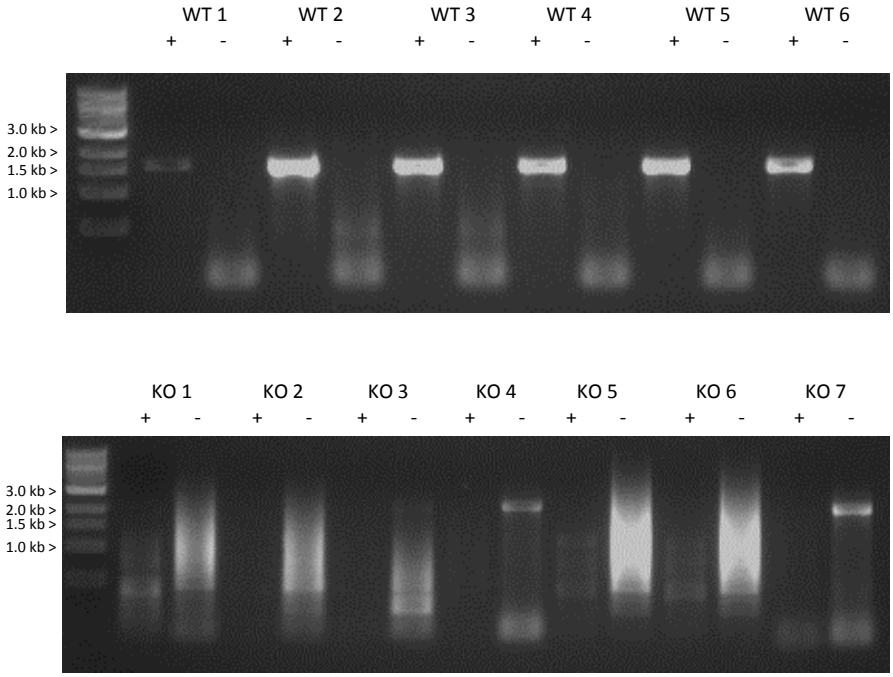

(B)

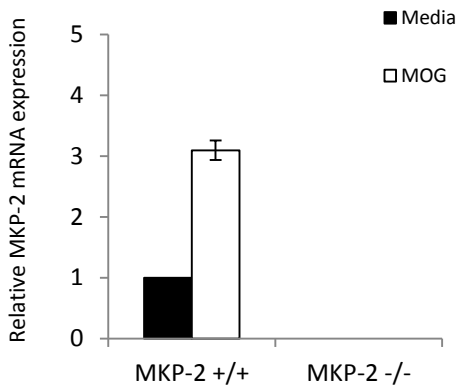

Figure 4.2: Confirmation of MKP-2 gene deletion by genotyping and analysis of mRNA expression. (A) DNA was extracted from MKP-2 +/+ and MKP-2 -/- tail tips and PCR performed using the GoTaq Polymerase kit. (B) RNA was extracted from MKP-2 +/+ and MKP-2 -/- spleen cells cultured with medium or 40 µg/ml MOG_{35-55} peptide and reverse transcribed to cDNA. MKP-2 mRNA expression was analysed by qPCR using Fast Sybr green master mix. Graph shows representative results (mean ± SEM) from one of two experiments. n=6 spleen samples pooled for cell culture.

4.2.3 Does MKP-2 gene deletion affect development of EAE?

In order to determine how prominent MKP-2 is in EAE development, we investigated the effect of MKP-2 gene disruption on disease development and progression. EAE was induced in MKP-2 KO and WT littermates following active immunization with MOG_{35-55} emulsified in complete freunds adjuvant (CFA) injected subcutaneously on day 0, and pertussis toxin (PTX) injected intraperitoneally on day 0 and day 2. Mice were monitored daily for signs of EAE and given a clinical score of between 0 and 5 based on severity of symptoms, as detailed in Fig 3.1.

Initial experiments were performed on MKP-2 KO mice from a 5^{th} generation backcross (termed PLE-5). Within the 4 experiments carried out, 2 contrasting EAE clinical phenotypes developed. On 2 occasions PLE-5 MKP-2 KO mice developed less disease than their WT counterparts (Fig 4.3 A). However EAE was more severe in MKP-2 KO mice in the other 2 repeats (Fig 4.3 B). There were no statistical differences between WT and KO within these experiments.

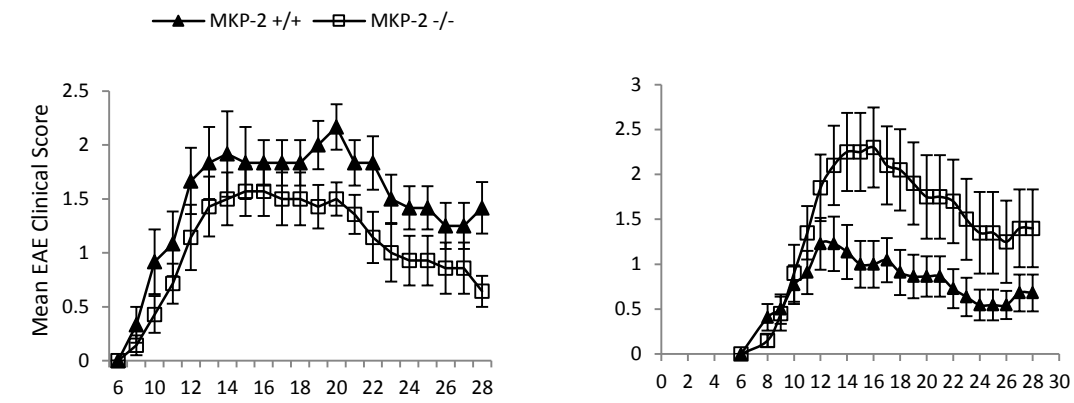

Figure 4.3: Mean EAE clinical score. PLE-5 MKP-2 +/+ and -/- mice (female, 7-8 weeks old) were injected subcutaneously with 100 µg MOG_{35-55} in CFA on Day 0 as well as 100 ng of PTX i.p. on day 0 and day 2. Results represent mean clinical score ± SEM of all animals in each group. Each graph represents one of two experiments. (A) n=7 per group. (B) n=6 per group. Not statistically significant, Two-way repeated measures ANOVA with bonferroni post-hoc test.

The inconsistency in results led us to repeat the immunisations, this time in 6th generation MKP-2 mice (PLE-6). As these are the product of another cross with naïve C57BL/6 mice, there should be less chance of genetic variation caused by going from a 129Sv background to a C57BL/6 mouse. Therefore we hoped that any results obtained from these mice could be considered more reliable, however a similar pattern emerged.

EAE was reduced in PLE-6 MKP-2 KO mice in 2 / 3 experiments (Fig 4.4 A) but in the final repeat EAE was more severe compared to MKP-2 WT mice (Fig 4.4 B). These data suggested that there was a difference in disease phenotype between the MKP-2 WT and KO animals, but it remained unclear if absence of the gene resulted in more or less severe EAE.

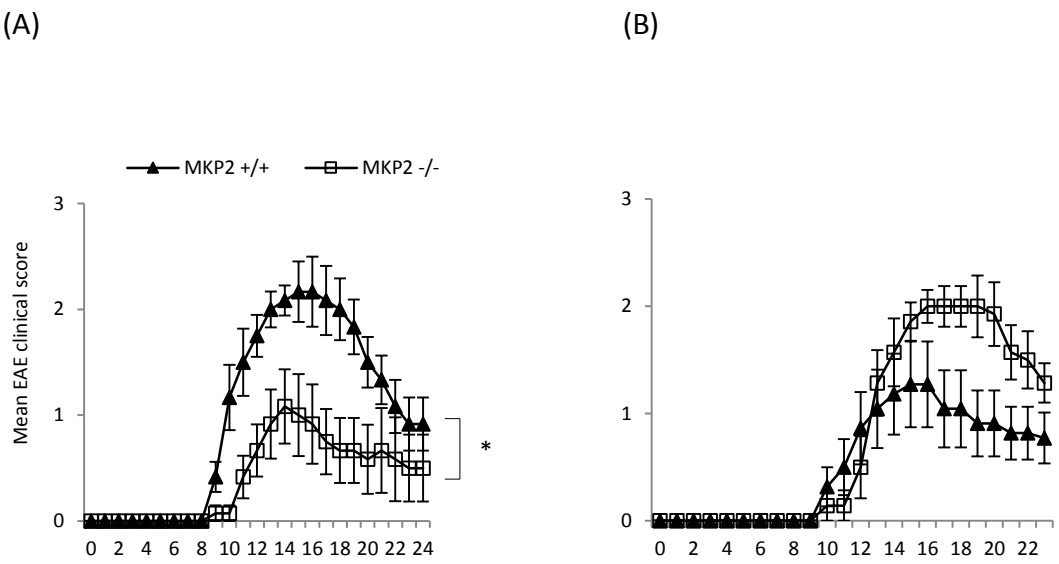

Figure 4.4: Effect of further background crossing of MKP-2 deletion on mean EAE clinical score. PLE-6 MKP-2 +/+ and -/- mice (female, 7-8 weeks old) were injected subcutaneously with 100 µg MOG_{35-55} in CFA on Day 0 as well as 100 ng of PTX i.p. on day 0 and day 2. Results represent mean clinical score ± SEM of all animals in each group. Each graph represents one experiment. (A) n=7 per group, (B) n=7 per group. *P<0.05, Two-way repeated measures ANOVA; bonferroni post-hoc test showed no statistical significance at any specific time point.

In an attempt to resolve this, experiments were further repeated in PLE-7 (7^{th} generation) mice which gave a stable, consistent phenotype. Our data show that in all 7 experiments performed, EAE disease severity was reduced in MKP-2 KO mice. KO mice showed significantly decreased EAE clinical severity compared to WT littermates (Fig 4.5 A). There was also a delay in the onset of symptoms. On average, MKP-2 KO mice developed EAE around day 11, 2 days later than WT counterparts which began to show clinical signs of disease by day 9 (Fig 4.5 B). WT mice reached 100 % disease incidence between days 11-14, while it took 15-18 days for symptoms to present in all KO mice. A significant decrease in cumulative disease score was observed in MKP-2 KO mice, with an average of just 20.4±2.4 (mean±SEM) compared to 30.8±2.3 in MKP-2 WT counterparts (Fig 4.5 C). Maximal disease severity was also significantly reduced upon MKP-2 deletion; from an average of 3.13±0.07 in WT animals to 2.22±0.18 (Figure 4.5 D).

Mice were also weighed daily from Day 0, and percentage weight change relative to this day calculated. A negative correlation between weight change and disease progression was observed, with weight decreasing at disease onset before beginning to increase again as they recovered (Figure 4.5 E). However there was no statistical difference in weight change between WT and KO mice.

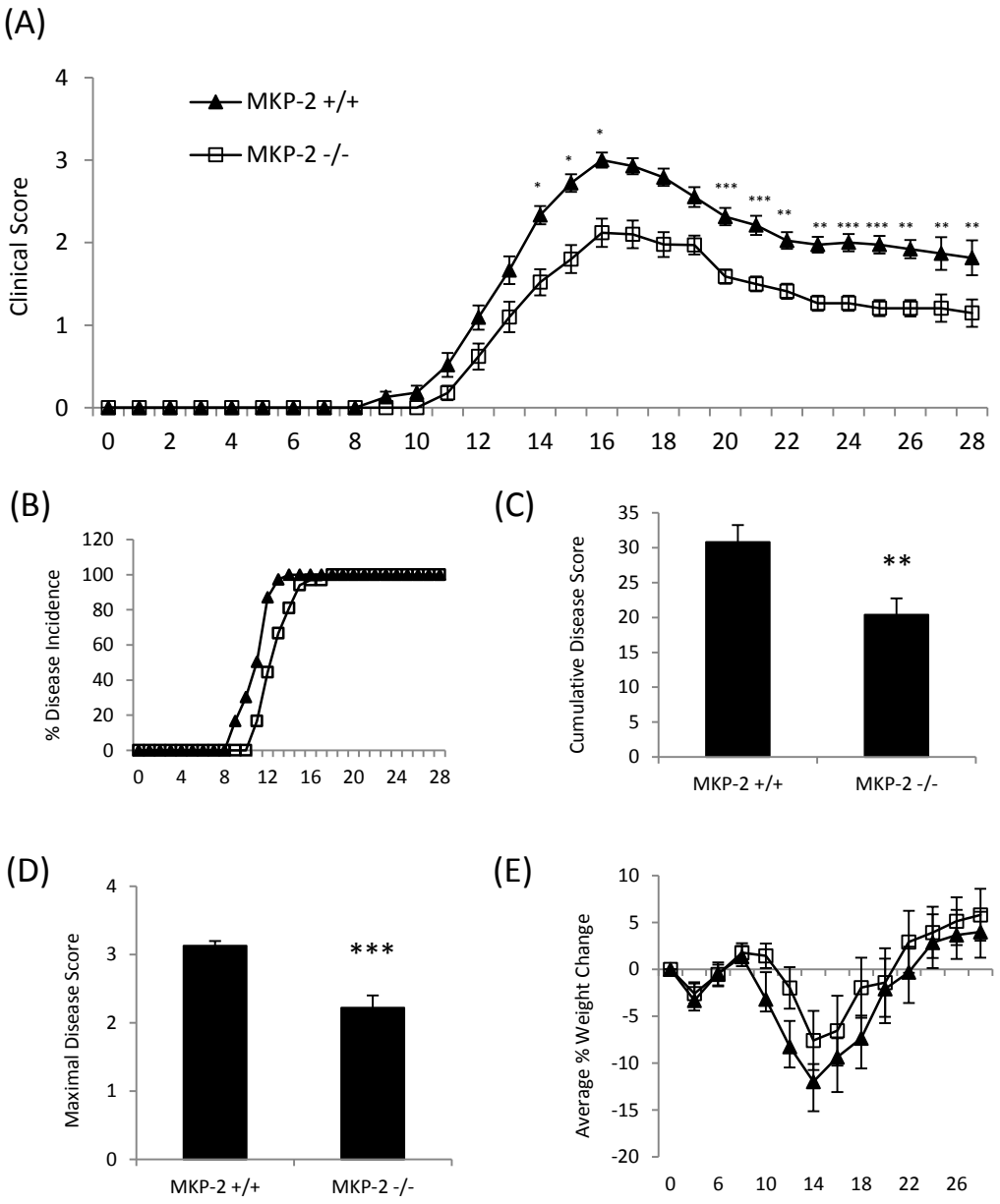

Figure 4.5: EAE clinical disease data in 7th generation backcross MKP-2 -/- mice and +/+ littermates. PLE-7 MKP-2 +/+ and -/- mice (female, 8 weeks) were injected subcutaneously with 100 µg MOG_{35-55} in CFA on day 0 as well as 100 ng of PTX i.p. on day 0 and day 2. Results represent (A) mean clinical score ± SEM of all animals in each group. (B) Percentage of mice which developed any clinical signs of EAE in each group. (C) Maximal clinical score reached during the course of disease ± SEM. (D) Cumulative disease score over the entire course of EAE ± SEM. (E) Percentage weight change within each group ± SEM. Two-tailed unpaired student's t test. Graphs show combined data from three experiments (n=27 WT mice; n=25 KO mice). *P<0.05; **P<0.01; ***P<0.001, (A) Two-way repeated measures ANOVA with bonferroni post-hoc test; (C) and (D) Mann-Whitney U test.

4.2.4 Histological analysis of CNS tissue

To investigate the extent of inflammation and cellular infiltration in mouse spinal cords at the peak disease, as well as at the end of the disease course when clinical severity has declined, we used histological examination. Tissue was removed, flash frozen and cut into 7 micron sections. Firstly, haematoxylin and eosin (H & E) staining was carried out.

Confirming the clinical data that less severe EAE was observed in MKP2 KO mice, the histology data showed a greater number of infiltrating cells in the white matter of WT spinal cord sections compared to KO mice tissue at the peak of disease severity, day 17 post disease induction (Figure 4.6 A). By day 28, when the mean EAE clinical score had decreased from a peak of 3.0±0.1 to 1.8±0.2 in WT mice and 2.1±0.2 to 1.1±0.2 in MKP-2 KO mice, the level of cell migration into the CNS had greatly reduced (Fig 4.6 B). Therefore there was minimal difference between WT and KO tissue in terms of overall cellular infiltration at this time point.

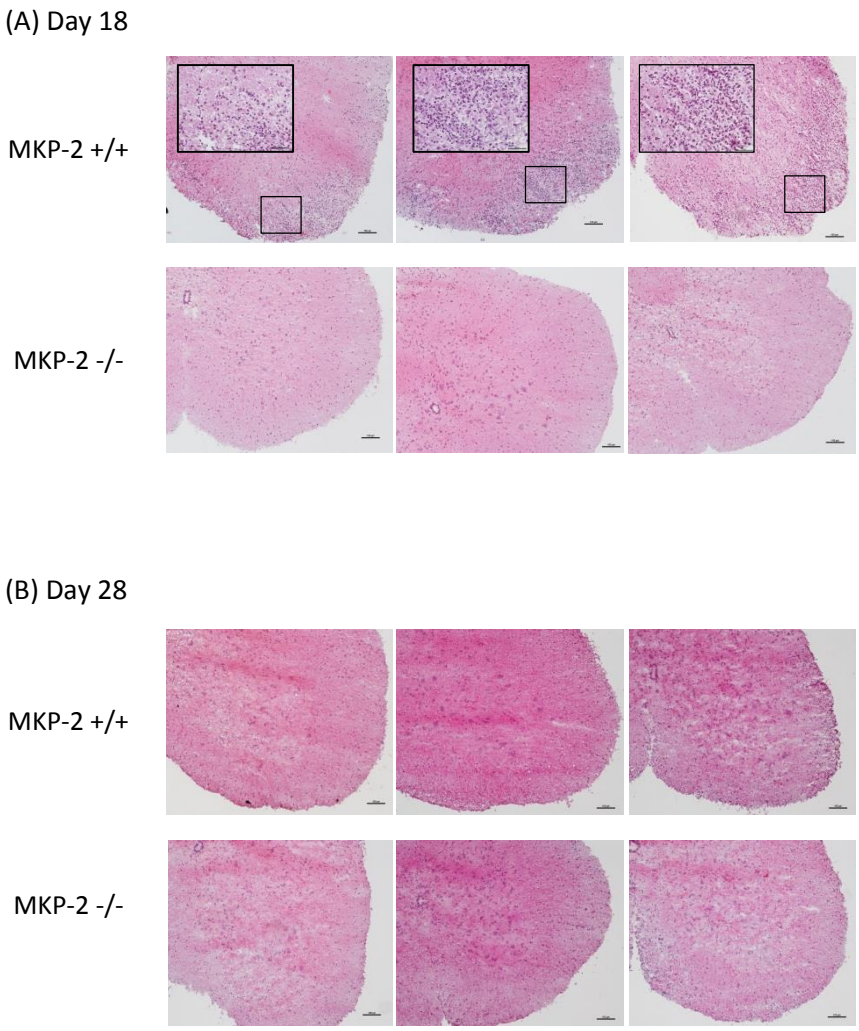

Figure 4.6: Immunopathology of EAE-induced MKP-2 +/+ and MKP-2 -/- mouse spinal cords. Spinal cords were removed (A) 17 or (B) 28 days post EAE-induction and flash-frozen in OCT. Seven micron sections were cut and stained with H&E. Primary images 100X magnification, scale bars = 100µm; Secondary images 400X magnification, scale bars = 50µm. Images are representative of 7 mice per group (n=3 experiments).

Following that, we then performed immunohistochemical staining of specific cell surface markers to identify the CNS infiltrating cell phenotype. Firstly, we confirmed that these were in fact infiltrating, and not CNS-resident, cells by anti-CD45 staining (Fig 4.7) which is a marker present on all hematopoietic cells (excluding mature erythrocytes and platelets).

To ascertain which particular cell types formed the clusters of invading peripheral cells, spinal cord sections were stained for some common immune cell surface markers. Our images show that the majority of infiltrating cells were found to be $CD4^+$ T cells or $F4/80^+$ macrophages (Fig 4.7 A, B). We also stained for $CD19^+$ B cells however no positive staining was achieved (not shown).

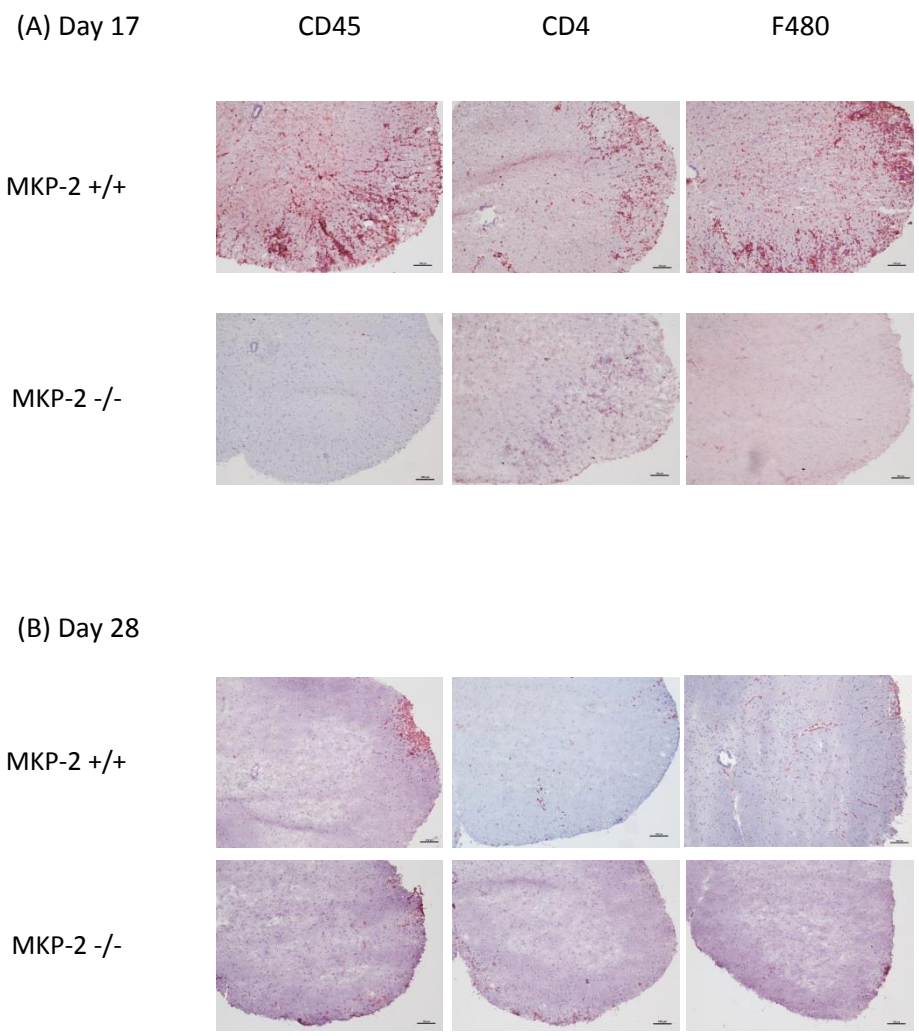

Figure 4.7: Immunopathology of EAE-induced MKP-2 +/+ and MKP-2 -/- mouse spinal cords. Spinal cords were removed (A) 17 or (B) 28 days post EAE-induction and flash-frozen in OCT. Seven micrometre sections were cut and stained for different cell surface markers as indicated (CD45, CD4 and F4/80) before counterstaining in hematoxylin. Blue = nuclei; Red = surface marker. 100X magnification, scale bars=100 µm. Images are representative of 7 mice per group (n=3 experiments).

4.2.5 Antigen-specific cytokine production in EAE day 17 MKP-2 WT and MKP-2 KO secondary lymphoid organs

To try and understand the mechanistic basis of reduced EAE observed in MKP-2 KO mice, spleen and draining lymph node (inguinal lymph nodes; dLN) cells were collected from MOG immunized WT and KO mice at the peak of EAE severity, day 17. Cells were cultured for 24, 48 or 72 hours with or without MOG_{35-55} and supernatants collected for analysis of cytokine concentration by ELISA to examine whether MOG-specific T cells generated in mice deficient in MKP-2 respond differently to WT cells when re-challenged ex-vivo with MOG peptide.

4.2.5.1 Interleukin 17 (IL-17)

In both WT and KO mice cells, supernatants from cultures with medium only had undetectable or very low levels of cytokine. In contrast, antigen specific production of IL-17 was significantly decreased in day 17 MKP-2 KO spleen cell cultures following 24, 48 and 72 hour MOG stimulation (Fig 4.8 A). No IL-17 was detected in KO cells at 24 hours, compared to 371±22 pg/ml in WT cells. After 48 and 72 hours, IL-17 production was downregulated from 1727±68 to 1290±39 pg/ml and from 3059±99 to 2662±10 pg/ml respectively in MOG stimulated MKP-2 KO cell cultures compared to WT. The levels of IL-17 were below detectable limits in WT and KO EAE day 17 dLN cultures following 24 hour MOG re-challenge (Fig 4.8 B). However, after 48 hours, IL-17 production was reduced in MKP-2 KO mice and was significantly decreased in 72 hour KO MOG cultures (1251±411 pg/ml) relative to WT cultures (2778±436 pg/ml).

4.2.5.2 Interferon gamma (IFNγ)

Cells cultured with medium alone produced undetectable levels of the Th1 cytokine IFNγ. However IFNγ levels were significantly reduced in KO spleen cell cultures at disease peak following MOG stimulation (Fig 4.8 A). MKP-2 KO cultures contained 20±12, 2798±141 and 5097±30 pg/ml of IFNγ in response to 24, 48 and 72 hour MOG

stimulation respectively. These were all significantly less than the 2318±65, 5796±74 and 6667±46 pg/ml of IFNγ produced by WT cells. In day 17 dLN cells, no IFNγ was detected in WT or KO cultures after 24 hours (Fig 4.8 B). Following 48 hours of MOG culture, comparable levels of IFNγ were detected between WT and KO mice. By 72 hours, IFNγ production was significantly lower in MKP-2 KO dLNs (2242±38 pg/ml) compared to WT counterparts (1723±48 pg/ml).

4.2.5.3 Interleukin 6 (IL-6)

IL-6 production was significantly reduced in MOG-stimulated MKP-2 KO cells relative to WT, with no cytokine detected in KO 24 hour MOG culture or any media cultures (Fig 4.8 A). After 48 hours of antigen challenge, MKP-2 KO cells produced just 86±22 pg/ml IL-6, compared to 553±66 pg/ml by WT cells. Similarly, by 72 hours, KO cultures still contained significantly less IL-6 than WT (249±65 compared to 771±22 pg/ml). No IL-6 could be detected in any stimulated day 17 dLN cell cultures.

4.2.5.4 Interleukin 22 (IL-22)

No IL-22 was detected in any media cultures. IL-22 levels significantly decreased in day 17 KO spleen cells compared to WT after 48 and 72 hour MOG stimulation (Fig 4.8 A). Antigen challenged MKP-2 KO cells produced 503±16 and 1258±22 pg/ml IL-22 after 48 and 72 hours respectively. In comparison, WT cultures contained 941±28 and 1992±17 pg/ml. No expression was detected in WT or KO spleen cultures after 24 hours. IL-22 production was also significantly downregulated in KO dLN cultures compared to WT after 48 and 72 hour MOG stimulation (Fig 4.8 B). WT cells produced 90±16, 598±102 and 1872±169 pg/ml IL-22 in response to 24, 48 and 72 hour MOG stimulation respectively. KO cells produced no detectable IL-22 after 24 hours, and only 310±73 and 1232±303 pg/ml IL-22 at 48 and 72 hours.

4.2.5.5 Interleukin 2 (IL-2)

Both WT and KO cells cultured with medium alone expressed undetectable or very low levels of IL-2. In contrast, following 24 and 48 hour MOG re-challenge, MKP-2 KO spleen cells produced 358±11 and 565±39 pg/ml IL-2 respectively (Fig 4.8 A). This was significantly less than WT cells which produced 779±22 pg/ml after 24 hours and 901±99 pg/ml at 48 hours. After 72 hours, IL-2 levels continued to increase in MKP-2 KO cells, but decreased in WT cells relative to 48 hour stimulations. Therefore by 72 hours, MKP-2 WT and KO cultures contained comparable amounts of IL-2. Conversely, in MOG stimulated dLN cells, IL-2 production remained consistent between WT and KO mice after 24 and 48 hours but was moderately decreased in KO cultures by 72 hours, however this difference was not significant (Fig 4.8 B).

4.2.5.6 Chemokine Ligand 2 (CCL2)

Production of the chemokine CCL2 was significantly decreased in antigen re-challenged MKP-2 KO spleen cells compared to WT counterparts (Fig 4.8 A). WT cells produced 738±57, 2445±45 and 4534±49 pg/ml CCL2 in response to 24, 48 and 72 hour MOG stimulation respectively. In comparison, KO cultures contained just 258±46, 1806±135 and 3803±36 pg/ml. No statistical differences in CCL2 expression were observed in KO dLN cultures following MOG stimulation (Fig 4.8 B).

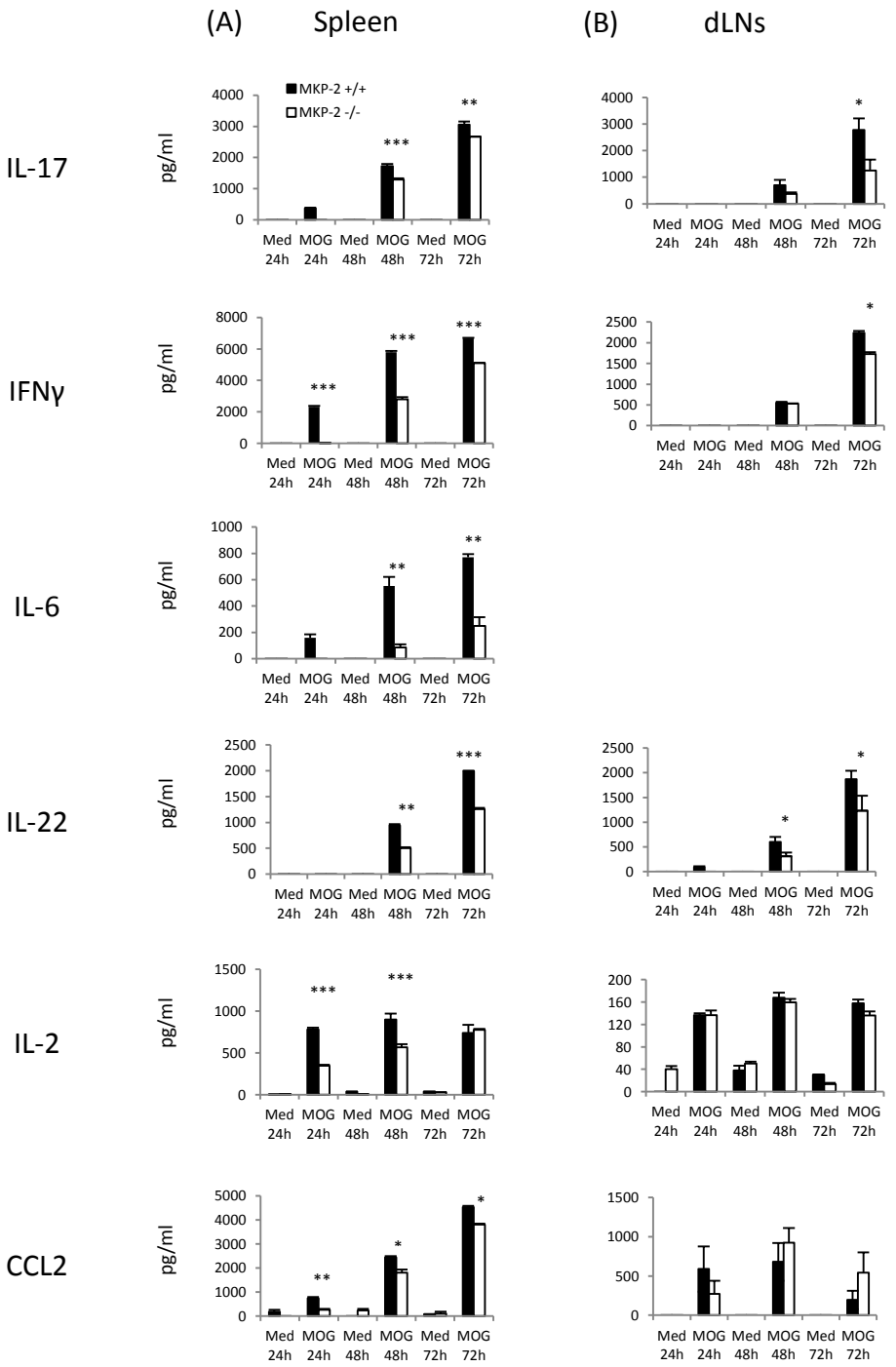

Figure 4.8: Cytokine expression in EAE day 17 MKP-2 +/+ and MKP-2 -/- spleen and inguinal lymph node cells. Spleen and dLNs were harvested at Day 17 post EAE-induction and cells (4 x10^6 for spleen; 2 x10^6 for dLNs) extracted and incubated for 24, 48 or 72 hours (h) at 37°C and 5% CO_2 in presence of RPMI alone or RPMI supplemented with 40µg / ml MOG. Supernatants were collected and cytokine expression analysed by ELISA. Graphs show representative data from one of at least three individual experiments performed in quadruplicate (n=7 mice per group; n=3 experiments). *P<0.05; **P<0.01; ***P<0.001 compared to WT, two-tailed unpaired student's t test.

4.2.6 EAE day 28 spleen and dLNs

We then repeated with cells cultured from MKP-2 WT and KO EAE day 28 spleen and dLNs in order to determine whether the changes observed at the peak of disease are maintained at later stages of EAE. As before, cells were cultured for 24, 48 or 72 hours with or without MOG_{35-55} and supernatants collected for analysis of cytokine expression by ELISA.

4.2.6.1 Interleukin 17 (IL-17)

No IL-17 was detected in any WT or KO medium-only spleen and dLN cultures. In MOG-stimulated KO spleen cells, IL-17 production was significantly reduced compared to WT counterparts (Fig 4.9 A). Following 24, 48 and 72 hour antigen challenge, MKP-2 KO cells produced 71± 38, 1336±75 and 1790±43 pg/ml IL-17 respectively. In comparison, WT cells produced significantly more (248±7, 1591±22 and 1977±26 pg/ml). However, although these differences are statistically significant, they may not represent a large change in a biological context. IL-17 expression was also significantly decreased in day 28 MKP-2 KO dLN cells after 48 and 72 hours of MOG culture compared to WT (Fig 4.9 B). IL-17 production was downregulated from 753±85 and 1042±45 pg/ml in WT cells to 153±15 and 577±43 pg/ml in KO cells at 48 and 72 hours respectively. No IL-17 was detected in MOG KO cell culture after 24 hours.

4.2.6.2 Interferon gamma (IFNγ)

IFNγ production was not altered in spleen cells at EAE day 28, with almost identical levels observed between WT and KO samples after 48 and 72 hours of MOG stimulation (Fig 4.9 A). No IFNγ was detected in 24 hour WT and KO MOG culture supernatants. IFNγ production was significantly downregulated in MKP-2 KO dLN cells after 48 and 72 hour MOG re-challenge (Fig 4.9 B). KO cells produced just 26±18 and 416±132 pg/ml IFNγ at 48 and 72 hours respectively, compared to 1247±51 and 1815±47 pg/ml in WT cultured following MOG challenge. IFNγ was undetectable

in 24 hour KO MOG cultures. Also, WT and KO spleen and dLN cells cultured with medium alone contained no, or very low levels of IFNγ.

4.2.6.3 Interleukin 6 (IL-6)

Antigen re-challenged spleen cells produced less IL-6, a decrease which was significant after 48 and 72 hours (Fig 4.9 A). Following MOG stimulation, KO cultures contained 1122±49 and 1113±68 pg/ml IL-6 at 48 and 72 hours respectively. In comparison, WT cells produced 1360±41 and 1496±22 pg/ml. As with IL-17, these differences are perhaps not biologically significant but they are statistically significant. IL-6 production was also diminished in day 28 MKP-2 KO dLNs compared to WT following MOG stimulation (Fig 4.9 B). Only moderate reductions were observed at 24 and 48 hours. However this amelioration was significant after 72 hours of MOG challenge. KO cultures contained 56±3 pg/ml IL-6 while WT cells produced 151±15 pg/ml. A small decrease in IL-6 levels was also observed in 72 hour media-cultured KO spleen and dLN cells. No cytokine was detected in 24 or 48 hour media culture.

4.2.6.4 Interleukin 22 (IL-22)

IL-22 levels were below detectable limits in both WT and KO 24 hour MOG cultures, as well as all media cultures (Fig 4.9 A). Following 48 hour MOG challenge, KO cells produced 1073± 9 IL-22 which was significantly more than WT counterparts at 745±24 pg/ml. No IL-22 was detected in any supernatants from dLN cells cultured with medium only (Fig 4.9 B). Also, KO MOG cultures contained no detectable levels of IL-22 after 24 and 48 hour stimulation, and only very low levels after 72 hours. Therefore IL-22 production was significantly downregulated in MKP-2 KO dLN cells compared to WT, as WT cells produced 55±33, 371±35 and 685±27 pg/ml IL-22 following 24, 48 and 72 hour antigen challenge respectively.

4.2.6.5 Interleukin 2 (IL-2)

Both spleen and dLN WT and KO cells cultured without MOG produced low levels of IL-2, with no, or only very moderate differences between WT and KO. Following MOG stimulation, IL-2 levels remained unchanged between WT and KO spleen cells (Fig 4.9 A). In dLNs, IL-2 production was significantly downregulated in MKP-2 KO cells (57±3 pg/ml) compared to WT cells (108±7 pg/ml) following 24 hour MOG culture (Fig 4.9 B). However by 48 and 72 hours there were no longer any differences between WT and KO.

4.2.6.6 Chemokine Ligand 2 (CCL2)

CCL2 production was significantly downregulated in MKP-2 KO spleen cells following MOG stimulation compared to WT (Fig 4.9 A). KO cultures contained 98±61, 1719±190 and 2439±84 pg/ml after 24, 48 and 72 hours respectively. In contrast, WT cells produced significantly more CCL2 at all time points: 1334±99, 2795±110 and 4216±203 pg/ml. A more moderate decrease was also observed in KO spleen cells cultured with media alone for 24, 48 and 72 hours. No detectable expression was observed in any media or MOG dLN cultures.

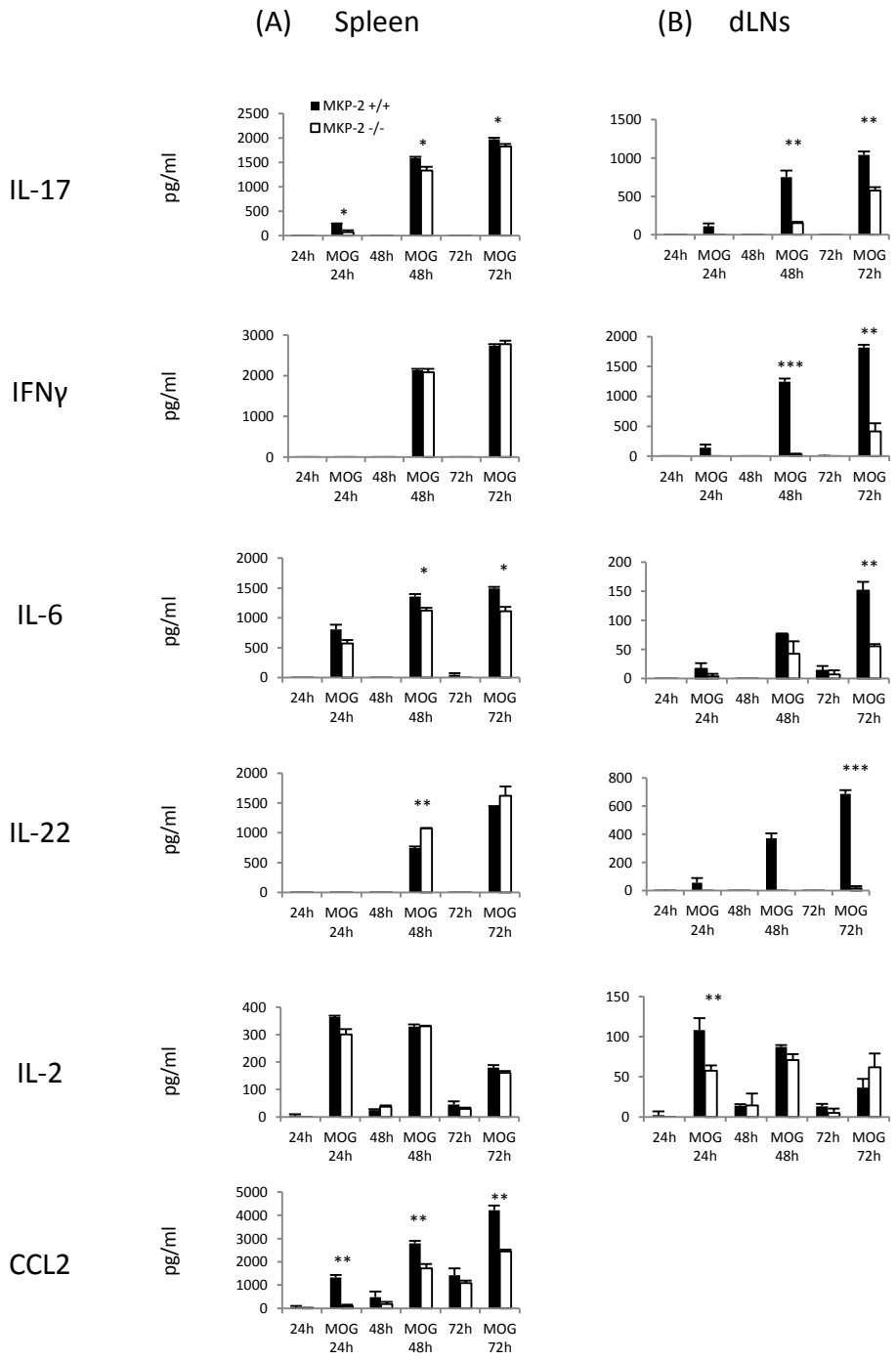

Figure 4.9: Cytokine expression in EAE day 28 MKP-2 +/+ and MKP-2 -/- spleen and inguinal lymph node cells. Spleen and dLNs were harvested at Day 28 post EAE-induction and cells (4 x10^6 for spleen; 2 x10^6 for dLNs) extracted and incubated for 24, 48 or 72 hours (h) at 37°C and 5% CO_2 in presence of RPMI alone or RPMI supplemented with 40µg / ml MOG. Supernatants were collected and cytokine expression analysed by ELISA. Graphs show representative data from one of at least three individual experiment performed in quadruplicate (n=7 mice per group; n=3 experiments). *P<0.05; **P<0.01; ***P<0.001 compared to WT, two-tailed unpaired student's t test.

4.2.7 MKP mRNA expression in MKP-2 WT and KO spleen cells

We next wanted to determine if the expression of MKP-2 mRNA, along with selected other MKPs, was altered in correlation with this immune response. Spleen cells from MKP-2 WT and KO mice were collected at day 17 after immunisation and cultured for 72 hours with or without MOG_{35-55} peptide. RNA from these cells was then extracted and reverse transcribed to cDNA to allow analysis by qPCR. The data in Fig 4.10 A show that MKP-2 expression by WT spleen cells was more than 3-fold higher upon stimulation with MOG peptide compared to culture with media alone however this was not statistically significant. As expected, no MKP-2 expression was detected in MKP-2 KO cells.

MKP-1 was analysed as it has previously been associated with EAE pathogenesis. In WT spleen cells, upon MOG antigen challenge, MKP-1 mRNA expression was unchanged relative to cells cultured with media (Fig 4.10 B). However, after the same challenge in MKP-2 KO cells, MKP-1 expression was 3.2-fold greater relative to cells incubated with media alone. MKP-5 and DUSP5 were also analysed as these MKPs have previously been shown to be involved in the pathogenesis of EAE and CIA respectively. DUSP5 mRNA expression was increased in both WT (3.5-fold) and MKP-2 KO cells (4.8-fold) following antigen stimulation, but with no statistical difference (Fig 4.10 C) between WT and KO. MKP-5 expression was unaltered in WT spleen cells relative to naïve (Fig 4.10 D). However there was a possible upregulation in KO cells; with MKP-5 mRNA levels double that of unstimulated equivalents. However again this was not statistically significant and overall expression levels of this phosphatase were very low compared to the other MKPs analysed based on Ct values.

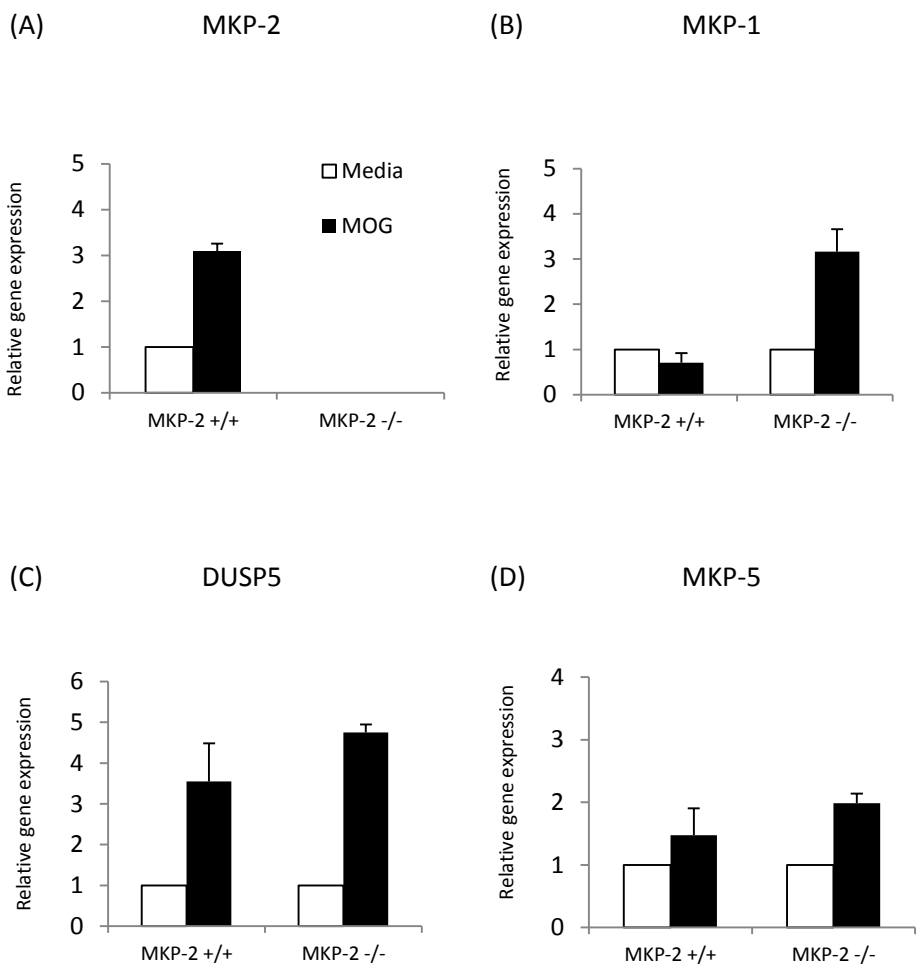

Figure 4.10: MKP mRNA expression in MKP-2 +/+ and MKP-2 -/- EAE spleen cells re-challenged with MOG. Spleens were harvested and pooled for both groups and cells extracted. Cells were incubated in a 24-well tissue culture plate (4 x 10^6 / well) for 72 hours in presence of RPMI alone or RPMI supplemented with 40µg / ml MOG. Supernatant was collected and RNA isolation performed using the RNeasy mini kit (Qiagen) and reverse transcribed to cDNA to allow analysis of MKP mRNA expression by qPCR. The housekeeping gene GAPDH was analysed simultaneously to allow normalisation of relative MKP mRNA expression. Graph show data from two experiments (MKP-2 KO n = 13; WT n = 12). Not statistically significant, Mann-Whitney U test.

4.2.8 MKP mRNA expression in MKP-2 WT and KO EAE spinal cord tissue

As well as examining MKP expression in MKP-2 WT and KO EAE spleen cells, we also analysed MKP levels in CNS tissue by analysing mRNA expression in EAE spinal cords. Tissues were removed from MKP-2 WT and KO mice at EAE day 28. RNA was extracted and reverse transcribed to cDNA to allow analysis by qPCR. MKP mRNA levels in KO mice are expressed as relative to WT littermates (Fig 4.11).

As expected, while WT mice spinal cord tissues expressed MKP-2 mRNA, no MKP-2 expression was detected in KO spinal cords confirming these mice were indeed gene deficient (Fig 4.11 A). No differences in the mRNA expression levels of MKP-1, MKP-5, MKP-7 or MKP-x mRNA were observed between WT and KO samples (Fig 4.11 B-D, F). In contrast, DUSP5 mRNA expression was significantly increased by 2.8-fold in KO EAE mice relative to WT controls (Fig 4.11 E).

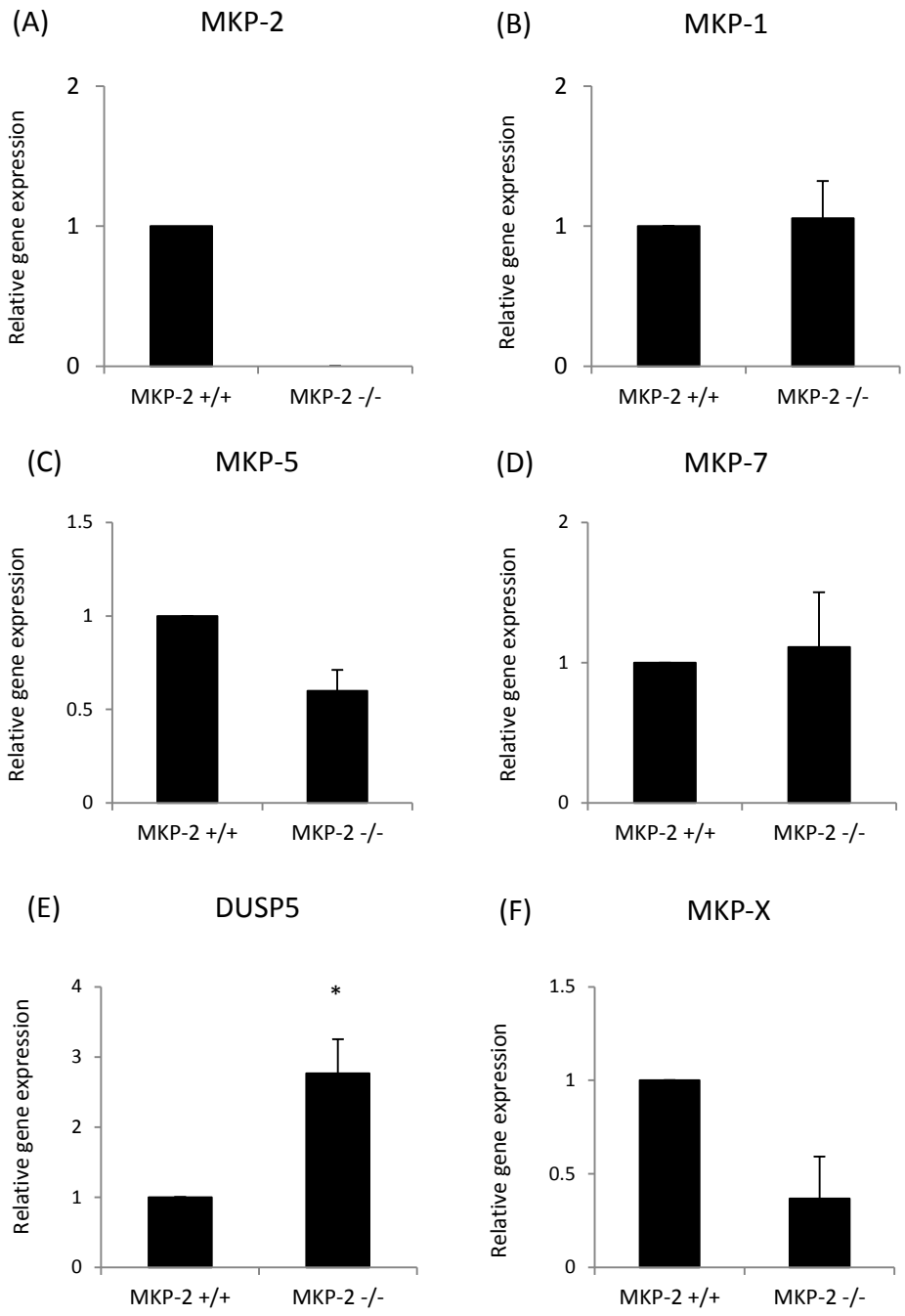

Figure 4.11: mRNA expression of selected MKPs in MKP-2 +/+ and MKP-2 -/- EAE day 28 spinal cords. Tissue was harvested 28 days post EAE-induction and flash frozen. RNA was extracted using TRIzol and reverse transcribed to cDNA to allow analysis of MKP mRNA expression by qPCR. The housekeeping gene tubulin beta 5 was analysed simultaneously to allow normalisation of relative MKP mRNA expression. Graph show data from two experiments (WT n = 7; KO n = 6). *P<0.05, Mann-Whitney U test.

4.2.9 MAPK mRNA expression in MKP-2 WT and KO EAE spinal cord tissue

Having observed altered MKP expression in EAE spinal cord tissue as a consequence of MKP-2 deletion, MAPK mRNA expression in WT and KO EAE spinal cords was subsequently examined as we hypothesised that changes in MKP expression would affect MAPK levels. Spinal cords were removed from MKP-2 WT and KO mice at EAE day 28. RNA was extracted and reverse transcribed to cDNA to allow analysis by qPCR. MAPK mRNA levels in KO EAE mice are expressed as relative to WT littermates (Fig 4.12).

In KO EAE mice, our data suggest a potential increase in ERK1 mRNA levels, with a 2.5-fold increase observed relative to WT (Fig 4.12 A). However this was not statistically significant. And there was no difference in ERK2, JNK1, JNK2 or p38 mRNA expression levels between WT and KO EAE spinal cord samples (Fig 4.12 B-E).

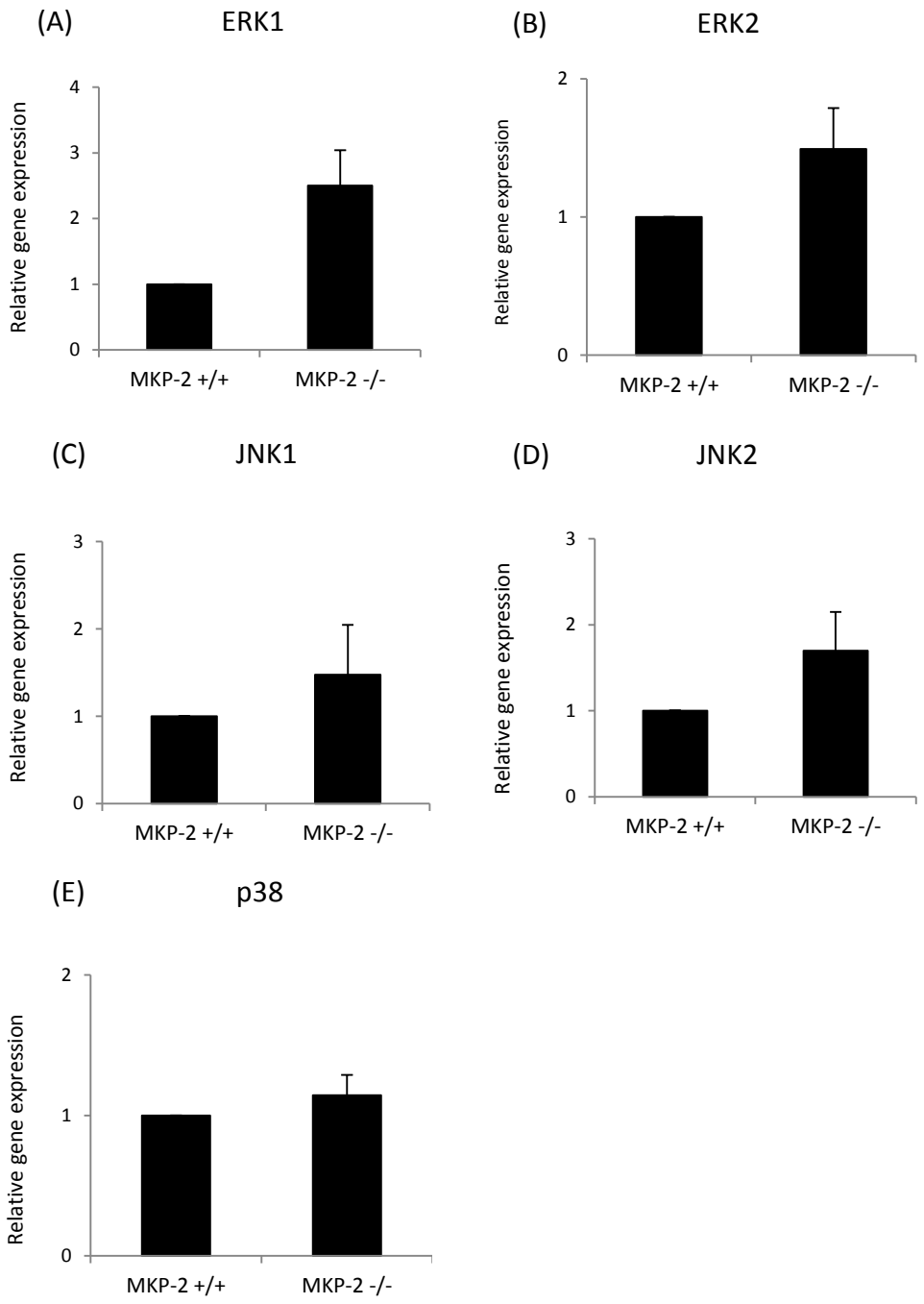

Figure 4.12: MAPK mRNA expression in MKP-2 +/+ and MKP-2 -/- EAE day 28 spinal cords. Tissue was harvested 28 days post EAE-induction and flash frozen. RNA was extracted using TRIzol and reverse transcribed to cDNA to allow analysis of MAPK mRNA expression by qPCR. The housekeeping gene tubulin beta 5 was analysed simultaneously to allow normalisation of relative MAPK mRNA expression. Graph show data from two experiment (WT n = 7; KO n = 6). Not statistically significant, Mann-Whitney U test.

4.2.10 ERK and JNK phosphorylation in MKP-2 WT and KO EAE CNS tissue

As previously mentioned, MKP-2 is involved in the regulation of signalling via MAPK dephosphorylation. MKP-2 substrate specificity varies between different cells and tissue types and so it remains unclear how, if at all, MKP-2 affects phosphorylation of these kinases during EAE development and progression. Therefore, to investigate this, we analysed ERK and JNK phosphorylation in the CNS of MKP-2 WT and KO EAE mice.

Whole brain and spinal cord tissue was harvested from WT and KO mice at different time points over the course of an EAE model and proteins isolated using RIPA buffer. Expression of p-ERK and p-JNK was then analysed by western blot. Membranes were probed for phospho-ERK / JNK, then stripped and re-probed for respective total kinase levels as well as GAPDH. For densitometry analysis, GAPDH levels were used as a loading control. Levels of phosphorylated ERK and JNK were expressed as relative to their equivalent total ERK / JNK.

4.2.10.1 p-ERK1 and p-ERK2

Firstly, the expression levels of p-ERK1 and p-ERK2 in MKP-2 WT and KO EAE spinal cords at day 9, 17 and 28 post-immunisation were examined by western blot (Fig 4.13 A-C; Fig 4.14 A-C). We observed no changes in the level of phosphorylation of either ERK isoform at any of the time points tested between WT and KO mice (Fig 4.13 D-F; Fig 4.14 D, E).

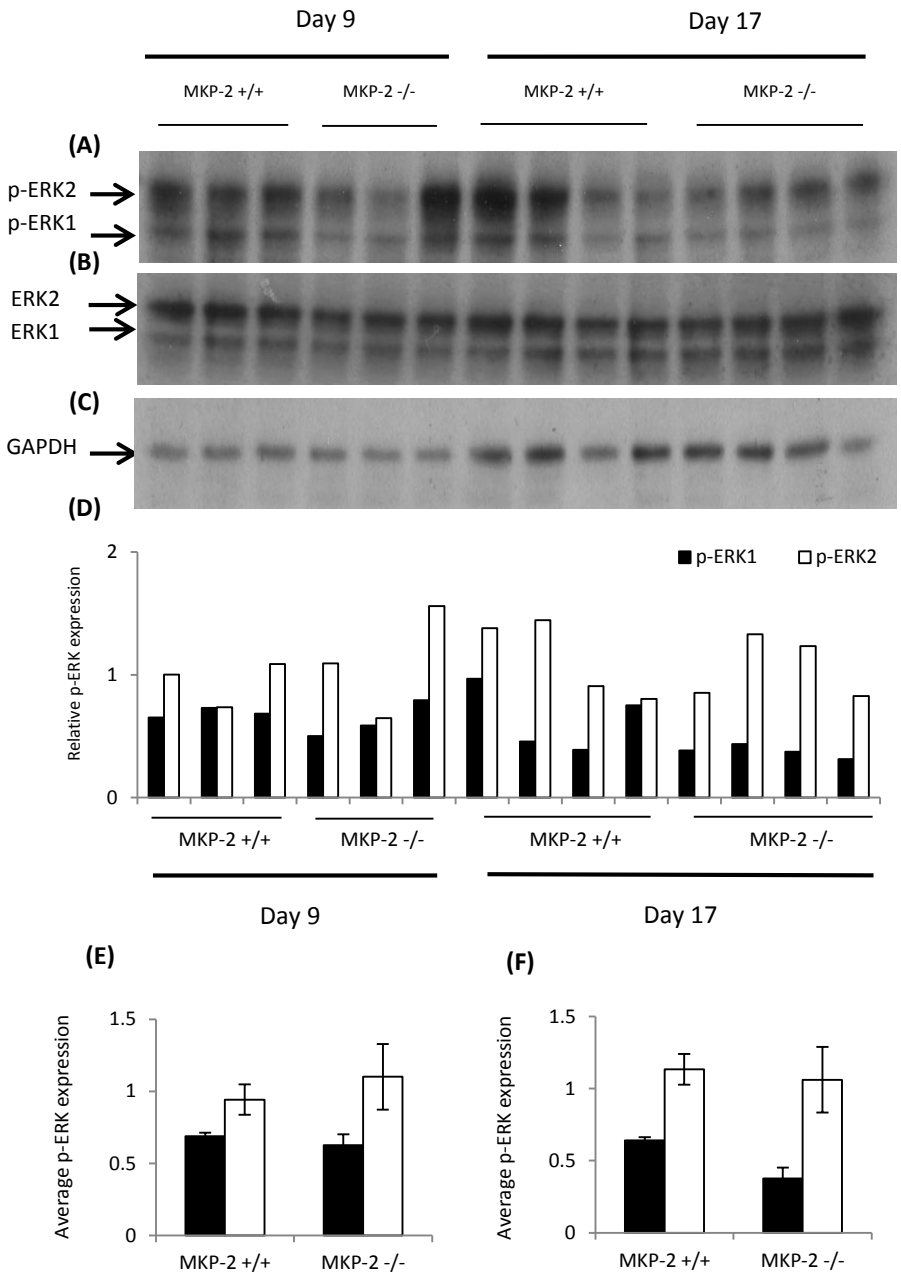

Figure 4.13: p-ERK expression in MKP-2 +/+ and MKP-2 -/- EAE day 9 and day 17 spinal cord tissue. Spinal cords were harvested from day 9 or 17 EAE mice and whole protein lysate prepared using RIPA buffer. (A) p-ERK expression was analysed by western blotting. Membranes were stripped and re-probed for (B) total ERK and (C) GAPDH. (D) Densitometry was utilised to determine changes in p-ERK expression relative to total ERK, with GAPDH used as a loading control and total ERK used as a control for variances in overall ERK levels between samples. (E) Day 9 and (F) day 17 graphs show mean ± SEM p-ERK expression in EAE MKP-2 +/+ or MKP-2 -/- mice. Data shown is from one experiment, n=3 at day 9 and n=4 at day 17 per group. Not statistically significant, two-tailed unpaired student's t test.

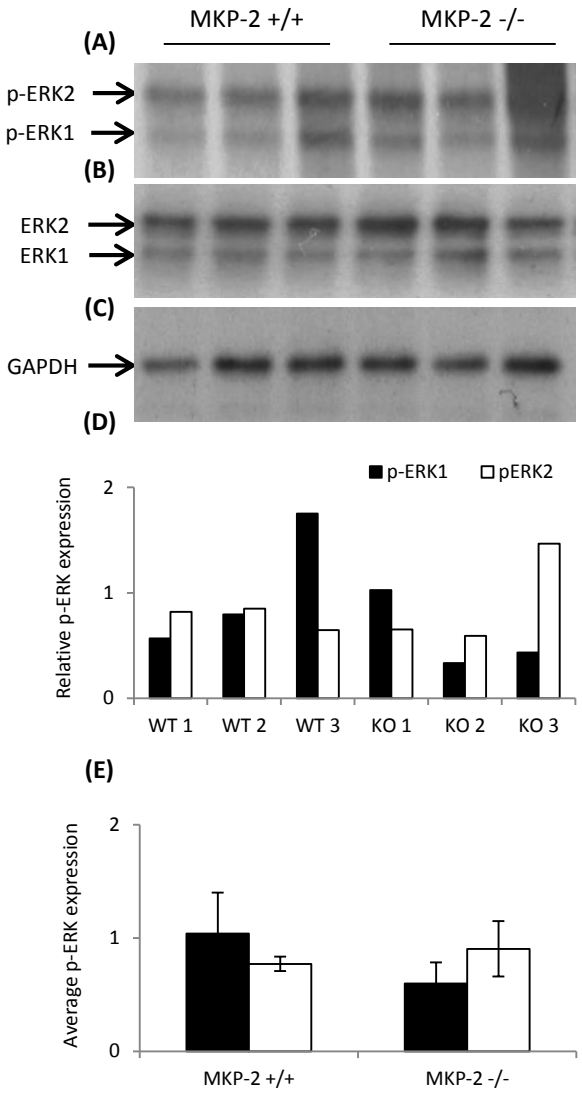

Figure 4.14: p-ERK expression in MKP-2 +/+ and MKP-2 -/- EAE day 28 spinal cord tissue. Spinal cords were harvested from day 28 EAE mice and whole protein lysate prepared using RIPA buffer. (A) p-ERK expression was analysed by western blotting. Membranes were stripped and re-probed for (B) total ERK and (C) GAPDH. (D) Densitometry was utilised to determine changes in p-ERK expression relative to total ERK, with GAPDH used as a loading control and total ERK used as a control for variances in overall ERK levels between samples. (E) Graph represents mean ± SEM p-ERK expression in EAE MKP-2 +/+ or MKP-2 -/- mice. Data shown is from one experiment, n=3 per group. Not statistically significant, two-tailed unpaired student's t test.

We next analysed p-ERK expression in EAE brain tissue (Fig 4.15 A-C; Fig 4.16 A-C). Similarly to the spinal cord, there was no difference in ERK1 or ERK2 phosphorylation between WT and MKP-2 KO EAE brain samples at either day 9, day 17 or day 28 (Fig 4.15 D-F, Fig 4.16 D, E).

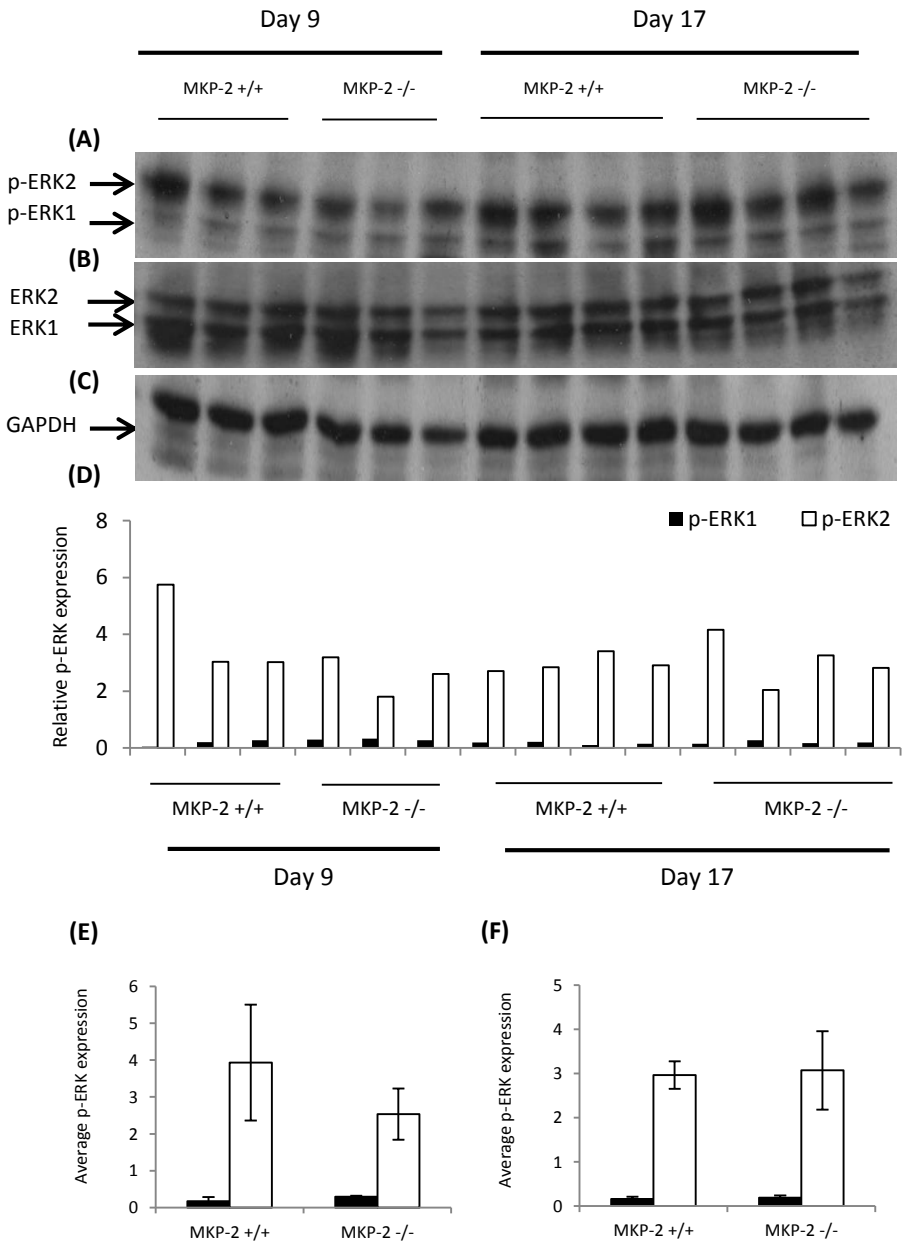

Figure 4.15: p-ERK expression in MKP-2 +/+ and MKP-2 -/- EAE day 9 and day 17 brain tissue. Brains were harvested from day 9 or 17 EAE mice and whole protein lysate prepared using RIPA buffer. (A) p-ERK expression was analysed by western blotting. Membranes were stripped and re-probed for (B) total ERK and (C) GAPDH. (D) Densitometry was utilised to determine changes in p-ERK expression relative to total ERK, with GAPDH used as a loading control and total-ERK used as a control for variances in overall ERK levels between samples. (E) Day 9 and (F) day 17 graphs represent mean ± SEM p-ERK expression in EAE MKP-2 +/+ or MKP-2 -/- mice. Data shown is from one experiment, n=3 at day 9 and n=4 at day 17 per group. Not statistically significant, two-tailed unpaired student's t test.

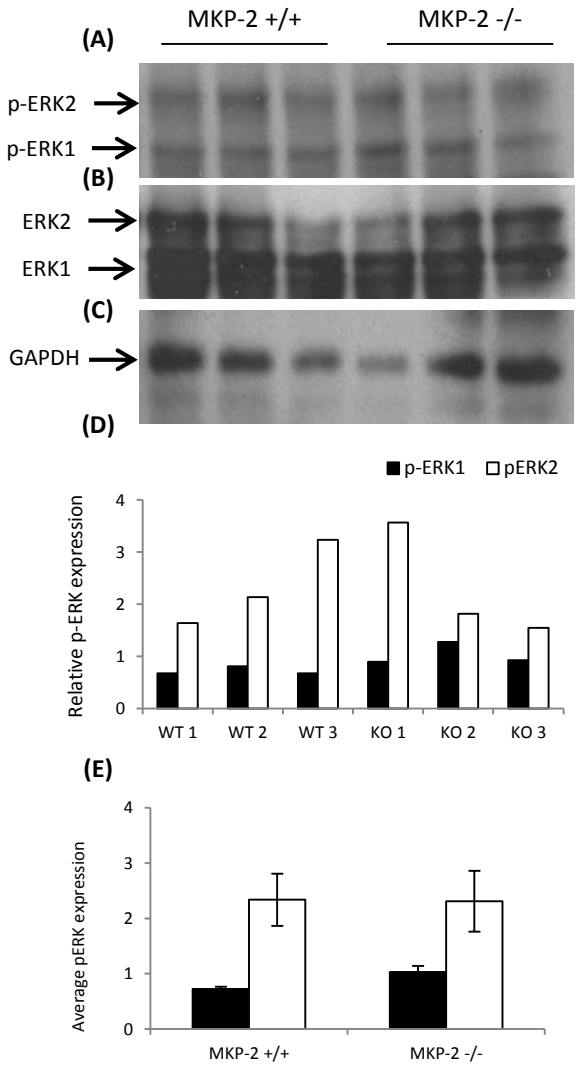

Figure 4.16: p-ERK expression in MKP-2 +/+ and MKP-2 -/- EAE day 28 brain tissue. Brains were harvested from day 28 EAE mice and whole protein lysate prepared using RIPA buffer. (A) p-ERK expression was analysed by western blotting. Membranes were stripped and re-probed for (B) total ERK and (C) GAPDH. (D) Densitometry was utilised to determine changes in p-ERK expression relative to total ERK, with GAPDH used as a loading control and total ERK used as a control for variances in overall ERK levels between samples. (E) Graph shows mean ± SEM p-ERK expression in EAE MKP-2 +/+ or MKP-2 -/- mice. Data shown is from one experiment, n=3 per group. Not statistically significant, two-tailed unpaired student's t test.

4.2.10.2 p-JNK1 and p-JNK2

Following examination of p-ERK, we next investigated JNK phosphorylation in MKP-2 WT and KO EAE CNS tissue, with focus on the two primary genes which encode the JNK family, JNK1 and JNK2 (Fig 4.17 – Fig.4.20 A-C). Within spinal cord samples, phosphorylation of JNK1 and JNK2 remained unaffected by MKP-2 gene deletion, with comparable levels of p-JNK1 and p-JNK2 observed between MKP-2 KO and WT littermates (Fig 4.17 D-F; Fig 4.18 D, E).

Fig 4.18 E suggests a potential upregulation in JNK2 phosphorylation in KO mice compared to WT, however this increase was primarily due to one outlier which was likely caused by a poorly developed total JNK2 band (Fig 4.18 B), resulting in an average relative expression of 3.09±1.44 compared to 1.23±0.3 in WT samples and therefore this is unlikely to be an accurate result.

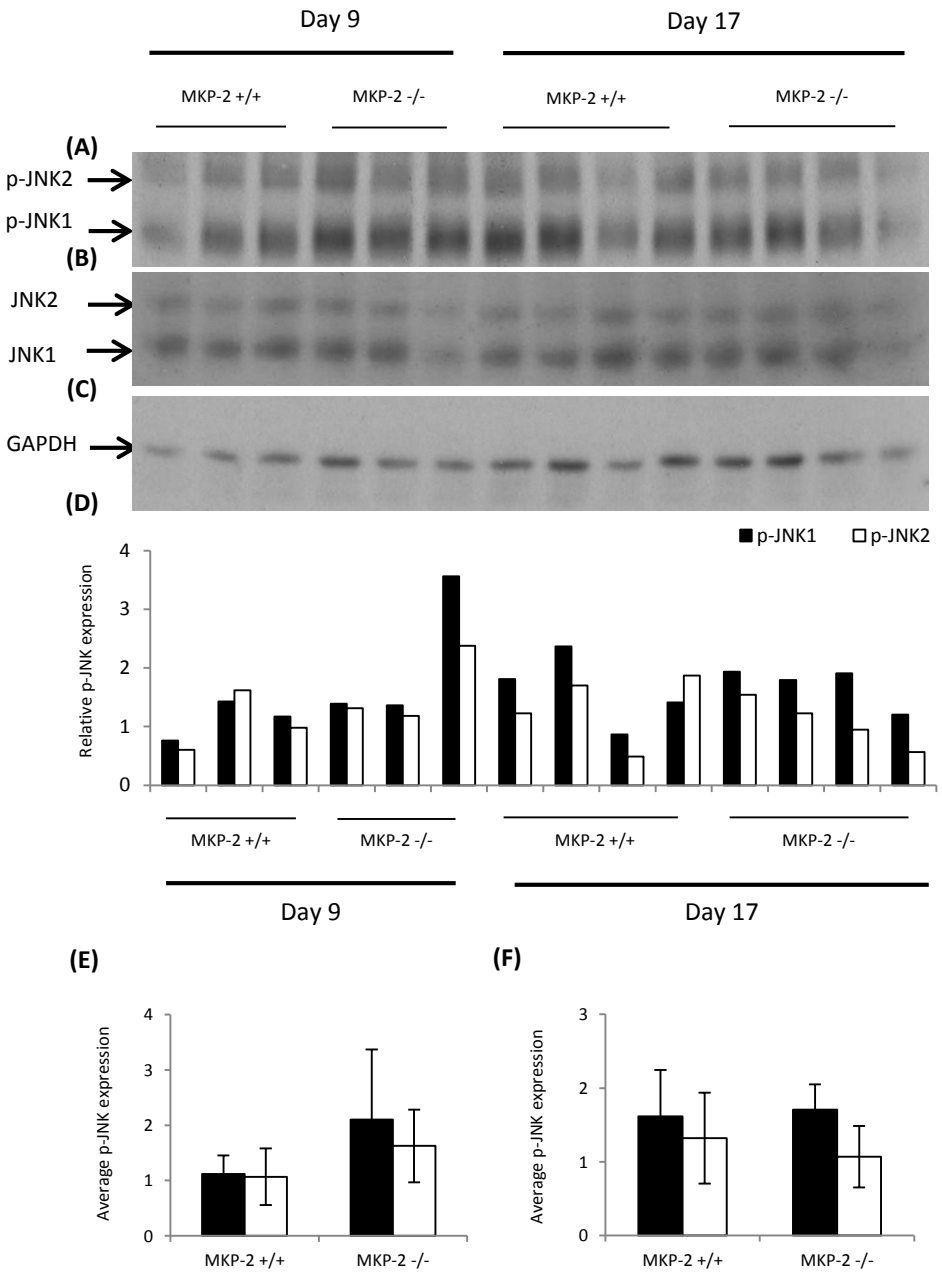

Figure 4.17: p-JNK expression in MKP-2 +/+ and MKP-2 -/- EAE day 9 and day 17 spinal cord tissue. Spinal cords were harvested from day 9 or 17 EAE mice and whole protein lysate prepared using RIPA buffer. (A) p-JNK expression was analysed by western blotting. Membranes were stripped and re-probed for (B) total JNK and (C) GAPDH. (D) Densitometry was utilised to determine changes in p-JNK expression relative to total JNK, with GAPDH used as a loading control and total JNK used as a control for variances in overall JNK levels between samples. (E) Day 9 and (F) day 17 graphs show mean ± SEM p-JNK expression in EAE MKP-2 +/+ or MKP-2 -/- mice. Data shown is from one experiment, n=3 at day 9 and n=4 at day 17 per group. Not statistically significant, two-tailed unpaired student's t test.

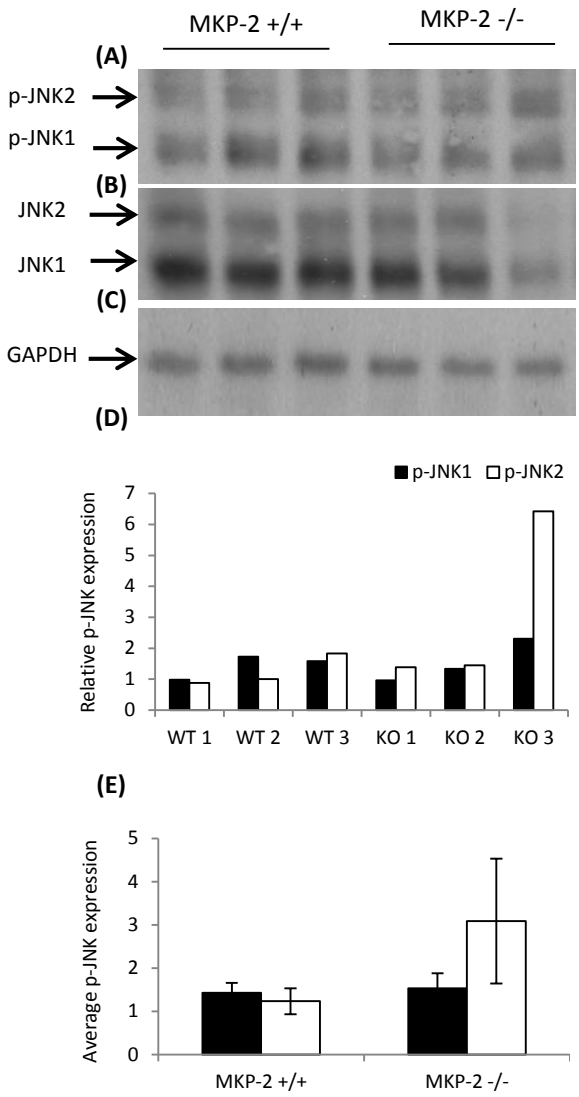

Figure 4.18: p-JNK expression in MKP-2 +/+ and MKP-2 -/- EAE day 28 spinal cord tissue. Spinal cords were harvested from day 28 EAE mice and whole protein lysate prepared using RIPA buffer. (A) p-JNK expression was analysed by western blotting. Membranes were stripped and re-probed for (B) total JNK and (C) GAPDH. (D) Densitometry was utilised to determine changes in p-JNK expression relative to total JNK, with GAPDH used as a loading control and total JNK used as a control for variances in overall JNK levels between samples. (E) Graph represents mean ± SEM p-JNK expression in EAE MKP-2 +/+ or MKP-2 -/- mice. Data shown is from one experiment, n=3 per group. Not statistically significant, two-tailed unpaired student's t test.

Similarly to our results obtained in spinal cord tissue, phosphorylation of JNK1 and JNK2 remained unchanged in MKP-2 KO brain samples relative to WT at day 9, day 17 and day 28 (Fig 4.19 D-F, Fig 4.20 A-E)).

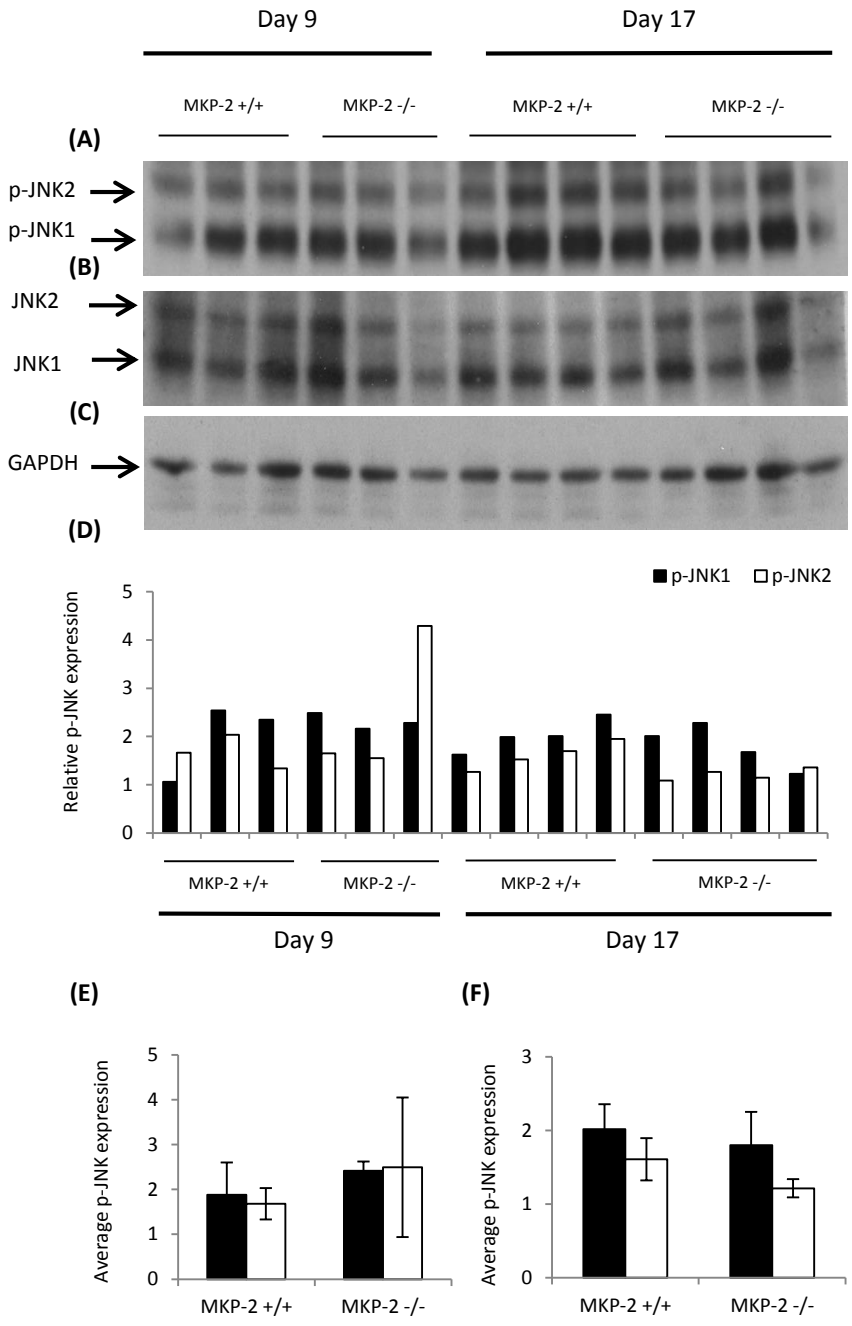

Figure 4.19: p-JNK expression in MKP-2 +/+ and MKP-2 -/- EAE day 9 and day 17 brain tissue. Brains were harvested from day 9 or 17 EAE mice and whole protein lysate prepared using RIPA buffer. (A) p-JNK expression was analysed by western blotting. Membranes were stripped and re-probed for (B) total JNK and (C) GAPDH. (D) Densitometry was utilised to determine changes in p-JNK expression relative to total JNK, with GAPDH used as a loading control and total JNK used as a control for variances in overall JNK levels between samples. (E) Day 9 and (F) day 17 average p-JNK expression in EAE MKP-2 +/+ or MKP-2 -/- mice. Data shown is from one experiment, n=3 at day 9, n=4 at day 17 per group. Not statistically significant, two-tailed unpaired student's t test.

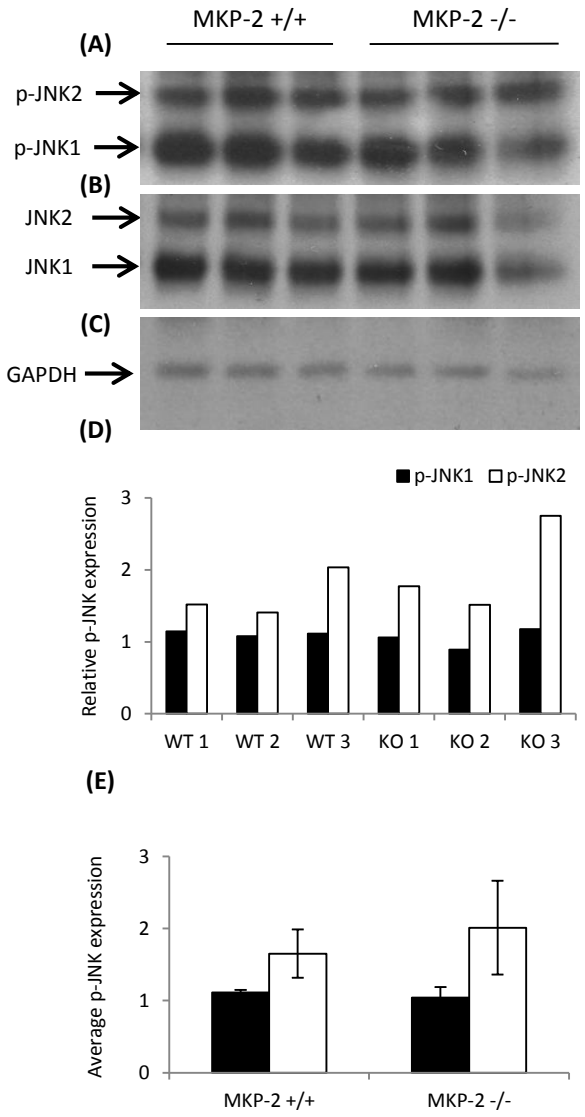

Figure 4.20: p-JNK expression in MKP-2 +/+ and MKP-2 -/- EAE day 28 brain tissue. Brains were harvested from day 28 EAE mice and whole protein lysate prepared using RIPA buffer. (A) p-JNK expression was analysed by western blotting. Membranes were stripped and re-probed for (B) total JNK and (C) GAPDH. (D) Densitometry was utilised to determine changes in p-JNK expression relative to total JNK, with GAPDH used as a loading control and total JNK used as a control for variances in overall JNK levels between samples. (E) Average p-JNK expression in EAE MKP-2 +/+ or MKP-2 -/- mice. Data shown is from one experiment, n=3 per group. Not statistically significant, two-tailed unpaired student's t test.

4.2.11 Flow cytometric analysis of cellular phenotypes in MKP-2 WT and KO spleen, lymph node and CNS tissue

EAE is an autoimmune disease driven by host autoreactive cells damaging self; therefore we sought to investigate any potential changes in the cellular phenotype within secondary lymphoid tissues due to MKP-2 deletion. Spleen and dLNs were harvested from naïve MKP-2 WT and KO mice. From this tissue, cell suspensions were formed to allow analysis of various cell surface markers by flow cytometry and assess any intrinsic differences in percentage and total number of various cell types.

Following analysis of baseline differences in cell phenotype frequencies in the absence of MKP-2, we then investigated changes occurring as a result of EAE onset and progression within MKP-2 KO mice. Spleen, dLN, brain and spinal cord tissue were harvested from MKP-2 WT and KO EAE mice and, again, cell suspensions formed to allow flow cytometric analysis of various cell surface markers.

4.2.11.1 $CD4^+$ $CD8^+$ T cells

Both $CD8^+$ T cells and, in particular, $CD4^+$ T cells are known to be essential in EAE pathogenesis therefore we examined these markers first, using FITC-conjugated anti-CD4 and PerCP-Cy5.5-conjugated anti-CD8 antibodies (Fig 4.21 A, B). Firstly naïve spleen and dLN cells from MKP-2 WT and KO mice were analysed. $CD4^+$ and $CD8^+$ populations were gated on all cells. The total cell number was calculated using the percentage positive cells and the total cell count from each spleen and dLN cell preparation counted before FACS staining.

Neither the percentage nor the overall number of $CD4^+$ T cells or $CD8^+$ T cells was altered in MKP-2 KO spleen or LN tissue compared with WT controls (Fig 4.21 C, D).

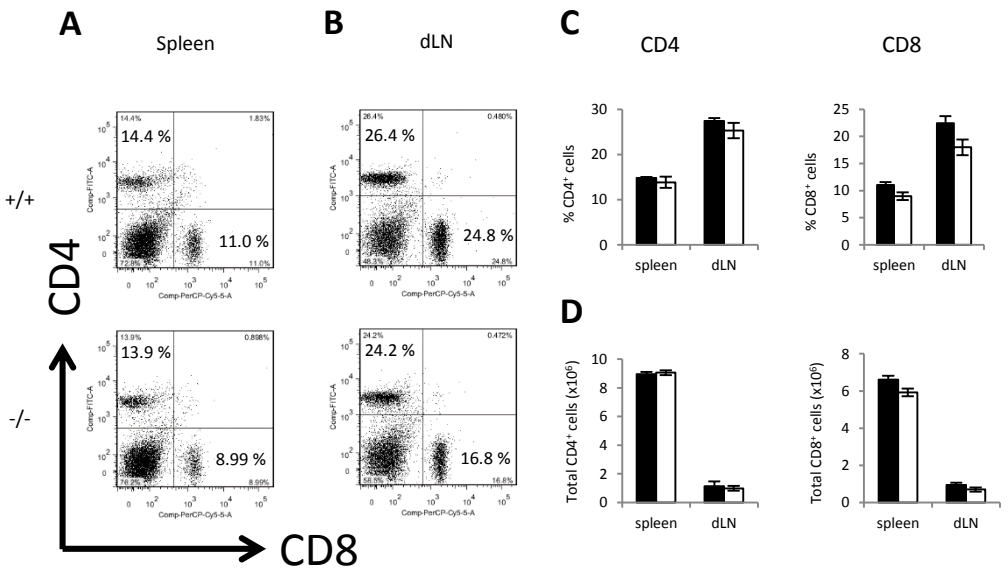

Figure 4.21: Frequency and total number of CD4$^+$ and CD8$^+$ cells in naïve MKP-2 +/+ and MKP-2 -/- spleen and dLNs. (A) Spleen and (B) dLNs were harvested from naïve MKP-2 +/+ and MKP-2 -/- mice and disrupted to form individual cell suspensions. Cells (0.5 x 10^6) were added to each relevant FACS tube and stained for FITC-conjugated CD4 and PE-conjugated CD8 and analysed by flow cytometry. Both the (C) percentage and (D) total number of positive cells were calculated. Graphs show mean ± SEM of one experiment (n=4 mice per group). Not statistically significant, two-tailed unpaired student's t test.

Following this, examination of $CD4^+$ and $CD8^+$ T cells in MKP-2 WT and KO EAE mice was carried out, firstly in spleen and dLN tissue at 3 separate time points (Fig. 4.22). Upon disease onset at day 9 post-immunisation, no difference in $CD4^+$ or $CD8^+$ cell percentage or total number was observed in either tissue type (Fig 4.22 A-D).

However by day 17, which corresponds to the stage of maximal disease severity, MKP-2 KO mice displayed significantly reduced frequency of $CD4^+$ and $CD8^+$ T cells (Fig 4.22 E-H). In KO spleens, only 12.5±1.0 % of cells were $CD4^+$, a decrease of 4.1 % from 16.6±0.5 % in WT samples, while $CD8^+$ cells made up just 8.1±1.5 % of the KO spleen cell population compared to 11.7±1.2 % in WT counterparts.

MKP-2 KO dLNs also contained lower percentages of $CD4^+$ and $CD8^+$ cells. $CD4^+$ cell frequency significantly decreased from 27.5±0.9 % to 23.8±0.9 % and $CD8^+$ cells from 21.9±1.0 % in WT mice to 16.9±1.2 %, a statistically significant 5 % reduction in MKP-2 KO animals. However the reduced frequency of $CD4^+$ and $CD8^+$ cells did not corresponded with any reduction in the total number of these cells in KO EAE day 17 spleen or dLNs, suggesting an increase in the overall number of immune cells in these tissues in KO EAE mice relative to WT.

At day 28 post immunisation, no change in $CD4^+$ or $CD8^+$ T cell frequency or total cell number was detected between MKP-2 WT and KO spleen and dLN tissue (Fig 4.22 l-L).

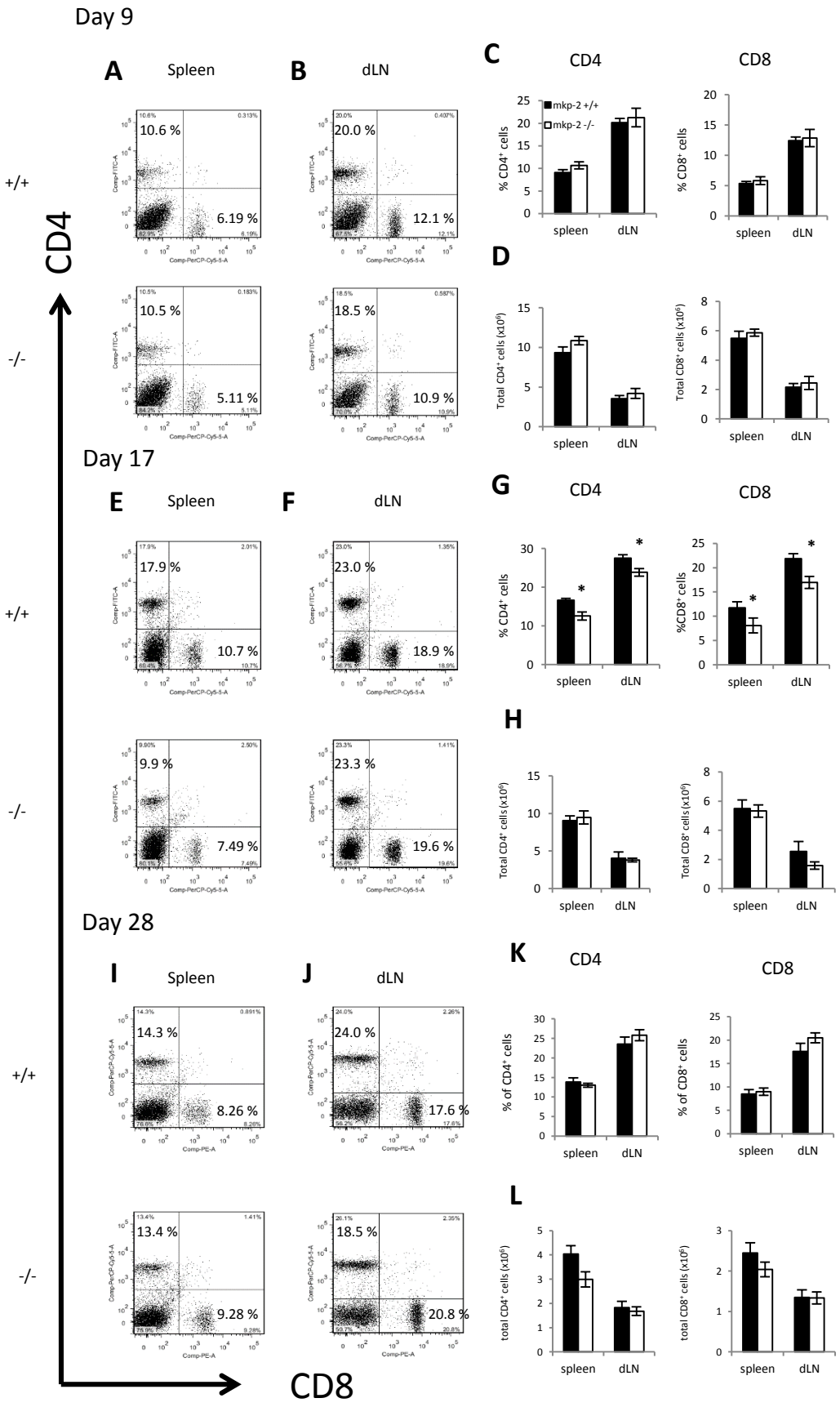
Day 9
A
Spleen
B
dLN
C
CD4
CD8
mkp-2 +/+
mkp-2 -/-
+/+
-/-
CD4
10.6 %
6.19 %
20.0 %
12.1 %
10.5 %
5.11 %
18.5 %
10.9 %
% CD4+ cells
% CD8+ cells
spleen
dLN
D
Total CD4+ cells (x10⁶)
Total CD8+ cells (x10⁶)
Day 17
E
Spleen
F
dLN
G
CD4
CD8
17.9 %
10.7 %
23.0 %
18.9 %
9.9 %
7.49 %
23.3 %
19.6 %
% CD4+ cells
%CD8+ cells
H
Total CD4+ cells (x10⁶)
Total CD8+ cells (x10⁶)
Day 28
I
Spleen
J
dLN
K
CD4
CD8
14.3 %
8.26 %
24.0 %
17.6 %
13.4 %
9.28 %
18.5 %
20.8 %
% of CD4+ cells
% of CD8+ cells
L
total CD4+ cells (x10⁶)
total CD8+ cells (x10⁶)
CD8

Figure 4.22: Frequency and total number of $CD4^+$ and $CD8^+$ cells in MKP-2 +/+ and MKP-2 -/- EAE spleen and dLNs. Spleen and lymph nodes were harvested at (A, B) day 9, (E, F) day 17 or (I, J) day 28 post EAE induction and disrupted to form individual cell suspensions. 0.5×10^6 cells were added to each relevant FACS tube and stained for FITC-conjugated CD4 and PE-conjugated CD8 and analysed by flow cytometry. The (C, G, K) percentage and total number (D, H, L) of positive cells were calculated. Graphs show mean ± SEM of three experiments, with representative FACS plots (n=10 mice per group). *P<0.05, two-tailed unpaired student's t test.

In naïve conditions, few $CD4^+$ and $CD8^+$ T cells are found within the CNS. However, a key event in EAE development is the migration of large numbers of autoreactive T cells across the BBB, allowing infiltration into the CNS to damage myelin antigens. Therefore we next analysed the immune cell phenotype in CNS tissues. Cells were isolated from brain and spinal cord tissue by percoll gradient as described in Materials and Methods Chapter 2, and analysed by flow cytometry (Fig 4.23). Cells were stained with FITC-conjugated anti-CD4 and PerCP-Cy5.5-conjugated anti-CD8 antibodies. $CD4^+$ and $CD8^+$ populations were gated on all cells. The total cell number was calculated using the percentage positive cells and the total cell count from each CNS cell preparation counter before FACS staining.

Comparable levels of $CD4^+$ and $CD8^+$ cells were found in MKP-2 WT and KO CNS tissue at disease onset, day 9 after immunisation (Fig 4.23 A-C). By day 17, the stage of peak disease severity, the percentage - but not total number - of $CD4^+$ and $CD8^+$ cells had increased compared to day 9 samples (Fig 4.23 D-F). However the frequency of $CD4^+$ cells between WT and KO tissue remained equivalent. In contrast, there was a significantly lower frequency of $CD8^+$ T cells within the CNS of MKP-2 KO mice relative to WT counterparts, down from 7.6±1.1 % to 3.6±0.5 %. Total CD8+ cell number was unchanged.

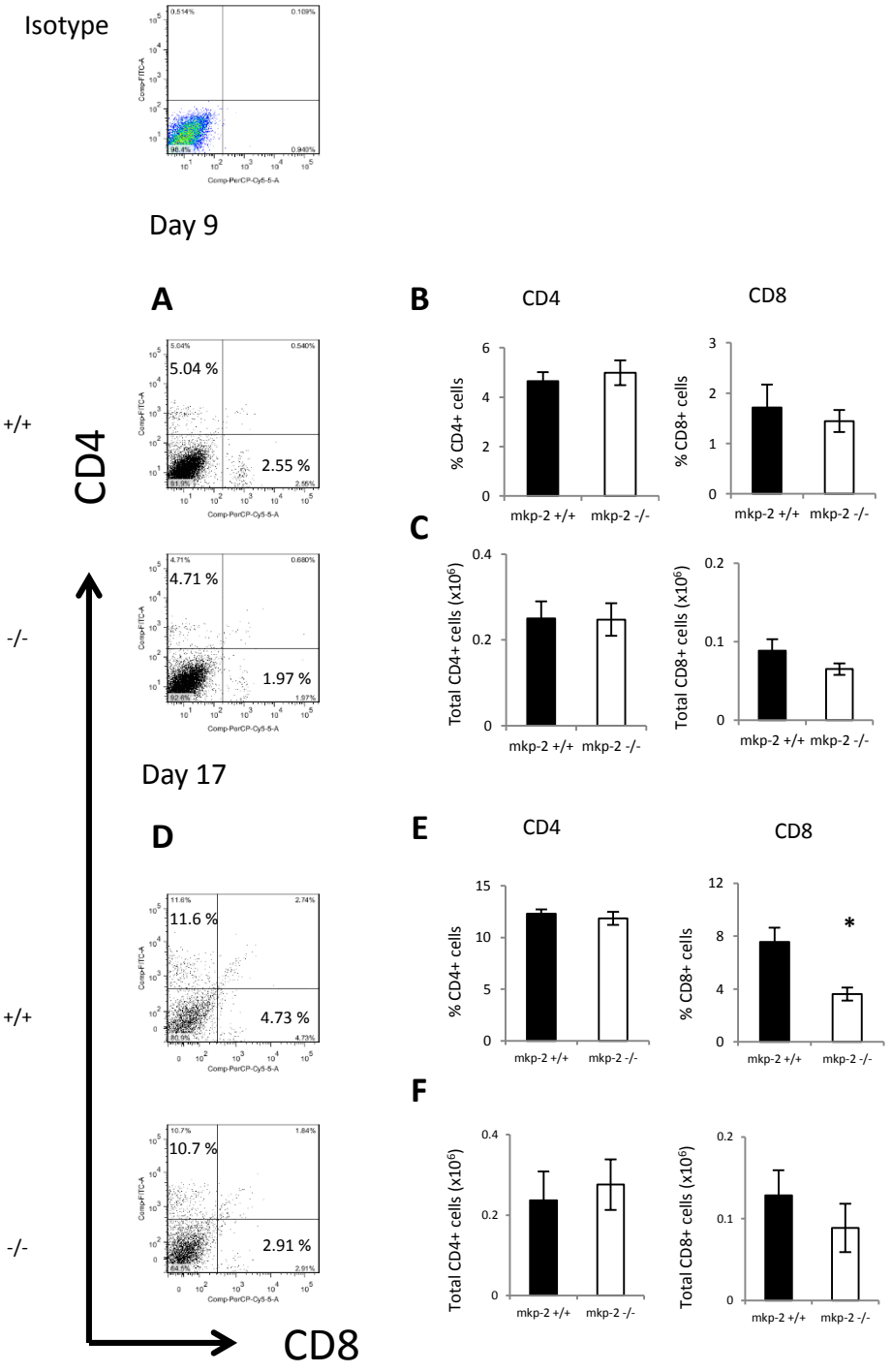

Figure 4.23: Frequency and total number of CD4$^+$ and CD8$^+$ cells in MKP-2 +/+ and MKP-2 -/- EAE CNS tissue. Brain and spinal cords were harvested at (A) day 9 and (D) day 17 post EAE induction. Tissue was pooled and cells isolated using percoll gradient. 0.2 x 10^6 cells were added to each relevant FACS tube and stained for FITC-conjugated CD4 and PE-conjugated CD8 and analysed by flow cytometry. The (B, E) percentage and (C, F) total number of positive cells were calculated. Graphs show mean ± SEM of two experiments with representative FACS plots (n=6 mice per group). *P<0.05, two-tailed unpaired student's t test

4.2.11.2 $CD4^+$ $CD25^+$ T cells

Activated mature T cells express CD25 on their cell surface; therefore we analysed the frequency of $CD4^+$ $CD25^+$ cells to establish whether the significant reduction in $CD4^+$ cells seen in spleen and dLNs of MKP-2 KO EAE mice compared to WT was due to a decreased repertoire of activated $CD4^+$ T cells. Cells were stained with PerCP-Cy5.5-conjugated anti-CD4 and FITC-conjugated anti-CD25 antibodies (Fig 4.24). $CD4^+$ $CD25^+$ populations were gated on all cells. The total cell number was calculated using the percentage of positive cells and the total cell count from each spleen and dLN cell preparation counted before FACS staining

However no change in the percentage of $CD4^+$ $CD25^+$ cells within total cell preparations was observed between WT and KO spleen or dLNs at any time point (Fig 4.24 A-C, E-G, I-K). The percentage of $CD25^+$ cells within $CD4^+$ cell populations was also analysed, and again there was no difference between WT and KO tissue at EAE day 9, day 17 or day 28 (data not shown). The total number of $CD4^+$ $CD25^+$ T cells was also unchanged at any time point.

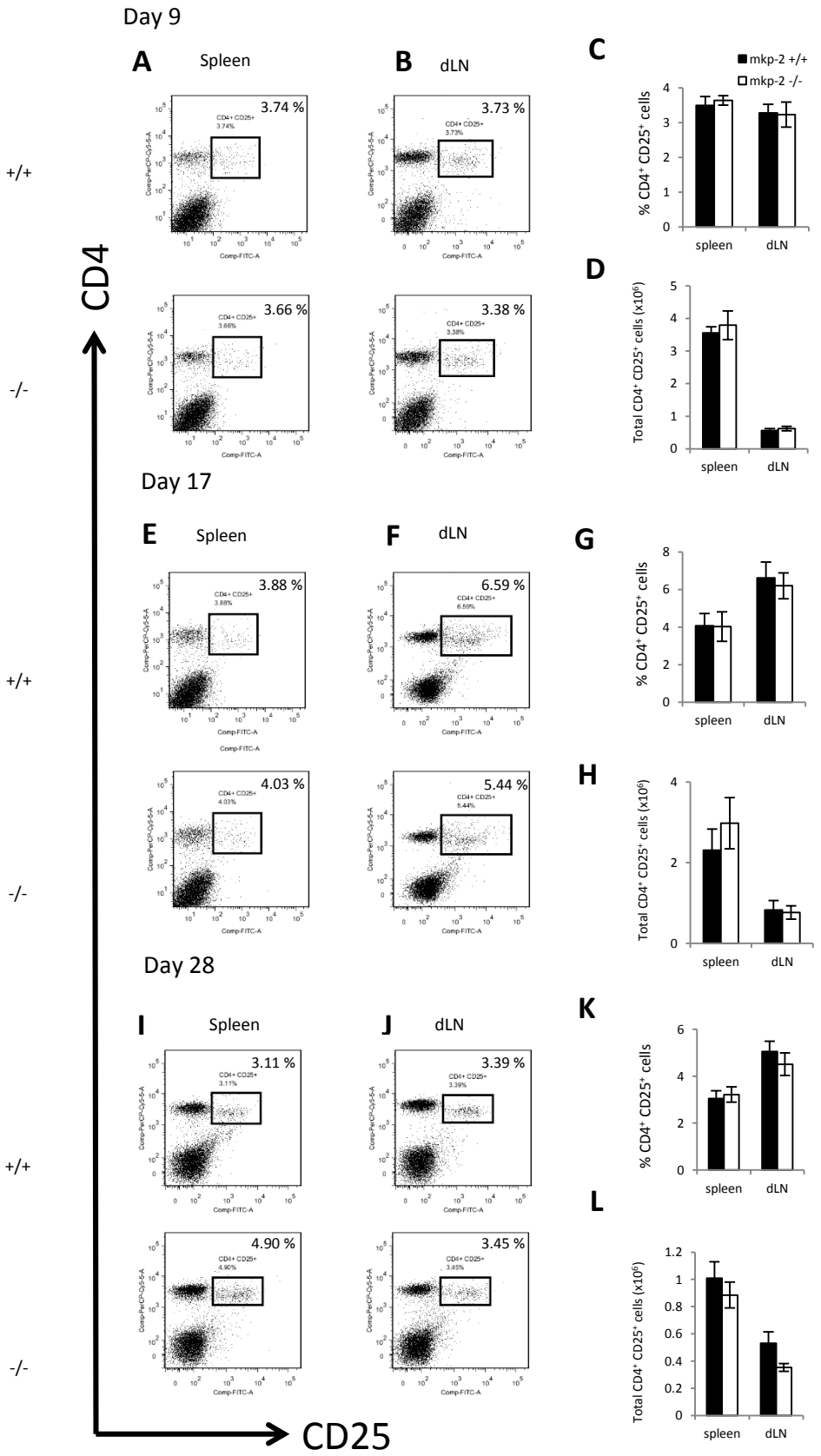
Day 9
A
Spleen
B
dLN
C
mkp-2 +/+
mkp-2 -/-
% CD4+ CD25+ cells
spleen
dLN
+/+
-/-
3.74 %
3.73 %
3.66 %
3.38 %
D
Total CD4+ CD25+ cells (x10^6)
Day 17
E
Spleen
F
dLN
G
% CD4+ CD25+ cells
3.88 %
6.59 %
4.03 %
5.44 %
H
Total CD4+ CD25+ cells (x10^6)
Day 28
I
Spleen
J
dLN
K
% CD4+ CD25+ cells
3.11 %
3.39 %
4.90 %
3.45 %
L
Total CD4+ CD25+ cells (x10^6)
CD4
CD25

Figure 4.24: Frequency and total number of $CD4^+$ $CD25^+$ cells in MKP-2 +/+ and MKP-2 -/- EAE spleen and dLNs. Spleen and dLNs were harvested at (A, B) day 9, (E, F) day 17 or (I, J) day 28 post EAE induction and disrupted to form individual cell suspensions. Cells (0.5×10^6) were added to each relevant FACS tube and stained for PerCPCy5.5-conjugated CD4 and FITC-conjugated CD25 and analysed by flow cytometry. The (C, G, K) percentage and (D, H, L) total number of positive cells were calculated. Graphs show mean ± SEM of three experiments with representative FACS plots (n=10 mice per group). Not statistically significant, two-tailed unpaired student's t test.

MKP-2 KO spleen and dLNs contained a reduced frequency of $CD4^+$ T cells compared to WT counterparts at day 17 after immunisation, yet this did not correspond with any changes in the frequency of activated T cells within these tissues. It was hypothesised that this may have been the result of more activated T cells migrating to the CNS in WT mice, therefore the expression of $CD4^+$ $CD25^+$ cells in MKP-2 WT and KO EAE day 17 CNS tissue was analysed. However the frequency and total number of $CD4^+$ $CD25^+$ cells remained unchanged in KO CNS samples relative to WT (Fig 4.25 A-C).

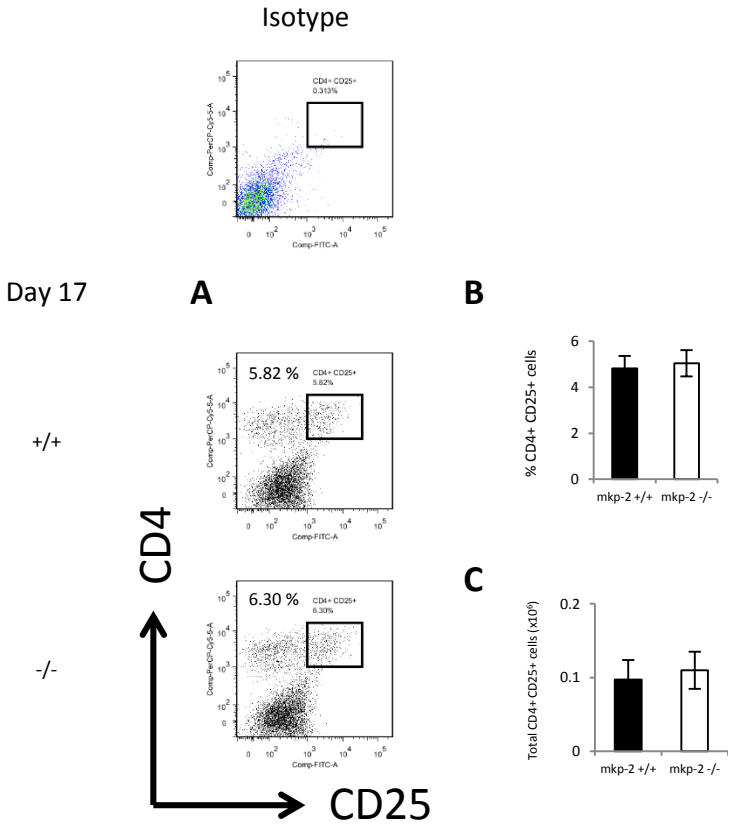

Figure 4.25: Frequency and total number of CD4$^+$ CD25$^+$ cells in MKP-2 WT and KO EAE CNS tissue. Brain and spinal cords were harvested at day 17 post EAE induction. Tissue was pooled and cells isolated using percoll gradient. Cells (0.2 x 10^6) were added to each relevant FACS tube and stained for PerCPCy5.5-conjugated CD4 and FITC-conjugated CD25 and analysed by flow cytometry. The (B) percentage and (C) total number of positive cells were calculated. Graphs show mean ± SEM of two experiments with representative FACS plots (n=6 mice per group). Not statistically significant, two-tailed unpaired student's t test.

4.2.11.3 $CD19^+$ $CD40^+$ B cells

As well as T cells, the important role of B cells in EAE development has been highlighted in recent literature. Therefore we next investigated the expression of B cells in naïve, as well as EAE, MKP-2 WT and KO lymphoid tissue. Cells were stained with APC-conjugated anti-CD19 and FITC-conjugated anti-CD40 antibodies, two markers expressed by B cells at almost all stages of development, including mature naïve B cells, activated B cells, memory B cells and regulatory B cells. However it should be noted that CD40 is also expressed on other immune cells, including macrophages and dendritic cells and therefore a more B cell-specific marker could have been chosen. $CD19^+$ $CD40^+$ populations were gated on all cells. The total cell number was calculated using the percentage of positive cells and the total cell count from each spleen and dLN cell preparation counted before FACS staining.

Firstly naïve spleen and dLN cells from MKP-2 WT and KO mice were analysed. We observed no changes in the percentage (Fig 4.26 A-C) or the total number (Fig 4.26 A, B, D) of $CD19^+$ $CD40^+$ cells in spleen or dLNs between naïve WT and KO mice.

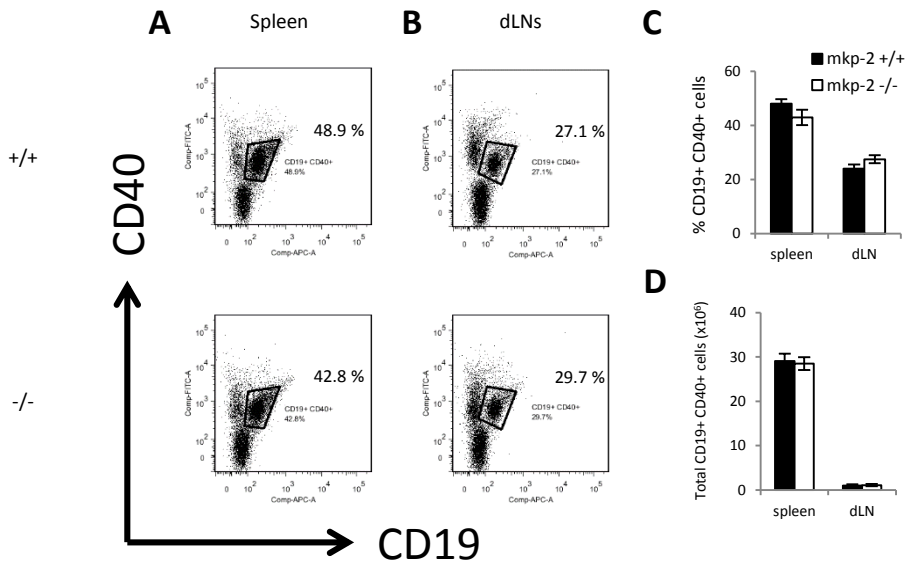

Figure 4.26: Frequency and total number of CD19$^+$ CD40$^+$ B cells in naïve MKP-2 +/+ and MKP-2 -/- spleen and dLNs. (A) Spleen and (B) dLNs were harvested from naïve MKP-2 +/+ and MKP-2 -/- mice and disrupted to form individual cell suspensions. Cells (0.5 x 10^6) were added to each relevant FACS tube and stained for FITC-conjugated CD40 and APC-conjugated CD19 and analysed by flow cytometry. Both the (C) percentage and (D) total number of positive cells were calculated. Graphs show mean ± SEM of one experiment (n=4 mice per group). Not statistically significant, two-tailed unpaired student's t test.

Upon EAE onset at day 9, MKP-2 KO spleen and dLNs still contained a comparable percentage and total number of $CD19^+$ $CD40^+$ cells compared to WT tissue (Fig 4.27 A-D).

In contrast, at day 17 post immunisation, B cell frequency was found to be significantly lower in MKP-2 KO spleen and dLNs relative to WT mice (Fig 4.27 E-G). WT spleens contained, on average, 27.7±2.6 % $CD19^+$ $CD40^+$ B cells compared to just 19.8±0.5 % in KO mice. In dLN tissue, B cells made up 29.5±1.2 % of the cell population of MKP-2 WT mice, but only 23.7±1.4 % in KO tissue. Surprisingly this did not corresponded with any change in the total number of $CD19^+$ $CD40^+$ cells in KO spleen or dLN tissues compared to WT (Fig 4.27 H).

By day 28 we observed no difference in either the percentage or the total number of B cells in MKP-2 KO lymphoid tissue relative to that of WT counterparts (Fig 4.27 I-L).

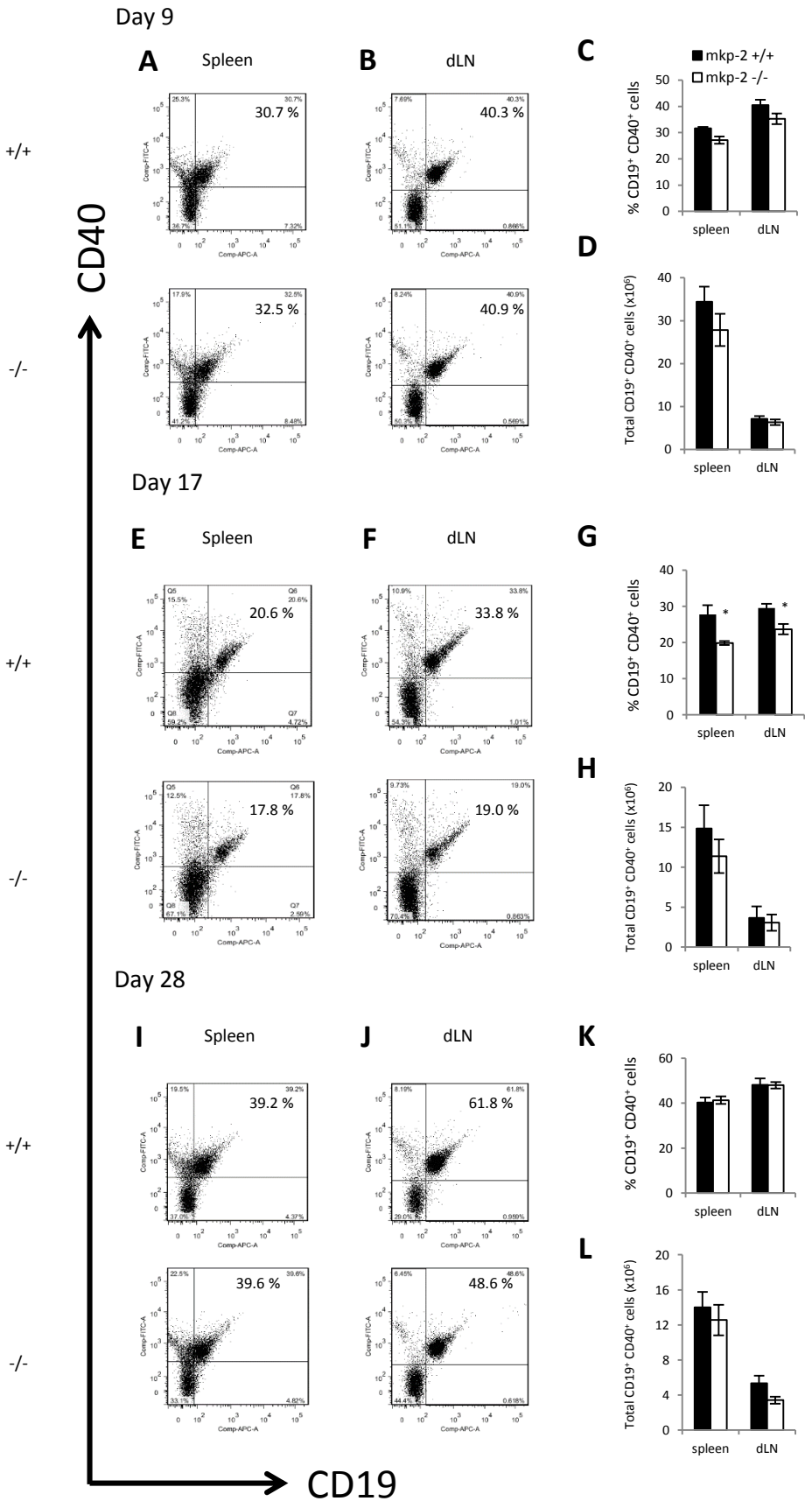
Day 9
A
Spleen
B
dLN
C
mkp-2 +/+
mkp-2 -/-
+/+
-/-
30.7 %
40.3 %
32.5 %
40.9 %
% CD19+ CD40+ cells
spleen
dLN
D
Total CD19+ CD40+ cells (x10^6)
CD40
Day 17
E
Spleen
F
dLN
G
20.6 %
33.8 %
17.8 %
19.0 %
% CD19+ CD40+ cells
H
Total CD19+ CD40+ cells (x10^6)
Day 28
I
Spleen
J
dLN
K
39.2 %
61.8 %
39.6 %
48.6 %
% CD19+ CD40+ cells
L
Total CD19+ CD40+ cells (x10^6)
CD19

Figure 4.27: Frequency and total number of $CD19^+$ $CD40^+$ B cells in MKP-2 +/+ and MKP-2 -/- EAE spleen and dLNs. Spleen and dLNs were harvested at (A, B) day 9, (E, F) day 17 or (I, J) day 28 post EAE induction and disrupted to form individual cell suspensions. Cells (0.5×10^6) were added to each relevant FACS tube and stained for APC-conjugated CD19 and FITC-conjugated CD40 and analysed by flow cytometry. The (C, G, K) percentage and (D, H, L) total number of positive cells were calculated. Graphs show mean ± SEM of 3 experiments with representative FACS plots (n=10). *P<0.05, two-tailed unpaired student's t test.

In addition to autoreactive T cell infiltration, B cell migration into the CNS is also a key event in EAE pathogenesis. Once there, B cells can reactivate autoreactive T cells and produce MOG-specific autoantibodies which contributes to demyelination and inflammation. Therefore we analysed the percentage and total number of $CD19^+$ $CD40^+$ B cells within MKP-2 WT and KO EAE CNS tissue.

MKP-2 deletion did not affect the percentage of CNS infiltrating $CD19^+$ $CD40^+$ B cells in the brain and spinal cord tissues within EAE mice at either day 9 or day 17 post-immunisation (Fig 4.28 A, B, D, E). In addition, the total number of B cells was comparable between WT and KO mice samples at both time points (Fig 4.28 C, F).

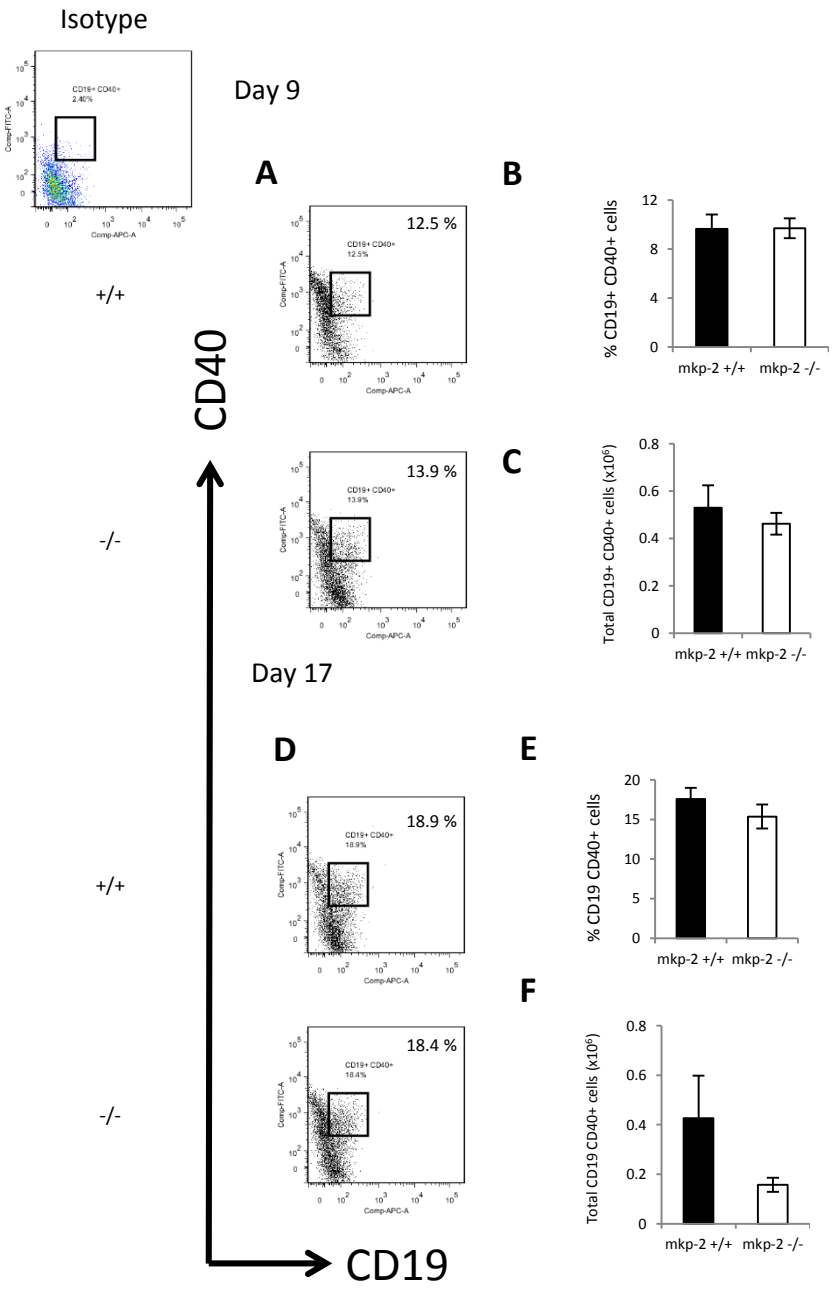

Figure 4.28: Frequency and total number of CD19$^+$ CD40$^+$ cells in MKP-2 +/+ and MKP-2 -/- EAE CNS tissue. Brain and spinal cords were harvested at (A) day 9 or (D) day17 post EAE induction. Tissue was pooled and cells isolated using percoll gradient. Cells (0.2 x 10^6 cells) were added to each relevant FACS tube and stained for FITC-conjugated CD19 and PE-conjugated CD40 and analysed by flow cytometry. The (B, E) percentage and (C, F) total number of positive cells were calculated. Graphs show mean ± SEM of two experiments (n=6 mice per group). Not statistically significant, two-tailed unpaired student's t test.

4.2.11.4 CD11c$^+$ DCs and MHC-II$^+$ cells

Autoreactive T cells are primed by antigen presenting cells (APCs) displaying the relevant antigen via MHC-II molecules. In EAE, DCs are one of the most important APCs and thus we investigated any potential variations in expression of these cells in mice tissues upon MKP-2 deletion. The frequency of CD11c$^+$ DCs and MHC-II$^+$ expression on APCs, including DCs, in naïve, as well as EAE, MKP-2 WT and KO lymphoid tissue was analysed. Cells were stained with PE-conjugated anti-CD11c and APC-conjugated anti-MHC-II antibodies. CD11c$^+$ and MHC-II$^+$ populations were gated on all cells. The total cell number was calculated using the percentage positive cells and the total cell count from each spleen and dLN cell preparation counted before FACS staining. It should be noted that, while CD11c is a common marker of DCs, it is also expressed on other cells including monocytes and macrophages.

The frequency and total number of CD11c$^+$ DCs remained unchanged in naive MKP-2 KO spleen and dLN samples compared to WT (Fig 4.29 A-D). In addition, the percentage and overall number of spleen and dLN cells which were MHC-II$^+$ did not change in KO mice compared to WT (Fig 4.29 A-D). Upon immune activation, APCs including DCs, B cells and macrophages increase surface expression of MHC-II. In EAE, DCs are the primary APCs that prime autoreactive T cells via presentation of antigen on MHC-II, therefore we also analysed the frequency of CD11c$^+$ MHC-II$^+$ cells in naïve MKP-2 KO mice and WT littermates. We observed comparable levels of MHC-II$^+$ DCs between KO and WT mice in spleen and dLNs (Fig 4.29 A-D).

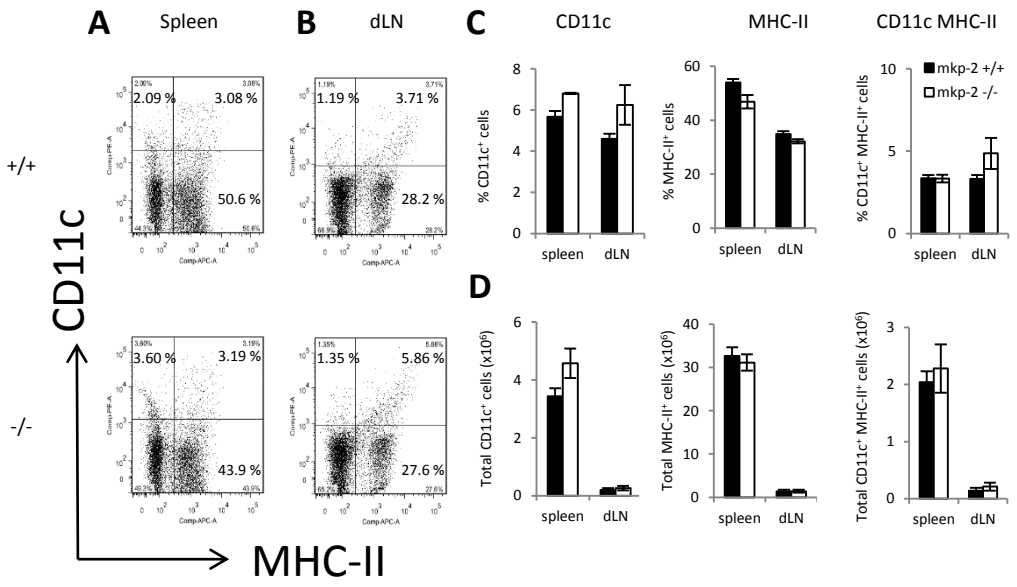

Figure 4.29: Frequency and total number of CD11c$^+$ and MHC-II$^+$ cells in naïve MKP-2 +/+ and MKP-2 -/- spleen and dLNs. (A) Spleen and (B) dLNs were harvested from naïve MKP-2 +/+ and MKP-2 -/- mice and disrupted to form individual cell suspensions. Cells (0.5 x 10^6) were added to each relevant FACS tube and stained for PE-conjugated CD11c and APC-conjugated MHC-II and analysed by flow cytometry. The (C) percentage and (D) total number of positive cells were calculated. Graphs show mean ± SEM of one experiment (n=4 mice per group). Not statistically significant, two-tailed unpaired student's t test.

Subsequently we assessed $CD11c^+$ and $MHC\text{-}II^+$ cell numbers in MKP-2 WT and KO lymphoid tissue during EAE onset, peak and recovery. $CD11c^+$ DC frequency and total cell number were not altered by the absence of MKP-2 in day 9 spleen and dLN tissue (Fig 4.30 A-D). This was also true of $MHC\text{-}II^+$ cells as well as $MHC\text{-}II^+$ $CD11c^+$ DCs.

DC expression remained unaffected by MKP-2 deletion in day 17 and day 28 samples (Fig 4.30 E-H; Fig 4.30 I-L). Similarly, the frequency and total number of $MHC\text{-}II^+$ APCs was again unchanged in both spleen and dLN tissue as a result of MKP-2 KO. While the percentage of $CD11c^+$ DCs which were $MHC\text{-}II^+$ was also comparable between WT and KO samples at day 17 and day 28.

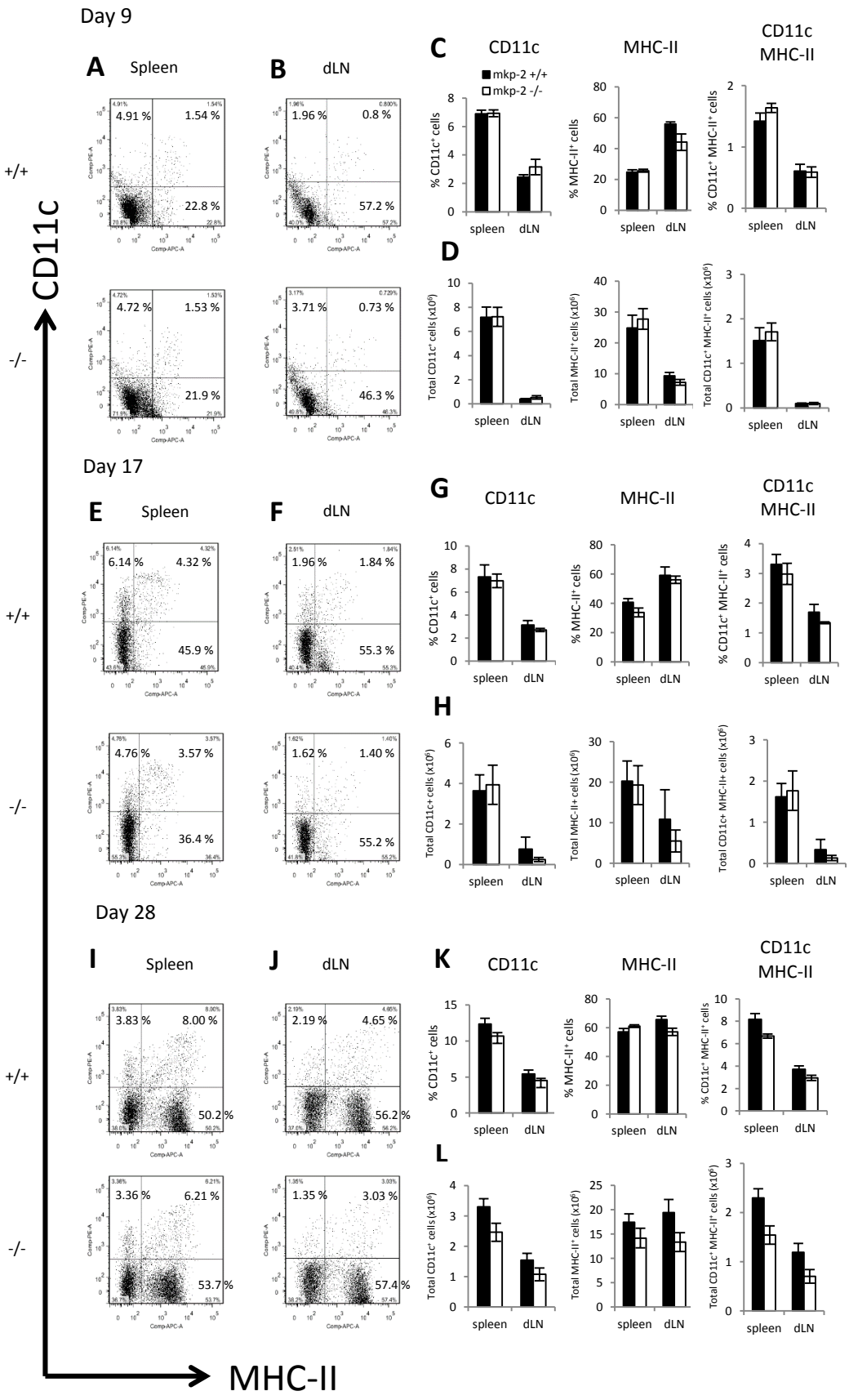
Day 9
A Spleen
B dLN
C CD11c
MHC-II
CD11c MHC-II
mkp-2 +/+
mkp-2 -/-
4.91 %
1.54 %
22.8 %
1.96 %
0.8 %
57.2 %
4.72 %
1.53 %
21.9 %
3.71 %
0.73 %
46.3 %
% CD11c+ cells
% MHC-II+ cells
% CD11c+ MHC-II+ cells
Total CD11c+ cells (x10⁶)
Total MHC-II+ cells (x10⁶)
Total CD11c+ MHC-II+ cells (x10⁶)
spleen
dLN
Day 17
E Spleen
F dLN
G CD11c
MHC-II
CD11c MHC-II
6.14 %
4.32 %
45.9 %
1.96 %
1.84 %
55.3 %
4.76 %
3.57 %
36.4 %
1.62 %
1.40 %
55.2 %
Total CD11c+ cells (x10⁶)
Total MHC-II+ cells (x10⁶)
Total CD11c+ MHC-II+ cells (x10⁶)
Day 28
I Spleen
J dLN
K CD11c
MHC-II
CD11c MHC-II
3.83 %
8.00 %
50.2 %
2.19 %
4.65 %
56.2 %
3.36 %
6.21 %
53.7 %
1.35 %
3.03 %
57.4 %
% CD11c+ cells
% MHC-II+ cells
% CD11c+ MHC-II+ cells
Total CD11c+ cells (x10⁶)
Total MHC-II+ cells (x10⁶)
Total CD11c+ MHC-II+ cells (x10⁶)
+/+
-/-
CD11c
MHC-II

Figure 4.30: Frequency and total number of CD11c$^+$ and MHC-II$^+$ cells in MKP-2 +/+ and MKP-2 -/- EAE spleen and dLNs. Spleen and lymph nodes were harvested at (A, B) day 9, (E, F) day 17 or (I, J) day 28 post EAE induction and disrupted to form individual cell suspensions. Cells (0.5×10^6) were added to each relevant FACS tube and stained for PE-conjugated CD11c and APC-conjugated MHC-II and analysed by flow cytometry. The (C, G, K) percentage and (D, H, L) total number of positive cells were calculated. Graphs show mean ± SEM of three experiments (n=10 mice per group). Not statistically significant, two-tailed unpaired student's t test.

4.2.11.5 CD11b$^+$ macrophages

Macrophages are another important population of cells in EAE pathogenesis with both detrimental, as well as protective, effects. MKP-2 deletion has previously been shown to alter macrophage function in disease conditions. Therefore we analysed macrophage expression in MKP-2 WT and KO mice during EAE development by flow cytometry, using CD11b as a positive marker for macrophages. Tissue-resident macrophages within the spleen include red pulp, marginal zone, metallophilic and tangible macrophages. In lymph nodes there are also subpopulations of sinus-resident and parenchymal macrophages.

No variance in CD11b$^+$ cell frequency or total number was observed between day 9 EAE WT and KO spleen and dLNs (Fig 4.31 A-D). By day 17 our data suggest that the frequency, but not total number, of splenic CD11b$^+$ macrophages in KO mice may be upregulated at 26.8±1.6 % relative to WT counterparts with 18.4±1.3 % (Fig 4.31 E-H). However this difference is not statistically significant and thus has to be confirmed. No difference in CD11b$^+$ cells was observed in dLNs at day 17. Similarly, the frequency and total number of macrophages in day 28 EAE lymphoid tissue was comparable between WT and KO mice (Fig 4.31 I-L). Overall, CD11b$^+$ macrophages were found to be far more abundant in spleen tissue compared to dLNs at all time points.

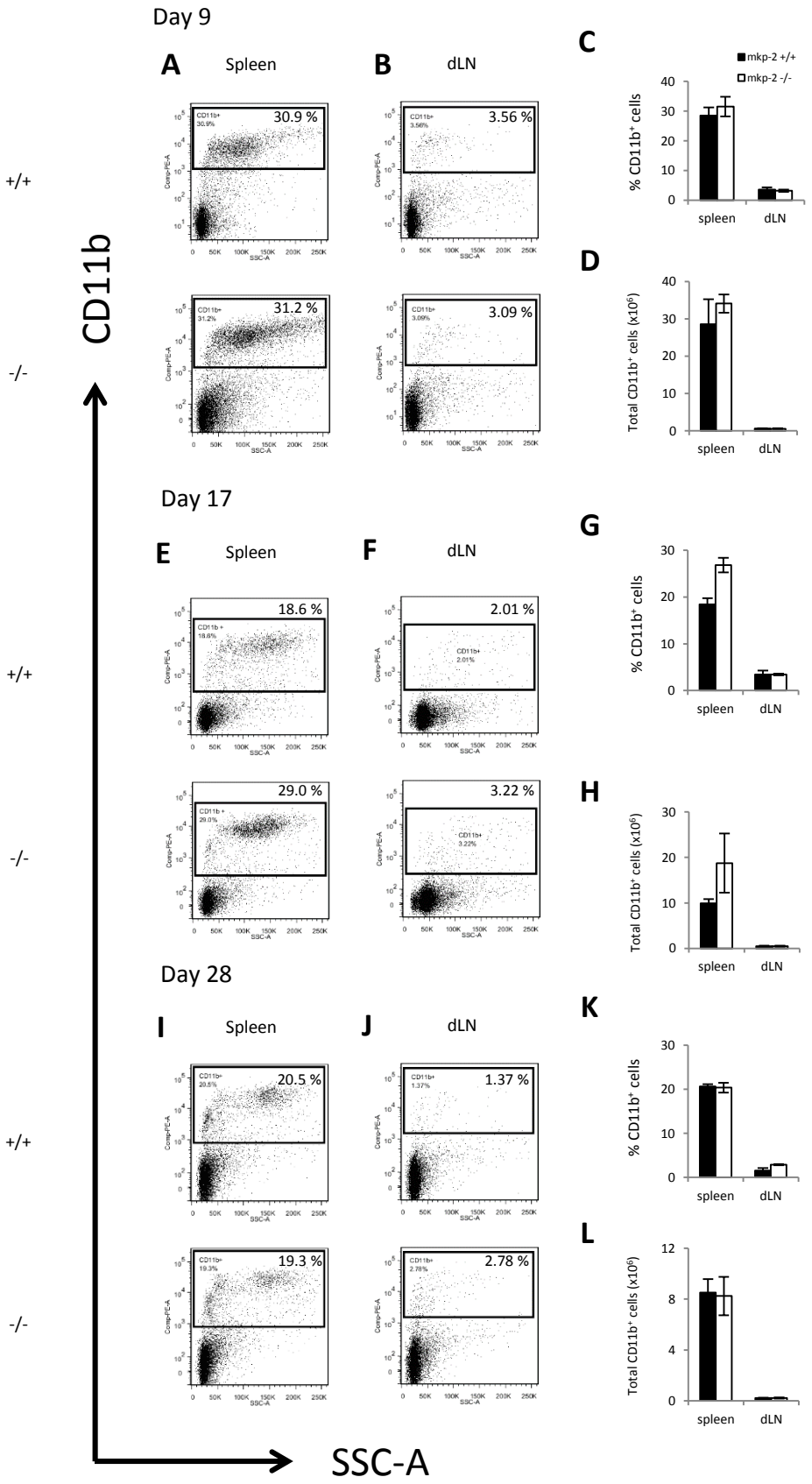
Day 9
A
Spleen
B
dLN
C
mkp-2 +/+
mkp-2 -/-
30.9 %
3.56 %
31.2 %
3.09 %
+/+
-/-
CD11b
% CD11b+ cells
Total CD11b+ cells (x10^6)
spleen
dLN
D
Day 17
E
Spleen
F
dLN
G
18.6 %
2.01 %
29.0 %
3.22 %
H
Day 28
I
Spleen
J
dLN
K
20.5 %
1.37 %
19.3 %
2.78 %
L
SSC-A

Figure 4.31: Frequency and total number of CD11b$^+$ cells in MKP-2 +/+ and MKP-2 -/- EAE spleen and dLNs. Spleen and dLNs were harvested at (A, B) day 9, (E, F) day 17 or (I, J) day 28 post EAE induction and disrupted to form individual cell suspensions. Cells (0.5×10^6) were added to each relevant FACS tube and stained for PE-conjugated CD11b and analysed by flow cytometry. The (C, G, K) percentage and (D, H, L) total number of positive cells were calculated. Graphs show mean ± SEM of two experiments (n=6). Not statistically significant, two-tailed unpaired student's t test.

4.2.12 Serum nitrite levels in MKP-2 WT and MKP-2 KO EAE mice

An important inflammatory mediator involved in the pathogenesis of EAE is NO. Changes in NO production in MKP-2 deficient mice have also been observed in recent publications [228], therefore we next analysed any potential differences in NO formation between MKP-2 WT and KO mice in our disease model. This was performed using a Griess reagent system to measure a breakdown product of NO, nitrite, in mice serum samples.

Nitrite levels increased in EAE mice compared to naïve controls (data not shown) but there was no difference between MKP-2 WT and KO samples at day 17 of EAE development (Fig 4.32 A). However, by day 28, KO mice were producing significantly less nitrite relative to WT, decreasing from 161.8±21.9 to 80±12.8 µM / L (Fig 4.32 B).

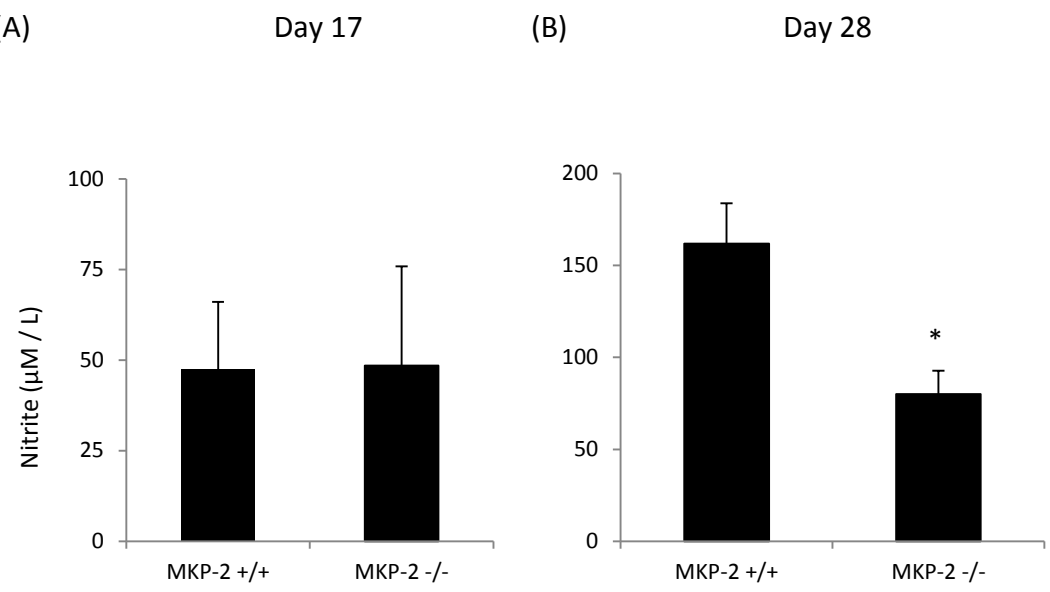

Figure 4.32: Nitrite expression in MKP-2 +/+ and MKP-2 -/- serum. Whole blood was harvested at (A) day 17 or (B) day 28 post EAE-induction and centrifuged at full speed for 15 minutes to pellet clotted blood. Serum supernatant was retained and 15 mg/ml $ZnSO_4$ added to allow deproteinization of samples. Following this, nitrite concentrations were determined by Griess Assay, using a standard curve of known nitrite concentrations. Graphs show mean ± SEM of two experiments (n=4 naïve; n=7 MKP-2 +/+; n=8 MKP-2 -/-). *$P < 0.05$, two-tailed unpaired student's t test.

4.3 Discussion

MKP-2 mRNA expression was significantly upregulated in the CNS of day 17 MOG immunised mice compared to PBS controls (Fig 3.17 B), suggesting a potential role of this kinase in EAE development. The present study is the first to confirm an important role for MKP-2 in EAE development as disease severity is significantly ameliorated in mice deficient in this gene compared with WT littermate controls.

However our early experiments in either 5^{th} or 6^{th} backcross generation mice were not conclusive. In 4/7 experiments conducted in PLE-5 and PLE-6 mice, EAE development was reduced in MKP-2 KO mice compared to WT littermates. In contrast, disease severity was enhanced in KO mice relative to WT counterparts on 3/7 occasions. The lack of reproducibility of these results highlighted the inherent problems associated with studies using KO mice.

Mice used in these experiments were either a 5^{th} or 6^{th} generation backcross (male chimeras of a 129/sv background crossed with female C57BL/6) following MKP-2 gene deletion. Therefore the inconsistency in EAE development was most likely the result of genetic variability due to an insufficient number of backcrosses, meaning these mice could still contain genetic material from the donor 129/sv strain. The optimal number of backcrosses is at least 10, at which stage there is only a 0.1% chance of retaining loci from the donor background, and thus the strain is considered fully congenic (when it differs from the inbred strain at only a single locus). Previous studies have observed similar effects, with changes in disease incidence and phenotype in KO mice with insufficient backcrossing [303], [304]. As 129/sv mice are resistant to MOG-induced EAE [92], [305], [306], this could potentially affect EAE development in our MKP-2 WT and KO mice. Repeated crossing into C57BL/6 mice should reduce the likelihood of this happening [304]. This was confirmed when a 7^{th} generation (PLE-7) was tested, in which a stable disease phenotype was obtained. In 7/7 EAE experiments, MKP-2 deletion resulted in significantly decreased clinical severity compared to WT littermates, thus confirming MKP-2 as a critical component in the autoimmune response of EAE. This is in support of previous reports which have also observed reduced EAE severity in mice deficient in MKP-1 [217] and MKP-5 [243].

Once this had been established, our next aim was to determine how MKP-2 gene deletion affects key aspects of this disease model. Firstly, inflammatory cell infiltration into the spinal cord was reduced in MKP-2 deficient mice. Even at day 17, when clinical symptoms are at their peak, far fewer cells were observed crossing the BBB into the CNS in these KO mice. In contrast, WT spinal cords all contained several large areas of inflammatory cell accumulation in the white matter, particularly $CD4^+$ T cells and $F4/80^+$ macrophage/microglial cells. Surprisingly, although with fewer cells in the spinal cord tissues, these KO mice still displayed clinical symptoms of EAE at an average of around 2.1 at this time point. The reduced number of infiltrating cells in the CNS of KO mice may indicate that MKP-2 deletion could also potentially affect BBB permeability resulting in less cells trafficking to the CNS. Although I was not able to investigate the difference in BBB permeability between WT and KO EAE mice in my thesis, this could be tested by Evans Blue assay. A potential effect of MKPs on BBB permeability would be in line with a previous report which found increased BBB disruption following subarachnoid haemorrhage in rats was associated with decreased MKP-1 and in increase in ERK, JNK and p38 phosphorylation [307]. Treatment with recombinant osteopontin restored BBB integrity, with increased MKP-1 expression. This suggests MKPs may be involved in regulation of BBB integrity via regulation of MAPK activation.

Another possible explanation for decreased CNS infiltration in MKP-2 KO EAE mice may be altered chemokine expression in the absence of MKP-2, affecting cell migration to areas of inflammation. Previous literature supports this hypothesis. As mentioned briefly in Section 4.1, MKP-2 is involved in regulation of the early inflammatory response in mouse models of ALI [232]; this is associated with significantly decreased MIP-1α expression in BAL fluids following intratracheal LPS challenge. Furthermore, other MKPs have also been implicated in control of chemokine expression, including MKP-1 which negatively regulates expression of CXCL1 and CXCL2 in periodontal disease, contributing to osteoclast formation [212]. In addition, Hammer et al observed upregulated CCL3, CCL4 and CXCL2 mRNA expression in MKP-1 KO spleen tissue, as well as protein expression in serum, in response to LPS administration [211]. Similarly, serum CCL2 levels are increased in MKP-1 KO mice following LPS challenge [210]. Our study found that CCL2

expression was significantly decreased in EAE day 17 and day 28 MKP-2 KO spleen cells following MOG stimulation. CCL2 acts as a chemoattractant for a variety of cells, including macrophages, T lymphocytes, natural killer (NK) cells and DCs. By regulating migration of these cells, it can indirectly lead to an increase in the inflammatory response at specific sites. Therefore, through regulation of chemokine expression, MKP-2 can potentially affect the level of cell migration to sites of inflammation, thereby increasing autoimmune pathology. WT and KO dLN cells expressed similar levels of CCL2 expression, suggesting MKP-2 may exert tissue-specific effects on chemokine production.

A further possible mechanism of action of MKP-2 during EAE pathogenesis and progression may be in contributing to the regulation of cytokine production. Upon MOG_{35-55} peptide re-challenge in ex vivo cell cultures, in addition to upregulated CCL2 production, the expression of several cytokines by spleen and dLN cells was altered in MKP-2 KO mice compared to WT counterparts. Both Th17 and Th1 cells are known to play a crucial role in EAE pathogenesis [98], [308]. Antigen specific production of the most prominent cytokine within the Th17 family, IL-17A, and the archetypal Th1 cytokine, IFNγ, was significantly downregulated in KO spleen and dLN cells compared to WT. Other pro-inflammatory cytokines are also very important in this particular disease model. IL-6, which is secreted by a variety of cells including Th2 cells, macrophages, DCs, and B cells [309]–[312], is a prominent cytokine in the development of inflammatory responses. Our data show that IL-6 expression was also significantly lower in MKP-2 KO spleen and dLN cells compared to WT. The reduction of all these proinflammatory cytokines in KO mice is correlated with the reduced disease severity seen in KO mice, highlighting how critical they are in EAE disease development. It also suggests MKP-2 may be involved in regulating production of these cytokines by reducing activity of the cells producing them or downregulating gene transcription.

This is in agreement with previous reports utilising MKP-2 KO mice. Upon LPS stimulation, Al-Mutairi *et al* showed that MKP-2 KO macrophages produce significantly less IL-6, IL-12 and TNFα but more IL-10 [228]. In addition, following i.p LPS administration, levels of IL-6, TNFα, IL-1β and IL-10 significantly decrease

in MKP-2 KO serum compared to WT [233]. MKP-2 can also alter Th2 responses, with significantly reduced IL-4 produced by MKP-2 KO splenic $CD4^+$ T cells in response to *L.major* infection compared to WT [231]. Taken together with our results, MKP-2 is clearly involved in regulating production of several different cytokines from a variety of cells. However, particularly in the case of IFNγ, the level of regulation may vary between different tissues and cell types. It is also likely that the function of MKP-2 in regulating these cytokines is dynamic and influenced by the stages of EAE pathogenesis as well as the overall cytokine milieu in vivo, e.g. naïve mice versus mice at the onset, peak or resolution stages of EAE. In each of these studies, altered cytokine production was associated with changes in MAPK phosphorylation and therefore a similar mechanism of action may be taking place in our model. For IFNγ and, in particular, IL-6, increased p38 and JNK activation in MKP-1 deficient mice appears to be involved in increased cytokine production [208], [313]. MKP-2 may also be acting through other cells (e.g. DCs) to regulate Th1 and Th17 responses as a similar function with MKP-1 has previously been established [314]. The development of Th1 and Th17 cells was altered in MKP-1 KO mice as a result of increased IL-6 and decreased IL-12 expression in KO DCs (via increased p38 activation) which enhanced STAT3 phosphorylation but downregulated STAT4 phosphorylation in MKP-1 KO T cells, downstream targets of IL-6 and IL-12 respectively.

IL-22 is a member of the IL-10 cytokine family which is linked to both innate and adaptive immune responses [315], [316]. A variety of cell types are known to produce IL-22, including Th1 cells, Th17 cells, Th22 cells, $CD8^+$ T cells and NK cells [317]–[319]. Previous studies have reported both inflammatory as well as protective effects exerted by IL-22 [320]–[323]. In the present study we found that expression of this cytokine was significantly reduced in MKP-2 KO day 17 spleen and dLNs, suggesting that, similarly to IL-17, IL-6 and IFNγ, IL-22 expression is positively regulated by MKP-2 and that IL-22 may exacerbate the inflammatory response at the peak of disease severity. However this may not be a crucial part of the autoimmune pathogenesis of EAE as IL-22 KO mice are fully susceptible to EAE [324]. By day 28, IL-22 expression remained downregulated in KO dLNs, however an increase was observed in corresponding spleen samples. Perhaps splenic IL-22 can aid in EAE recovery at the latter stages of disease progression, thus explaining the increased IL-

22 correlating with lower clinical scores observed in KO mice. These results also suggest MKP-2 may be able to act as both a positive and negative regulator of IL-22 expression, and therefore can potentially increase or decrease IL-22 production at different times.

Antigen specific production of IL-2 was downregulated in MKP-2 deficient day 17 EAE spleen and dLN cells following 24 hour and 48 hour MOG re-stimulation but not 72 hours. This implies an initial defect in IL-2 production in the absence of MKP-2 which is overcome in the event of continued cell stimulation. The mechanism through which this occurs is unknown, but is perhaps the result of delayed compensation by another MKP. IL-2 plays a role in many functions which are essential in EAE, including mediating differentiation and proliferation of antigen-specific T cells and B cells [325]–[328], as well as regulating the expression of the inflammatory cytokine IFNγ [329]. Therefore decreased IL-2 production in MKP-2 KO mice may result in reduced T cell and B cell differentiation and proliferation, which correlates with the lower clinical disease scores observed. The implication that MKP-2 is needed for T cell activation and proliferation is similar to results previously seen in MKP-1 deficient mice. Upon stimulation with anti-CD3 and anti-CD28, MKP-1 KO $CD4^+$ T and $CD8^+$ T cells produced less IL-2 and proliferated less than WT counterparts [217].

Although not statistically significant, MKP-2 mRNA expression was 3-fold higher in MOG stimulated WT spleen cells compared to unstimulated controls. This suggests MKP-2 may be upregulated in cells involved in the antigen-specific immune response of EAE, and thus may contribute to the altered functioning of these cells which leads to disease pathogenesis. However, as whole spleen cell preparations were used, it remains unclear in which cells MKP-2 is most strongly expressed, as well as which cells are contributing most to production of these cytokines. MKP-2 deficient cells displayed an altered profile of cytokine production but these results again do not conclusively reveal which cells are most affected by the absence of MKP-2. MKP-2 has been shown to have diverse functions depending on which type of cell it is expressed in [223], [225], [226]; therefore deletion of this enzyme would likely have varying effects in different cell types. As EAE pathophysiology involves several different cell types, including $CD4^+$ T cells, $CD8^+$ T cells, B cells, DCs and

macrophages, decreased disease severity due to MKP-2 deficiency may be the result of unique alterations in cellular functionality of some or all of these immune cells. Previous reports have observed changes in $CD4^+$ T cell responses and proliferation in MKP-2 KO mice [330], as well as alterations in phenotype and cytokine production in MKP-2 KO macrophages [228], [233] therefore these cells are likely contributing to the amelioration of EAE in MKP-2 KO mice.

MKP-1 is the most widely studied and well defined of the MKPs to date. Similarly to MKP-2, it is ubiquitously expressed throughout the body [201], is localised to the nucleus [202] and has varied substrate specificity in different cells [205], [206]. When spleen cells from WT and MKP-2 KO mice were stimulated with MOG peptide *ex vivo*, our data show that MKP-1 mRNA expression was increased by over 3-fold in MKP-2 KO cells relative to WT controls. This may represent a form of redundancy, whereby if MKP-2 is depleted, expression of other MKPs will increase to try and compensate for the lack of MKP-2 function. Previous studies have alluded to potential compensation from other MKPs in T cell development and T helper cell-mediated antibody production [330] as well as in inflammatory conditions such as ALI [232] and sepsis [232] following MKP-2 deletion but without conclusive evidence. However, in our model, increased MKP-1 expression was unable to fully compensate for MKP-2 as EAE severity was not comparable with WT mice.

Unlike in spleen cells, no change in MKP-1 expression was observed between WT and KO EAE spinal cord tissue. This would suggest that any compensatory mechanisms by MKP-1 may be localised to specific tissues. In contrast, DUSP5 expression more than doubled in MKP-2 deficient spinal cord tissue. The significant upregulation of DUSP5 expression within the CNS of MKP-2 KO mice implies another possible attempt to compensate for the absence of MKP-2 by enhancing expression of this phosphatase. As mentioned in section 3.3, DUSP5 is known to ameliorate CIA via T cell regulation [262]. Therefore increased DUSP5 expression is perhaps contributing to the reduced clinical severity of EAE in MKP-2 KO mice.

Surprisingly MKP-2 deletion had no effect on the level of phosphorylation of ERK or JNK in EAE spinal cord and brain samples relative to WT littermates. This would perhaps suggest that MKP-2 is largely dispensable for ERK and JNK phosphorylation

in EAE CNS tissue, either because MKP-2 is not the primary regulator of ERK and JNK activity in this particular tissue, or is the result of compensation, perhaps via DUSP5. However DUSP5 is specific for ERK, not JNK or p38 [260], therefore other MKPs would also have to be involved. Due to time constraints, these conclusions are based on data from one experiment, with only 3 or 4 mice per group per time point. Therefore it is more likely that upon repeating these blots, the small changes observed in MAPK phosphorylation would become more conclusive. In addition, whole brain and spinal cord tissue was used which may mask any differences in MAPK phosphorylation within individual cell types such as key cells involved in EAE pathogenesis.

Naïve (Day 0) MKP-2 WT and KO mice were found to contain comparable amounts of $CD4^+$ T cells and $CD8^+$ T cells in spleen and dLNs which is in agreement with previous work carried out in MKP-2 KO mice [330]. This suggests MKP-2 is not required for T cell development or lineage commitment within the thymus.

In day 17 EAE mice, the total numbers remained similar, but a substantial increase in the frequency of $CD4^+$ and $CD8^+$ T cells was observed in both WT and KO mice compared to naïve and day 9 EAE mice, confirming the importance of both $CD4^+$ T cells as well as $CD8^+$ T cells in EAE pathogenesis, particularly at this stage of disease progression. MKP-2 KO EAE day 17 spleen and dLNs contained a significantly lower percentage of $CD4^+$ and $CD8^+$ cells compared to WT. These results indicate MKP-2 may have a role in autoreactive $CD4^+$ and $CD8^+$ T cell expansion in secondary lymphoid organs during EAE, which would be similar to previous findings with MKP-1 [217] and MKP-5 [243]. However this was not reflected in the absolute number of $CD4^+$ and $CD8^+$ T cells which remained unchanged between WT and KO mice and therefore the effect of MKP-2 deletion on T cell number and function requires further investigation. In addition, reduced T cell frequency was not associated with any changes in $CD4^+$ T cell activation, as determined by analysing the frequency of $CD4^+$ $CD25^+$ cells. WT and KO mice contained equivalent percentages of activated $CD4^+$ T cells, with the total number steadily declining from day 9 to day 28. This reflects the change in immune response over the course of this monophasic animal model towards mouse recovery. In addition, $CD8^+$ T cell expression was significantly

reduced in KO CNS tissue, suggesting $CD8^+$, but not $CD4^+$ T cell migration and/or infiltration into the CNS appears to be regulated by MKP-2. In MS and EAE, several chemokines have been associated with T cell migration into the CNS such as CCL1-CCL5 and CXCL9-CXCL11 [331], [332]. In addition, T cells found in the CNS of MS patients and EAE mice have been found to express various chemokine receptors including CCR1-CCR5 and CXCR1-CXCR6 [331]–[334]. Our data, as well as results from other groups, have indicated a role for MKP-2 in regulation of chemokine expression. Therefore this would be a potential mechanism for the decreased $CD8^+$ T cell migration into the CNS of EAE mice.

MKP-2 does not appear to be integral to naïve mature B cell development as $CD19^+$ $CD40^+$ B cell frequency and total number was unchanged in naïve MKP-2 KO spleen and dLN tissue relative to WT littermate controls. In contrast, the frequency of $CD19^+$ $CD40^+$ B cells was significantly downregulated in EAE day 17 MKP-2 KO lymphoid tissues compared to WT counterparts. No similar research has previously been carried out looking at the role of MKP-2, or any other MKPs, in relation to B cells. STAT5 is essential in the early development of B cells [335] via its effect on transcription factors such as Pax5 [336]. However it is not required for late stage B cell development or mature B cell proliferation, therefore it is unlikely that this is the cause of reduced B cells in EAE mice in the absence of MKP-2 as no change in the amount of naïve B cells was observed. Activation of B cells occurs within the germinal centres of spleen and lymph nodes in response to antigen stimulation via the B cell receptor [337]. Subsequent activation of the MAPKs (ERK, JNK and p38) leads to phosphorylation of various transcription factors which are involved in B cell survival and proliferation [272], [294]. Taken together, this suggests that reduced $CD19^+$ $CD40^+$ B cell frequency in MKP-2 deficient EAE spleen and dLNs is potentially the result of changes in MAPK phosphorylation due to the absence of MKP-2. The corresponding amelioration of disease severity would confirm a detrimental role for B cells in EAE pathogenesis. No change in percentage of $CD19^+$ $CD40^+$ B cells was detected in EAE day 9 or day 17 CNS tissue following MKP-2 deletion, suggesting MKP-2 is not critical for B cell migration and subsequent entry into the CNS.

In the absence of MKP-2, there was no difference in the frequency and total number of $CD11c^+$ DCs in naïve spleen and dLNs compared to WT. This was also true upon EAE onset and progression, with WT and KO tissue containing comparable levels throughout disease. These results indicate that MKP-2 does not appear to be involved in regulation of DC development. This is in support of similar data obtained with MKP-1, as Huang et al observed no change in $CD11c^+$ frequency in MKP-1 KO spleens relative to WT [314]. Similarly, our data showed that the percentage and total number of $MHC\text{-}II^+$ cells were also unchanged in naïve and EAE KO mice compared to WT, suggesting MKP-2 may not be involved in MHC-II transcription or cell surface expression.

Previous research has shown that macrophages can exert contrasting effects during EAE pathogenesis and thus have the potential to be damaging [134] as well as beneficial [138]. In the absence of MKP-2, the frequency and total number of $CD11b^+$ cells did not change relative to WT littermates, suggesting MKP-2 is not likely to be involved in macrophage proliferation.

It is well recognised that NO is involved in the inflammatory response of MS [338], [339] and EAE [340], [341], contributing to myelin destruction and oligodendrocyte damage [342], [343]. On the other hand, conflicting reports have observed protective effects exerted by NO in EAE [344]–[346]. Data from this study showed that, at the peak of EAE clinical severity, equivalent levels of NO were observed in the serum samples of WT and KO EAE mice. In contrast, by day 28 the level of NO was significantly lower in MKP-2 KO serum compared to MKP-2 WT littermates. This suggests the pathways involved in NO production are unaffected by a lack of MKP-2 until the latter stages of EAE, at which point MKP-2 deficiency results in reduced serum NO. The mechanism through which this occurs remains unknown. Altered NO production as a result of MKP-2 deletion has previously been demonstrated in LPS-stimulated bone marrow-derived MKP-2 KO macrophages [228], with NO levels also downregulated in KO cells compared to WT. The paper also suggested a shift of macrophages toward an M2 phenotype. The opposing roles of macrophages in EAE have been attributed to the differences in phenotype and function between the classically activated M1 and alternatively activated M2 macrophages, with M1 linked

to pathogenic responses and M2 protective [137], [346]. Thus the reduced NO levels observed in day 28 EAE KO mice could be due to the altered activation of macrophages in vivo.

In conclusion, this is the first study to show that MKP-2 appears to be critical in the pathogenesis of EAE, as deletion of this gene results in significantly decreased severity of CNS inflammation. This is associated with changes in several immune mechanisms in MKP-2 deficient mice following EAE induction. These include diminished inflammation and cellular infiltration in the CNS, decreased expression of cytokines and chemokines known to be important in EAE (IL-17, IFNγ, IL-6, IL-2 and CCL2), reduced frequency of $CD4^+$ T cells, $CD8^+$ T cells and B cells, and downregulated NO production. However MAPK phosphorylation within CNS tissues was unchanged in MKP-2 deficient mice relative to WT littermates. The current study also suggests potential compensatory mechanisms following MKP-2 deletion, e.g. via upregulation of MKP-1 and DUSP5 expression.

5 Investigating the role of MKP-2 in regulating DC and macrophage phenotype and function

5.1 Introduction

We have already shown in chapters 3 and 4 of this study that MKP-2 is significantly upregulated in CNS tissues at the peak of EAE severity, and that deletion of this gene results in significantly decreased EAE severity. We found that the reduced EAE severity is associated with changes in CNS inflammation, cytokine production, frequency of $CD4^+$ T cells, $CD8^+$ T cells and B cells and NO production but not MAPK expression or phosphorylation in MKP-2 deficient mice. However these changes were observed in whole spleen and dLN cell cultures, as well as whole CNS tissue. Therefore the effect of MKP-2 deletion on specific cells of the immune system during EAE pathogenesis remains unknown.

The development of a complex autoimmune disease such as EAE involves many different cell types, therefore the changes we observed in the tissues and cell cultures of MKP-2 KO EAE mice may be the result of altered functioning in a number of different immune and CNS cells. Previous research, predominantly using KO mice, has shown that MKP-2 function, and the related signalling pathways, can vary between different cells. MKP-2 has been shown to be essential for cell proliferation and survival in mouse fibroblasts and macrophages [225]. In fibroblasts, MKP-2 induced cell proliferation is associated with dephosphorylation of ERK. However contrasting changes in ERK phosphorylation have been observed in MKP-2 KO macrophages, with MKP-2 deletion either having no effect [228] or resulting in increased ERK phosphotylation [233] . Another report found that over-expression of MKP-2 in human endothelial cells protects against apoptosis via selective inhibition of TNF-α-induced JNK, but not ERK or p38, phosphorylation [223]. In $CD4^+$ T cells, MKP-2

deletion does not affect phosphorylation of ERK, JNK or p38 but instead results in enhanced STAT5 phosphorylation, leading to hyperproliferative cells [330]. Taken together, MKP-2 clearly has variable substrate specificity between different cell types, and thus is involved in unique effector functions within different cells.

It is well established that $CD4^+$ T cells, $CD8^+$ T cells and B cells are key mediators of the inflammatory response in EAE [124], [308]. However other immune cells also have significant roles in disease pathogenesis. These include DCs, which present antigen to T cells, leading to priming of antigen-specific T cells [130]. Adoptive transfer of DCs presenting MOG peptide can also induce EAE in naïve mice [128]. In addition, macrophages are known to be important in EAE, with both deleterious and protective effects previously observed [134], [138].

MKPs, including MKP-2, have previously been shown to play an important role in the function of DCs and/or macrophages [216], [228], [313], and both cells have essential roles in the initiation and development of EAE. While we did not observe any differences in the frequency of $CD11c^+$ or $CD11b^+$ cells in EAE spleen and dLN tissues between WT and KO mice, the alternation in antigen specific cytokine production by immune cells, as well as the reduced NO production in MKP-2 KO EAE mice may suggest a functional change of these cells. We therefore aimed to determine the role of MKP-2 on DC and macrophage cell phenotype and function by using bone-marrow derived DCs (bmDCs) and bone marrow-derived macrophages (BMMs) from MKP-2 WT and KO mice. The cells were generated in culture from WT and KO mice as described in Chapter 2. Cell phenotype, cytokine production and MAPK mRNAexpression were analysed following *in vitro* stimulation with the toll-like receptor agonist, *Salmonella*-derived lipopolysaccharide (LPS).

5.2 Results

5.2.1 MKP-2 KO bmDCs express lower levels of MHC-II

DCs are one of the most important APCs in immune responses, thus playing a key role in the development of MS and EAE. Foreign antigenic material is phagocytosed by DCs and transported to lysosomes where they are degraded into fragments (e.g. peptides). These peptides are subsequently loaded onto an MHC-II molecule before trafficking to the plasma membrane to be displayed on the cell surface which allows presentation to, and activation of, T cells. Therefore, in an autoimmune disease such as EAE, MHC-II molecules are an essential part of disease pathogenesis. In Chapter 4, although not statistically significant, we observed a modest reduction in the frequency of MHC-II$^+$ CD11c$^+$ cells in the spleen and dLN of MKP-2 KO mice at EAE day 17 and day 28, as well as reduced total cell number at day 28. Therefore to further determine whether MKP-2 may be important for the expression of MHC-II in DCs, the level at which bmDCs are able to express MHC-II following MKP-2 deletion was investigated.

Bone marrow cells were obtained from MKP-2 KO mice and WT littermates. Both tibia and femurs were removed and bone marrow flushed out. The bmDCs were obtained by adding 10 % GM-CSF containing supernatant (from X-63 cell line) in the culture medium at day 0, day 3 and day 5 of culture. After 7 days, cells were harvested and counted before being stimulated with 100 ng/ml LPS for 4, 24 and 48 hours. Cells were collected and CD11c and MHC-II expression analysed by flow cytometry using PE-conjugated anti-CD11c and APC-conjugated anti-MHC-II antibodies. Cells were initially gated for CD11c$^+$ cells and MHC-II expression assessed within these populations. Our results show that samples were, on average, 75-80 % CD11c$^+$, suggesting the majority of GM-CSF cultured bone marrow-derived cells were DCs (Fig 5.1 A). However it should be noted that GMCSF can also promote macrophage differentiation, and therefore a more appropriate DC growth factor could have been used, such as Flt3 ligand. Alternatively we could have initially gated on F4/80$^-$ populations to remove any macrophages from our analysis prior to gating on CD11c$^+$ which is a marker also expressed at low levels on macrophages.

We examined MHC-II expression by the $CD11c^+$ cells. Our data shows that just 53.6±6.6 % of MKP-2 KO $CD11c^+$ bmDCs cultured in media alone for 4 hours were found to be $MHC\text{-}II^+$, significantly less than WT cells with 62.0±1.6 % (Fig 5.1 B, D). Following LPS stimulation, the proportion of $MHC\text{-}II^+$ $CD11c^+$ MKP-2 WT cells increased to 71.4±0.9 % (Fig 5.1 C, D), an increase of 15 % compared to unstimulated cells. In contrast, MKP-2 KO bmDCs displayed only a moderate increase (6.5 %) in MHC-II expression relative to unstimulated cells, to 57.1±1.6 %. Therefore our data show that KO bmDCs express less MHC-II than WT littermate counterparts and may be less capable of upregulating MHC-II in response to LPS compared to WT.

After 24 and 48 hours of culture in media alone, MHC-II expression in MKP-2 KO $CD11c^+$ DCs was only slightly lower than WT cells with no statistical difference (Fig 5.1 E, G, H, J). As expected, MHC-II levels increased as a result of LPS stimulation in both WT and KO cells (Fig 5.1 F, G, I, J). Again, cells deficient in MKP-2 expressed significantly less MHC-II (61.9±3.1 %) than WT counterparts with 75.4±0.8 %, an average reduction of 13.8 % at 24 hours. MHC-II expression remained decreased in LPS-stimulated KO cells after 48 hours compared to WT, but this was not significant.

After 24 and 48 hours with LPS stimulation, WT MHC-II expression increased by 15.3 % and 18.4 % respectively relative to unstimulated cells whereas KO MHC-II expression increased by only 11.5 % and 11.3 %, further suggesting MKP-2 deficiency not only results in reduced MHC-II expression on DCs but also reduces the capacity for DCs to upregulate MHC-II following immune challenge.

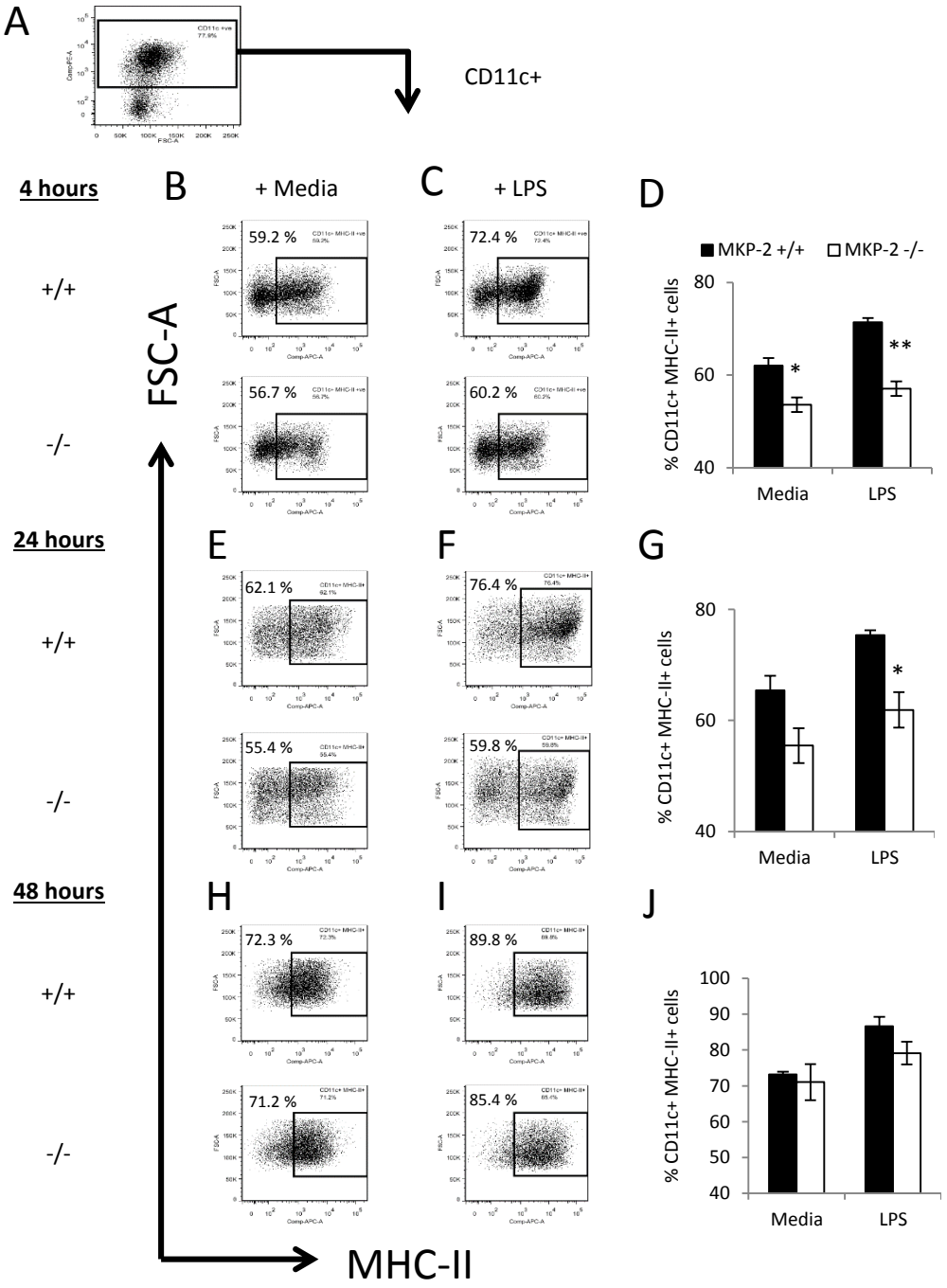

Figure 5.1: MKP-2 +/+ and MKP-2 -/- bone marrow-derived dendritic cell MHC-II expression. bmDCs were generated from the culture of bone marrow from 7–8 week old MKP-2 +/+ and MKP-2 -/- mice. Cells were harvested on day 7 and single cell suspensions added to 12-well plates ($2x10^6$ cells per well) for stimulation with media alone or media supplemented with LPS (100 ng/ml). Cells were collected at 4, 24 and 48 hours and CD11c and MHC-II expression analysed by flow cytometry. A, B, C, E, F, H and I show representative plots from one experiment. D, G and J show combined data from three individual experiments, bars represent mean ± SEM. *P<0.05; **P<0.01, two-tailed unpaired student's t test.

5.2.2 MKP-2 deficient macrophages display an altered phenotype

Macrophages are key cells in EAE, with the potential for contrasting functions. Previous studies have revealed detrimental as well as ameliorating effects exerted by these cells during disease. Macrophages can release inflammatory mediators such as NO, IL-6 and TNF-α which contribute to the inflammatory response and demyelination [134], [347]. In addition, macrophages can present antigen to T cells, enhancing T cell activation [136]. In contrast, they have been shown to aid in recovery by clearing tissue debris via phagocytosis [139].

These contrasting actions may be the result of different forms of macrophage activation producing unique phenotypes. Macrophages which are activated by LPS, IFNγ and TNF-α are known as classically activated (M1) macrophages. These cells predominantly produce NO, TNF-α, IL-6 and IL-12 and upregulate MHC-II expression. In contrast, IL-4 and IL-13 activation induces the so-called alternatively activated (M2) macrophages. This phenotype preferentially produces arginase-1 (Arg1) and IL-10 while reducing production of M1 cytokines. M2-specific macrophage markers also include CD163 and CD206 (mannose receptor).

Taken together, the balance between M1 and M2 macrophages in EAE is an important determinant of disease severity. In Chapter 4 we showed that nitrite, and thus NO production, was downregulated in MKP-2 KO day 28 EAE serum samples relative to WT. As M1 macrophages are a key source of NO, it would perhaps suggest a reduction in the number or function of classically activated macrophages in MKP-2 deficient mice. One previous report has suggested a potential role for MKP-2 in regulating macrophage phenotypes [228]. Therefore we wanted to investigate the effect of MKP-2 deletion on macrophage activation.

Bone marrow cells were obtained from femurs and tibias of MKP-2 KO mice and WT littermates. BMMs were obtained by adding 30 % L-cell conditioned medium in the culture medium at day 0, day 3 and day 5 of culture. After 7 days, cells were harvested and counted before being stimulated with 100 ng/ml LPS for 24 hours and both the supernatant and cells were collected.

5.2.2.1 Classical macrophage activation

From culture supernatants we analysed the production of NO, which is widely regarded as a key marker for classical macrophage activation. To do this we measured the concentration of nitrite, a breakdown product of the highly unstable NO, in the cell culture supernatants by Griess assay. Unstimulated WT, as well as MKP-2 KO BMMs produced low levels of nitrite, with no difference between WT and KO observed (Fig 5.2). Upon LPS stimulation, nitrite concentrations increased in the supernatants of both WT and KO cell cultures. However, nitrite production was significantly reduced in MKP-2 KO BMMs (29.1±1.3 μM) compared to WT counterparts (38.2±3.4 μM), a decrease of 23.8 %.

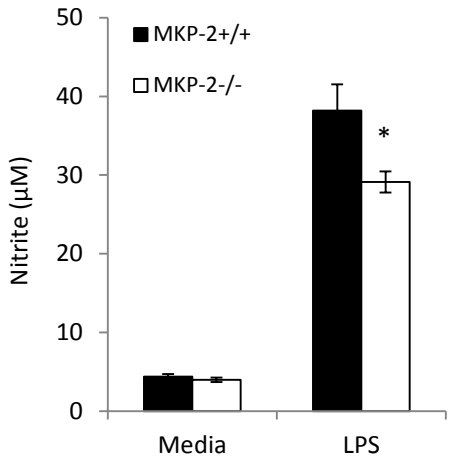

Figure 5.2: Nitrite expression in LPS–stimulated MKP-2 +/+ and MKP-2 -/- macrophages. BMMs were generated from the culture of bone marrow from 7-8 week old MKP-2 +/+ and MKP-2 -/- mice. Cells were harvested on Day 7 and added to 12-well plates ($2x10^6$ cells per well) for stimulation with media alone or media supplemented with LPS (100 ng/ml) for 24 hours. Culture supernatant was collected and nitrite concentrations determined by Griess Assay using a standard curve of known nitrite concentrations. Graph shows data from two individual experiments performed in triplicate. Bars represent mean ± SEM. *P<0.05, two-tailed unpaired student's t test.

5.2.2.2 Alternative macrophage activation

The reduction in nitrite production by KO mice BMMs further suggests a change of macrophage phenotype and functional switch in the absence of MKP-2 when taken together with our EAE serum results (Chapter 4). Therefore we next investigated the percentage of alternatively activated macrophages in LPS-stimulated cells. Expression of the surface marker CD206, also known as the mannose receptor, and a marker of alternative activation, was analysed by flow cytometry. Cells were initially gated for $CD11b^+$ cells and CD206 expression assessed within these populations (Fig 5.3 A). FITC-conjugated anti-CD11b and PE-conjugated anti-CD206 antibodies were used.

Indeed, our data show that unstimulated MKP-2 KO BMMs contained a higher frequency of $CD206^+$ M2 macrophages at 4.26±0.4 % compared to just 1.76±0.06 % of WT cells (Fig 5.3 B, D). Interestingly, following LPS stimulation, an inducer of classical activation, the percentage of M2 macrophages increased to 9.69±0.4 % in KO cultures while only a moderate increase was observed in WT cells to 2.84±0.4 % (Fig 5.3 C, D). Therefore LPS-cultured MKP-2 KO cells contained 3.5-fold as many M2 macrophages relative to WT, a significant increase.

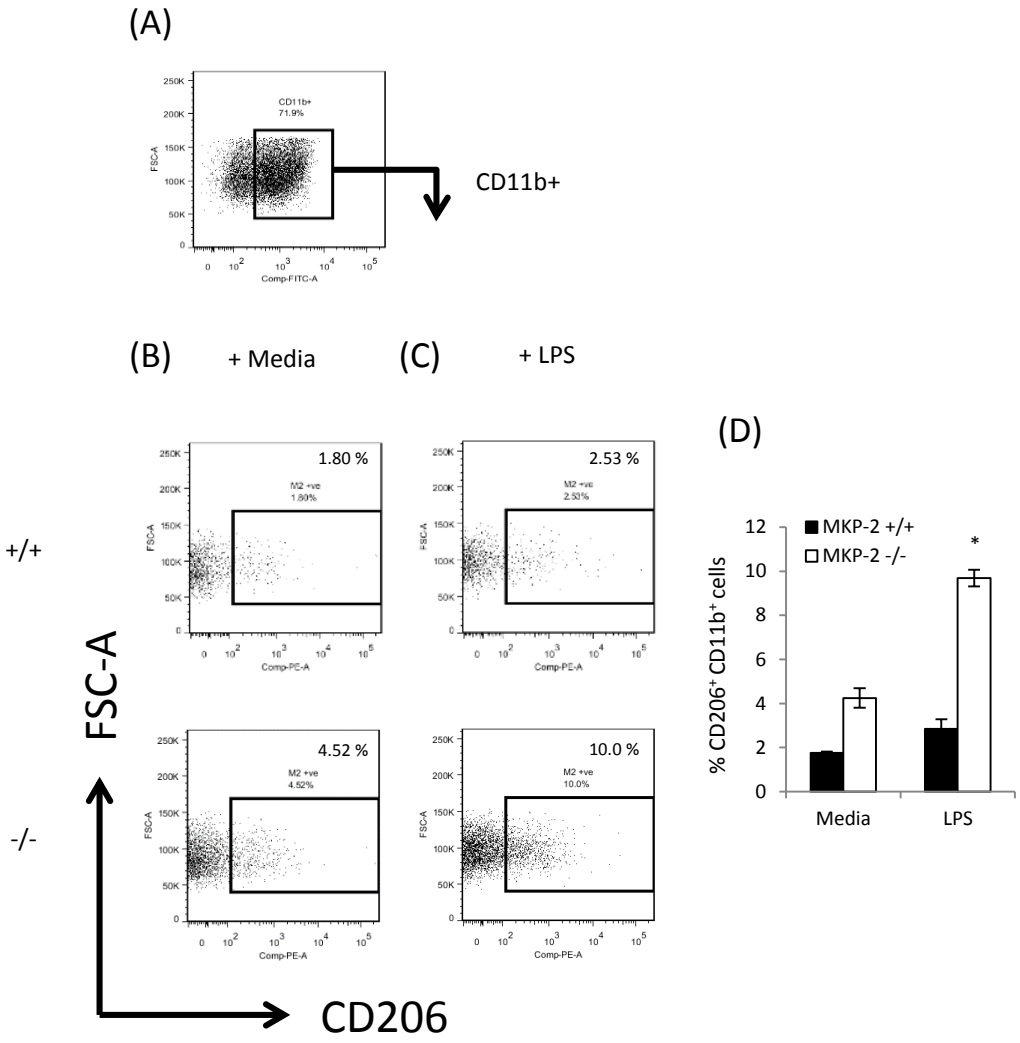

Figure 5.3: Alternative macrophage activation in MKP-2 +/+ and MKP-2 -/- macrophages. BMMs were generated from the culture of bone marrow from 7–8 week old MKP-2 +/+ and MKP-2 -/- mice. Cells were harvested on day 7 and added to 12-well plates ($2x10^6$ cells per well) for stimulation with media alone or media supplemented with LPS (100 ng/ml). Cells were collected after 24 hours and CD11b and CD206 expression analysed by flow cytometry. (A), (B) and (C) show representative plots, (D) data show mean±SEM of two individual experiments performed in triplicate. *P<0.05, two-tailed unpaired student's t test.

5.2.3 MKP-2 KO bmDCs and BMMs have altered cytokine profiles

In chapter 4 we found significantly reduced antigen-specific cytokine production in MKP-2 KO spleen and dLN cells, suggesting MKP-2 may be involved in regulation of cytokine production in immune cells. Both DCs and macrophages can release a range of key pro- and anti-inflammatory cytokines which contribute to immune responses via effects on neighbouring cells. Changes in phenotype and activation status can alter the secretion profile of these cells. In addition, cytokine expression is regulated by MAPK activation.

Therefore we sought to determine whether MKP-2 deletion alters cytokine production by DCs and macrophages from MKP-2 WT and KO mice following stimulation with LPS. MKP-2 WT and KO bmDCs and BMMs were generated as described above (section 5.2.1; section 5.2.2 respectively) and cells were stimulated for 2-72 hours with 100 ng/ml LPS. The supernatant was collected at different time points and IL-6, TNF-α and IL-10 production analysed by ELISA.

5.2.3.1 bmDCs

Supernatants from both WT and KO bmDCs cultured with media alone contained no detectable levels of IL-6 at any time point (Fig 5.4 A). With LPS in the culture, IL-6 levels steadily increased and reached a peak at 24 hours in both WT and KO cells. IL-6 production by KO bmDCs was significantly upregulated (6369±98 pg/ml) compared to WT cells after 4 hours (5386±109 pg/ml) which corresponds to an increase of 18.2 %.

Supernatants from both WT and KO bmDCs cultured with media alone contained no detectable levels of TNF-α at any time point (Fig 5.4 B). Cells from both MKP-2 WT and KO mice displayed almost identical patterns of change in cytokine levels over the course of LPS stimulation. TNF-α production rapidly increased between 2 and 4 hours, reaching maximal output by 6 hours. MKP-2 KO bmDCs produced significantly more TNF-α in response to LPS stimulation compared to WT cells at 48 and 72 hours with increases of 57.0 % and 31.9 % respectively. WT cells produced 1141±32 and 1188±47 pg/ml TNF-α while KO cells produced 1792±48 and 1567±40 pg/ml after 48 and 72 hours.

Both WT and KO bmDCs cultured in media produced low, but detectable levels of IL-10 (Fig 5.4 C). MKP-2 deletion had no effect on basal IL-10 levels, with comparable cytokine expression between WT and KO cultures. IL-10 production by both WT and KO bmDCs peaked at 8 hours following gradual increases at each preceding time point, before steadily declining. A significant upregulation in IL-10 production was observed at 6, 8 and 48 hours, with KO cultures containing 3293±39, 4776±115 and 4357±16 pg/ml IL-10 respectively compared to 2797±75, 4123±25 and 4086±102 pg/ml in WT cultures, constituting increases of 17.7 %, 15.8 % and 20.7 %.

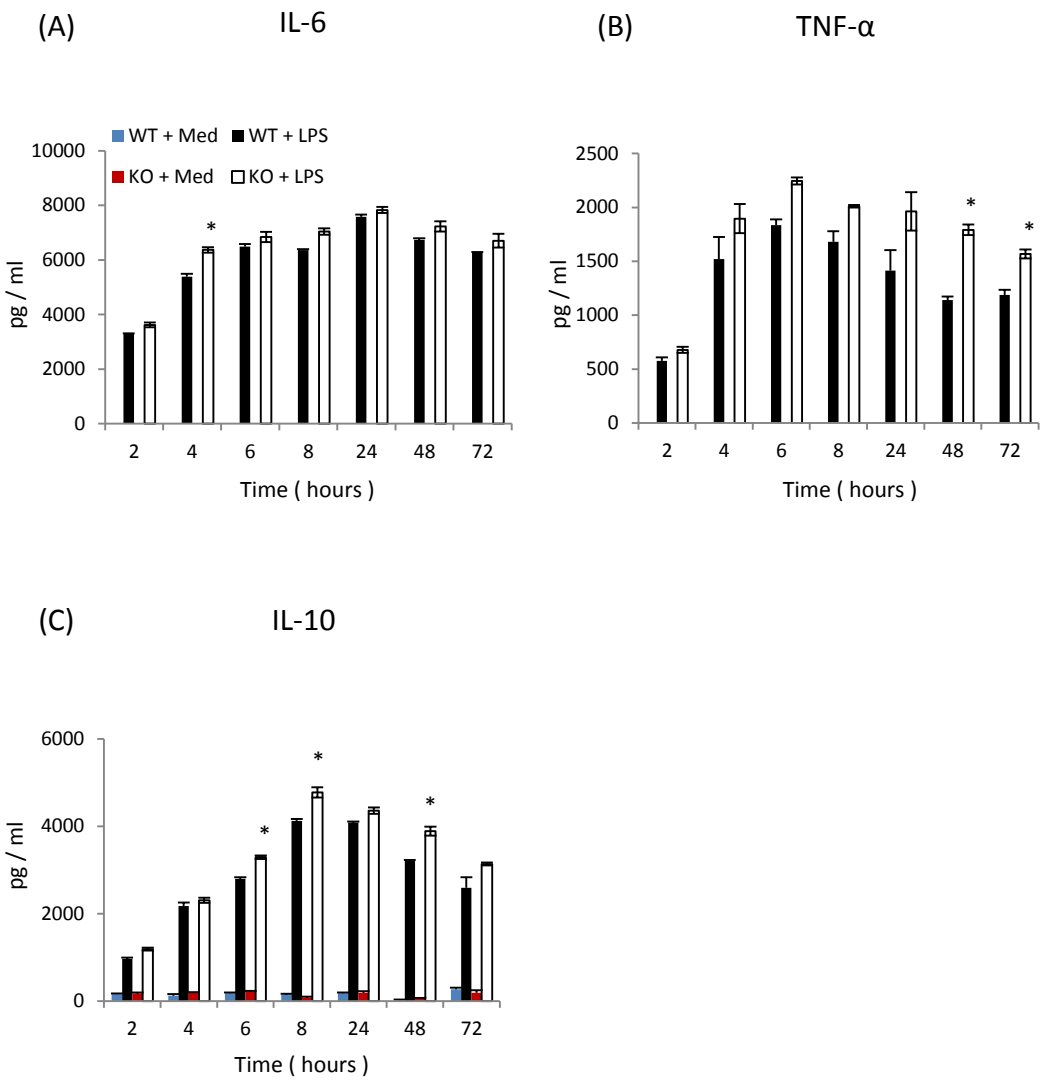

Figure 5.4: Cytokine production in LPS-stimulated bmDCs from MKP-2 +/+ and MKP-2 -/- mice. Bone marrow-derived dendritic cells (bmDCs) were generated from the culture of bone marrow from 7–8 week old MKP-2 +/+ and MKP-2 -/- mice. Both tibia and femurs were removed and bone marrow flushed out. Cells were resuspended in RPMI supplemented with 10 % GM-CSF and cultured at 37 °C and 5 % CO_2. The bmDCs were harvested on day 7 and single cell suspensions were added to 12-well plates ($2x10^6$ cells per well) for stimulation with media alone or media supplemented with LPS (100 ng/ml) for the times indicated. Supernatant was collected and cytokine expression analysed by ELISA. Results show representative data from one of three individual experiments performed in quadruplicate, mean ± SEM. *P<0.05, two-tailed unpaired student's t test.

5.2.3.2 BMMs

Supernatants from MKP-2 WT and KO macrophages cultured in the presence of media alone contained no detectable levels of IL-6 at any time point (Fig 5.5 A). Also, no IL-6 expression was detected in WT or KO cells after 2 hours of LPS stimulation. However IL-6 production by the cells gradually increased in both WT and KO cultures from 4 hours until 24 hours, before decreasing at 48 and 72 hours. MKP-2 KO macrophages produced 88.8 % more IL-6 (3506±149 pg/ml) than WT counterparts (1856±239 pg/ml) following 4 hour LPS stimulation, a significant increase. KO culture supernatant again contained significantly more IL-6 (31.8 %) compared to WT (6122±95 and 4643± 116 pg/ml respectively) after 6 hours.

No TNF-α was detected in the supernatants of MKP-2 WT and KO BMMs cultured in medium alone (Fig 5.5 B). WT macrophages reached maximum levels of TNF-α production after 4 hours of LPS stimulation, which remained consistent at 6 and 8 hours, before a decrease in cytokine production after 24 hours. Equivalent levels were observed between 24, 48 and 72 hour WT LPS cultures. In contrast, TNF-α expression in MKP-2 KO cells also peaked at 4 hours but then displayed a cyclic phenotype of TNF-α production between 6 and 72 hours after LPS stimulation. This pattern occurred in 2/3 experiment repeats. TNF-α production was significantly enhanced in MKP-2 KO BMM LPS cultures compared to WT at 2, 4, 24 and 48 hours. KO cells produced 470±24 pg/ml TNF-α, 2.5-fold more than WT following 2 hour LPS stimulation (190±16 pg/ml). After 4 hours, cytokine levels were 97.1 % higher in KO cells (1558±13 compared to 790±36 pg/ml). Following 24 hour LPS culture, KO cells produced 7147±50 pg/ml while WT cells produced just 512±15, an upregulation of 39.4 % in KO cells. 48 hour KO cultures contained 110 % more TNF-α (1157±12 pg/ml) compared to WT (549±19).

Similar to bmDCs, MKP-2 WT and KO BMM media cultures contained low, but detectable levels of IL-10 (Fig 5.5 C). However MKP-2 deletion had no effect on baseline IL-10 levels, with equivalent cytokine expression between WT and KO medium-only cultures. IL-10 levels steadily increased in response to LPS stimulation, and were significantly upregulated in MKP-2 KO cultures after 2 and 4 hours (5235±15 and 6921±106 pg/ml) compared to WT counterparts (3480±46 and

4996±304), increases of 50.4 % and 38.5 % respectively. IL-10 production decreased at 24 hours in both WT and KO LPS stimulated cells. Interestingly, significantly less IL-10 was detected in the supernatants of KO BMMs compared to WT cells at 24 and 48 hours, with 9079±265 and 8014±116 pg/ml respectively in KO cultures, compared to 11891±139 and 9635±61 pg/ml, decreases of 23.6 % and 20.2 %.

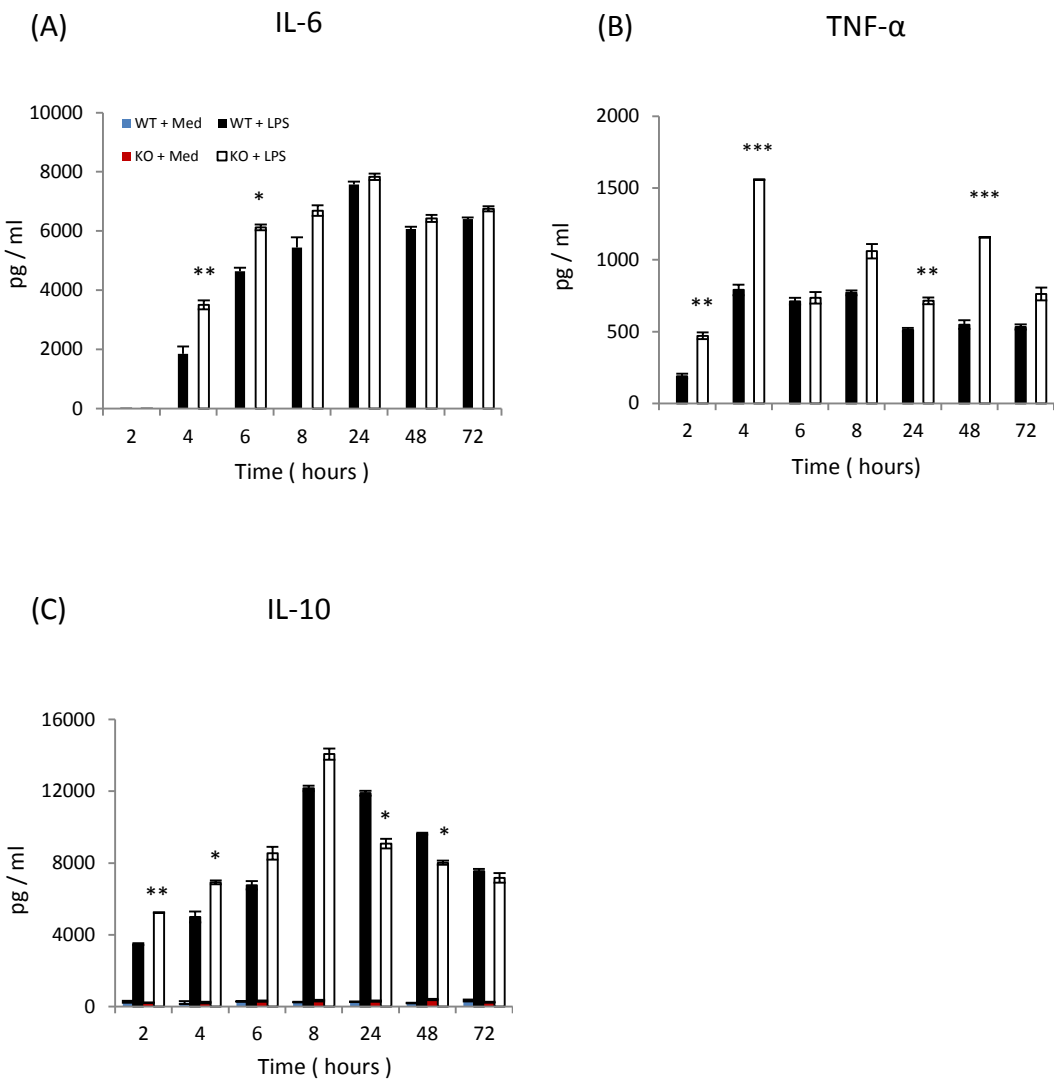

Figure 5.5: Cytokine production by LPS-stimulated bone marrow-derived macrophages from MKP-2 +/+ and MKP-2 -/- mice. Bone marrow-derived macrophages (BMMs) were generated from the culture of bone marrow from 7-8 week old MKP-2 +/+ and MKP-2 -/- mice. The BMMs were harvested after 7 days of culture and single cell suspensions added to 12-well plates ($2x10^6$ cells per well) for stimulation with media alone or media supplemented with LPS (100 ng/ml). Supernatant was collected at different time points and cytokine expression analysed by ELISA. Results show representative data from one of three individual experiments performed in quadruplicate, mean ± SEM. *P<0.05; **P<0.01; ***P<0.001, two-tailed unpaired student's t test..

5.2.4 MAPK expression is unchanged in MKP-2 KO bmDCs and BMMs

We have shown that MKP-2 deletion in bmDCs and BMMs results in altered phenotypes as well as changes in cytokine production within both cells. MAPK signalling is known to be involved in cytokine production and MHC-II expression. As the main function of MKP-2 is in regulation of the MAPK pathway, the changes observed in MKP-2 KO cell phenotype and cytokine profile may be the result of altered MAPK expression following MKP-2 deletion. Therefore MAPK mRNA levels in MKP-2 WT and KO LPS-stimulated DCs and macrophages were analysed.

MKP-2 WT and KO bmDCs and BMMs were obtained and stimulated as described above (section 5.2.1). Cells were then collected and RNA isolated which was then reverse transcribed and cDNA analysed by qPCR. The mRNA levels of MAPKs, including ERK1, ERK2, JNK1, JNK2 and p38 are expressed as relative to GAPDH for each sample to allow changes over time, as well as differences between WT and KO cells, to be displayed simultaneously.

5.2.4.1 bmDCs

Our data show no difference in the levels of mRNA expression of any of the MAPKs analysed, ERK1, ERK2, JNK1, JNK2 or p38 between MKP-2 KO and WT bmDCs following 15, 30, 60, 120 and 240 minutes LPS stimulation (Fig 5.6 A).

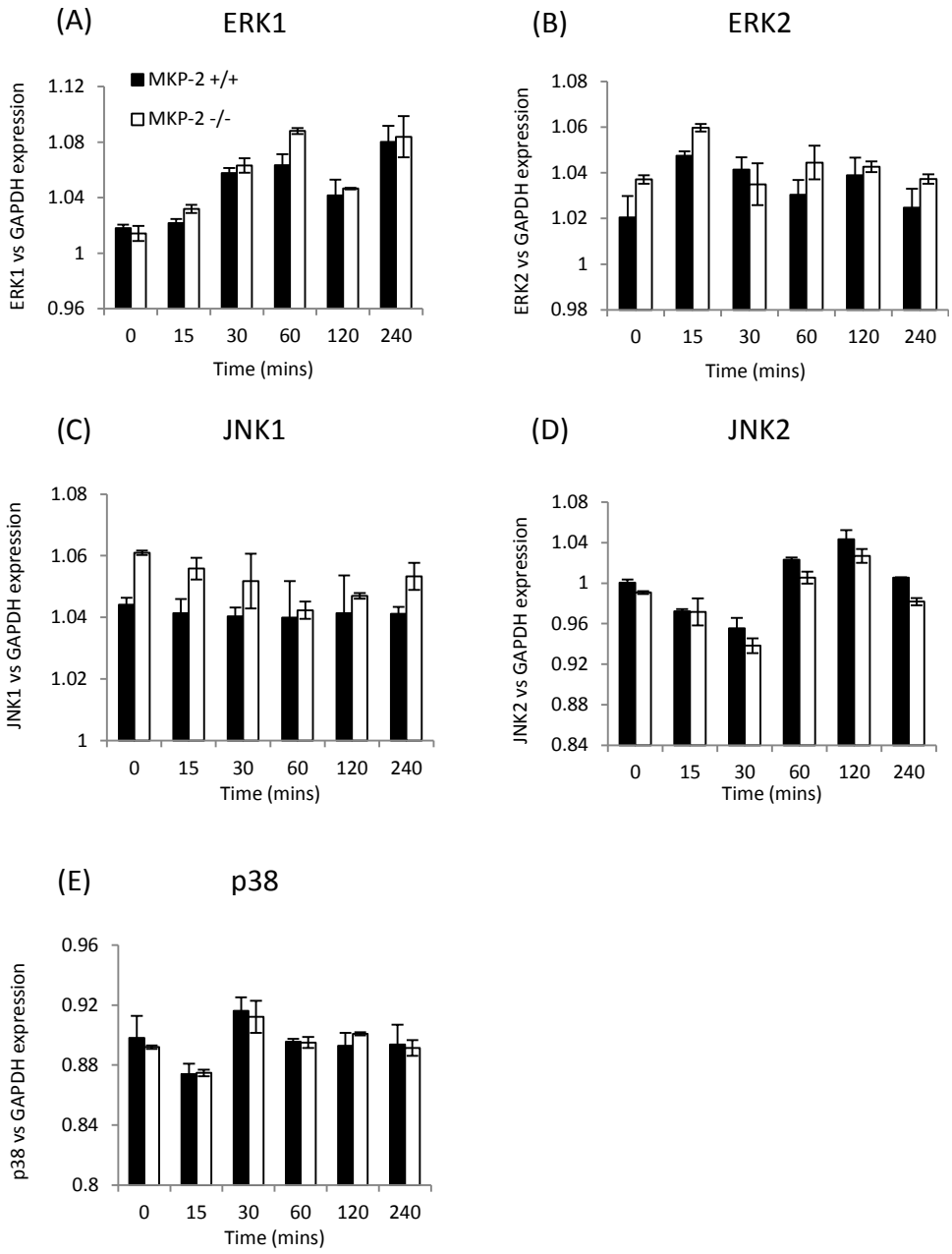

Figure 5.6: MAPK mRNA expression in LPS-stimulated MKP-2 +/+ and MKP-2 -/- DCs. bmDCs were generated from the culture of bone marrow from 7 – 8 week old MKP-2 +/+ and MKP-2 -/- mice. Cells were harvested on Day 7 and added to 12-well plates ($2x10^6$ cells per well) for stimulation with media alone or media supplemented with LPS (100 ng/ml) and collected at various time points. RNA was extracted using TRIzol and reverse transcribed to cDNA to allow analysis of MAPK mRNA expression by qPCR. GAPDH was analysed simultaneously to allow normalisation of relative MAPK mRNA expression. Graphs show data from two individual experiments. Not statistically significant, Mann-Whitney U test.

5.2.4.2 BMMs

We next examined MAPK expression by the BMMs with or without LPS stimulation. Similar to our results observed in bmDCs, we observed comparable levels of ERK1, ERK2, JNK1, JNK2 and p38 mRNA expression between unstimulated and LPS cultured WT and KO BMMs (Fig 5.7 A).

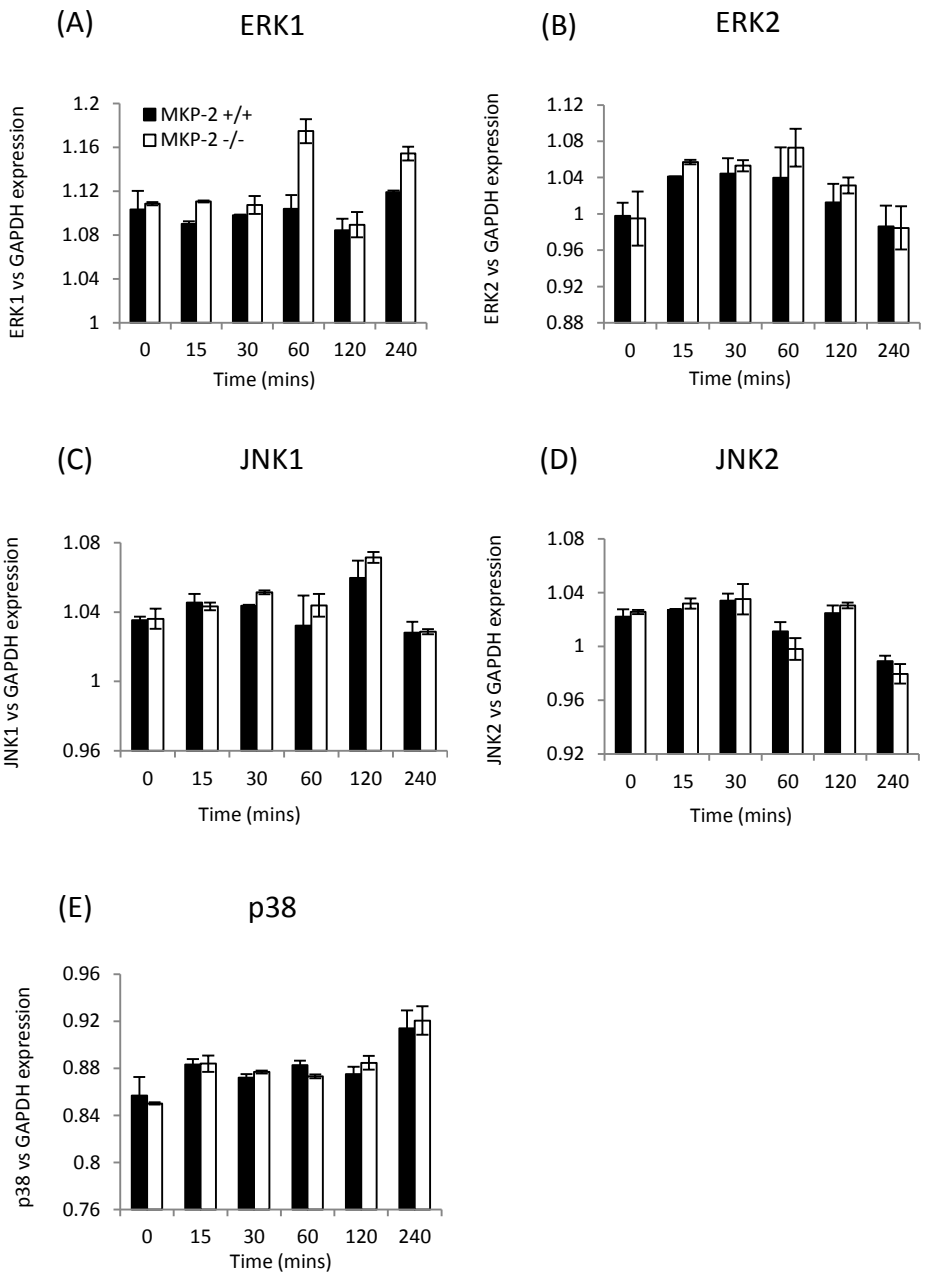

Figure 5.7: MAPK mRNA expression in LPS-stimulated MKP-2 +/+ and KO macrophages. BMMs were generated from the culture of bone marrow from 7 – 8 week old MKP-2 +/+ and MKP-2 -/- mice. Cells were harvested on Day 7 and added to 12-well plates ($2x10^6$ cells per well) for stimulation with media alone or media supplemented with LPS (100 ng/ml) and collected at various time points. RNA was extracted using TRIzol and reverse transcribed to cDNA to allow analysis of MAPK mRNA expression by qPCR. GAPDH was analysed simultaneously to allow normalisation of relative MAPK mRNA expression. Graphs show data from two individual experiments. Not statistically significant, Mann-Whitney U test.

5.3 Discussion

Previous studies utilising KO mice have confirmed a role for MKP-2 in a variety of immune-mediated conditions, however the exact role of MKP-2 in cells of the immune system remains poorly characterised. MKP-2 deficient mice are more susceptible to *L.mexicana* infection [228], with enhanced Th2 responses (increased IL-4, IL-13 and IgG1) and reduced Th1 responses (decreased IFNγ and IgG2a). MKP-2 KO mice are also more susceptible to *T.gondii* infection [230]; however in this model there are no differences in T cell response, with comparable levels of IFNγ, IL-4, IL-5 and IL-10 observed between WT and KO antigen-challenged splencoytes. In addition, MKP-2 deletion ameliorates the severity of acute lung injury (ALI) [232] and sepsis [233], associated with reduced TNFα levels in KO BAL fluid and decreased serum IL-6, TNF-α and IL-1β respectively, however this was not conclusively attributed to any particular cell types. MKP-2 also appears to be involved in regulation of macrophage cytokine production, though conflicting changes have been observed. One group detected increased IL-6 and TNF-α production in KO macrophages following LPS stimulation [228], while another found decreased levels of TNF-α in the absence of MKP-2 [233]. To date, no work has been carried out investigating the role of MKP-2 in other important immune cells such as B cells or DCs

My study has confirmed that MKP-2 is involved in the pathogenic response of EAE as disease severity is significantly decreased in the absence of this gene (Chapter 4). The attenuation of EAE in MKP-2 deficient mice was confirmed with reduced CNS inflammation and cellular infiltration, and was associated with reduced antigen-specific cytokine/chemokine production in spleen and dLN cells (IL-17, IFNγ, IL-6, IL-22, IL-2 and CCL2) together with reduced frequency of $CD4^+$ T cells, $CD8^+$ T cells and B cells as well as reduced NO production. MAPK expression and phosphorylation were both unchanged in MKP-2 KO EAE mice compared to WT counterparts. However these results were based on whole tissue preparations, therefore the exact mediating cells of MKP-2 function during EAE pathogenesis remains unknown.

As discussed in previous chapters, macrophages and DCs are important mediators of the immune response in EAE; therefore the effect of MKP-2 deletion on the functioning of these cells upon immune activation was investigated. Therefore we

firstly wanted to investigate the level of MHC-II expression on MKP-2 WT and KO bmDCs following LPS stimulation to determine if MKP-2 deletion has any effect on DC activation and their potential ability to present antigen to T cells. We observed that the percentage of MHC-II$^+$ CD11c$^+$ cells was reduced in KO bmDC cultures compared to WT cells cultured in media alone, significantly so at shorter time periods (4 hours). Following LPS stimulation, the frequency of MHC-II$^+$ DCs increased in both WT and KO cultures, but remained significantly downregulated in MKP-2 KO mice after 4 hours and 24 hours, but not 48 hours, of LPS challenge relative to WT. In the context of EAE/MS, decreased MHC-II expression would mean a potential reduction in antigen presentation and thus a decrease in autoreactive T cell priming/activation and therefore reduced inflammation, demyelination and axonal damage MHC-II gene expression is regulated by the transcriptional coactivators RFX [348] and CIITA [349], which is regarded as the master controller of MHC-II genes. CIITA expression, at least within DCs and macrophages, is controlled by ERK and p38 activity through a negative feedback loop [350]. In addition, ERK and JNK regulate CIITA transcription in melanoma [351]. Therefore MKP-2 may alter CIITA expression via MAPK dephosphorylation, reducing ERK and/or p38 MAPK activity, allowing continued expression of CIITA and thus increasing synthesis of MHC-II. This hypothesis is supported by results previously observed in MKP-1 deficient LPS-stimulated DCs and IFNγ-stimulated macrophages which displayed reduced CIITA and MHC-II expression [350]. In addition, MKP-1 overexpresison upregulated both MHC-II and CIITA expression in stimulated DCs and macrophages

Following LPS stimulation, production of the inflammatory cytokines TNF-α and IL-6, as well as the anti-inflammatory cytokine IL-10 was significantly increased in MKP-2 KO DCs compared to WT. This suggests that MKP-2 negatively regulates production of TNF-α, IL-6 and IL-10 in DCs. Previous literature suggests that ERK is crucial for TNF-α production in DCs as treatment of these cells with a specific inhibitor of MEK, a protein kinase that phosphorylates ERK1/ERK2, prior to LPS stimulation results in decreased TNF-α levels [295]. ERK activation also regulates DC IL-10 production as LPS-stimulated DCs from ERK1 deficient mice produce less IL-10 than WT controls [297], [352]. In addition, pre-treatment of WT DCs with a MEK inhibitor before LPS culture further downregulates IL-10 levels; thus confirming

a positive role for both ERK1 and ERK2 in DC IL-10 production [352]. IL-6 levels were unaltered in LPS stimulated ERK1 KO DCs or in inhibitor-treated DCs cultured with LPS. Therefore this perhaps suggests that MKP-2 may be involved in negatively regulating DC TNF-α and IL-10, but not IL-6 production via ERK dephosphorylation.

Similar to our results obtained here with MKP-2 KO DCs, TNF-α, IL-6 and IL-10 production is significantly upregulated in MKP-1 KO bmDCs following LPS stimulation, which is attributed to enhanced JNK and p38 phosphorylation [313]. Thus MKP-2 may also regulate production of these cytokines by decreasing JNK and p38 activity. Other reports have linked IL-6 production in DCs to p38 activity. The use of a p38 inhibitor by Yanagawa *et al* led to significantly decreased CD40-mediated IL-6 production in mature DCs [271]. Furthermore, upon induction of EAE in mice with p38 selectively deleted only in DCs, IL-6 mRNA levels are reduced compared to WT counterparts [275]. Taken together, the above evidence supports the involvement of p38 in IL-6 production by DCs via positive regulation. Therefore p38 dephosphorylation is a potential mechanism through which MKP-2 may control IL-6 expression in DCs, however further work is required to confirm this.

Macrophages can exert both deleterious as well as beneficial effects during EAE pathogenesis. These opposing effects are due to the presence of contrasting macrophage phenotypes resulting from different activation stimuli. Classically activated (M1) macrophages have been associated with detrimental functions in EAE. They are known to contribute to the formation of lesions [134] and axonal damage [347] by releasing inflammatory mediators such as TNF-α, IL-6 and NO, as well as interacting with autoreactive T cells in their role as APCs [136]. In addition, the elimination of macrophages using mannosylated liposomes containing dichloromethylene diphoshonate (Cl_2MDP) reduces the clinical severity of EAE [133]. In contrast, macrophage depletion using these clodronate liposomes also results in impaired remyelination due to decreased oligodendrocyte progenitor cell differentiation and altered expression of growth factors involved in remyelination [353]. Furthermore, treatment of mice with alternatively activated (M2) macrophages can protect against the development of EAE [137], [138]. M2 microglia/macrophages can also promote removal of tissue debris by phagocytosis [139]. Therefore it is clear

that macrophages are key immune cells during the development of EAE, and that the balance between M1 and M2 phenotypes can determine whether these cells will primarily be pathogenic or aid in recovery and amelioration of disease.

Interestingly, upon stimulation with LPS, MKP-2 KO macrophages produced significantly less NO in conjunction with increased expression of CD206 compared to WT cells, which is more indicative of M2 macrophages. This is supported by Al Mutairi *et al* who also observed reduced NO levels, with increased arginase 1 expression, in LPS-stimulated MKP-2 KO macrophages, suggesting a shift towards the M2 phenotype [228]. However the means by which MKP-2 alters the balance between NO and arginase levels and M1/M2 surface marker expression remains unclear. In response to inflammatory stimuli, NO is produced by inducible NO synthase (iNOS), which catalyses the conversion of NO from L-arginine, the same substrate utilised by arginase [354]. Therefore MKP-2 may affect the pathways that lead to expression of iNOS and/or arginase. Blocking p38 or ERK activity in macrophage cell lines using specific inhibitors results in decreased iNOS induction following LPS or IFNγ stimulation [179], [355]. In addition, arginase expression is increased in BMMs and macrophage cell lines following treatment with *Trypanosoma cruzi* (*T.cruzi*) trypomastigotes and the *T.cruzi* antigen Cruzipain, an increase which is, in part, mediated by increased p38 activity [356], [357].

These data suggest that p38 and ERK are involved in the production of iNOS and arginase; however it provides conflicting evidence for the exact role of MAPK activity. Blocking p38 activity leads to decreased iNOS, thus suggesting a subsequent increase in arginase production (M2>M1), yet increased p38 activity in macrophages regulates increased arginase which itself would suggest decreased NO. Therefore MKP-2 may alter the balance between iNOS/NO and arginase in macrophages via regulation of p38 and ERK activation. This is supported by previous research which has shown that phosphorylation of ERK [228] and p38 [233] is upregulated in MKP-2 KO cells, confirming these MAPKs as likely substrates for MKP-2 in macrophages.

MKP-2 KO macrophages produced significantly more IL-6 and TNF-α when cultured with LPS. As with the altered cytokine production in DCs, this is likely due to changes in MAPK phosphorylation in MKP-2 deficient mice. These results back up previous

work. By using inhibitors specific for ERK, JNK or p38, Rego *et al* found that preventing ERK activity (but not JNK or p38) reduced IL-6 production [358], suggesting ERK is more important for macrophage IL-6 production than JNK or p38. ERK activation has also been linked to IL-6 production in a macrophage murine cell line, RAW264.7 [359]. In contrast, other studies using MKP-2 KO macrophages have shown enhanced JNK and p38 activity [228]. In particular, p38 has been identified as a key component of IL-6 and TNF-α production in macrophages [270], [360].

In addition, ERK is thought to regulate the translocation of TNF-α mRNA from the nucleus to the cytoplasm [361] and thus, like JNK and p38, also appears to be important in macrophage TNF-α production. Taken together, the MAPKs are clearly involved in the production of IL-6 and TNF-α by macrophages, and MKP-2 is likely to exert its effects on macrophage IL-6 and TNF-α production via regulation of MAPK activity. Therefore, although we observed no changes in total MAPK mRNA expression in LPS-stimulated MKP-2 KO BMMs, the phosphorylation and activity of ERK, JNK and p38 need to be analysed in WT and KO BMMs to confirm which, if any, are altered due to MKP-2 deletion and thus may regulate cytokine production.

Regulation of macrophage IL-10 production by MKP-2 appears to be a more complex situation. At earlier time points of LPS stimulation (2 and 4 hours), IL-10 production was significantly upregulated in KO cells relative to WT counterparts. In contrast, following prolonged LPS exposure (24 and 48 hours); KO cultures contained significantly less IL-10. The significant reduction in IL-10 levels from 24 hours onwards is in agreement with Al-Mutairi *et al* who reported similar results [228]. However they did not analyse earlier time points therefore it is unclear if they would have also observed any differences in IL-10 regulation by MKP-2 at different time points following antigen challenge.

Another report found no change in IL-10 production in BMMs following 2, 4 and 6 hour LPS stimulation, but a significant decrease in MKP-2 KO cells after 8 hours [233]. No later times were analysed. This would, to some degree, support our data and give further credence to the theory that MKP-2 regulation of IL-10 production in macrophages appears to change with continued challenge. However it is not clear why there is a difference between our data of IL-10 production by macrophages and reports

from other laboratories. One possible explanation is perhaps the differences in the culture and stimulation protocol. Whereas we added generated macrophages to multi-well plates and immediately added LPS, they incubated their cells overnight before LPS culture. It has previously been shown that delaying the addition of LPS to bmDC cultures alters IL-10 production, with a longer delay associated with much lower levels of IL-10 compared to immediate stimulation [362]. Therefore the timing of stimulation appears to be a crucial factor in cell activation which can alter the subsequent cellular responses.

Multiple studies have confirmed that blocking ERK activation in either BMMs or macrophage cell lines with a specific MEK inhibitor reduces IL-10 production [363], [364]. In addition, p38 inhibition also decreases macrophage IL-10 production [363]. This would confirm that ERK and p38 are involved in IL-10 production in these cells and are the likely targets for MKP-2 through which regulation of IL-10 occurs. IL-10 levels are upregulated in MKP-1 KO BMMs stimulated with LPS [209], [210], [313], an effect which is predominantly attributed to increased p38 and JNK phosphorylation, suggesting MKP-1 negatively regulates IL-10 production in macrophages. As MKP-1 is upregulated in tissues of MKP-2 KO EAE mice, there may be delayed compensation by MKP-1 following LPS challenge in MKP-2 KO macrophages, suggesting both MKPs are prominently involved in IL-10 production via opposing mechanisms of action.

When these results are taken together: decreased NO production, increased CD206 expression, increased IL-6 and TNF-α production, and altered IL-10 production in MKP-2 KO BMMs, it suggests a unique alteration in macrophage phenotype in the absence of MKP-2 with a mostly M1 cytokine profile, but decreased NO production and increased Arg1 and CD206 expression in KO cells compared to WT, which is more indicative of an M2 phenotype. As mentioned above, this is supported by previous research carried out by another group who also observed reduced NO levels with increased arg1 expression in LPS-stimulated MKP-2 KO macrophages, suggesting a shift towards the M2 phenotype [228]. However, similar to our results, their cytokine data did not match this, with increased IL-6, TNF-α and IL-12, but decreased IL-10 (from 24 hours of LPS culture onwards) – a cytokine profile closer to

M1 macrophages. MKP-2 may therefore be involved in a variety of macrophage responses in vivo rather than simply promoting M1 or M2 phenotypes, most likely by regulating MAPK activity. As a result of this it remains unclear exactly how MKP-2 deletion affects macrophage functioning in EAE. With M1 thought to drive the pathogenic responses of macrophages in EAE and M2 associated with protective effects, the unique mixed phenotype observed in MKP-2 KO mice must be fully characterised in vivo to understand how these cells are affected by the absence of MKP-2.

In conclusion, MKP-2 deficient bmDCs cultured with LPS express less MHC-II and produce more IL-6, TNF-α and IL-10. LPS-stimulated macrophages, in the absence of MKP-2, display a unique M1 and M2 mixed phenotype. This is associated with reduced NO, a classically activated M1 marker and increased CD206, a marker for alternatively activated M2 macrophages. However production of IL-6 and TNF-α, which are more associated with M1 responses, are increased by MKP-2 KO macrophages compared to WT cells after LPS stimulation. In addition, IL-10 is initially upregulated in KO cells following LPS stimulation, but is decreased with prolonged challenge. Therefore the function of MKP-2 in DC and macrophage activation, and in EAE development, is likely to be complex however it appears to be involved in several key functions within these immune cells, possibly through regulation of MAPK activity.

6 General Discussion

6.1 Discussion

In this report we have shown that MAPK mRNA expression is altered in the CNS of EAE mice in conjunction with a significant increase in ERK2 phosphorylation in EAE day 9 brain tissues relative to PBS controls. In addition, we observed possible but as yet inconclusive increases in JNK phosphorylation in EAE spinal cord tissue. In particular, our results suggest ERK2 and JNK1 may be involved in EAE, with potential roles within the CNS. Previous literature provides conflicting evidence for the involvement of ERK in EAE, with disease severity either enhanced or unchanged in the absence of ERK1 alone or ameliorated when ERK1 and ERK2 activity are both blocked [273], [297], [298]. This may suggest a compensatory mechanism between ERK1 and ERK2 in EAE pathogenesis, and thus both ERK1 and ERK2 would have to be targeted. Furthermore, JNK1 deficient mice are less susceptible to EAE [274] while JNK2 KO mice remain fully susceptible [299] suggesting JNK1, but not JNK2, is essential in EAE pathogenesis.

As MAPK activity is regulated by MKPs we next investigated expression of these phosphatases in EAE CNS tissue. We found that MKP-2 expression is significantly upregulated in the CNS of MOG immunised mice compared to PBS controls, which suggests that MKP-2 may be involved in EAE pathogenesis. The important role of MKP-2 in the development of EAE was confirmed using MKP-2 deficient mice, with EAE severity significantly ameliorated in the absence of MKP-2. Several aspects of the immune response were altered in MKP-2 KO mice during EAE which may represent the underlying mechanisms through which EAE severity is decreased. This includes reduced inflammation and cellular infiltration in the CNS, decreased expression of cytokines and chemokines known to be important in EAE (IL-17, IFNγ, IL-6, IL-2 and CCL2), reduced frequency of $CD4^+$ T cells, $CD8^+$ T cells and B cells and downregulated NO production. However the MAPK pathway in MKP-2 KO mice was unchanged compared to WT littermates in our EAE model, with no differences in MAPK mRNA expression or phosphorylation of these kinases in brain and spinal cord

tissues. Interestingly we also observed potential compensatory mechanisms by other MKPs following MKP-2 deletion, via upregulation of MKP-1 (although not statistically significant) and DUSP5 expression. To my knowledge this thesis is the first study to investigate the role of MKP-2 in EAE development and examine the potential underlying cellular and molecular mechanisms (Figure 6.1).

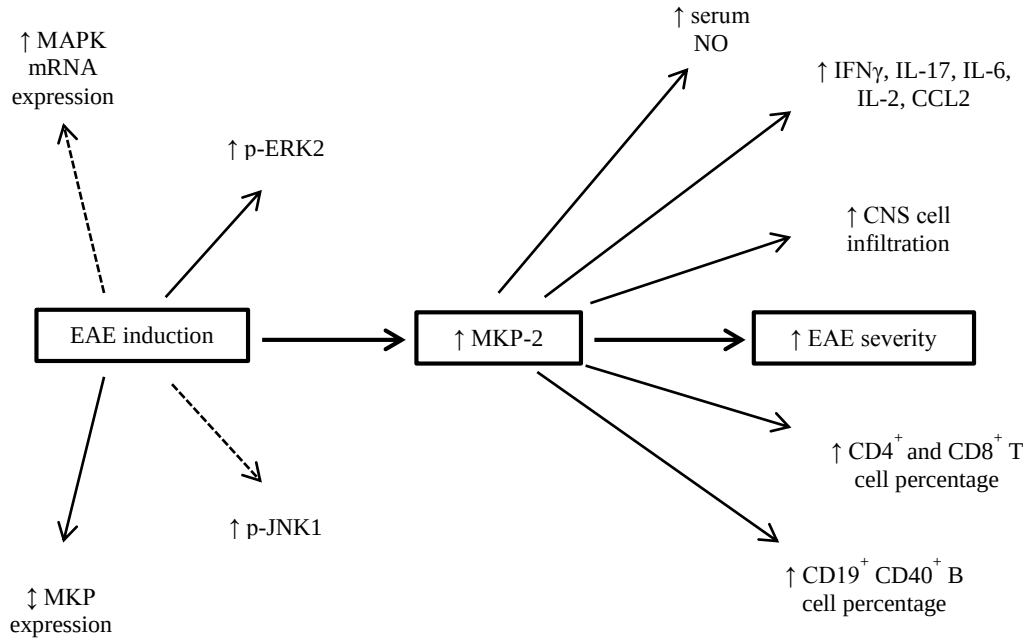

Figure 6.1: Schematic diagram summarising the key findings from Chapter 3 and Chapter 4 of my thesis. Dashed lines indicate data that suggests a change but is not yet conclusive from this study.

Our results, taken together with previous literature, support the hypothesis that MKP-2 is integral to the regulation of numerous cellular functions, ranging from cell survival, proliferation and differentiation [225], [330] to cytokine/chemokine production and antigen presentation [228], [231]. These previous reports suggest that these effects are predominantly mediated by the ability of MKP-2 to control MAPK activation via dephosphorylation [225], [228], [231]–[233]. In particular, we have shown that MKP-2 may have an important role in two key immune cells involved in EAE pathogenesis. Our data from in vitro cultured bmDCs suggest that MKP-2 may be a positive regulator of MHC-II expression while also negatively regulating IL-6,

TNF-α and IL-10 production (Fig 6.2 A). It is not clear why the significant reduction of MHC-II expression on bmDCs of MKP-2KO mice was not confirmed in vivo in EAE mice. The disagreement between these data may be due to the complexity of the in vivo environment, with many organs, cells and molecules interacting with each other simultaneously. Also, while we investigated DC phenotype at day 9, 17 and 28 after immunisation, it is possible that we have missed the optimal time points with the dynamic immune responses during the development of EAE. Nonetheless, increased MHC-II expression would likely contribute to EAE pathogenesis via activation of myelin specific T cells.

Furthermore, our data using BMMs show that MKP-2 deletion results in a unique M1 and M2 mixed macrophage phenotype, with reduced NO production, increased CD206 expression and increased IL-6 and TNF-α production (Fig 6.2 B). IL-10 is also initially increased in LPS-cultured KO macrophages but is downregulated with sustained stimulation. Therefore it remains unclear exactly how MKP-2 regulates macrophage functioning. While M1 is thought to be responsible for the pathogenic responses of macrophages in EAE, M2 is associated with the protective effects, Although no difference in frequency or total number of $CD11b^+$ cells was observed in EAE spleen and dLNs between WT and KO mice, future studies using better defined markers will be important to fully characterise the unique mixed phenotype of macrophages observed in MKP-2 KO BMM cells *in vivo*.

In the context of EAE, MKP-2 positively regulating NO production would enhance disease pathogenesis as NO is known to contribute to the inflammatory response and demyelination of MS/EAE [338]–[340]. In day 28 EAE serum samples we showed that NO levels are significantly decreased in MKP-2 deficient mice, which thus supports this hypothesis and suggests reduced NO production by macrophages contributes to the overall reduction in serum NO.

In summary our study suggests that DCs and macrophages may be the potential mediating cells of MKP-2 effects on exacerbating EAE disease, however further studies are required to confirm our findings *in vivo* using better defined markers for both cells.

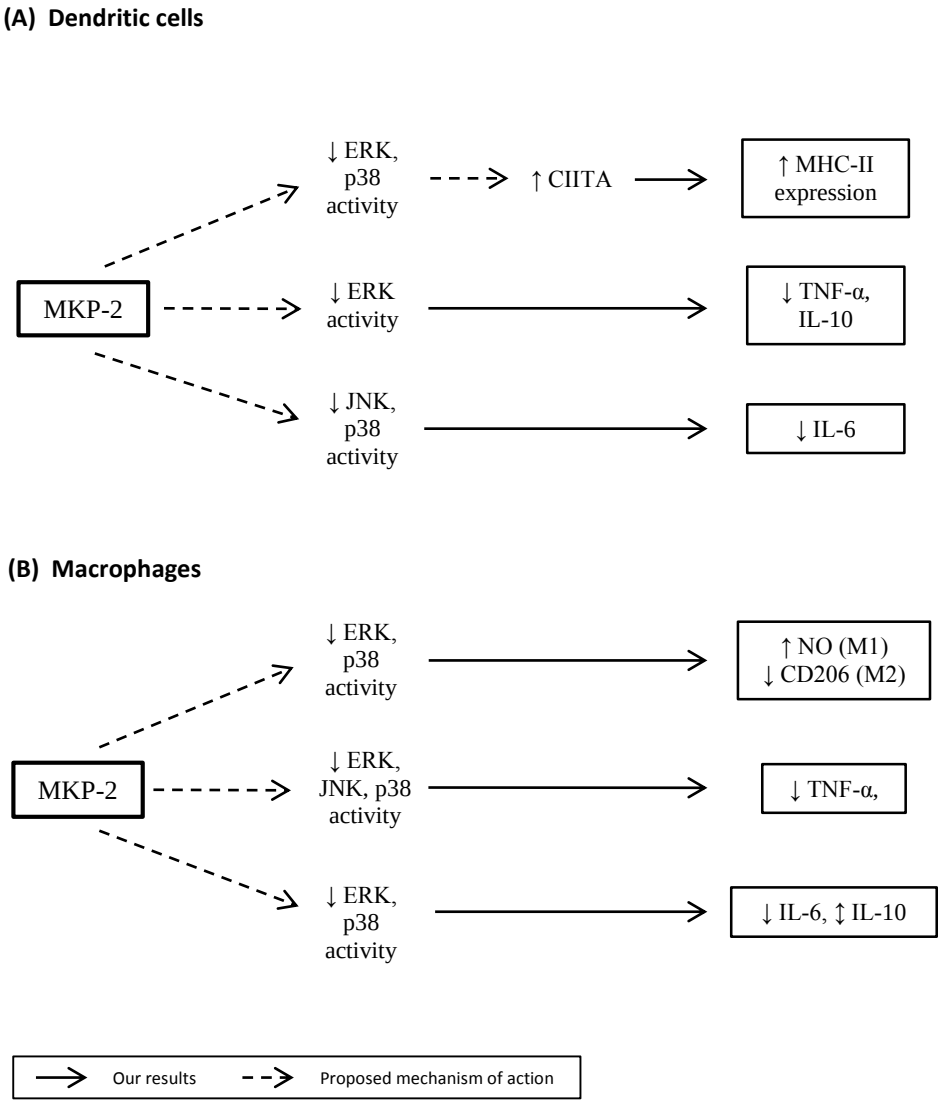

Figure 6.2: Schematic diagram summarising the role of MKP-2 in (A) DCs and (B) macrophages elucidated in this thesis. Solid arrows represent our results and dashed arrows represent the proposed mechanism of action through which MKP-2 may regulate each function based on conclusions from previous literature.

6.2 Future Work

Our data has confirmed that MKP-2 is important in the pathogenesis of EAE. We have also identified changes in the immune response which may contribute to the

amelioration of disease. However more work must be done to fully elucidate the exact mechanisms of action of MKP-2 in EAE in order for this phosphatase to be considered a potential novel therapeutic target in the treatment of MS.

Firstly, as shown in Chapters 4 and 5, we have characterised the potential role of MKP-2 in DCs and macrophages. However we still need to establish the phenotype of macrophages in MKP-2 deficient mice at different stages of EAE to determine whether the unique phenotype we observed in vitro also occurs in vivo. We then have to perform functional assays to understand how these macrophages function in autoimmune conditions such as EAE. These would include testing the phagocytic ability of the cells, which could be done using various available kits or by flow cytometry, as well as their production of reactive oxygen species which can again be assessed by flow cytometry.

In addition, as MHC-II expression appears to be downregulated in MKP-2 deficient bmDCs, we need to investigate the effect this has on antigen presentation as this is an essential step in EAE disease pathogenesis. This could be done by using an assay to measure antigen presentation, for example by analysing the ability of MKP-2 WT and KO DCs to present ovalbumin (OVA) to OT-II T cells ($CD4^+$ T cells specific for OVA). The potential for MKP-2 to regulate MHC-II expression on other APCs (e.g. B cells, macrophages), and the subsequent alteration in antigen presentation should also be determined.

Furthermore, we have yet to investigate the cellular/immune functions regulated by MKP-2 in other key immune cells involved in EAE (e.g. $CD4^+$ T cells, $CD8^+$ T cells, B cells) as well as CNS-resident cells such as microglia, astrocytes and oligodendrocytes which are also very important in EAE. Previous reports have shown potential defects in $CD4^+$ T cell proliferation and cytokine production in the absence of MKP-2 [330], therefore it is important to study the role of MKP-2 in $CD4^+$ T cell function in our EAE model using MKP-2 deficient mice. Similar analysis on $CD8^+$ T cells should also be performed as these cells contribute greatly to inflammatory cytokine production and demyelination. No work has previously been carried out investigating the potential role of MKP-2 in B cells, a crucial population of immune

cells in the pathogenesis of MS/EAE, and therefore any data would greatly enhance the knowledge in this area.

As regulatory T cells (Tregs) are crucial to MS/EAE recovery, I also attempted to analyse the frequency of FoxP3$^+$ Treg cells present in EAE spleen and dLN tissue (data not shown). As Foxp3 is an intracellular antigen, cells must first be fixed and permeabilized before detection with antibody. After successfully staining for Foxp3 on one occasion, I was unable to successfully repeat this, perhaps due to problems with the fixation and permeabilization steps as all surface marker staining worked. When successful staining was achieved I found an increased percentage of CD4$^+$ Foxp3$^+$ Treg cells in EAE day 17 MKP-2 KO spleens, however in KO dLNs the frequency of Tregs was moderately reduced compared to WT (n=3 mice per group). These results must therefore be repeated to confirm the potential effect of MKP-2 deletion on Treg cell development. A potential increase of Treg cell populations in MKP-2 deficient mice would highlight another important mechanism which strengthens the theory that MKP-2 is a viable candidate for consideration in future therapeutic intervention strategies.

The significantly increased frequency of B cell population in MKP-2 KO mice suggests MKP-2 may be involved in regulation of B cell expansion. As B cells play key roles in EAE/MS pathogenesis and recovery, it is very important next to establish the role of MKP-2 in the immune mechanisms of B cells during EAE, including autoantibody production and antigen presentation by measuring antigen-specific antibody levels and expression of MHC-II and co-receptors for T cell activation. Furthermore, the protective effects of B cells, such as IL-10 production, may also be regulated by MKP-2 and therefore this should also be investigated. A potential strategy for investigating the role of MKP-2 in individual cell types would be to utilise inducible cell-specific KO mice, allowing examination of MKP-2 function in specific cell types without affecting its function in other cells. Alternatively, bone marrow chimeras and could be utilised to look at cell-specific functions.

The significant increase in MKP-2 mRNA expression in spinal cord tissues at the peak of EAE severity suggests a role for this phosphatase in the CNS compartment. While our study has focused on the effects of MKP-2 on peripheral immune cells and immune

responses, it is also important to understand the role of MKP-2 in CNS resident cell function. To investigate the role of MKP-2 in cells of the CNS we could use isolated cell cultures, as well as mixed glial cultures, from WT and KO mice to examine any potential phenotypical/functional changes in these cells (neurons, astrocytes, microglia), including proliferation, secretion profile, antigen presentation and phagocytosis. In addition, any alterations in the interactions between microglia/astrocytes could be examined as this is an important aspect of EAE pathogenesis.

It would also be of benefit to analyse whether MKP-2 has a role in remyelination as this is a crucial step in EAE/MS recovery wherein oligodendrocytes generate new myelin sheaths around damaged axons. To do this, ex vivo slice culture systems could be used [365]. Based on existing protocols, dissected slices of brain or spinal cord tissue from MKP-2 WT and KO mouse pups would be cultured and allowed to myelinate before induced demyelination with compounds such as lysophosphatidylcholine. Cultures would then be maintained for around 14 days before assessing the level of remyelination by immunofluorescent staining of myelin with an anti-myelin basic protein antibody.

Furthermore, it is also important to determine the substrate specificity of MKP-2 in these cells to understand how MKP-2 is regulating cellular function. The best method for this is by western blot. I was only able to analyse ERK and JNK phosphorylation in whole MKP-2 WT and KO EAE CNS tissue samples from one experiment with small sample numbers (3 or 4 mice per group per time point). This was primarily due to time constraints therefore these experiments need to be repeated with increased sample numbers. Nonetheless our preliminary data shows that, in the absence of MKP-2, ERK and JNK phosphorylation in brain and spinal cord tissue may be altered, suggesting MKP-2 may be crucial in regulating the activity of these kinases within the CNS. However it would be more useful to isolate individual cell populations and analyse changes in ERK and JNK phosphorylation caused by MKP-2 deletion as this would be more relevant to the potential effects on disease pathogenesis.

Again, due to time constraints, I was unable to investigate the levels of p-p38 expression in EAE CNS tissue, however activity of this MAPK is also regulated by

MKP-2 in a number of cells [228], [233], therefore this should be analysed along with ERK and JNK. In addition, non-MAPK substrates have recently been identified for MKP dephosphorylation [256]–[258], including STAT5 for MKP-2 [330], suggesting that we have to expand our search beyond the MAPKs when investigating the potential effector targets of MKP-2.

6.3 Conclusion

In conclusion, although EAE is not a perfect representation of MS, it is still a very useful animal model which shares many of the pathophysiological aspects of MS, including CNS inflammation, demyelination and axonal damage. For that reason, novel findings obtained in this model have the potential to further our knowledge and understanding of the pathological mechanisms of MS. By using gene deficient mice we have confirmed a role for MKP-2 in EAE pathogenesis, and thus possibly in MS as well. We have also highlighted a number of potential mechanisms of action through which MKP-2 may be contributing to the pathogenesis of EAE, including increased expansion of key immune cells, increased production of inflammatory mediators and enhanced CNS immune cell infiltration.

Therefore the primary findings that we present in the current study, that MKP-2 is essential to the pathogenic response of EAE, suggests that inhibition of MKP-2 expression or function may be a viable strategy in the treatment of autoimmune inflammatory diseases such as MS.

References

[1] A. Rivallan, “3/6 Jean-Martin Charcot,” *Soins Psychiatr.*, vol. 33, pp. 45–46, 2012.

[2] A. Compston, H. Lassmann, and I. McDonald, “The story of multiple sclerosis,” in *McAlpine’s Multiple Sclerosis: Fourth Edition*, 2005, pp. 3–68.

[3] D. K. Hartline and D. R. Colman, “Rapid conduction and the evolution of giant axons and myelinated fibers.,” *Curr. Biol.*, vol. 17, no. 1, pp. R29–35, Jan. 2007.

[4] M. Pugliatti, S. Sotgiu, and G. Rosati, “The worldwide prevalence of multiple sclerosis,” *Clin. Neurol. Neurosurg.*, vol. 104, no. 3, pp. 182–191, 2002.

[5] I. S. Mackenzie, S. V Morant, G. a Bloomfield, T. M. MacDonald, and J. O’Riordan, “Incidence and prevalence of multiple sclerosis in the UK 1990-2010: a descriptive study in the General Practice Research Database.,” *J. Neurol. Neurosurg. Psychiatry*, vol. 85, no. 1, pp. 76–84, Jan. 2014.

[6] S.-M. Orton, B. M. Herrera, I. M. Yee, W. Valdar, S. V Ramagopalan, a D. Sadovnick, and G. C. Ebers, “Sex ratio of multiple sclerosis in Canada: a longitudinal study.,” *Lancet. Neurol.*, vol. 5, no. 11, pp. 932–6, Nov. 2006.

[7] J. Kurtzke, “Multiple sclerosis in time and space-geographic clues to cause,” *J. Neurovirol.*, vol. 215, pp. 134–140, 2000.

[8] S. Simpson, L. Blizzard, P. Otahal, I. Van der Mei, and B. Taylor, “Latitude is significantly associated with the prevalence of multiple sclerosis: a meta-analysis.,” *J. Neurol. Neurosurg. Psychiatry*, vol. 82, no. 10, pp. 1132–41, Oct. 2011.

[9] D. S. Goodin, “The causal cascade to multiple sclerosis: a model for MS pathogenesis.,” *PLoS One*, vol. 4, no. 2, p. e4565, Jan. 2009.

[10] J. F. Pearson, S. Alla, G. Clarke, B. V Taylor, D. H. Miller, A. Richardson, and D. F. Mason, “Multiple sclerosis in New Zealand Māori.,” *Mult. Scler. J.*, vol. 20, no. 14, pp. 1892–5, Dec. 2014.

[11] A. Compston, “Genetic epidemiology of multiple sclerosis.,” *J. Neurol. Neurosurg. Psychiatry*, vol. 62, pp. 553–561, 1997.

[12] C. H. Polman, S. C. Reingold, B. Banwell, M. Clanet, J. a Cohen, M. Filippi, K. Fujihara, E. Havrdova, M. Hutchinson, L. Kappos, F. D. Lublin, X. Montalban, P. O’Connor, M. Sandberg-Wollheim, A. J. Thompson, E. Waubant, B. Weinshenker, and J. S. Wolinsky, “Diagnostic criteria for

multiple sclerosis: 2010 revisions to the McDonald criteria.," *Ann. Neurol.*, vol. 69, no. 2, pp. 292–302, Feb. 2011.

[13] H. Link and Y.-M. Huang, "Oligoclonal bands in multiple sclerosis cerebrospinal fluid: an update on methodology and clinical usefulness.," *J. Neuroimmunol.*, vol. 180, no. 1–2, pp. 17–28, Nov. 2006.

[14] J. Lechner-Scott, B. Spencer, T. de Malmanche, J. Attia, M. Fitzgerald, M. Trojano, F. Grand'Maison, J. A. C. Gomez, G. Izquierdo, P. Duquette, M. Girard, P. Grammond, C. Oreja-Guevara, R. Hupperts, R. Bergamaschi, C. Boz, G. Giuliani, V. van Pesch, G. Iuliano, M. Fiol, E. Cristiano, F. Verheul, M. L. Saladino, M. Slee, M. Barnett, N. Deri, S. Flechter, N. Vella, C. Shaw, J. Herbert, F. Moore, T. Petkovska-Boskova, V. Jokubaitis, and H. Butzkueven, "The frequency of CSF oligoclonal banding in multiple sclerosis increases with latitude.," *Mult. Scler. J.*, vol. 18, no. 7, pp. 974–82, Jul. 2012.

[15] D. Hafler, A. Compston, and S. Sawcer, "Risk alleles for multiple sclerosis identified by a genomewide study.," *New Engl.*, 2007.

[16] M. Ban, A. Goris, A. R. Lorentzen, A. Baker, T. Mihalova, G. Ingram, D. R. Booth, R. N. Heard, G. J. Stewart, E. Bogaert, B. Dubois, H. F. Harbo, E. G. Celius, A. Spurkland, R. Strange, C. Hawkins, N. P. Robertson, F. Dudbridge, J. Wason, P. L. De Jager, D. Hafler, J. D. Rioux, A. J. Ivinson, J. L. McCauley, M. Pericak-Vance, J. R. Oksenberg, S. L. Hauser, D. Sexton, J. Haines, S. Sawcer, and A. Compston, "Replication analysis identifies TYK2 as a multiple sclerosis susceptibility factor.," *Eur. J. Hum. Genet.*, vol. 17, no. 10, pp. 1309–13, Oct. 2009.

[17] S. Kerlan-Candon, B. Combe, R. Vincent, J. Clot, V. Pinet, and J. F. Eliaou, "HLA-DRB1 gene transcripts in rheumatoid arthritis," *Clin. Exp. Immunol.*, vol. 124, pp. 142–149, 2001.

[18] H. Erlich, A. M. Valdes, J. Noble, J. a Carlson, M. Varney, P. Concannon, J. C. Mychaleckyj, J. a Todd, P. Bonella, A. L. Fear, E. Lavant, A. Louey, P. Moonsamy, and T. 1 D. G. Consortium, "HLA DR-DQ Haplotypes and Genotypes and Type 1 Diabetes Risk," *Diabetes*, vol. 57, no. April, pp. 1084–1092, 2008.

[19] N. a Patsopoulos, F. Esposito, J. Reischl, S. Lehr, D. Bauer, J. Heubach, R. Sandbrink, C. Pohl, G. Edan, L. Kappos, D. Miller, J. Montalbán, C. H. Polman, M. S. Freedman, H.-P. Hartung, B. G. W. Arnason, G. Comi, S. Cook, M. Filippi, D. S. Goodin, D. Jeffery, P. O'Connor, G. C. Ebers, D. Langdon, A. T. Reder, A. Traboulsee, F. Zipp, S. Schimrigk, J. Hillert, M. Bahlo, D. R. Booth, S. Broadley, M. a Brown, B. L. Browning, S. R. Browning, H. Butzkueven, W. M. Carroll, C. Chapman, S. J. Foote, L. Griffiths, A. G. Kermode, T. J. Kilpatrick, J. Lechner-Scott, M. Marriott, D. Mason, P. Moscato, R. N. Heard, M. P. Pender, V. M. Perreau, D. Perera, J. P. Rubio, R. J. Scott, M. Slee, J. Stankovich, G. J. Stewart, B. V Taylor, N.

Tubridy, E. Willoughby, J. Wiley, P. Matthews, F. M. Boneschi, A. Compston, J. Haines, S. L. Hauser, J. McCauley, A. Ivinson, J. R. Oksenberg, M. Pericak-Vance, S. J. Sawcer, P. L. De Jager, D. a Hafler, and P. I. W. de Bakker, "Genome-wide meta-analysis identifies novel multiple sclerosis susceptibility loci.," *Ann. Neurol.*, vol. 70, no. 6, pp. 897–912, Dec. 2011.

[20] P.-A. Gourraud, H. F. Harbo, S. L. Hauser, and S. E. Baranzini, "The genetics of multiple sclerosis: an up-to-date review.," *Immunol. Rev.*, vol. 248, no. 1, pp. 87–103, Jul. 2012.

[21] S. Sawcer, G. Hellenthal, M. Pirinen, C. C. a Spencer, N. a Patsopoulos, L. Moutsianas, A. Dilthey, Z. Su, C. Freeman, S. E. Hunt, S. Edkins, E. Gray, D. R. Booth, S. C. Potter, A. Goris, G. Band, A. B. Oturai, A. Strange, J. Saarela, C. Bellenguez, B. Fontaine, M. Gillman, B. Hemmer, R. Gwilliam, F. Zipp, A. Jayakumar, R. Martin, S. Leslie, S. Hawkins, E. Giannoulatou, S. D'alfonso, H. Blackburn, F. Martinelli Boneschi, J. Liddle, H. F. Harbo, M. L. Perez, A. Spurkland, M. J. Waller, M. P. Mycko, M. Ricketts, M. Comabella, N. Hammond, I. Kockum, O. T. McCann, M. Ban, P. Whittaker, A. Kemppinen, P. Weston, C. Hawkins, S. Widaa, J. Zajicek, S. Dronov, N. Robertson, S. J. Bumpstead, L. F. Barcellos, R. Ravindrarajah, R. Abraham, L. Alfredsson, K. Ardlie, C. Aubin, A. Baker, K. Baker, S. E. Baranzini, L. Bergamaschi, R. Bergamaschi, A. Bernstein, A. Berthele, M. Boggild, J. P. Bradfield, D. Brassat, S. a Broadley, D. Buck, H. Butzkueven, R. Capra, W. M. Carroll, P. Cavalla, E. G. Celius, S. Cepok, R. Chiavacci, F. Clerget-Darpoux, K. Clysters, G. Comi, M. Cossburn, I. Cournu-Rebeix, M. B. Cox, W. Cozen, B. a C. Cree, A. H. Cross, D. Cusi, M. J. Daly, E. Davis, P. I. W. de Bakker, M. Debouverie, M. B. D'hooghe, K. Dixon, R. Dobosi, B. Dubois, D. Ellinghaus, I. Elovaara, F. Esposito, C. Fontenille, S. Foote, A. Franke, D. Galimberti, A. Ghezzi, J. Glessner, R. Gomez, O. Gout, C. Graham, S. F. a Grant, F. R. Guerini, H. Hakonarson, P. Hall, A. Hamsten, H.-P. Hartung, R. N. Heard, S. Heath, J. Hobart, M. Hoshi, C. Infante-Duarte, G. Ingram, W. Ingram, T. Islam, M. Jagodic, M. Kabesch, A. G. Kermode, T. J. Kilpatrick, C. Kim, N. Klopp, K. Koivisto, M. Larsson, M. Lathrop, J. S. Lechner-Scott, M. a Leone, V. Leppä, U. Liljedahl, I. L. Bomfim, R. R. Lincoln, J. Link, J. Liu, A. R. Lorentzen, S. Lupoli, F. Macciardi, T. Mack, M. Marriott, V. Martinelli, D. Mason, J. L. McCauley, F. Mentch, I.-L. Mero, T. Mihalova, X. Montalban, J. Mottershead, K.-M. Myhr, P. Naldi, W. Ollier, A. Page, A. Palotie, J. Pelletier, L. Piccio, T. Pickersgill, F. Piehl, S. Pobywajlo, H. L. Quach, P. P. Ramsay, M. Reunanen, R. Reynolds, J. D. Rioux, M. Rodegher, S. Roesner, J. P. Rubio, I.-M. Rückert, M. Salvetti, E. Salvi, A. Santaniello, C. a Schaefer, S. Schreiber, C. Schulze, R. J. Scott, F. Sellebjerg, K. W. Selmaj, D. Sexton, L. Shen, B. Simms-Acuna, S. Skidmore, P. M. a Sleiman, C. Smestad, P. S. Sørensen, H. B. Søndergaard, J. Stankovich, R. C. Strange, A.-M. Sulonen, E. Sundqvist, A.-C. Syvänen, F. Taddeo, B. Taylor, J. M. Blackwell, P. Tienari, E. Bramon, A. Tourbah, M. a Brown, E. Tronczynska, J. P. Casas, N. Tubridy, A. Corvin, J. Vickery, J. Jankowski, P. Villoslada, H. S. Markus, K. Wang, C. G. Mathew, J. Wason, C. N. a Palmer, H.-E. Wichmann, R. Plomin, E. Willoughby, A. Rautanen, J. Winkelmann, M. Wittig, R. C. Trembath, J.

Yaouanq, A. C. Viswanathan, H. Zhang, N. W. Wood, R. Zuvich, P. Deloukas, C. Langford, A. Duncanson, J. R. Oksenberg, M. a Pericak-Vance, J. L. Haines, T. Olsson, J. Hillert, A. J. Ivinson, P. L. De Jager, L. Peltonen, G. J. Stewart, D. a Hafler, S. L. Hauser, G. McVean, P. Donnelly, and A. Compston, "Genetic risk and a primary role for cell-mediated immune mechanisms in multiple sclerosis.," *Nature*, vol. 476, no. 7359, pp. 214–9, Aug. 2011.

[22] D. Pohl, "Epstein-Barr virus and multiple sclerosis.," *J. Neurol. Sci.*, vol. 286, no. 1–2, pp. 62–4, Nov. 2009.

[23] M. Fga and W. C. Human, "Human herpes virus 6 and multiple sclerosis," pp. 63–83, 2002.

[24] A. Ascherio and K. L. Munger, "Environmental Risk Factors for Multiple Sclerosis . Part II : Noninfectious Factors," *Ann. Neurol.*, pp. 1–3, 2007.

[25] P. Goldberg, "Multiple sclerosis: vitamin D and calcium as environmental determinants of prevalence," *Int. J. Environ. Stud.*, vol. 6, no. 1, pp. 19–27, Feb. 1974.

[26] K. Munger, L. Levin, B. Hollis, N. Howard, and A. Ascherio, "Serum 25-hydroxyvitamin D levels and risk of multiple sclerosis," *JAMA*, vol. 296, no. 23, pp. 2832–2838, 2006.

[27] K. Munger, S. Zhang, E. O'reilly, M. Hernan, M. Olek, W. Willett, and A. Ascherio, "Vitamin D intake and incidence of multiple sclerosis," *Neurology*, vol. 62, pp. 60–65, 2004.

[28] M. Soilu-Hänninen, L. Airas, I. Mononen, A. Heikkila, M. Viljanen, and A. Hanninen, "25-Hydroxyvitamin D levels in serum at the onset of multiple sclerosis," *Mult. Scler.*, vol. 11, pp. 266–271, 2005.

[29] S. Ozgocmen, S. Bulut, N. Ilhan, A. Gulkesen, O. Ardicoglu, and Y. Ozkan, "Vitamin D deficiency and reduced bone mineral density in multiple sclerosis: effect of ambulatory status and functional capacity.," *J. Bone Miner. Metab.*, vol. 23, no. 4, pp. 309–13, Jan. 2005.

[30] D. M. Wingerchuk, "Smoking: effects on multiple sclerosis susceptibility and disease progression.," *Ther. Adv. Neurol. Disord.*, vol. 5, no. 1, pp. 13–22, Jan. 2012.

[31] A. Manouchehrinia, C. R. Tench, J. Maxted, R. H. Bibani, J. Britton, and C. S. Constantinescu, "Tobacco smoking and disability progression in multiple sclerosis: United Kingdom cohort study.," *Brain*, vol. 136, no. Pt 7, pp. 2298–304, Jul. 2013.

[32] A. E. Handel, A. J. Williamson, G. Disanto, R. Dobson, G. Giovannoni, and S. V Ramagopalan, “Smoking and multiple sclerosis: an updated meta-analysis.,” *PLoS One*, vol. 6, no. 1, p. e16149, Jan. 2011.

[33] B. C. Healy, E. N. Ali, C. R. G. Guttmann, T. Chitnis, B. I. Glanz, G. Buckle, M. Houtchens, L. Stazzone, J. Moodie, A. M. Berger, Y. Duan, R. Bakshi, S. Khoury, H. Weiner, and A. Ascherio, “Smoking and disease progression in multiple sclerosis,” *Arch. Neurol.*, vol. 66, no. 7, pp. 858–864, 2009.

[34] E. L. Thacker, F. Mirzaei, and A. Ascherio, “Infectious mononucleosis and risk for multiple sclerosis: a meta-analysis.,” *Ann. Neurol.*, vol. 59, no. 3, pp. 499–503, Mar. 2006.

[35] R. a Farrell, D. Antony, G. R. Wall, D. a Clark, L. Fisniku, J. Swanton, Z. Khaleeli, K. Schmierer, D. H. Miller, and G. Giovannoni, “Humoral immune response to EBV in multiple sclerosis is associated with disease activity on MRI.,” *Neurology*, vol. 73, no. 1, pp. 32–8, Jul. 2009.

[36] A. Ascherio, K. L. Munger, D. Spiegelman, M. A. Herna, S. E. Hankinson, and D. J. Hunter, “Epstein-Barr Virus Antibodies and Risk of Multiple Sclerosis A Prospective Study,” *JAMA*, vol. 286, no. 24, pp. 3083–3088, 2001.

[37] A. Ascherio and K. L. Munger, “Environmental risk factors for multiple sclerosis. Part I: the role of infection.,” *Ann. Neurol.*, vol. 61, no. 4, pp. 288–99, Apr. 2007.

[38] J. Pakpoor, G. Disanto, J. E. Gerber, R. Dobson, U. C. Meier, G. Giovannoni, and S. V Ramagopalan, “The risk of developing multiple sclerosis in individuals seronegative for Epstein-Barr virus: a meta-analysis.,” *Mult. Scler. J.*, vol. 19, no. 2, pp. 162–6, Feb. 2013.

[39] N. Ben-Fredj, W. Ben-Selma, A. Rotola, F. Nefzi, S. Benedetti, M. Frih-Ayed, D. Di Luca, M. Aouni, and E. Caselli, “Prevalence of human herpesvirus U94/REP antibodies and DNA in Tunisian multiple sclerosis patients.,” *J. Neurovirol.*, vol. 19, no. 1, pp. 42–47, Feb. 2013.

[40] A. Behzad-Behbahani, M. H. Mikaeili, M. Entezam, A. Mojiri, G. Y. Pour, M. M. Arasteh, M. Rahsaz, M. Banihashemi, B. Khadang, A. Moaddeb, Z. Nematollahi, and N. Azarpira, “Human herpesvirus-6 viral load and antibody titer in serum samples of patients with multiple sclerosis.,” *J. Microbiol. Immunol. Infect.*, vol. 44, no. 4, pp. 247–51, Aug. 2011.

[41] S. Simpson, B. Taylor, D. E. Dwyer, J. Taylor, L. Blizzard, A.-L. Ponsonby, F. Pittas, T. Dwyer, and I. van der Mei, “Anti-HHV-6 IgG titer significantly predicts subsequent relapse risk in multiple sclerosis.,” *Mult. Scler. J.*, vol. 18, no. 6, pp. 799–806, Jun. 2012.

[42] M. Zorzon, R. de Masi, D. Nasuelli, M. Ukmar, R. P. Mucelli, G. Cazzato, a Bratina, and R. Zivadinov, “Depression and anxiety in multiple sclerosis. A clinical and MRI study in 95 subjects.,” *J. Neurol.*, vol. 248, pp. 416–421, 2001.

[43] D. Michalski, S. Liebig, E. Thomae, S. Singer, A. Hinz, and F. T. Bergh, “Anxiety, depression and impaired health-related quality of life are therapeutic challenges in patients with multiple sclerosis,” *Ment. Illn.*, vol. 2, pp. 20–24, 2010.

[44] M. M. Goldenberg, *Multiple sclerosis review.*, vol. 37, no. 3. 2012.

[45] A. Minagar, “Current and future therapies for multiple sclerosis.,” *Scientifica (Cairo).*, vol. 2013, p. 249101, Jan. 2013.

[46] S. Shapiro, Y. Galboiz, N. Lahat, A. Kinarty, and A. Miller, “The ‘Immunological-Synapse’ at its APC side in relapsing and secondary-progressive multiple sclerosis: Modulation by interferon-??,” *J. Neuroimmunol.*, vol. 144, pp. 116–124, 2003.

[47] Y. Zang, J. Hong, R. Robinson, S. Li, V. M. Rivera, and J. Z. Zhang, “Immune regulatory properties and interactions of Copolymer-I and beta-interferon 1a in multiple sclerosis,” *J. Neuroimmunol.*, vol. 137, pp. 144–153, 2003.

[48] V. Ozenci, M. Kouwenhoven, Y. M. Huang, P. Kivisäkk, and H. Link, “Multiple sclerosis is associated with an imbalance between tumour necrosis factor-alpha (TNF-alpha)- and IL-10-secreting blood cells that is corrected by interferon-beta (IFN-beta) treatment.,” *Clin. Exp. Immunol.*, vol. 120, pp. 147–153, 2000.

[49] D. K. Li and D. W. Paty, “Magnetic resonance imaging results of the PRISMS trial: a randomized, double-blind, placebo-controlled study of interferon-beta1a in relapsing-remitting multiple sclerosis. Prevention of Relapses and Disability by Interferon-beta1a Subcutaneously in Multi,” *Ann. Neurol.*, vol. 46, pp. 197–206, 1999.

[50] J. H. Simon, L. D. Jacobs, M. Campion, K. Wende, N. Simonian, S. S. D. L. Cookfair, R. a Rudick, R. M. Herndon, J. R. Richert, I. I. A. M. Salazar, J. J. Alam, J. S. Fischer, D. E. Goodkin, C. V Granger, M. Lajaunie, A. L. Martens-davidson, M. Meyer, J. Sheeder, K. Choi, A. L. Scherzinger, D. M. Bartoszak, D. N. Bourdette, J. Braiman, C. M. Brownscheidle, M. E. Coats, S. L. Cohan, D. S. Dougherty, R. P. Kinkel, M. K. Mass, F. E. Munschauer, P. M. Pullicino, B. J. Scherokman, and S. S. B. Weinstock-guttman, “Magnetic Resonance Studies of Intramuscular Interferon P-la for Relapsing Multiple Sclerosis,” *Ann. Neurol.*, vol. 43, pp. 79–87, 1998.

[51] G. P. Rice, J. Oger, P. Duquette, G. S. Francis, M. Bélanger, S. Laplante, and J. F. Grenier, “Treatment with interferon beta-1b improves quality of life in multiple sclerosis.,” *Can. J. Neurol. Sci.*, vol. 26, pp. 276–282, 1999.

[52] J. S. Fischer, R. L. Priore, L. D. Jacobs, D. L. Cookfair, R. a Rudick, R. M. Herndon, J. R. Richert, a M. Salazar, D. E. Goodkin, C. V Granger, J. H. Simon, J. H. Grafman, M. D. Lezak, K. M. O’Reilly Hovey, K. K. Perkins, D. Barilla-Clark, M. Schacter, D. W. Shucard, a L. Davidson, K. E. Wende, D. N. Bourdette, and M. F. Kooijmans-Coutinho, “Neuropsychological effects of interferon beta-1a in relapsing multiple sclerosis. Multiple Sclerosis Collaborative Research Group.,” *Ann. Neurol.*, vol. 48, pp. 885–892, 2000.

[53] C. Ford, a D. Goodman, K. Johnson, N. Kachuck, J. W. Lindsey, R. Lisak, C. Luzzio, L. Myers, H. Panitch, J. Preiningerova, A. Pruitt, J. Rose, H. Rus, and J. Wolinsky, “Continuous long-term immunomodulatory therapy in relapsing multiple sclerosis: results from the 15-year analysis of the US prospective open-label study of glatiramer acetate.,” *Mult. Scler. J.*, vol. 16, no. 3, pp. 342–350, 2010.

[54] G. Comi, M. Filippi, and J. S. Wolinsky, “European/Canadian multicenter, double-blind, randomized, placebo-controlled study of the effects of glatiramer acetate on magnetic resonance imaging--measured disease activity and burden in patients with relapsing multiple sclerosis. European/Canadian Gla,” *Ann. Neurol.*, vol. 49, pp. 290–7, 2001.

[55] K. P. Johnson, B. R. Brooks, C. C. Ford, a. Goodman, J. Guarnaccia, R. P. Lisak, L. W. Myers, H. S. Panitch, a. Pruitt, J. W. Rose, N. Kachuck, and J. S. Wolinsky, “Sustained clinical benefits of glatiramer acetate in relapsing multiple sclerosis patients observed for 6 years,” *Mult. Scler.*, vol. 6, no. January 2000, pp. 255–266, 2000.

[56] M. Fridkis-Hareli, D. Teitelbaum, I. Pecht, R. Arnon, and M. Sela, “Binding of copolymer 1 and myelin basic protein leads to clustering of class II MHC molecules on antigen-presenting cells,” *Int. Immunol.*, vol. 9, no. 7, pp. 925–934, 1997.

[57] B. Bellosillo, D. Colomer, G. Pons, and J. Gil, “Mitoxantrone, a topoisomerase II inhibitor, induces apoptosis of B-chronic lymphocytic leukaemia cells.,” *Br. J. Haematol.*, vol. 100, pp. 142–6, 1998.

[58] L. S. Rosenberg, M. J. Carvlin, and T. R. Krugh, “The antitumor agent mitoxantrone binds cooperatively to DNA: evidence for heterogeneity in DNA conformation.,” *Biochemistry*, vol. 25, no. 1984, pp. 1002–1008, 1986.

[59] J. M. Fidler, S. Q. DeJoy, and J. J. Gibbons, “Selective immunomodulation by the antineoplastic agent mitoxantrone. I. Suppression of B lymphocyte function.,” *J. Immunol.*, vol. 137, no. 3, pp. 727–732, 1986.

[60] H.-P. Hartung, R. Gonsette, N. König, H. Kwiecinski, A. Guseo, S. P. Morrissey, H. Krapf, and T. Zwingers, "Mitoxantrone in progressive multiple sclerosis: a placebo-controlled, double-blind, randomised, multicentre trial.," *Lancet*, vol. 360, pp. 2018–25, 2002.

[61] E. J. Fox, "Management of worsening multiple sclerosis with mitoxantrone: A review," *Clin. Ther.*, vol. 28, no. 4, pp. 461–474, 2006.

[62] B. Engelhardt and L. Kappos, "Natalizumab: targeting alpha4-integrins in multiple sclerosis.," *Neurodegener. Dis.*, vol. 5, pp. 16–22, 2008.

[63] W. a. Sheremata, A. Minagar, J. S. Alexander, and T. Vollmer, "The role of alpha-4 integrin in the aetiology of multiple sclerosis: Current knowledge and therapeutic implications," *CNS Drugs*, vol. 19, no. 11, pp. 909–922, 2005.

[64] D. H. Miller, O. a Khan, W. a Sheremata, L. D. Blumhardt, G. P. a Rice, M. a Libonati, A. J. Willmer-Hulme, C. M. Dalton, K. a Miszkiel, and P. W. O'Connor, "A controlled trial of natalizumab for relapsing multiple sclerosis.," *N. Engl. J. Med.*, vol. 348, pp. 15–23, 2003.

[65] C. H. Polman, P. W. O'Connor, E. Havrdova, M. Hutchinson, L. Kappos, D. H. Miller, J. T. Phillips, F. D. Lublin, G. Giovannoni, A. Wajgt, M. Toal, F. Lynn, M. a Panzara, and A. W. Sandrock, "A randomized, placebo-controlled trial of natalizumab for relapsing multiple sclerosis.," *N. Engl. J. Med.*, vol. 354, no. 9, pp. 899–910, 2006.

[66] G. Bloomgren, S. Richman, C. Hotermans, M. Subramanyam, S. Goelz, A. Natarajan, S. Lee, T. Plavina, J. V. Scanlon, A. Sandrock, and C. Bozic, "Risk of Natalizumab-Associated Progressive Multifocal Leukoencephalopathy," *N. Engl. J. Med.*, vol. 366, pp. 1870–1880, 2012.

[67] M. Matloubian, C. G. Lo, G. Cinamon, M. J. Lesneski, Y. Xu, V. Brinkmann, M. L. Allende, R. L. Proia, and J. G. Cyster, "Lymphocyte egress from thymus and peripheral lymphoid organs is dependent on S1P receptor 1.," *Nature*, vol. 427, pp. 355–360, 2004.

[68] G. Comi, P. O'Connor, X. Montalban, J. Antel, E.-W. Radue, G. Karlsson, H. Pohlmann, S. Aradhye, and L. Kappos, "Phase II study of oral fingolimod (FTY720) in multiple sclerosis: 3-year results.," *Mult. Scler. J.*, vol. 16, no. 2, pp. 197–207, 2010.

[69] L. Steinman and S. S. Zamvil, "How to successfully apply animal studies in experimental allergic encephalomyelitis to research on multiple sclerosis.," *Ann. Neurol.*, vol. 60, no. 1, pp. 12–21, Jul. 2006.

[70] R. Gold, C. Linington, and H. Lassmann, "Understanding pathogenesis and therapy of multiple sclerosis via animal models: 70 years of merits and

culprits in experimental autoimmune encephalomyelitis research.," *Brain*, vol. 129, no. Pt 8, pp. 1953–71, Aug. 2006.

[71] T. M. Rivers, D. H. Sprunt, and G. P. Berry, "Observations an attempts to produce acute disseminated encephalomyelitis in monkeys.," *J. Exp. Med.*, 1933.

[72] J. L. Berard, K. Wolak, S. Fournier, and S. David, "Characterization of relapsing-remitting and chronic forms of experimental autoimmune encephalomyelitis in C57BL/6 mice," *Glia*, vol. 58, no. August 2009, pp. 434–445, 2010.

[73] C. S. Constantinescu, N. Farooqi, K. O'Brien, and B. Gran, "Experimental autoimmune encephalomyelitis (EAE) as a model for multiple sclerosis (MS).," *Br. J. Pharmacol.*, vol. 164, no. 4, pp. 1079–106, Oct. 2011.

[74] K. E. Bruckener, "Permeabilization in a cerebral endothelial barrier model by pertussis toxin involves the PKC effector pathway and is abolished by elevated levels of cAMP," *J. Cell Sci.*, vol. 116, no. 9, pp. 1837–1846, Mar. 2003.

[75] R. K. Bergman, J. J. Munoz, I. Diseases, and F. Lewis, "Vascular Permeability Changes in the Central Nervous System of Rats with Hyperacute Experimental Allergic Encephalomyelitis Induced with the Aid of a Substance from Bordetella pertussis," vol. 21, no. 2, pp. 627–637, 1978.

[76] S. M. Kerfoot, E. M. Long, M. J. Hickey, G. Andonegui, B. M. Lapointe, C. O. Renata, C. Bonder, W. G. James, M. Stephen, R. C. O. Zanardo, S. M. Robbins, and P. Kubes, "TLR4 contributes to Disease-Inducing mechanisms in Central Nervous System Autoimmune Disease," *J. Immunol.*, vol. 173, pp. 7070–7077, 2004.

[77] H. H. Hofstetter, C. L. Shive, and G. Thomas, "Pertussis Toxin Modulates the Immune Response to Neuroantigens Injected in Incomplete Freund's Adjuvant: Induction of Th1 Cells and Experimental Autoimmune Encephalomyelitis in the Presence of High Frequencies of Th2 Cells," *J. Immunol.*, vol. 169, no. 1, pp. 117–125, 2002.

[78] P. K. Olitsky and R. H. Yager, "Experimental disseminated encephalomyelitis in white mice.," *J. Exp. Med.*, vol. 90, no. 3, pp. 213–224, 1949.

[79] a Ben-Nun, H. Wekerle, and I. R. Cohen, "The rapid isolation of clonable antigen-specific T lymphocyte lines capable of mediating autoimmune encephalomyelitis.," *Eur. J. Immunol.*, vol. 11, no. 3, pp. 195–9, Mar. 1981.

[80] M. L. Ford and B. D. Evavold, "Specificity, magnitude, and kinetics of MOG-specific CD8+ T cell responses during experimental autoimmune encephalomyelitis.," *Eur. J. Immunol.*, vol. 35, no. 1, pp. 76–85, Jan. 2005.

[81] G. Krishnamoorthy, H. Lassmann, H. Wekerle, and A. Holz, “Spontaneous opticospinal encephalomyelitis in a double-transgenic mouse model of autoimmune T cell / B cell cooperation,” vol. 116, no. 9, pp. 2385–2392, 2006.

[82] B. Pöllinger, G. Krishnamoorthy, K. Berer, H. Lassmann, M. R. Bösl, R. Dunn, H. S. Domingues, A. Holz, F. C. Kurschus, and H. Wekerle, “Spontaneous relapsing-remitting EAE in the SJL/J mouse: MOG-reactive transgenic T cells recruit endogenous MOG-specific B cells.,” *J. Exp. Med.*, vol. 206, no. 6, pp. 1303–16, Jun. 2009.

[83] S. Kuerten, D. Kostova-Bales, and L. Frenzel, “MP4- and MOG:35–55-induced EAE in C57BL/6 mice differentially targets brain, spinal cord and cerebellum,” *J. Neuroimmunol.*, vol. 189, pp. 31–40, 2007.

[84] A. Compston and A. Coles, “Multiple sclerosis.,” *Lancet*, vol. 372, no. 9648, pp. 1502–17, Oct. 2008.

[85] L. J. Bagley, R. I. Grossman, S. L. Galetta, G. P. Sinson, M. Kotapka, and J. C. McGowan, “Characterization of white matter lesions in multiple sclerosis and traumatic brain injury as revealed by magnetization transfer contour plots,” *Am. J. Neuroradiol.*, vol. 20, no. July, pp. 977–981, 1999.

[86] D. Kidd, F. Barkhof, R. McConnell, P. Algra, I. Allen, and T. Revesz, “Cortical lesions in multiple sclerosis,” *Brain*, vol. 122, pp. 17–26, 1999.

[87] J. J. G. Geurts, L. Bo, P. J. W. Pouwels, J. A. Castelijns, C. H. Polman, and F. Barkhof, “Cortical Lesions in Multiple Sclerosis : Combined Postmortem MR Imaging and Histopathology,” no. March, pp. 572–577, 2005.

[88] J. E. Merrill, D. H. Kono, J. Clayton, D. G. Ando, D. R. Hinton, and F. M. Hofman, “Inflammatory leukocytes and cytokines in the peptide-induced disease of experimental allergic encephalomyelitis in SJL and B10.PL mice.,” *Proc. Natl. Acad. Sci. U. S. A.*, vol. 89, no. January, pp. 574–578, 1992.

[89] J. R. Lees and A. H. Cross, “A little stress is good: IFN-γ, demyelination, and multiple sclerosis,” *J. Clin. Invest.*, vol. 117, no. 2, pp. 297–299, 2007.

[90] H. S. Panitch, R. L. Hirsch, J. Schindler, and K. P. Johnson, “Treatment of multiple sclerosis with gamma interferon: exacerbations associated with activation of the immune system.,” *Neurology*, vol. 37, no. July, pp. 1097–1102, 1987.

[91] I. A. Ferber, S. Brocke, C. Taylor-Edwards, W. Ridgway, C. Dinisco, L. Steinman, D. Dalton, and C. G. Fathman, “Mice with a disrupted IFN-gamma gene are susceptible to the induction of experimental autoimmune encephalomyelitis (EAE).,” *J. Immunol.*, vol. 156, pp. 5–7, 1996.

[92] D. O. Willenborg, S. Fordham, C. C. Bernard, W. B. Cowden, and I. A. Ramshaw, “IFN-gamma plays a critical down-regulatory role in the induction and effector phase of myelin oligodendrocyte glycoprotein-induced autoimmune encephalomyelitis.,” *J. Immunol.*, vol. 157, pp. 3223–3227, 1996.

[93] B. Becher, B. G. Durell, and R. J. Noelle, “Experimental autoimmune encephalitis and inflammation in the absence of interleukin-12,” *J. Clin. Invest.*, vol. 110, no. 4, pp. 493–497, 2002.

[94] B. Gran, G.-X. Zhang, S. Yu, J. Li, X.-H. Chen, E. S. Ventura, M. Kamoun, and A. Rostami, “IL-12p35-deficient mice are susceptible to experimental autoimmune encephalomyelitis: evidence for redundancy in the IL-12 system in the induction of central nervous system autoimmune demyelination.,” *J. Immunol.*, vol. 169, pp. 7104–7110, 2002.

[95] D. J. Cua, J. Sherlock, Y. Chen, C. a Murphy, B. Joyce, B. Seymour, L. Lucian, W. To, S. Kwan, T. Churakova, S. Zurawski, M. Wiekowski, S. a Lira, D. Gorman, R. a Kastelein, and J. D. Sedgwick, “Interleukin-23 rather than interleukin-12 is the critical cytokine for autoimmune inflammation of the brain.,” *Nature*, vol. 421, no. February, pp. 744–748, 2003.

[96] L. E. Harrington, R. D. Hatton, P. R. Mangan, H. Turner, T. L. Murphy, K. M. Murphy, and C. T. Weaver, “Interleukin 17-producing CD4+ effector T cells develop via a lineage distinct from the T helper type 1 and 2 lineages.,” *Nat. Immunol.*, vol. 6, no. 11, pp. 1123–1132, 2005.

[97] C. L. Langrish, Y. Chen, W. M. Blumenschein, J. Mattson, B. Basham, J. D. Sedgwick, T. McClanahan, R. a Kastelein, and D. J. Cua, “IL-23 drives a pathogenic T cell population that induces autoimmune inflammation.,” *J. Exp. Med.*, vol. 201, no. 2, pp. 233–40, Jan. 2005.

[98] A. Jäger, V. Dardalhon, R. a Sobel, E. Bettelli, and V. K. Kuchroo, “Th1, Th17, and Th9 effector cells induce experimental autoimmune encephalomyelitis with different pathological phenotypes.,” *J. Immunol.*, vol. 183, pp. 7169–7177, 2009.

[99] a. P. Kohm, P. a. Carpentier, H. a. Anger, and S. D. Miller, “Cutting Edge: CD4+CD25+ Regulatory T Cells Suppress Antigen-Specific Autoreactive Immune Responses and Central Nervous System Inflammation During Active Experimental Autoimmune Encephalomyelitis,” *J. Immunol.*, vol. 169, pp. 4712–4716, 2002.

[100] M. J. McGeachy, L. a. Stephens, and S. M. Anderton, “Natural Recovery and Protection from Autoimmune Encephalomyelitis: Contribution of CD4+CD25+ Regulatory Cells within the Central Nervous System,” *J. Immunol.*, vol. 175, no. 5, pp. 3025–3032, Aug. 2005.

[101] J. Reddy, H. Waldner, X. Zhang, Z. Illes, K. W. Wucherpfennig, R. a Sobel, and V. K. Kuchroo, “Cutting edge: CD4+CD25+ regulatory T cells contribute to gender differences in susceptibility to experimental autoimmune encephalomyelitis.,” *J. Immunol.*, vol. 175, pp. 5591–5595, 2005.

[102] M. a. Friese and L. Fugger, “Pathogenic CD8 + T cells in multiple sclerosis,” *Ann. Neurol.*, vol. 66, pp. 132–141, 2009.

[103] E. S. Huseby, P. G. Huseby, S. Shah, R. Smith, and B. D. Stadinski, “Pathogenic CD8 T cells in multiple sclerosis and its experimental models.,” *Front. Immunol.*, vol. 3, no. March, p. 64, Jan. 2012.

[104] H. Babbe, a Roers, a Waisman, H. Lassmann, N. Goebels, R. Hohlfeld, M. Friese, R. Schröder, M. Deckert, S. Schmidt, R. Ravid, and K. Rajewsky, “Clonal expansions of CD8(+) T cells dominate the T cell infiltrate in active multiple sclerosis lesions as shown by micromanipulation and single cell polymerase chain reaction.,” *J. Exp. Med.*, vol. 192, no. 3, pp. 393–404, 2000.

[105] F. W. Gay, T. J. Drye, G. W. a Dick, and M. M. Esiri, “The application of multifactorial cluster analysis in the staging of plaques in early multiple sclerosis: Identification and characterization of the primary demyelinating lesion,” *Brain*, vol. 120, pp. 1461–1483, 1997.

[106] S. Jilek, M. Schluep, A. O. Rossetti, L. Guignard, G. Le Goff, G. Pantaleo, and R. a. Du Pasquier, “CSF enrichment of highly differentiated CD8+ T cells in early multiple sclerosis,” *Clin. Immunol.*, vol. 123, pp. 105–113, 2007.

[107] C. Skulina, S. Schmidt, K. Dornmair, H. Babbe, A. Roers, K. Rajewsky, H. Wekerle, R. Hohlfeld, and N. Goebels, “Multiple sclerosis: brain-infiltrating CD8+ T cells persist as clonal expansions in the cerebrospinal fluid and blood.,” *Proc. Natl. Acad. Sci. U. S. A.*, vol. 101, no. 8, pp. 2428–2433, 2004.

[108] A. Bitsch, J. Schuchardt, S. Bunkowski, T. Kuhlmann, and W. Brück, “Acute axonal injury in multiple sclerosis. Correlation with demyelination and inflammation.,” *Brain*, vol. 123, pp. 1174–1183, 2000.

[109] T. Kuhlmann, G. Lingfeld, A. Bitsch, J. Schuchardt, and W. Brück, “Acute axonal damage in multiple sclerosis is most extensive in early disease stages and decreases over time.,” *Brain*, vol. 125, pp. 2202–2212, 2002.

[110] A. J. Coles, M. G. Wing, P. Molyneux, A. Paolillo, C. M. Davie, G. Hale, D. Miller, H. Waldmann, and A. Compston, “Monoclonal antibody treatment exposes three mechanisms underlying the clinical course of multiple sclerosis.,” *Ann. Neurol.*, vol. 46, no. 3, pp. 296–304, Sep. 1999.

[111] R. Höftberger, W. Brueck, C. Lucchinetti, M. Rodriguez, M. Schmidbauer, K. Jellinger, and H. Lassmann, “Expression of Major Histocompatibility

Complex Class I Molecules on the Different Cell Types in Multiple Sclerosis Lesions," *Brain Pathol.*, vol. 14, pp. 43–50, 2004.

[112] N. Melzer, S. G. Meuth, and H. Wiendl, "CD8+ T cells and neuronal damage: direct and collateral mechanisms of cytotoxicity and impaired electrical excitability.," *FASEB J.*, vol. 23, pp. 3659–3673, 2009.

[113] L. T. Mars, P. Saikali, R. S. Liblau, and N. Arbour, "Contribution of CD8 T lymphocytes to the immuno-pathogenesis of multiple sclerosis and its animal models," *Biochim. Biophys. Acta*, vol. 1812, no. 2, pp. 151–161, 2011.

[114] A. Saxena, J. Bauer, T. Scheikl, J. Zappulla, M. Audebert, S. Desbois, A. Waisman, H. Lassmann, R. S. Liblau, and L. T. Mars, "Cutting edge: Multiple sclerosis-like lesions induced by effector CD8 T cells recognizing a sequestered antigen on oligodendrocytes.," *J. Immunol.*, vol. 181, pp. 1617–1621, 2008.

[115] Y. Matsumoto, K. Kohyama, Y. Aikawa, T. Shin, Y. Kawazoe, Y. Suzuki, and N. Tanuma, "Role of natural killer cells and TCR q p T cells in acute autoimmune encephalomyelitis," *Mult. Scler.*, pp. 1681–1688, 1998.

[116] D. M. Karussis, D. Lehmann, S. Slavin, U. Vourka-karussis, and R. Mizrachi-koll, "Ihbition of Acute , Experimental Autoimmune Encephalomyelitis by the Synthetic Immunomodulator Lrnomide," *Control*, 1993.

[117] R. B. Fritz, M. Zhao, C. B. L. Mouse, and T. Cells, "Regulation of Experimental Autoimmune Encephalomyelitis in the C57BL/6J Mouse by NK1.1 + , DX5 + , α β + T Cells," *Culture*, 2011.

[118] M. S. Freedman, E. J. Thompson, F. Deisenhammer, G. Giovannoni, G. Grimsley, G. Keir, S. Ohman, M. K. Racke, M. Sharief, C. J. M. Sindic, F. Sellebjerg, and W. W. Tourtellotte, "Recommended standard of cerebrospinal fluid analysis in the diagnosis of multiple sclerosis: a consensus statement.," *Arch. Neurol.*, vol. 62, no. June 2005, pp. 865–870, 2005.

[119] B. Obermeier, L. Lovato, R. Mentele, W. Brück, I. Forne, A. Imhof, F. Lottspeich, K. W. Turk, S. N. Willis, H. Wekerle, R. Hohlfeld, D. a. Hafler, K. C. O'Connor, and K. Dornmair, "Related B cell clones that populate the CSF and CNS of patients with multiple sclerosis produce CSF immunoglobulin," *J. Neuroimmunol.*, vol. 233, pp. 245–248, 2011.

[120] A. P. D. Henderson, M. H. Barnett, J. D. E. Parratt, and J. W. Prineas, "Multiple sclerosis: Distribution of inflammatory cells in newly forming lesions," *Ann. Neurol.*, vol. 66, pp. 739–753, 2009.

[121] E. C. W. Breij, B. P. Brink, R. Veerhuis, C. Van Den Berg, R. Vloet, R. Yan, C. D. Dijkstra, P. Van Der Valk, and L. Bö, "Homogeneity of active

demyelinating lesions in established multiple sclerosis," *Ann. Neurol.*, vol. 63, no. 16, pp. 16–25, 2008.

[122] S. Hauser, E. Waubant, D. L. Arnold, T. Vollmer, J. Antel, R. J. Fox, A. Bar-or, M. Panzara, N. Sarkar, S. Agarwal, and A. Langer-gould, "B-Cell Depletion with Rituximab in Relapsing–Remitting Multiple Sclerosis," *N. Engl. J. Med.*, no. 358, pp. 678–688, 2008.

[123] C. Linington, M. Bradl, H. Lassmann, C. Brunner, and K. Vass, "Augmentation of demyelination in rat acute allergic encephalomyelitis by circulating mouse monoclonal antibodies directed against a myelin/oligodendrocyte glycoprotein," *Am. J. Pathol.*, vol. 3, no. 130, pp. 443–454, 1988.

[124] E. R. Pierson, I. M. Stromnes, and J. M. Goverman, "B cells promote induction of experimental autoimmune encephalomyelitis by facilitating reactivation of T cells in the central nervous system.," *J. Immunol.*, vol. 192, no. 3, pp. 929–39, Feb. 2014.

[125] S. Wolf, B. Dittel, F. Hardardottir, and C. Janeway, "Experimental autoimmune encephalomyelitis induction in genetically B cell–deficient mice," *J. Exp. Med.*, vol. 184, no. December, pp. 2271–2278, 1996.

[126] T. Matsushita, K. Yanaba, J. D. Bouaziz, M. Fujimoto, and T. F. Tedder, "Regulatory B cells inhibit EAE initiation in mice while other B cells promote disease progression," *J. Clin. Invest.*, vol. 118, no. 10, pp. 3420–3430, 2008.

[127] S. Fillatreau, C. H. Sweenie, M. J. McGeachy, D. Gray, and S. M. Anderton, "B cells regulate autoimmunity by provision of IL-10.," *Nat. Immunol.*, vol. 3, no. 10, pp. 944–50, Oct. 2002.

[128] C. R. Weir, K. Nicolson, and B. T. Bäckström, "Experimental autoimmune encephalomyelitis induction in naive mice by dendritic cells presenting a self-peptide," *Immunol. Cell Biol.*, pp. 14–20, 2002.

[129] T. Suter, U. Malipiero, L. Otten, B. Ludewig, A. Muelethaler-, B. Mach, W. Reith, and A. Fontana, "Dendritic cells and differential usage of the MHC class II transactivator promoters in the central nervous system in experimental autoimmune encephalitis," *Genetics*, pp. 794–802, 2000.

[130] S. L. Bailey, B. Schreiner, E. J. McMahon, and S. D. Miller, "CNS myeloid DCs presenting endogenous myelin peptides 'preferentially' polarize CD4+ T(H)-17 cells in relapsing EAE.," *Nat. Immunol.*, vol. 8, no. 2, pp. 172–80, Feb. 2007.

[131] S. L. Bailey-Bucktrout, S. C. Caulkins, G. Goings, J. a. a. Fischer, a. Dzionek, and S. D. Miller, "Cutting Edge: Central Nervous System Plasmacytoid

Dendritic Cells Regulate the Severity of Relapsing Experimental Autoimmune Encephalomyelitis," *J. Immunol.*, vol. 180, no. 10, pp. 6457–6461, May 2008.

[132] E. Gomez Perdiguero, K. Klapproth, C. Schulz, K. Busch, E. Azzoni, L. Crozet, H. Garner, C. Trouillet, M. F. de Bruijn, F. Geissmann, and H.-R. Rodewald, "Tissue-resident macrophages originate from yolk-sac-derived erythro-myeloid progenitors," *Nature*, vol. 518, no. 7540, pp. 547–551, 2014.

[133] B. I. Huitinga, N. Van Rooijen, C. J. A. De Groot, B. M. J. Uitdehaag, and C. D. Dijkstra, "Suppression of Experimental Allergic Encephalomyelitis in Lewis Rats After Elimination of Macrophages," *J. Exp. Med.*, vol. 172, pp. 1025–1033, 1990.

[134] J. A. Martiney, A. J. Rajan, P. C. Charles, A. Cerami, P. C. Ulrich, S. Macphail, K. J. Tracey, and C. F. Brosnan, "Prevention and treatment of experimental autoimmune encephalomyelitis by CNI-1493, a macrophage-deactivating agent," *J. Immunol.*, no. 160, pp. 5588–5595, 1998.

[135] F. L. Heppner, M. Greter, D. Marino, J. Falsig, G. Raivich, N. Hövelmeyer, A. Waisman, T. Rülicke, M. Prinz, J. Priller, B. Becher, and A. Aguzzi, "Experimental autoimmune encephalomyelitis repressed by microglial paralysis.," *Nat. Med.*, vol. 11, no. 2, pp. 146–52, Feb. 2005.

[136] E. M. L. Chastain, D. S. Duncan, J. M. Rodgers, and S. D. Miller, "The role of antigen presenting cells in multiple sclerosis.," *Biochim. Biophys. Acta*, vol. 1812, no. 2, pp. 265–74, Feb. 2011.

[137] J. Mikita, N. Dubourdieu-Cassagno, M. S. Deloire, A. Vekris, M. Biran, G. Raffard, B. Brochet, M.-H. Canron, J.-M. Franconi, C. Boiziau, and K. G. Petry, "Altered M1/M2 activation patterns of monocytes in severe relapsing experimental rat model of multiple sclerosis. Amelioration of clinical status by M2 activated monocyte administration.," *Mult. Scler. J.*, vol. 17, no. 1, pp. 2–15, Jan. 2011.

[138] J. B. Tierney, M. Kharkrang, and A. C. La Flamme, "Type II-activated macrophages suppress the development of experimental autoimmune encephalomyelitis.," *Immunol. Cell Biol.*, vol. 87, no. 3, pp. 235–40, 2009.

[139] R. Shechter, A. London, C. Varol, C. Raposo, M. Cusimano, G. Yovel, A. Rolls, M. Mack, S. Pluchino, G. Martino, S. Jung, and M. Schwartz, "Infiltrating blood-derived macrophages are vital cells playing an anti-inflammatory role in recovery from spinal cord injury in mice.," *PLoS Med.*, vol. 6, no. 7, p. e1000113, Jul. 2009.

[140] M. R. Kotter, W.-W. Li, C. Zhao, and R. J. M. Franklin, "Myelin impairs CNS remyelination by inhibiting oligodendrocyte precursor cell differentiation.," *J. Neurosci.*, vol. 26, no. 1, pp. 328–32, Jan. 2006.

[141] C. Brosnan and C. Raine, “The astrocyte in multiple sclerosis revisited,” *Glia*, vol. 61, no. 4, pp. 453–65, Apr. 2013.

[142] P. Jukkola, T. Guerrero, V. Gray, and C. Gu, “Astrocytes differentially respond to inflammatory autoimmune insults and imbalances of neural activity.,” *Acta Neuropathol. Commun.*, vol. 1, no. 1, p. 70, Jan. 2013.

[143] D. Wang, M. M. Ayers, D. V Catmull, L. J. Hazelwood, C. C. a Bernard, and J. M. Orian, “Astrocyte-associated axonal damage in pre-onset stages of experimental autoimmune encephalomyelitis.,” *Glia*, vol. 51, no. 3, pp. 235–40, Aug. 2005.

[144] R. Brambilla, T. Persaud, X. Hu, S. Karmally, V. I. Shestopalov, G. Dvoriantchikova, D. Ivanov, L. Nathanson, S. R. Barnum, and J. R. Bethea, “Transgenic inhibition of astroglial NF-kappa B improves functional outcome in experimental autoimmune encephalomyelitis by suppressing chronic central nervous system inflammation.,” *J. Immunol.*, vol. 182, no. 5, pp. 2628–40, Mar. 2009.

[145] R. Brambilla, P. D. Morton, J. J. Ashbaugh, S. Karmally, K. L. Lambertsen, and J. R. Bethea, “Astrocytes play a key role in EAE pathophysiology by orchestrating in the CNS the inflammatory response of resident and peripheral immune cells and by suppressing remyelination.,” *Glia*, vol. 62, no. 3, pp. 452–67, Mar. 2014.

[146] C. S. Constantinescu, M. Tani, R. M. Ransohoff, M. Wysocka, B. Hilliard, T. Fujioka, S. Murphy, P. J. Tighe, J. Das Sarma, G. Trinchieri, and A. Rostami, “Astrocytes as antigen-presenting cells: expression of IL-12/IL-23.,” *J. Neurochem.*, vol. 95, no. 2, pp. 331–40, Oct. 2005.

[147] C. Jack, J. Antel, W. Brück, and T. Kuhlmann, “Contrasting potential of nitric oxide and peroxynitrite to mediate oligodendrocyte injury in multiple sclerosis,” *Glia*, vol. 934, no. August 2006, pp. 926–934, 2007.

[148] F. Aloisi, G. Penna, and J. Cerase, “IL-12 production by central nervous system microglia is inhibited by astrocytes.,” *J. Immunol.*, vol. 1, no. 159, pp. 1604–1612, 1997.

[149] J. Xu and P. D. Drew, “Peroxisome Proliferator-Activated Receptor- Agonists Suppress the Production of IL-12 Family Cytokines by Activated Glia,” *J. Immunol.*, vol. 178, no. 3, pp. 1904–1913, Jan. 2007.

[150] J. S. Stumhofer, A. Laurence, E. H. Wilson, E. Huang, C. M. Tato, L. M. Johnson, A. V Villarino, Q. Huang, A. Yoshimura, D. Sehy, C. J. M. Saris, J. J. O’Shea, L. Hennighausen, M. Ernst, and C. a Hunter, “Interleukin 27 negatively regulates the development of interleukin 17-producing T helper cells during chronic inflammation of the central nervous system.,” *Nat. Immunol.*, vol. 7, no. 9, pp. 937–45, Sep. 2006.

[151] D. C. Fitzgerald, B. Ciric, T. Touil, H. Harle, J. Grammatikopolou, J. Das Sarma, B. Gran, G. Zhang, and A. Rostami, "Suppressive Effect of IL-27 on Encephalitogenic Th17 Cells and the Effector Phase of Experimental Autoimmune," vol. 3, no. 17.

[152] M. Batten, J. Li, S. Yi, N. M. Kljavin, D. M. Danilenko, S. Lucas, J. Lee, F. J. de Sauvage, and N. Ghilardi, "Interleukin 27 limits autoimmune encephalomyelitis by suppressing the development of interleukin 17-producing T cells.," *Nat. Immunol.*, vol. 7, no. 9, pp. 929–36, Sep. 2006.

[153] C. Mc Guire, T. Volckaert, U. Wolke, M. Sze, R. de Rycke, A. Waisman, M. Prinz, R. Beyaert, M. Pasparakis, and G. van Loo, "Oligodendrocyte-specific FADD deletion protects mice from autoimmune-mediated demyelination.," *J. Immunol.*, vol. 185, no. 12, pp. 7646–53, Dec. 2010.

[154] N. Hovelmeyer, Z. Hao, K. Kranidioti, G. Kassiotis, T. Buch, F. Frommer, L. von Hoch, D. Kramer, L. Minichiello, G. Kollias, H. Lassmann, and a. Waisman, "Apoptosis of Oligodendrocytes via Fas and TNF-R1 Is a Key Event in the Induction of Experimental Autoimmune Encephalomyelitis," *J. Immunol.*, vol. 175, no. 9, pp. 5875–5884, Oct. 2005.

[155] Y. A. Yeo, J. M. Martínez Gómez, J. L. Croxford, S. Gasser, E.-A. Ling, and H. Schwarz, "CD137 ligand activated microglia induces oligodendrocyte apoptosis via reactive oxygen species.," *J. Neuroinflammation*, vol. 9, p. 173, Jan. 2012.

[156] T. Vartanian, Y. Li, M. Zhao, and K. Stefansson, "Interferon-gamma-induced oligodendrocyte cell death: implications for the pathogenesis of multiple sclerosis.," *Mol. Med.*, vol. 1, no. 7, pp. 732–743, 1995.

[157] M. Raman, W. Chen, and M. H. Cobb, "Differential regulation and properties of MAPKs," *Oncogene*, pp. 3100–3112, 2007.

[158] T. Boutros, E. Chevet, and P. Metrakos, "Mitogen-Activated Protein (MAP) Kinase / MAP Kinase Phosphatase Regulation : Roles in Cell Growth , Death , and Cancer," *Pharmacol. Rev.*, vol. 60, no. 3, pp. 261–310, 2008.

[159] J. Yasuda, A. J. Whitmarsh, J. Cavanagh, M. Sharma, and R. J. Davis, "The JIP group of mitogen-activated protein kinase scaffold proteins," *Mol. Cell. Biol.*, vol. 19, no. 10, p. 7245, 1999.

[160] H. J. Schaeffer, "MP1: A MEK Binding Partner That Enhances Enzymatic Activation of the MAP Kinase Cascade," *Science (80-.).*, vol. 281, no. 5383, pp. 1668–1671, Sep. 1998.

[161] T. G. Boulton, G. D. Yancopoulos, J. S. Gregory, C. Slaughter, C. Moomaw, J. Hsu, and M. H. Cobb, "An insulin-stimulated protein kinase similar to yeast

kinases involved in cell cycle control," *Science (80-.).*, vol. 249, no. 4964, p. 64, 1990.

[162] T. G. Boulton and M. H. Cobb, "Identification of multiple extracellular signal-regulated kinases (ERKs) with antipeptide antibodies.," *Cell Regul.*, vol. 2, no. 5, pp. 357–71, May 1991.

[163] a G. Turjanski, J. P. Vaqué, and J. S. Gutkind, "MAP kinases and the control of nuclear events.," *Oncogene*, vol. 26, no. 22, pp. 3240–53, May 2007.

[164] C. P. Gayer, D. H. Craig, T. L. Flanigan, T. D. Reed, D. E. Cress, and M. D. Basson, "ERK regulates strain-induced migration and proliferation from different subcellular locations.," *J. Cell. Biochem.*, vol. 109, no. 4, pp. 711–25, Mar. 2010.

[165] R. Ley, K. Balmanno, K. Hadfield, C. Weston, and S. J. Cook, "Activation of the ERK1/2 signaling pathway promotes phosphorylation and proteasome-dependent degradation of the BH3-only protein, Bim.," *J. Biol. Chem.*, vol. 278, no. 21, pp. 18811–6, May 2003.

[166] H. Harada, B. Quearry, A. Ruiz-Vela, and S. J. Korsmeyer, "Survival factor-induced extracellular signal-regulated kinase phosphorylates BIM, inhibiting its association with BAX and proapoptotic activity," *Proc. Natl. Acad. Sci. U. S. A.*, vol. 101, no. 43, pp. 15313–15317, 2004.

[167] M. Hibi, A. Lin, T. Smeal, M. Hibi, A. Lin, T. Smeal, A. Minden, and M. Karin, "Identification of an oncoprotein- and UV-responsive protein kinase that binds and potentiates the c-Jun activation domain," *Genes Dev.*, pp. 2135–2148, 1993.

[168] H. K. Sluss, T. Barrett, B. Derijard, and R. J. Davis, "Signal transduction by tumor necrosis factor mediated by JNK protein kinases.," *Mol. Cell. Biol.*, vol. 14, no. 12, p. 8376, 1994.

[169] S. Gupta, T. Barrett, A. J. Whitmarshl, J. Cavanagh, H. K. Sluss, B. Derijard, and R. J. Davis, "Selective interaction of JNK protein kinase isoforms with transcription factors," *EMBO J.*, vol. 15, no. 11, pp. 2760–2770, 1996.

[170] R. Davis, "Signal transduction by the JNK group of MAP kinases," *Cell*, vol. 2, no. 103, pp. 239–252, 2000.

[171] C. Weston and R. Davis, "The JNK signal transduction pathway," *Curr. Opin. Genet. Dev.*, vol. 1, no. 12, pp. 14–21, 2002.

[172] A. M. Bode and Z. Dong, "The Functional Contrariety of JNK," *Mol. Carcinog.*, vol. 598, no. April, pp. 591–598, 2007.

[173] K. Maundrell, B. Antonsson, E. Magnenat, M. Camps, M. Muda, C. Chabert, C. Gillieron, U. Boschert, E. Vial-Knecht, J. C. Martinou, and S. Arkinstall, "Bcl-2 undergoes phosphorylation by c-Jun N-terminal kinase/stress-activated protein kinases in the presence of the constitutively active GTP-binding protein Rac1.," *J. Biol. Chem.*, vol. 272, no. 40, pp. 25238–42, Oct. 1997.

[174] J. Lamb, J. Ventura, P. Hess, and R. Flavell, "JunD mediates survival signaling by the JNK signal transduction pathway," *Mol. Cell*, vol. 11, pp. 1479–1489, 2003.

[175] Z. Huang, D.-P. Yan, and B.-X. Ge, "JNK regulates cell migration through promotion of tyrosine phosphorylation of paxillin.," *Cell. Signal.*, vol. 20, no. 11, pp. 2002–12, Nov. 2008.

[176] T. K. P. Doan, K. S. Park, H. K. Kim, D. S. Park, J. H. Kim, and T. R. Yoon, "Inhibition of JNK and ERK pathways by SP600125- and U0126-enhanced osteogenic differentiation of bone marrow stromal cells," *Tissue Eng. Regen. Med.*, vol. 9, no. 6, pp. 283–294, Nov. 2012.

[177] C. Dong, D. Yang, C. Tournier, and A. Whitmarsh, "JNK is required for effector T-cell function but not for T-cell activation," *Nature*, vol. 405, no. May, pp. 91–94, 2000.

[178] V. Waetzig, K. Czeloth, U. Hidding, K. Mielke, M. Kanzow, S. Brecht, M. Goetz, R. Lucius, T. Herdegen, and U.-K. Hanisch, "c-Jun N-terminal kinases (JNKs) mediate pro-inflammatory actions of microglia.," *Glia*, vol. 50, no. 3, pp. 235–46, May 2005.

[179] E. Chan and D. Riches, "IFN-γ+ LPS induction of iNOS is modulated by ERK, JNK/SAPK, and p38 mapk in a mouse macrophage cell line," *Am. J. Physiol. Physiol.*, no. 280, pp. 441–450, 2001.

[180] Y. Jiang, C. Chen, Z. Li, W. Guo, and J. Gegner, "Characterization of the structure and function of a new mitogen-activated protein kinase (p38β)," *J. Biol. Chem.*, vol. 271, no. 30, pp. 17920–17926, 1996.

[181] S. Mertens, M. Craxton, and M. Goedert, "SAP kinase-3, a new member of the family of mammalian stress-activated protein kinases," *FEBS Lett.*, vol. 383, pp. 273–276, 1996.

[182] Y. Jiang, H. Gram, M. Zhao, L. New, and J. Gu, "Characterization of the structure and function of the fourth member of p38 group mitogen-activated protein kinases, p38δ," *J. Biol. Chem.*, vol. 272, no. 48, pp. 30122–30128, 1997.

[183] A. Cuadrado and A. R. Nebreda, "Mechanisms and functions of p38 MAPK signalling.," *Biochem. J.*, vol. 429, no. 3, pp. 403–17, Aug. 2010.

[184] H. Enslen, J. Raingeaud, and R. Davis, “Selective activation of p38 mitogen-activated protein (MAP) kinase isoforms by the MAP kinase kinases MKK3 and MKK6,” *J. Biol. Chem.*, vol. 273, no. 3, pp. 1741–1748, 1998.

[185] K. Deacon and J. Blank, “Characterization of the Mitogen-activated Protein Kinase Kinase 4 (MKK4)/c-Jun NH2-terminal kinase 1 and MKK3/p38 Pathways Regulated by MEK Kinases 2 and 3,” *J. Biol. Chem.*, vol. 272, no. 22, pp. 14489–14496, 1997.

[186] D. Brancho and N. Tanaka, “Mechanism of p38 MAP kinase activation in vivo,” *Genes Dev.*, no. 17, pp. 1969–1978, 2003.

[187] S. H. Ridley, J. L. Dean, S. J. Sarsfield, M. Brook, a R. Clark, and J. Saklatvala, “A p38 MAP kinase inhibitor regulates stability of interleukin-1-induced cyclooxygenase-2 mRNA.,” *FEBS Lett.*, vol. 439, no. 1–2, pp. 75–80, Nov. 1998.

[188] Y. L. Zu, J. Qi, a Gilchrist, G. a Fernandez, D. Vazquez-Abad, D. L. Kreutzer, C. K. Huang, and R. I. Sha’afi, “p38 mitogen-activated protein kinase activation is required for human neutrophil function triggered by TNF-alpha or FMLP stimulation.,” *J. Immunol.*, vol. 160, no. 4, pp. 1982–9, Feb. 1998.

[189] T. Ishizuka, F. Okajima, M. Ishiwara, K. Iizuka, I. Ichimonji, T. Kawata, H. Tsukagoshi, K. Dobashi, T. Nakazawa, and M. Mori, “Sensitized Mast Cells Migrate Toward the Agen: A Response Regulated by p38 Mitogen-Activated Protein Kinase and Rho-Associated Coiled-Coil-Forming Protein Kinase,” *J. Immunol.*, vol. 167, no. 4, pp. 2298–2304, Aug. 2001.

[190] Y. Li, B. Jiang, W. E. Jr, P. Vogt, and J. Han, “Myogenic differentiation requires signalling through both phosphatidylinositol 3-kinase and p38 MAP kinase,” *Cell. Signal.*, vol. 12, pp. 751–757, 2000.

[191] R. Eckert and T. Efimova, “p38 mitogen-activated protein kinases on the body surface–a function for p38δ,” *J. Invest. Dermatol.*, vol. 5, no. 120, pp. 823–828, 2003.

[192] J. Lee, J. Laydon, and P. McDonnell, “A protein kinase involved in the regulation of inflammatory cytokine biosynthesis,” *Nature*, no. 372, pp. 739–746, 1994.

[193] A. D. Bachstetter, B. Xing, and L. J. Van Eldik, “The p38alpha mitogen-activated protein kinase limits the CNS proinflammatory cytokine response to systemic lipopolysaccharide, potentially through an IL-10 dependent mechanism.,” *J. Neuroinflammation*, vol. 11, p. 175, Jan. 2014.

[194] S. M. Keyse and M. Ginsburg, “Amino acid sequence similarity between CL100, a dual-specificity MAP kinase phosphatase and cdc25.,” *Trends Biochem. Sci.*, vol. 18, no. 10, p. 377, 1993.

[195] T. Tanoue, M. Adachi, T. Moriguchi, and E. Nishida, “A conserved docking motif in MAP kinases common to substrates , activators and regulators,” *Nat. Cell Biol.*, vol. 2, no. February, 2000.

[196] T. Tanoue, T. Yamamoto, and E. Nishida, “Modular structure of a docking surface on MAPK phosphatases,” *J. Biol. Chem.*, vol. 277, no. 25, p. 22942, 2002.

[197] M. J. Wishart, J. M. Denu, J. A. Williams, and J. E. Dixon, “Communication A Single Mutation Converts a Novel Phosphotyrosine Binding Domain into a Dual-specificity Phosphatase *,” *Biochemistry*, pp. 26782–26785, 1995.

[198] A. Theodosiou and A. Ashworth, “Protein family review MAP kinase phosphatases Gene organization and evolutionary history,” *Genome*, pp. 1–10, 2002.

[199] L. F. Lau and D. Nathans, “Identification of a set of genes expressed during the GO / Gi transition of cultured mouse cells,” vol. 4, no. 12, pp. 3145–3151, 1985.

[200] S. M. Keyse and E. A. Emslie, “Oxidative stress and heat shock induce a human gene encoding a protein-tyrosine phosphatase,” *Nature*, vol. 359, pp. 644–647, 1992.

[201] H. Sun, C. H. Charles, L. F. Lau, and N. K. Tonks, “MKP-1 (3CH134), an immediate early gene product, is a dual specificity phosphatase that dephosphorylates MAP kinase in vivo.,” *Cell*, vol. 75, pp. 487–493, 1993.

[202] P. J. Rohan, P. Davis, C. A. Moskaluk, M. Kearns, H. Krutzsch, U. Siebenlist, and K. Kelly, “PAC-1 : A Mitogen-Induced Nuclear Protein Tyrosine Phosphatase,” *Science (80-.).*, vol. 259, pp. 1763–1766, 1993.

[203] C. H. Charles, H. Sun, L. F. Lau, and N. K. Tonks, “The growth factor-inducible immediate-early gene 3CH134 encodes a protein-tyrosine-phosphatase.,” *Proc. Natl. Acad. Sci. U. S. A.*, vol. 90, no. June, pp. 5292–5296, 1993.

[204] J. J. Wu and A. M. Bennett, “Essential Role for Mitogen-activated Protein (MAP) Kinase Phosphatase-1 in Stress-responsive MAP Kinase and Cell Survival Signaling *,” *Biochemistry*, vol. 280, no. 16, pp. 16461–16466, 2005.

[205] Q. Zhao, E. G. Shepherd, M. E. Manson, L. D. Nelin, A. Sorokin, and Y. Liu, “The role of mitogen-activated protein kinase phosphatase-1 in the response of alveolar macrophages to lipopolysaccharide: attenuation of proinflammatory cytokine biosynthesis via feedback control of p38.,” *J. Biol. Chem.*, vol. 280, no. 9, pp. 8101–8, Mar. 2005.

[206] C. C. Chen, D. B. Hardy, and C. R. Mendelson, “Progesterone receptor (PR) inhibits proliferation of human breast cancer cells via induction of MAPK phosphatase 1 (MKP-1/DUSP1).,” *J. Biol. Chem.*, vol. 1, no. 2, Oct. 2011.

[207] E. G. Shepherd, Q. Zhao, S. E. Welty, T. N. Hansen, C. V Smith, and Y. Liu, “The function of mitogen-activated protein kinase phosphatase-1 in peptidoglycan-stimulated macrophages.,” *J. Biol. Chem.*, vol. 279, no. 52, pp. 54023–31, Dec. 2004.

[208] P. Chen, J. Li, J. Barnes, G. C. Kokkonen, J. C. Lee, and Y. Liu, “Restraint of Proinflammatory Cytokine Biosynthesis by Mitogen-Activated Protein Kinase Phosphatase-1 in Lipopolysaccharide-Stimulated Macrophages,” *J. Immunol.*, vol. 169, no. 11, pp. 6408–6416, Dec. 2002.

[209] H. Chi, S. P. Barry, R. J. Roth, J. J. Wu, E. a Jones, A. M. Bennett, and R. a Flavell, “Dynamic regulation of pro- and anti-inflammatory cytokines by MAPK phosphatase 1 (MKP-1) in innate immune responses.,” *Proc. Natl. Acad. Sci. U. S. A.*, vol. 103, no. 7, pp. 2274–9, Feb. 2006.

[210] K. V. Salojin, I. B. Owusu, K. a. Millerchip, M. Potter, K. a. Platt, and T. Oravecz, “Essential Role of MAPK Phosphatase-1 in the Negative Control of Innate Immune Responses,” *J. Immunol.*, vol. 176, no. 3, pp. 1899–1907, Jan. 2006.

[211] M. Hammer, J. Mages, H. Dietrich, A. Servatius, N. Howells, A. C. B. Cato, and R. Lang, “Dual specificity phosphatase 1 (DUSP1) regulates a subset of LPS-induced genes and protects mice from lethal endotoxin shock.,” *J. Exp. Med.*, vol. 203, no. 1, pp. 15–20, Jan. 2006.

[212] M. S. Valerio, B. a Herbert, D. S. Basilakos, C. Browne, H. Yu, and K. L. Kirkwood, “Critical role of MKP-1 in lipopolysaccharide-induced osteoclast formation through CXCL1 and CXCL2.,” *Cytokine*, vol. 71, no. 1, pp. 71–80, Sep. 2014.

[213] T. Turpeinen, R. Nieminen, V. Taimi, T. Heittola, O. Sareila, A. R. Clark, E. Moilanen, and R. Korhonen, “Dual Specificity Phosphatase 1 Regulates Human Inducible Nitric Oxide Synthase Expression by p38 MAP Kinase,” *Mediators Inflamm.*, vol. 2011, 2011.

[214] X. Wang, Q. Zhao, R. Matta, X. Meng, X. Liu, C.-G. Liu, L. D. Nelin, and Y. Liu, “Inducible nitric-oxide synthase expression is regulated by mitogen-activated protein kinase phosphatase-1.,” *J. Biol. Chem.*, vol. 284, no. 40, pp. 27123–34, Oct. 2009.

[215] M. Lasa, S. M. Abraham, C. Boucheron, J. Saklatvala, and a. R. Clark, “Dexamethasone Causes Sustained Expression of Mitogen-Activated Protein Kinase (MAPK) Phosphatase 1 and Phosphatase-Mediated Inhibition of MAPK p38,” *Mol. Cell. Biol.*, vol. 22, no. 22, pp. 7802–7811, Nov. 2002.

[216] N. Srivastava, R. Sudan, and B. Saha, “CD40-modulated dual-specificity phosphatases MAPK phosphatase (MKP)-1 and MKP-3 reciprocally regulate Leishmania major infection.,” *J. Immunol.*, vol. 186, no. 10, pp. 5863–72, May 2011.

[217] Y. Zhang, J. M. Reynolds, S. H. Chang, N. Martin-Orozco, Y. Chung, R. I. Nurieva, and C. Dong, “MKP-1 is necessary for T cell activation and function.,” *J. Biol. Chem.*, vol. 284, no. 45, pp. 30815–24, Nov. 2009.

[218] A. Misra-Press, C. S. Rim, H. Yao, M. S. Roberson, and P. J. Stork, “A Novel Mitogen-activated Protein Kinase Phosphatase.pdf,” *J. Biol. Chem.*, vol. 270, no. 24, pp. 14587–14596, 1995.

[219] C. M. Sloss, L. Cadalbert, S. G. Finn, S. J. Fuller, and R. Plevin, “Disruption of two putative nuclear localization sequences is required for cytosolic localization of mitogen-activated protein kinase phosphatase-2.,” *Cell. Signal.*, vol. 17, no. 6, pp. 709–16, Jun. 2005.

[220] P. Chen, D. Hutter, X. Yang, M. Gorospe, R. J. Davis, and Y. Liu, “Discordance between the binding affinity of mitogen-activated protein kinase subfamily members for MAP kinase phosphatase-2 and their ability to activate the phosphatase catalytically.,” *J. Biol. Chem.*, vol. 276, no. 31, pp. 29440–9, Aug. 2001.

[221] L. C. Cadalbert, C. M. Sloss, M. R. Cunningham, M. Al-Mutairi, A. McIntire, J. Shipley, and R. Plevin, “Differential regulation of MAP kinase activation by a novel splice variant of human MAP kinase phosphatase-2.,” *Cell. Signal.*, vol. 22, no. 3, pp. 357–65, Mar. 2010.

[222] L. Cadalbert, C. M. Sloss, P. Cameron, and R. Plevin, “Conditional expression of MAP kinase phosphatase-2 protects against genotoxic stress-induced apoptosis by binding and selective dephosphorylation of nuclear activated c-jun N-terminal kinase.,” *Cell. Signal.*, vol. 17, no. 10, pp. 1254–64, Oct. 2005.

[223] M. Al-Mutairi, S. Al-Harthi, L. Cadalbert, and R. Plevin, “Over-expression of mitogen-activated protein kinase phosphatase-2 enhances adhesion molecule expression and protects against apoptosis in human endothelial cells.,” *Br. J. Pharmacol.*, vol. 161, no. 4, pp. 782–98, Oct. 2010.

[224] J. Wang, W. H. Shen, Y. J. Jin, P. W. Brandt-rauf, and Y. Yin, “A Molecular Link between E2F-1 and the MAPK Cascade *,” *J. Biol. Chem.*, vol. 282, no. 25, pp. 18521–18531, 2007.

[225] A. Lawan, S. Al-Harthi, L. Cadalbert, A. G. McCluskey, M. Shweash, G. Grassia, A. Grant, M. Boyd, S. Currie, and R. Plevin, “Deletion of the dual specific phosphatase-4 (DUSP-4) gene reveals an essential non-redundant role for MAP kinase phosphatase-2 (MKP-2) in proliferation and cell survival.,” *J. Biol. Chem.*, vol. 286, no. 15, pp. 12933–43, Apr. 2011.

[226] T. Hasegawa, A. Enomoto, T. Kato, K. Kawai, R. Miyamoto, M. Jijiwa, M. Ichihara, M. Ishida, N. Asai, Y. Murakumo, K. Ohara, Y. Niwa, H. Goto, and M. Takahashi, "Roles of induced expression of MAPK phosphatase-2 in tumor development in RET-MEN2A transgenic mice," *Oncogene*, pp. 5684–5695, 2008.

[227] S. Saigusa, Y. Inoue, K. Tanaka, Y. Toiyama, Y. Okugawa, T. Shimura, J. Hiro, K. Uchida, Y. Mohri, and M. Kusunoki, "Decreased expression of DUSP4 is associated with liver and lung metastases in colorectal cancer.," *Med. Oncol.*, vol. 30, no. 3, p. 620, Jan. 2013.

[228] M. S. Al-Mutairi, L. C. Cadalbert, H. A. McGachy, M. Shweash, J. Schroeder, M. Kurnik, C. M. Sloss, C. E. Bryant, J. Alexander, and R. Plevin, "MAP kinase phosphatase-2 plays a critical role in response to infection by Leishmania mexicana.," *PLoS Pathog.*, vol. 6, no. 11, p. e1001192, Jan. 2010.

[229] D. McMahon-Pratt and J. Alexander, "Does the Leishmania major paradigm of pathogenesis and protection hold for New World cutaneous leishmaniases or the visceral disease?," *Immunol. Rev.*, vol. 201, pp. 206–24, Oct. 2004.

[230] S. Woods, J. Schroeder, H. a McGachy, R. Plevin, C. W. Roberts, and J. Alexander, "MAP kinase phosphatase-2 plays a key role in the control of infection with Toxoplasma gondii by modulating iNOS and arginase-1 activities in mice.," *PLoS Pathog.*, vol. 9, no. 8, p. e1003535, Aug. 2013.

[231] J. Schroeder, H. A. McGachy, S. Woods, R. Plevin, and J. Alexander, "T cell hypo-responsiveness against Leishmania major in MAP kinase phosphatase (MKP) 2 deficient C57BL/6 mice does not alter the healer disease phenotype.," *PLoS Negl. Trop. Dis.*, vol. 7, no. 2, p. e2064, Jan. 2013.

[232] T. T. Cornell, A. Fleszar, W. McHugh, N. B. Blatt, A. M. Le Vine, and T. P. Shanley, "Mitogen-activated protein kinase phosphatase 2, MKP-2, regulates early inflammation in acute lung injury.," *Am. J. Physiol. Lung Cell. Mol. Physiol.*, vol. 303, no. 3, pp. L251–8, Aug. 2012.

[233] T. T. Cornell, P. Rodenhouse, Q. Cai, L. Sun, and T. P. Shanley, "Mitogen-activated protein kinase phosphatase 2 regulates the inflammatory response in sepsis.," *Infect. Immun.*, vol. 78, no. 6, pp. 2868–76, Jun. 2010.

[234] M. Muda, U. Boschert, R. Dickinson, J. C. Martinou, I. Martinou, M. Camps, W. Schlegel, and S. Arkinstall, "MKP-3, a novel cytosolic protein-tyrosine phosphatase that exemplifies a new class of mitogen-activated protein kinase phosphatase.," *J. Biol. Chem.*, vol. 271, no. 8, pp. 4319–26, Feb. 1996.

[235] H. Lee, J. M. Kim, S.-M. Huang, S.-K. Park, D.-H. Kim, D. H. Kim, C. S. Lee, K. S. Suh, E. S. Yi, and K.-H. Kim, "Differential expression of DUSP6 with expression of ERK and Ki-67 in non-small cell lung carcinoma.," *Pathol. Res. Pract.*, vol. 207, no. 7, pp. 428–32, Jul. 2011.

[236] Z. Zhang, S. Kobayashi, A. C. Borczuk, R. S. Leidner, T. Laframboise, A. D. Levine, and B. Halmos, "Dual specificity phosphatase 6 (DUSP6) is an ETS-regulated negative feedback mediator of oncogenic ERK signaling in lung cancer cells.," *Carcinogenesis*, vol. 31, no. 4, pp. 577–86, Apr. 2010.

[237] Z. Wang, P. S. Reinach, F. Zhang, K. Vellonen, A. Urtti, H. Turner, and J. M. Wolosin, "DUSP5 and DUSP6 modulate corneal epithelial cell proliferation.," *Mol. Vis.*, vol. 16, no. June, pp. 1696–1704, 2010.

[238] B. Xu, L. Yang, R. J. Lye, and B. T. Hinton, "p-MAPK1/3 and DUSP6 regulate epididymal cell proliferation and survival in a region-specific manner in mice.," *Biol. Reprod.*, vol. 83, no. 5, pp. 807–17, Nov. 2010.

[239] M. Razmara, G. Eger, C. Rorsman, C.-H. Heldin, and J. Lennartsson, "MKP3 negatively modulates PDGF-induced Akt and Erk5 phosphorylation as well as chemotaxis.," *Cell. Signal.*, vol. 24, no. 3, pp. 635–40, Mar. 2012.

[240] M. Domercq, E. Alberdi, M. V. Sánchez-Gómez, U. Ariz, A. Pérez-Samartín, and C. Matute, "Dual-specific phosphatase-6 (Dusp6) and ERK mediate AMPA receptor-induced oligodendrocyte death.," *J. Biol. Chem.*, vol. 286, no. 13, pp. 11825–36, Apr. 2011.

[241] M. Saha, S. Skopelja, E. Martinez, D. L. Alvarez, B. S. Liponis, and E. A. Romero-Sandoval, "Spinal mitogen-activated protein kinase phosphatase-3 (MKP-3) is necessary for the normal resolution of mechanical allodynia in a mouse model of acute postoperative pain.," *J. Neurosci.*, vol. 33, no. 43, pp. 17182–7, Oct. 2013.

[242] T. Tanoue, T. Moriguchi, and E. Nishida, "Molecular cloning and characterization of a novel dual specificity phosphatase, MKP-5.," *J. Biol. Chem.*, vol. 274, no. 28, pp. 19949–56, Jul. 1999.

[243] Y. Zhang, J. Blattman, N. Kennedy, J. Duong, T. Nguyen, Y. Wang, R. Davis, P. Greenberg, R. Flavell, and C. Dong, "Regulation of innate and adaptive immune responses by MAP kinase phosphatase 5," *Nature*, vol. 430, no. August, pp. 793–797, 2004.

[244] F. Qian, J. Deng, N. Cheng, E. J. Welch, Y. Zhang, A. B. Malik, R. a Flavell, C. Dong, and R. D. Ye, "A non-redundant role for MKP5 in limiting ROS production and preventing LPS-induced vascular injury.," *EMBO J.*, vol. 28, no. 19, pp. 2896–907, Oct. 2009.

[245] Q. Cheng, Q. Zhang, X. Xu, L. Yin, L. Sun, X. Lin, C. Dong, and W. Pan, "MAPK phosphotase 5 deficiency contributes to protection against blood-stage Plasmodium yoelii 17XL infection in mice.," *J. Immunol.*, vol. 192, no. 8, pp. 3686–96, Apr. 2014.

[246] L. Nonn, D. Duong, and D. M. Peehl, “Chemopreventive anti-inflammatory activities of curcumin and other phytochemicals mediated by MAP kinase phosphatase-5 in prostate cells.,” *Carcinogenesis*, vol. 28, no. 6, pp. 1188–96, Jun. 2007.

[247] K. Masuda, H. Shima, M. Watanabe, and K. Kikuchi, “MKP-7, a novel mitogen-activated protein kinase phosphatase, functions as a shuttle protein.,” *J. Biol. Chem.*, vol. 276, no. 42, pp. 39002–11, Oct. 2001.

[248] T. Musikacharoen, K. Bandow, K. Kakimoto, J. Kusuyama, T. Onishi, Y. Yoshikai, and T. Matsuguchi, “Functional involvement of dual specificity phosphatase 16 (DUSP16), a c-Jun N-terminal kinase-specific phosphatase, in the regulation of T helper cell differentiation.,” *J. Biol. Chem.*, vol. 286, no. 28, pp. 24896–905, Jul. 2011.

[249] S. Kumabe, M. Itsumi, H. Yamada, T. Yajima, T. Matsuguchi, and Y. Yoshikai, “Dual specificity phosphatase16 is a negative regulator of c-Jun NH2-terminal kinase activity in T cells.,” *Microbiol. Immunol.*, vol. 54, no. 2, pp. 105–11, Mar. 2010.

[250] M. Niedzielska, B. Bodendorfer, S. Münch, A. Eichner, M. Derigs, O. da Costa, A. Schweizer, F. Neff, L. Nitschke, T. Sparwasser, S. M. Keyse, and R. Lang, “Gene trap mice reveal an essential function of dual specificity phosphatase Dusp16/MKP-7 in perinatal survival and regulation of Toll-like receptor (TLR)-induced cytokine production.,” *J. Biol. Chem.*, vol. 289, no. 4, pp. 2112–26, Jan. 2014.

[251] I. T. Nizamutdinova, Y. M. Kim, J. H. Lee, K. C. Chang, and H. J. Kim, “MKP-7, a negative regulator of JNK, regulates VCAM-1 expression through IRF-1.,” *Cell. Signal.*, vol. 24, no. 4, pp. 866–72, Apr. 2012.

[252] X. Pi, Y. Wu, J. E. Ferguson, A. L. Portbury, and C. Patterson, “SDF-1alpha stimulates JNK3 activity via eNOS-dependent nitrosylation of MKP7 to enhance endothelial migration.,” *Proc. Natl. Acad. Sci. U. S. A.*, vol. 106, no. 14, pp. 5675–80, Apr. 2009.

[253] A. J. Chen, G. Zhou, T. Juan, S. M. Colicos, J. P. Cannon, M. Cabriera-Hansen, C. F. Meyer, R. Jurecic, N. G. Copeland, D. J. Gilbert, N. a Jenkins, F. Fletcher, T.-H. Tan, and J. W. Belmont, “The dual specificity JKAP specifically activates the c-Jun N-terminal kinase pathway.,” *J. Biol. Chem.*, vol. 277, no. 39, pp. 36592–601, Sep. 2002.

[254] N. Aoki, K. Aoyama, M. Nagata, and T. Matsuda, “A Growing Family of Dual Specificity Phosphatases with Low Molecular Masses,” *J. Biochem.*, vol. 130, no. 1, pp. 133–140, Jul. 2001.

[255] K. Aoyama, M. Nagata, K. Oshima, T. Matsuda, and N. Aoki, “Molecular cloning and characterization of a novel dual specificity phosphatase, LMW-

DSP2, that lacks the cdc25 homology domain.," *J. Biol. Chem.*, vol. 276, no. 29, pp. 27575–83, Jul. 2001.

[256] Y. Sekine, S. Tsuji, O. Ikeda, N. Sato, N. Aoki, K. Aoyama, K. Sugiyama, and T. Matsuda, "Regulation of STAT3-mediated signaling by LMW-DSP2.," *Oncogene*, vol. 25, no. 42, pp. 5801–6, Sep. 2006.

[257] Y. Sekine, O. Ikeda, Y. Hayakawa, S. Tsuji, S. Imoto, N. Aoki, K. Sugiyama, and T. Matsuda, "DUSP22/LMW-DSP2 regulates estrogen receptor-alpha-mediated signaling through dephosphorylation of Ser-118.," *Oncogene*, vol. 26, no. 41, pp. 6038–49, Sep. 2007.

[258] J.-P. Li, Y.-N. Fu, Y.-R. Chen, and T.-H. Tan, "JNK pathway-associated phosphatase dephosphorylates focal adhesion kinase and suppresses cell migration.," *J. Biol. Chem.*, vol. 285, no. 8, pp. 5472–8, Mar. 2010.

[259] J.-P. Li, C.-Y. Yang, H.-C. Chuang, J.-L. Lan, D.-Y. Chen, Y.-M. Chen, X. Wang, A. J. Chen, J. W. Belmont, and T.-H. Tan, "The phosphatase JKAP/DUSP22 inhibits T-cell receptor signalling and autoimmunity by inactivating Lck.," *Nat. Commun.*, vol. 5, p. 3618, Jan. 2014.

[260] M. Mandl, D. N. Slack, and S. M. Keyse, "Specific inactivation and nuclear anchoring of extracellular signal-regulated kinase 2 by the inducible dual-specificity protein phosphatase DUSP5.," *Mol. Cell. Biol.*, vol. 25, no. 5, pp. 1830–45, Mar. 2005.

[261] P. E. Kovanen, J. Bernard, A. Al-Shami, C. Liu, J. Bollenbacher-Reilley, L. Young, C. Pise-Masison, R. Spolski, and W. J. Leonard, "T-cell development and function are modulated by dual specificity phosphatase DUSP5.," *J. Biol. Chem.*, vol. 283, no. 25, pp. 17362–9, Jun. 2008.

[262] S.-J. Moon, M.-A. Lim, J.-S. Park, J.-K. Byun, S.-M. Kim, M.-K. Park, E.-K. Kim, Y.-M. Moon, J.-K. Min, S.-M. Ahn, S.-H. Park, and M.-L. Cho, "Dual-Specificity Phosphatase 5 Attenuates Autoimmune Arthritis in Mice via Reciprocal Regulation of the Th17/Treg Cell Balance and Inhibition of Osteoclastogenesis.," *Arthritis Rheumatol. (Hoboken, N.J.)*, vol. 66, no. 11, pp. 3083–95, Nov. 2014.

[263] R. Echavarria and S. N. a Hussain, "Regulation of angiopoietin-1/Tie-2 receptor signaling in endothelial cells by dual-specificity phosphatases 1, 4, and 5.," *J. Am. Heart Assoc.*, vol. 2, no. 6, p. e000571, Jan. 2013.

[264] M.-F. Grasset, S. Gobert-Gosse, G. Mouchiroud, and R. P. Bourette, "Macrophage differentiation of myeloid progenitor cells in response to M-CSF is regulated by the dual-specificity phosphatase DUSP5.," *J. Leukoc. Biol.*, vol. 87, no. 1, pp. 127–35, Jan. 2010.

[265] B. S. Ferguson, B. C. Harrison, M. Y. Jeong, B. G. Reid, M. F. Wempe, F. F. Wagner, E. B. Holson, and T. A. Mckinsey, "Signal-dependent repression of DUSP5 by class I HDACs controls nuclear ERK activity and cardiomyocyte hypertrophy," 2013.

[266] N. T. Wickramasekera, D. Gebremedhin, K. a Carver, P. Vakeel, R. Ramchandran, A. Schuett, and D. R. Harder, "Role of dual-specificity protein phosphatase-5 in modulating the myogenic response in rat cerebral arteries.," *J. Appl. Physiol.*, vol. 114, no. 2, pp. 252–61, Jan. 2013.

[267] D. R. Harder, J. Narayanan, and D. Gebremedhin, "Pressure-induced myogenic tone and role of 20-HETE in mediating autoregulation of cerebral blood flow.," *Am. J. Physiol. Heart Circ. Physiol.*, vol. 300, no. 5, pp. H1557–65, May 2011.

[268] C. Kilkenny, W. J. Browne, I. C. Cuthill, M. Emerson, and D. G. Altman, "Improving bioscience research reporting: The arrive guidelines for reporting animal research," *Animals*, vol. 4, no. 1, pp. 35–44, 2013.

[269] W. N. D'Souza, C.-F. Chang, A. M. Fischer, M. Li, and S. M. Hedrick, "The Erk2 MAPK regulates CD8 T cell proliferation and survival.," *J. Immunol.*, vol. 181, pp. 7617–7629, 2008.

[270] Y. J. Kang, J. Chen, M. Otsuka, J. Mols, S. Ren, Y. Wang, and J. Han, "Macrophage Deletion of p38 Partially Impairs Lipopolysaccharide-Induced Cellular Activation," *J. Immunol.*, vol. 180, no. 7, pp. 5075–5082, Mar. 2008.

[271] Y. Yanagawa and K. Onoé, "Distinct regulation of CD40-mediated interleukin-6 and interleukin-12 productions via mitogen-activated protein kinase and nuclear factor kappaB-inducing kinase in mature dendritic cells.," *Immunology*, vol. 117, no. 4, pp. 526–35, Apr. 2006.

[272] J. M. Dal Porto, S. B. Gauld, K. T. Merrell, D. Mills, A. E. Pugh-Bernard, and J. Cambier, "B cell antigen receptor signaling 101.," *Mol. Immunol.*, vol. 41, no. 6–7, pp. 599–613, Jul. 2004.

[273] C. F. Brereton, C. E. Sutton, S. J. Lalor, E. C. Lavelle, and K. H. G. Mills, "Inhibition of ERK MAPK suppresses IL-23- and IL-1-driven IL-17 production and attenuates autoimmune disease.," *J. Immunol.*, vol. 183, no. 3, pp. 1715–23, Aug. 2009.

[274] E. H. Tran, Y.-T. Azuma, M. Chen, C. Weston, R. J. Davis, and R. a Flavell, "Inactivation of JNK1 enhances innate IL-10 production and dampens autoimmune inflammation in the brain.," *Proc. Natl. Acad. Sci. U. S. A.*, vol. 103, no. 36, pp. 13451–6, Sep. 2006.

[275] G. Huang, Y. Wang, P. Vogel, T.-D. Kanneganti, K. Otsu, and H. Chi, "Signaling via the kinase p38α programs dendritic cells to drive TH17

differentiation and autoimmune inflammation.," *Nat. Immunol.*, vol. 13, no. 2, pp. 152–61, Mar. 2012.

[276] C. J. Caunt and S. M. Keyse, "Dual-specificity MAP kinase phosphatases (MKPs): shaping the outcome of MAP kinase signalling.," *FEBS J.*, vol. 280, no. 2, pp. 489–504, Jan. 2013.

[277] D. M. Owens and S. M. Keyse, "Differential regulation of MAP kinase signalling by dual-specificity protein phosphatases," *Oncogene*, pp. 3203–3213, 2007.

[278] S. Bittner, A. M. Afzali, H. Wiendl, and S. G. Meuth, "Myelin oligodendrocyte glycoprotein (MOG35-55) induced experimental autoimmune encephalomyelitis (EAE) in C57BL/6 mice.," *J. Vis. Exp.*, no. 86, pp. 1–5, Jan. 2014.

[279] Z. Ji, Z.-J. Ke, and J.-G. Geng, "SAP suppresses the development of experimental autoimmune encephalomyelitis in C57BL/6 mice," *Immunology and Cell Biology*, vol. 90, no. 4. pp. 388–395, 2012.

[280] C. Malmeström, B. a. Andersson, S. Haghighi, and J. Lycke, "IL-6 and CCL2 levels in CSF are associated with the clinical course of MS: Implications for their possible immunopathogenic roles," *J. Neuroimmunol.*, vol. 175, pp. 176–182, 2006.

[281] D. Maimone, G. C. Guazzi, and P. Annunziata, "IL-6 detection in multiple sclerosis brain," *J. Neurol. Sci.*, vol. 146, pp. 59–65, 1997.

[282] K. Gijbels, J. Van Damme, P. Proost, W. Put, H. Carton, and a Billiau, "Interleukin 6 production in the central nervous system during experimental autoimmune encephalomyelitis.," *Eur. J. Immunol.*, vol. 20, pp. 233–235, 1990.

[283] M. Giralt, R. Ramos, A. Quintana, B. Ferrer, M. Erta, M. Castro-Freire, G. Comes, E. Sanz, M. Unzeta, P. Pifarré, A. García, I. L. Campbell, and J. Hidalgo, "Induction of atypical EAE mediated by transgenic production of IL-6 in astrocytes in the absence of systemic IL-6," *Glia*, vol. 61, pp. 587–600, 2013.

[284] E. B. Samoilova, J. L. Horton, B. Hilliard, T. S. Liu, and Y. Chen, "IL-6-deficient mice are resistant to experimental autoimmune encephalomyelitis: roles of IL-6 in the activation and differentiation of autoreactive T cells.," *J. Immunol.*, 1998.

[285] Y. Okuda, S. Sakoda, C. C. a Bernard, H. Fujimura, Y. Saeki, T. Kishimoto, and T. Yanagihara, "IL-6-deficient mice are resistant to the induction of experimental autoimmune encephalomyelitis provoked by myelin

oligodendrocyte glycoprotein," *Int. Immunol.*, vol. 10, no. 5, pp. 703–708, 1998.

[286] H. Pietro Eugster, K. Frei, M. Kopf, H. Lassmann, and A. Fontana, "IL-6-deficient mice resist myelin oligodendrocyte glycoprotein-induced autoimmune encephalomyelitis," *Eur. J. Immunol.*, vol. 28, pp. 2178–2187, 1998.

[287] J. S. Tzartos, M. a Friese, M. J. Craner, J. Palace, J. Newcombe, M. M. Esiri, and L. Fugger, "Interleukin-17 production in central nervous system-infiltrating T cells and glial cells is associated with active disease in multiple sclerosis.," *Am. J. Pathol.*, vol. 172, pp. 146–155, 2008.

[288] G.-X. Zhang, B. Gran, S. Yu, J. Li, I. Siglienti, X. Chen, M. Kamoun, and A. Rostami, "Induction of experimental autoimmune encephalomyelitis in IL-12 receptor-beta 2-deficient mice: IL-12 responsiveness is not required in the pathogenesis of inflammatory demyelination in the central nervous system.," *J. Immunol.*, vol. 170, pp. 2153–2160, 2003.

[289] T. Renno, M. Krakowski, C. Piccirillo, J. Y. Lin, and T. Owens, "TNF-alpha expression by resident microglia and infiltrating leukocytes in the central nervous system of mice with experimental allergic encephalomyelitis. Regulation by Th1 cytokines.," *J. Immunol.*, vol. 154, pp. 944–953, 1995.

[290] S. Serada, M. Fujimoto, M. Mihara, N. Koike, Y. Ohsugi, S. Nomura, H. Yoshida, T. Nishikawa, F. Terabe, T. Ohkawara, T. Takahashi, B. Ripley, A. Kimura, T. Kishimoto, and T. Naka, "IL-6 blockade inhibits the induction of myelin antigen-specific Th17 cells and Th1 cells in experimental autoimmune encephalomyelitis.," *Proc. Natl. Acad. Sci. U. S. A.*, vol. 105, no. 21, pp. 9041–9046, 2008.

[291] V. Sanna, A. Di Giacomo, A. La Cava, R. I. Lechler, S. Fontana, S. Zappacosta, and G. Matarese, "Leptin surge precedes onset of autoimmune encephalomyelitis and correlates with development of pathogenic T cell responses.," *J. Clin. Invest.*, vol. 111, no. 2, pp. 241–50, Jan. 2003.

[292] J. A. Encinas, M. B. Lees, R. A. Sobel, C. Symonowicz, H. L. Weiner, C. E. Seidman, J. G. Seidman, and V. K. Kuchroo, "Identification of genetic loci associated with paralysis, inflammation and weight loss in mouse experimental autoimmune encephalomyelitis.," *Int. Immunol.*, vol. 13, no. 3, pp. 257–264, 2001.

[293] L. L. Hua, M. Zhao, M. Cosenza, M. Kim, H. Huang, H. B. Tanowitz, C. F. Brosnan, and S. C. Lee, "Role of mitogen-activated protein kinases in inducible nitric oxide synthase and TNFalpha expression in human fetal astrocytes.," *J. Neuroimmunol.*, vol. 126, pp. 180–189, 2002.

[294] W. Wang, Q. Li, J. Zhang, H. Wu, Y. Yin, Q. Ge, and Y. Zhang, “Hemokinin-1 activates the MAPK pathway and enhances B cell proliferation and antibody production.,” *J. Immunol.*, vol. 184, no. 7, pp. 3590–7, Apr. 2010.

[295] K. Nakayama, Y. Ota, S. Okugawa, N. Ise, T. Kitazawa, K. Tsukada, M. Kawada, S. Yanagimoto, and S. Kimura, “Raf1 plays a pivotal role in lipopolysaccharide-induced activation of dendritic cells,” *Biochem. Biophys. Res. Commun.*, vol. 308, no. 2, pp. 353–360, Aug. 2003.

[296] T. Shin, M. Ahn, K. Jung, S. Heo, D. Kim, Y. Jee, Y. K. Lim, and E. J. Yeo, “Activation of mitogen-activated protein kinases in experimental autoimmune encephalomyelitis,” *J. Neuroimmunol.*, vol. 140, no. 1–2, pp. 118–125, Jul. 2003.

[297] A. Agrawal, S. Dillon, T. L. Denning, and B. Pulendran, “ERK1-/- Mice Exhibit Th1 Cell Polarization and Increased Susceptibility to Experimental Autoimmune Encephalomyelitis,” *J. Immunol.*, vol. 176, no. 10, pp. 5788–5796, May 2006.

[298] T. Nekrasova, C. Shive, Y. Gao, R. Guardia, G. Landreth, G. Thomas, and K. Kawamura, “ERK1-Deficient Mice Show Normal T Cell Effector Function and Are Highly Susceptible to Experimental Autoimmune Encephalomyelitis,” 2012.

[299] K. Nicolson, S. Freland, C. Weir, B. Delahunt, R. a Flavell, and B. T. Bäckström, “Induction of experimental autoimmune encephalomyelitis in the absence of c-Jun N-terminal kinase 2.,” *Int. Immunol.*, vol. 14, no. 8, pp. 849–56, 2002.

[300] K. Denninger, S. Rasmussen, J. M. Larsen, C. Orskov, S. Seier Poulsen, P. Sørensen, J. P. Christensen, H. Illges, N. Odum, and T. Labuda, “JNK1, but not JNK2, is required in two mechanistically distinct models of inflammatory arthritis.,” *Am. J. Pathol.*, vol. 179, no. 4, pp. 1884–93, Oct. 2011.

[301] R. Noubade, D. N. Krementsov, R. Del Rio, T. Thornton, V. Nagaleekar, N. Saligrama, A. Spitzack, K. Spach, G. Sabio, R. J. Davis, M. Rincon, and C. Teuscher, “Activation of p38 MAPK in CD4 T cells controls IL-17 production and autoimmune encephalomyelitis.,” *Blood*, vol. 118, no. 12, pp. 3290–300, Sep. 2011.

[302] Y. Chu, P. a Solski, R. Khosravi-Far, C. J. Der, and K. Kelly, “The mitogen-activated protein kinase phosphatases PAC1, MKP-1, and MKP-2 have unique substrate specificities and reduced activity in vivo toward the ERK2 sevenmaker mutation.,” *J. Biol. Chem.*, vol. 271, no. 11, pp. 6497–501, Mar. 1996.

[303] C. Mora, I. S. Grewal, F. S. Wong, and R. a. Flavell, “Role of L-selectin in the development of autoimmune diabetes in non-obese diabetic mice,” *Int. Immunol.*, vol. 16, no. 2, pp. 257–264, Feb. 2004.

[304] A. J. Lusis, J. Yu, and S. S. Wang, “The problem of passenger genes in transgenic mice.,” *Arterioscler. Thromb. Vasc. Biol.*, vol. 27, no. 10, pp. 2100–3, Oct. 2007.

[305] M. a Toscano, G. a Bianco, J. M. Ilarregui, D. O. Croci, J. Correale, J. D. Hernandez, N. W. Zwirner, F. Poirier, E. M. Riley, L. G. Baum, and G. a Rabinovich, “Differential glycosylation of TH1, TH2 and TH-17 effector cells selectively regulates susceptibility to cell death.,” *Nat. Immunol.*, vol. 8, no. 8, pp. 825–34, Aug. 2007.

[306] C. Dong, A. E. Juedes, U. A. Temann, S. Shresta, J. P. Allison, N. H. Ruddle, and R. A. Flavell, “ICOS co-stimulatory receptor is essential for T-cell activation and function.,” *Nature*, vol. 409, no. January, pp. 97–101, 2001.

[307] H. Suzuki, Y. Hasegawa, K. Kanamaru, and J. H. Zhang, “Mechanisms of osteopontin-induced stabilization of blood-brain barrier disruption after subarachnoid hemorrhage in rats,” *Stroke*, vol. 41, pp. 1783–1790, 2010.

[308] H. S. Domingues, M. Mues, H. Lassmann, H. Wekerle, and G. Krishnamoorthy, “Functional and pathogenic differences of Th1 and Th17 cells in experimental autoimmune encephalomyelitis.,” *PLoS One*, vol. 5, no. 11, p. e15531, Jan. 2010.

[309] A. M. Zubiaga, E. Munoz, M. Merrow, and B. T. Huber, “Regulation of interleukin 6 production in T helper cells,” *Int. Immunol.*, vol. 2, no. 11, pp. 1047–1054, 1990.

[310] G. Tosato and K. D. Jones, “Interleukin-1 induces interleukin-6 production in peripheral blood monocytes.,” *Blood*, vol. 75, pp. 1305–1310, 1990.

[311] J. Piercy, S. Petrova, E. Z. Tchilian, and P. C. L. Beverley, “CD45 negatively regulates tumour necrosis factor and interleukin-6 production in dendritic cells.,” *Immunology*, vol. 118, no. 2, pp. 250–6, Jun. 2006.

[312] T. Hirano, T. Matsuda, M. Turner, N. Miyasaka, G. Buchan, B. Tang, K. Sato, M. Shimizu, R. Maini, and M. Feldmann, “Excessive production of interleukin 6/B cell stimulatory factor-2 in rheumatoid arthritis.,” *Eur. J. Immunol.*, vol. 18, pp. 1797–1801, 1988.

[313] Q. Zhao, X. Wang, L. D. Nelin, Y. Yao, R. Matta, M. E. Manson, R. S. Baliga, X. Meng, C. V Smith, J. a Bauer, C.-H. Chang, and Y. Liu, “MAP kinase phosphatase 1 controls innate immune responses and suppresses endotoxic shock.,” *J. Exp. Med.*, vol. 203, no. 1, pp. 131–40, Jan. 2006.

[314] G. Huang, Y. Wang, L. Z. Shi, T.-D. Kanneganti, and H. Chi, “Signaling by the phosphatase MKP-1 in dendritic cells imprints distinct effector and regulatory T cell fates.,” *Immunity*, vol. 35, no. 1, pp. 45–58, Jul. 2011.

[315] A. Laurence, J. J. O’Shea, and W. T. Watford, “Interleukin-22: a sheep in wolf’s clothing.,” *Nat. Med.*, vol. 14, no. 3, pp. 247–9, Mar. 2008.

[316] a Eken, a K. Singh, P. M. Treuting, and M. Oukka, “IL-23R+ innate lymphoid cells induce colitis via interleukin-22-dependent mechanism.,” *Mucosal Immunol.*, vol. 7, no. 1, pp. 143–54, Jan. 2014.

[317] L. a Zenewicz and R. a Flavell, “Recent advances in IL-22 biology.,” *Int. Immunol.*, vol. 23, no. 3, pp. 159–63, Mar. 2011.

[318] C. J. Kim, a Nazli, O. L. Rojas, D. Chege, Z. Alidina, S. Huibner, S. Mujib, E. Benko, C. Kovacs, L. Y. Y. Shin, a Grin, G. Kandel, M. Loutfy, M. Ostrowski, J. L. Gommerman, C. Kaushic, and R. Kaul, “A role for mucosal IL-22 production and Th22 cells in HIV-associated mucosal immunopathogenesis,” *Mucosal Immunol.*, vol. 5, no. 6, pp. 670–680, 2012.

[319] S. Rutz, C. Eidenschenk, and W. Ouyang, “IL-22, not simply a Th17 cytokine,” *Immunol. Rev.*, vol. 252, pp. 116–132, 2013.

[320] Y. Zheng, D. M. Danilenko, P. Valdez, I. Kasman, J. Eastham-Anderson, J. Wu, and W. Ouyang, “Interleukin-22, a T(H)17 cytokine, mediates IL-23-induced dermal inflammation and acanthosis.,” *Nature*, vol. 445, no. 7128, pp. 648–651, Feb. 2007.

[321] H. Ma, S. Liang, J. Li, L. Napierata, T. Brown, S. Benoit, M. Senices, D. Gill, K. Dunussi-joannopoulos, M. Collins, C. Nickerson-nutter, L. A. Fouser, and D. A. Young, “IL-22 is required for Th17 cell – mediated pathology in a mouse model of psoriasis-like skin inflammation,” vol. 118, no. 2, pp. 597–607, 2008.

[322] L. a Zenewicz, G. D. Yancopoulos, D. M. Valenzuela, A. J. Murphy, M. Karow, and R. a Flavell, “IL-22 but not IL-17 provides protection to hepatocytes during acute liver inflammation,” *Immunity*, vol. 27, no. 4, pp. 647–659, 2007.

[323] R. Basu, D. B. O’Quinn, D. J. Silberger, T. R. Schoeb, L. Fouser, W. Ouyang, R. D. Hatton, and C. T. Weaver, “Th22 cells are an important source of IL-22 for host protection against enteropathogenic bacteria.,” *Immunity*, vol. 37, no. 6, pp. 1061–75, Dec. 2012.

[324] K. Kreymborg, R. Etzensperger, L. Dumoutier, S. Haak, A. Rebollo, T. Buch, F. L. Heppner, J.-C. Renauld, and B. Becher, “IL-22 is expressed by Th17 cells in an IL-23-dependent fashion, but not required for the development of autoimmune encephalomyelitis.,” *J. Immunol.*, vol. 179, pp. 8098–8104, 2007.

[325] J. Cote-Sierra, G. Foucras, L. Guo, L. Chiodetti, H. a Young, J. Hu-Li, J. Zhu, and W. E. Paul, “Interleukin 2 plays a central role in Th2 differentiation.,” *Proc. Natl. Acad. Sci. U. S. A.*, vol. 101, no. 11, pp. 3880–5, Mar. 2004.

[326] W. Liao, J.-X. Lin, L. Wang, P. Li, and W. J. Leonard, “Modulation of cytokine receptors by IL-2 broadly regulates differentiation into helper T cell lineages.,” *Nat. Immunol.*, vol. 12, no. 6, pp. 551–9, Jun. 2011.

[327] S. Le Gallou, G. Caron, C. Delaloy, D. Rossille, K. Tarte, and T. Fest, “IL-2 requirement for human plasma cell generation: coupling differentiation and proliferation by enhancing MAPK-ERK signaling.,” *J. Immunol.*, vol. 189, pp. 161–73, 2012.

[328] Y. H. Kim, M. J. Buchholz, and a a Nordin, “Murine T-lymphocyte proliferation induced by interleukin 2 correlates with a transient increase in p56lck kinase activity and the tyrosine phosphorylation of a 97-kDa protein.,” *Proc. Natl. Acad. Sci. U. S. A.*, vol. 90, no. April, pp. 3187–3191, 1993.

[329] T. Kasahara, J. J. Hooks, S. F. Dougherty, and J. J. Oppenheim, “Interleukin 2-mediated immune interferon (IFN-gamma) production by human T cells and T cell subsets.,” *J. Immunol.*, vol. 130, no. 4, pp. 1784–9, 1983.

[330] C.-Y. Huang, Y.-C. Lin, W.-Y. Hsiao, F.-H. Liao, P.-Y. Huang, and T.-H. Tan, “DUSP4 deficiency enhances CD25 expression and CD4+ T-cell proliferation without impeding T-cell development.,” *Eur. J. Immunol.*, vol. 42, no. 2, pp. 476–88, Mar. 2012.

[331] B. T. Fife, M. C. Paniagua, N. W. Lukacs, S. L. Kunkel, and W. J. Karpus, “Expression by Central Nervous System- Infiltrating Encephalitogenic T Cells During Encephalomyelitis,” vol. 714, no. April, pp. 705–714, 2001.

[332] A. Szczuciński and J. Losy, “Chemokines and chemokine receptors in multiple sclerosis. Potential targets for new therapies.,” *Acta Neurol. Scand.*, vol. 115, no. 3, pp. 137–46, Mar. 2007.

[333] R. Sporici and T. B. Issekutz, “CXCR3 blockade inhibits T-cell migration into the CNS during EAE and prevents development of adoptively transferred, but not actively induced, disease.,” *Eur. J. Immunol.*, vol. 40, no. 10, pp. 2751–61, Oct. 2010.

[334] K. E. Balashov, J. B. Rottman, H. L. Weiner, and W. W. Hancock, “CCR5(+) and CXCR3(+) T cells are increased in multiple sclerosis and their ligands MIP-1alpha and IP-10 are expressed in demyelinating brain lesions.,” *Proc. Natl. Acad. Sci. U. S. A.*, vol. 96, no. June, pp. 6873–6878, 1999.

[335] X. Dai, Y. Chen, L. Di, A. Podd, G. Li, K. D. Bunting, L. Hennighausen, R. Wen, and D. Wang, “Stat5 is essential for early B cell development but not for

B cell maturation and function.,” *J. Immunol.*, vol. 179, no. 2, pp. 1068–1079, Jul. 2007.

[336] S. Hirokawa, H. Sato, I. Kato, and A. Kudo, “EBF-regulating Pax5 transcription is enhanced by STAT5 in the early stage of B cells.,” *Eur. J. Immunol.*, vol. 33, no. 7, pp. 1824–9, Jul. 2003.

[337] C. D. C. Allen, T. Okada, and J. G. Cyster, “Germinal-center organization and cellular dynamics.,” *Immunity*, vol. 27, no. 2, pp. 190–202, Aug. 2007.

[338] N. Yuceyar, D. Taşkiran, and A. Sağduyu, “Serum and cerebrospinal fluid nitrite and nitrate levels in relapsing-remitting and secondary progressive multiple sclerosis patients.,” *Clin. Neurol. Neurosurg.*, vol. 103, pp. 206–211, 2001.

[339] G. Giovannoni, S. J. . Heales, N. . Silver, J. O’Riordan, R. . Miller, J. . Land, J. . Clark, and E. . Thompson, “Raised serum nitrate and nitrite levels in patients with multiple sclerosis,” *J. Neurol. Sci.*, vol. 145, no. 1, pp. 77–81, Jan. 1997.

[340] D. C. Hooper, O. Bagasra, J. C. Marini, A. Zborek, S. T. Ohnishi, R. Kean, J. M. Champion, A. B. Sarker, L. Bobroski, J. L. Farber, T. Akaike, H. Maeda, and H. Koprowski, “Prevention of experimental allergic encephalomyelitis by targeting nitric oxide and peroxynitrite: implications for the treatment of multiple sclerosis.,” *Proc. Natl. Acad. Sci. U. S. A.*, vol. 94, no. March, pp. 2528–2533, 1997.

[341] A. H. Cross, R. M. Keeling, S. Goorha, M. San, C. Rodi, P. S. Wyatt, P. T. Manning, and T. P. Misko, “Induciblenitric oxide synthasegene expressionand enzyme activity correlatewith disease activityin murine experimentalautoimmune encephalomyelitis,” vol. 71, pp. 145–153, 1996.

[342] D. Liñares, M. Taconis, P. Maña, M. Correcha, S. Fordham, M. Staykova, and D. O. Willenborg, “Neuronal nitric oxide synthase plays a key role in CNS demyelination.,” *J. Neurosci.*, vol. 26, no. 49, pp. 12672–12681, 2006.

[343] B. Mitrovic, L. J. Ignarro, H. V Vinters, M. A. Akers, I. Schmid, C. Uittenbogaart, and J. E. Merrill, “Nitric oxide induces necrotic but not apoptotic cell death in oligodendrocytes.,” *Neuroscience*, vol. 65, no. 2, pp. 531–539, 1995.

[344] L. Y. Xu, J. S. Yang, H. Link, and B. G. Xiao, “SIN-1, a nitric oxide donor, ameliorates experimental allergic encephalomyelitis in Lewis rats in the incipient phase: the importance of the time window.,” *J. Immunol.*, vol. 166, no. 9, pp. 5810–5816, May 2001.

[345] Y. Okuda, S. Sakoda, H. Fujimura, and T. Yanagihara, “Nitric oxide via an inducible isoform of nitric oxide synthase is a possible factor to eliminate

inflammatory cells from the central nervous system of mice with experimental allergic encephalomyelitis," *J. Neuroimmunol.*, vol. 73, no. 1–2, pp. 107–116, Mar. 1997.

[346] N. C. O'Brien, B. Charlton, W. B. Cowden, and D. O. Willenborg, "Nitric oxide plays a critical role in the recovery of Lewis rats from experimental autoimmune encephalomyelitis and the maintenance of resistance to reinduction.," *J. Immunol.*, 1999.

[347] I. Nikić, D. Merkler, C. Sorbara, M. Brinkoetter, M. Kreutzfeldt, F. M. Bareyre, W. Brück, D. Bishop, T. Misgeld, and M. Kerschensteiner, "A reversible form of axon damage in experimental autoimmune encephalomyelitis and multiple sclerosis.," *Nat. Med.*, vol. 17, no. 4, pp. 495–9, Apr. 2011.

[348] Q. Seguín-Estévez, R. De Palma, M. Krawczyk, E. Leimgruber, J. Villard, C. Picard, A. Tagliamacco, G. Abbate, J. Gorski, A. Nocera, and W. Reith, "The transcription factor RFX protects MHC class II genes against epigenetic silencing by DNA methylation.," *J. Immunol.*, vol. 183, no. 4, pp. 2545–53, Aug. 2009.

[349] K. Masternak, A. Muhlethaler-Mottet, J. Villard, M. Zufferey, V. Steimle, and W. Reith, "CIITA is a transcriptional coactivator that is recruited to MHC class II promoters by multiple synergistic interactions with an enhanceosome complex," *Genes Dev.*, 2000.

[350] Y. Yao, Q. Xu, M.-J. Kwon, R. Matta, Y. Liu, S.-C. Hong, and C.-H. Chang, "ERK and p38 MAPK Signaling Pathways Negatively Regulate CIITA Gene Expression in Dendritic Cells and Macrophages," *J. Immunol.*, vol. 177, no. 1, pp. 70–76, Jun. 2006.

[351] I. Martins, F. Deshayes, F. Baton, A. Forget, I. Ciechomska, K. Sylla, F. Aoudjit, D. Charron, R. Al-Daccak, and C. Alcaide-Loridan, "Pathologic expression of MHC class II is driven by mitogen-activated protein kinases.," *Eur. J. Immunol.*, vol. 37, no. 3, pp. 788–97, Mar. 2007.

[352] S. Dillon, a. Agrawal, T. Van Dyke, G. Landreth, L. McCauley, a. Koh, C. Maliszewski, S. Akira, and B. Pulendran, "A Toll-Like Receptor 2 Ligand Stimulates Th2 Responses In Vivo, via Induction of Extracellular Signal-Regulated Kinase Mitogen-Activated Protein Kinase and c-Fos in Dendritic Cells," *J. Immunol.*, vol. 172, no. 8, pp. 4733–4743, Apr. 2004.

[353] M. R. Kotter, C. Zhao, N. van Rooijen, and R. J. M. Franklin, "Macrophage-depletion induced impairment of experimental CNS remyelination is associated with a reduced oligodendrocyte progenitor cell response and altered growth factor expression.," *Neurobiol. Dis.*, vol. 18, no. 1, pp. 166–75, Feb. 2005.

[354] C. I. Chang, J. C. Liao, and L. Kuo, “Arginase modulates nitric oxide production in activated macrophages.,” *Am. J. Physiol.*, vol. 274, pp. H342–H348, 1998.

[355] S. J. Ajizian, B. K. English, and E. a Meals, “Specific inhibitors of p38 and extracellular signal-regulated kinase mitogen-activated protein kinase pathways block inducible nitric oxide synthase and tumor necrosis factor accumulation in murine macrophages stimulated with lipopolysaccharide and interf,” *J. Infect. Dis.*, vol. 179, no. 4, pp. 939–44, Apr. 1999.

[356] C. C. Stempin, V. V Garrido, L. R. Dulgerian, and F. M. Cerbán, “Cruzipain and SP600125 induce p38 activation, alter NO/arginase balance and favor the survival of Trypanosoma cruzi in macrophages.,” *Acta Trop.*, vol. 106, no. 2, pp. 119–27, May 2008.

[357] C. C. Stempin, T. B. Tanos, O. a Coso, and F. M. Cerbán, “Arginase induction promotes Trypanosoma cruzi intracellular replication in Cruzipain-treated J774 cells through the activation of multiple signaling pathways.,” *Eur. J. Immunol.*, vol. 34, no. 1, pp. 200–9, Jan. 2004.

[358] D. Rego, A. Kumar, L. Nilchi, K. Wright, S. Huang, and M. Kozlowski, “IL-6 production is positively regulated by two distinct Src homology domain 2-containing tyrosine phosphatase-1 (SHP-1)-dependent CCAAT/enhancer-binding protein β and NF-κB pathways and an SHP-1-independent NF-κB pathway in lipopolysaccharide-stimulated b,” *J. Immunol.*, vol. 186, no. 9, pp. 5443–56, May 2011.

[359] R. Tada, Y. Koide, M. Yamamuro, R. Tanaka, A. Hidaka, K. Nagao, and Y. Aramaki, “Maleylated-BSA suppresses lipopolysaccharide-induced IL-6 production by activating the ERK-signaling pathway in murine RAW264.7 cells.,” *Int. Immunopharmacol.*, vol. 19, no. 1, pp. 5–9, Mar. 2014.

[360] R. Craig, a Larkin, a M. Mingo, D. J. Thuerauf, C. Andrews, P. M. McDonough, and C. C. Glembotski, “p38 MAPK and NF-kappa B collaborate to induce interleukin-6 gene expression and release. Evidence for a cytoprotective autocrine signaling pathway in a cardiac myocyte model system.,” *J. Biol. Chem.*, vol. 275, no. 31, pp. 23814–24, Aug. 2000.

[361] C. D. Dumitru, J. D. Ceci, C. Tsatsanis, D. Kontoyiannis, K. Stamatakis, J. H. Lin, C. Patriotis, N. A. Jenkins, N. G. Copeland, G. Kollias, and P. N. Tsichlis, “TNF-α induction by LPS is regulated posttranscriptionally via a Tpl2/ERK-dependent pathway,” *Cell*, vol. 103, pp. 1071–1083, 2000.

[362] H. Jiang, E. Muckersie, M. Robertson, H. Xu, J. Liversidge, J. V Forrester, and D. J. Leu-, “Secretion of interleukin-10 or interleukin-12 by LPS-activated dendritic cells is critically dependent on time of stimulus relative to initiation of purified DC culture (LPS). We demonstrate here that LPS can stimu- but to differentiate toward an interl,” 2002.

[363] a.-K. Yi, J.-G. Yoon, S.-J. Yeo, S.-C. Hong, B. K. English, and a. M. Krieg, “Role of Mitogen-Activated Protein Kinases in CpG DNA-Mediated IL-10 and IL-12 Production: Central Role of Extracellular Signal-Regulated Kinase in the Negative Feedback Loop of the CpG DNA-Mediated Th1 Response,” *J. Immunol.*, vol. 168, no. 9, pp. 4711–4720, May 2002.

[364] F. Kaiser, D. Cook, S. Papoutsopoulou, R. Rajsbaum, X. Wu, H.-T. Yang, S. Grant, P. Ricciardi-Castagnoli, P. N. Tsichlis, S. C. Ley, and A. O’Garra, “TPL-2 negatively regulates interferon-beta production in macrophages and myeloid dendritic cells.,” *J. Exp. Med.*, vol. 206, no. 9, pp. 1863–71, Aug. 2009.

[365] H. Zhang, A. a Jarjour, A. Boyd, and A. Williams, “Central nervous system remyelination in culture--a tool for multiple sclerosis research.,” *Exp. Neurol.*, vol. 230, no. 1, pp. 138–48, Jul. 2011.